In vivo study of the suppression of cell-autonomous and systemic RNA silencing by the Peanut clump virus protein P15

Marco Incarbone

UNIVERSITÉ DE STRASBOURG

UNIVERSITÉ DE STRASBOURG

École Doctorale des Sciences de la Vie et de la Santé STRASBOURG

ECOLE DOCTORALE DE LA VIE ET DE LA SANTE

THÈSE

Présentée par

Marco INCARBONE

à

L'Institut de biologie moléculaire des plantes, CNRS

pour obtenir le grade de

DOCTEUR DE L'UNIVERSITÉ DE STRASBOURG

Spécialité : Aspects Moléculaires et Cellulaires de la Biologie

In vivo study of the suppression of cell-autonomous and systemic RNA silencing by the *Peanut clump virus* protein P15

Soutenue le 5 Décembre 2016 devant la Commission d'Examen :

Directeur de Thèse	**Dr Patrice DUNOYER**
Rapporteur Externe	**Dr Hervé VAUCHERET**
Rapporteur Externe	**Prof Peter BRODERSEN**
Examinateur Interne	**Dr Sébastien PFEFFER**

RNA networks Net RNA

ibmp www.ibmp.fr

cnrs

"Welcome. And congratulations. I am delighted that you could make it. Getting here wasn't easy, I know. In fact, I suspect it was a little tougher than you realize.

To begin with, for you to be here now trillions of drifting atoms had somehow to assemble in an intricate and intriguingly obliging manner to create you. It's an arrangement so specialized and particular that it has never been tried before and will only exist this once. For the next many years (we hope) these tiny particles will uncomplainingly engage in all the billions of deft, cooperative efforts necessary to keep you intact and let you experience the supremely agreeable but generally underappreciated state known as existence. (…)

So thank goodness for atoms. But the fact that you have atoms and that they assemble in such a willing manner is only part of what got you here. To be here now, alive in the twenty-first century and smart enough to know it, you also had to be the beneficiary of an extraordinary string of biological good fortune. Survival on earth is a surprisingly tricky business. Of the billions and billions of species of living things that have existed since the dawn of time, most – 99.99 percent – are no longer around. Life on earth, you see, is not only brief but dismayingly tenuous. It is a curious feature of our existence that we come from a planet that is very good at promoting life but even better at extinguishing it."

Bill Bryson, *A Short History of Nearly Everything*

Acknowledgements

First of all, I would like to thank my wonderful parents, Enrico and Karin, for always being patiently there to support, understand and motivate me. Equally, I'd like to thank my brother Roby and all the family in the Incarbone and Judkins/Mee clans. To all the friends from Torino and now in all corners of the globe, thanks guys!

These four years of PhD have been absolutely great, and I owe this mostly to all the beautiful people I have had the pleasure to meet here in Strasbourg. I would like to acknowledge the Garcia family, Adrien Pasquier, Jerome Zervudacki and my PhD brother Thomas Montavon. I'd also like to thank everybody at IBMP, but especially Yerim, Aude, Fabrice, Jean, Nina, Clement, Todd, Kamal, Khalid, Annette, Alyssa, Mattia, Elodie, Salah, Malek, Natka, Ahmed, Vianney, Ritz, David, Eduardo, Lea, Adrien and Thibaut, Clara, Esther, Christophe, the gardeners, Michelle, the administration staff. I would also like to thank CNRS and Labex for financing my works and providing many occasions to discuss with outstanding scientists. I am indebted to Sigrun Reumann, together with Delphine and Piotr, for teaching me the tricky business of peroxisome isolation.

A very special thanks goes to Patrice Dunoyer, who took me under his wing and coached me for four years, always pushing me to do better, to think, to hypothesize, to analyze, to try out new ideas, to try to be a good and thorough scientist. The fact that he continued to do so during some truly brutal times can only go to his credit.

Huge gratitude and affection goes to Marion Clavel for, well, everything.

I'd like to also express my gratitude to Sébastien Pfeffer, Hervé Vaucheret and Peter Brodersen for evaluating this work.

TABLE OF CONTENTS

Figure Index

INTRODUCTION

The year 1892 was an important one in biology. In an age when people were just starting to accept the fact that diseases were caused by specific and transmissible microscopical living things and not by “miasmas”, the Russian botanist Dmitri Ivanovsky made a truly sensational discovery, that would profoundly change biology and cause more than one headache to whoever has tried since then to provide a univocal and unambiguous definition of life. Ivanovsky observed that the agent causing tobacco mosaic disease was able to pass undisturbed through filters that retained bacteria, indicating that it was smaller than the smallest known living creature. Although at the time he didn’t have the tools to describe the true nature of what he had found, and as often happens in science he then proceeded to follow numerous valid yet ultimately false leads, Ivanovsky had discovered viruses.

Since then, more than a century of ingenuity, patient experimentation and stubborn investigation have yielded priceless evidence on what viruses are and how they go about the business of surviving and adapting to an ever changing world while not possessing the essential machinery to do so. Outside their host they are inorganic matter, not very different from a strand of hair or a microscopic grain of sand. However, when they come into contact with their host in the right conditions, viruses spring to life in ways that are fascinating to observe even through the indirect and partial view afforded by modern molecular biology. They hijack proteins, nucleic acids and membranes, they replicate, they mutate, they migrate, they fight efficient and diversified defensive host reactions, they board specific vectors and change their behavior to increase their chances of successfully reaching their next host. They achieve all this, and much else, mostly by using the host’s machinery for their own purposes, by warping the host’s vital mechanisms to fulfill their own agenda. Viruses are, in a way, the ultimate manipulators.

The main goal of this experimental work is to provide a clear snapshot of one such manipulation and place it in its context.

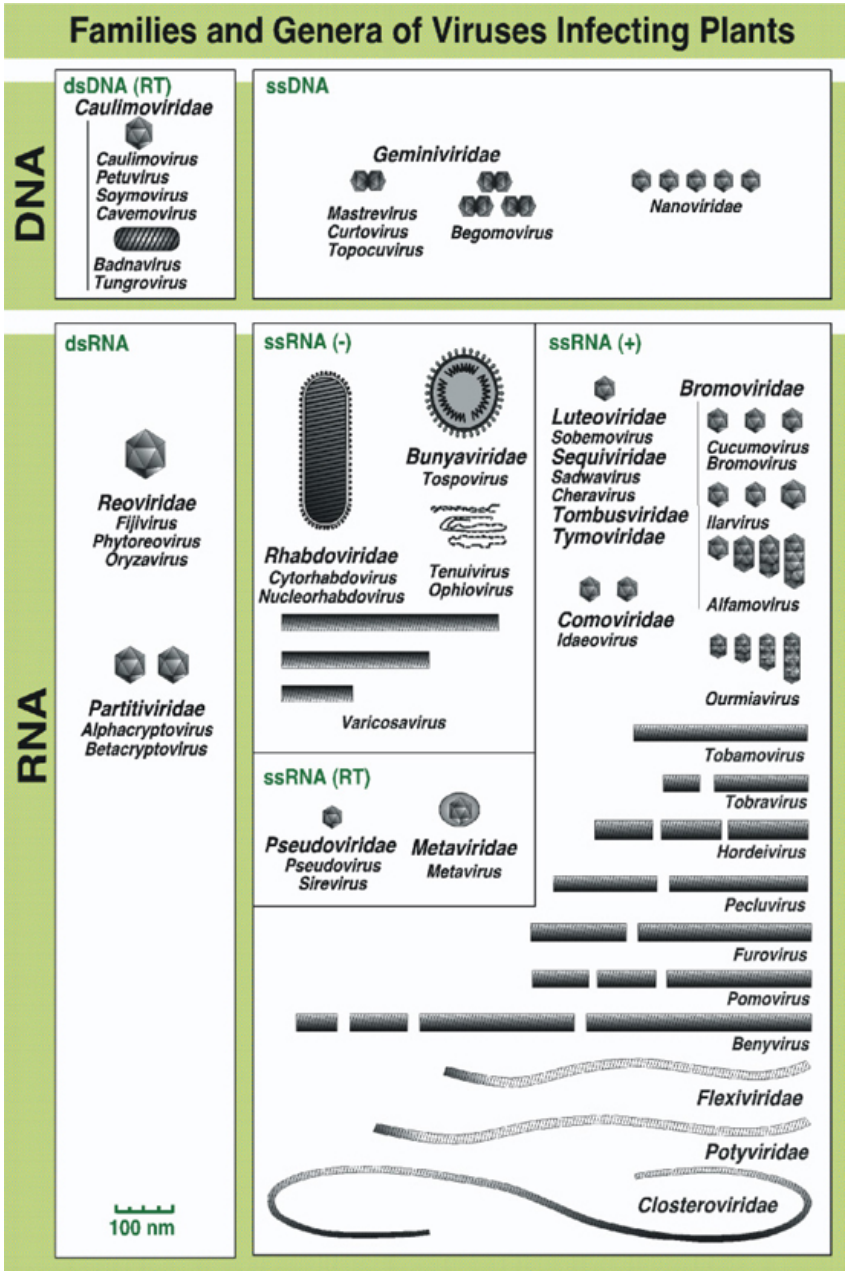

Figure I: Plant virus families and genera.
Plant virus families (suffix *–viridae*) and genera (suffix *–virus*). They are here divided according to the nature of their genome. The shape of the virion is depicted for each genus. Source: http://www.emporia.edu

I - Plant viruses and antiviral defense

A virus is defined as "a set of one or more nucleic acid template molecules, normally encased in a protective coat or coats of protein or lipoprotein, that is able to organize its own replication only within suitable host cells. It can usually be horizontally transmitted between hosts. Within such cells, virus replication is (1) dependent on the host's protein-synthesizing machinery, (2) organized from pools of the required materials rather than by binary fission, (3) located at sites that are not separated from the host cell contents by a lipoprotein bilayer membrane, and (4) continually giving rise to variants through various kinds of change in the viral nucleic acid" (Hull, 2002).

The general absence of proof-reading ability in viral replicases, leading to a high rate of mutation, coupled to the vast number of replication events taking place during a typical infection, have in time generated an almost boundless variety of shapes, strategies and tricks that viruses employ to successfully complete their infectious cycle. Broadly speaking, viruses are classified according to the nature of their genomic nucleic acid (DNA or RNA, single-strand or double-strand, coding or complementary strand) and the shape of their capsid. Other parameters of classification include replication strategy, host range and transmission vectors, among others. They are taxonomically classified into families, genera, species and strains, following a nomenclature that is different from the classical Linnaean binomial one used for all other forms of life. This nomenclature uses English and allows univocal abbreviation of virus names into acronyms to facilitate use (e.g. *Tobacco Mosaic Virus* becomes TMV, *Turnip Mosaic Virus* becomes TuMV, and so on). We shall here focus on plant viruses (**Fig. I**) and their interaction with and suppression of host antiviral mechanisms.

Plant DNA viruses count among their ranks species that are of great agricultural importance given the yield loss caused yearly, such as those belonging to the genus Geminivirus. However, the vast majority of plant viruses have an RNA genome. Of these, most species possess a single-stranded so-called (+)-polarity genome ((+)-ssRNA), meaning that the genomic RNA is the coding strand and can be directly translated into protein. The protein that is the object of this work is encoded by one such virus, *Peanut Clump Virus*. While our knowledge on plant RNA virus life cycles and strategies is the object of many detailed texts

and reviews, for the sake of fluidity it will here suffice to provide a very broad and largely simplistic overview of the typical life cycle of a plant (+)-ssRNA virus. Given the topic, there are probably several exceptions for each of the following statements.

A virus first enters its host as a virion (RNA + capsid) through direct contact with an infected host or through a vector. Upon entry the capsid (made up of coat protein) is removed and the genomic RNA is translated by ribosomes into key factors such as the replicase. The replicase is a viral RNA-dependent RNA-polymerase (RDRP), that uses the genomic RNA as a template to synthesize the (-) complementary strand. This step generates a double-stranded RNA that is probably short-lived, yet of paramount importance for the host (and of great danger for the virus) as it is a potent elicitor of RNA interference, a staple mechanism in plant antiviral defense. The freshly made (-) strand can then be used to synthesize more (+) RNA, that can in turn be translated into protein, copied, or encapsidated in newly generated coat protein to form new virions. Replication of (+)-ssRNA viruses usually takes place in the cytoplasm within membranous invaginations induced by the virus on specific subcellular compartments or organelles (reviewed in Grangeon *et al.*, 2012). Once the cells of entry are colonized, viruses proceed to move to neighboring cells through plasmodesmata (reviewed in Heinlein, 2015) and ultimately to distant tissues in the plant through the phloem (reviewed in Hipper *et al.*, 2013), in the form of virions or dedicated ribonucleoproteic (RNP) complexes, depending on the species, thereby colonizing new cells. As the last step of an infectious cycle the virus must reach a new host, most often by being acquired by a specific vector (ranging from fungi to insects) (reviewed in Blanc *et al.*, 2011). While typically encoding 5 to 10 essential and often multifunctional proteins, viruses largely rely on host proteins to complete their life cycle (reviewed in Hyodo *et al.*, 2014; Wang, 2014).

There are several reported cases of symbioses between viruses and their hosts, and several instances are described in which viruses provide their plant hosts with drought tolerance, cold tolerance and other advantages, though how they achieve this remains unclear (reviewed in Roossinck, 2011). Modern meta-genomic approaches have revealed many persistent viruses that cause no visible disease and may have co-evolved with their hosts for millennia. Despite this, and possibly because scientific enquiry has mostly focused on the

most evident, pathogenic and economically detrimental plant-virus interactions, viruses are generally considered selfish genetic elements that thrive at the expense of their hosts. Plants have thus evolved several layers of defense to hinder the establishment and propagation of viral infections.

The so-called *R*-gene (incompatible, or gene-for-gene) response, which is mostly virus-specific and results from prolonged virus-host coevolution, consists in the recognition of a viral avirulence (Avr) factor by a single dominant resistance (R) gene product (reviewed in de Ronde *et al.*, 2014; Mandadi and Scholthof, 2013; Dodds and Rathjen, 2010). This kind of response can be triggered by viruses, bacteria or fungi. The majority of these R genes belong to the NB-LRR family. Triggering of R genes generally leads to a programmed cell death response that is quite rapid (3 or 4 days post-infection) and contains the spread of the virus by killing the infected tissue. This hypersensitive response (HR) entails dramatic metabolic changes in the synthesis of hormones such as salicylic acid (SA), jasmonic acid (JA), ethylene and nitric oxide, the accumulation of reactive oxygen species, calcium ion influx, callose deposition at plasmodesmata, modification of membrane permeability and expression of pathogenesis-related (PR) proteins (Mandadi and Scholthof, 2013; Pallas and García, 2011). Avr/R protein interactions can also initiate systemic acquired resistance (SAR), whose exact mode of action remains unclear though it has been associated to an accumulation of SA and JA in tissues distant from the site of infection (Mandadi and Scholthof, 2013). SAR doesn't cause cell death, and provides a long-lasting systemic immune response against subsequent infections.

While dominant resistance has received a great deal of attention, there are other less investigated forms of antiviral defense. For example, *A. thaliana* proteins RTM1, RTM2 and RTM3 have been shown to restrict the movement of *Tobacco Etch Virus* (TEV) and other Potyviruses independently of HR/SAR through recognition of the 5' end of the coat protein (Chisholm *et al.*, 2001; Decroocq *et al.*, 2009). JAX1, a lectin protein closely related to RTM1, has been shown to inhibit *Plantago Asiatica Mosaic Virus* (PLAMV) replication (Yamaji *et al.*, 2012). Lectin proteins could therefore represent another barrier against viruses, possibly acting through recognition of viral glycosylated proteins (Chisholm *et al.*, 2000;

Yamaji *et al.*, 2012). Plants can also employ the ubiquitin proteasome pathway to target viral proteins for degradation, as for example happens to the movement proteins of *Tobacco Mosaic Virus* (TMV) and *Turnip Yellow Mosaic virus* (TYMV), thereby decreasing virulence and pathogenicity (Drugeon and Jupin, 2002; Reichel and Beachy, 2000). It has been recently shown that upon recognition of begomovirus NSP protein, *A. thaliana* NIK1 (a LRR receptor-like kinase) triggers global translational suppression (Zorzatto *et al.*, 2015). The authors of this study found that NIK1 activation leads to LIMYB-mediated downregulation of ribosomal protein gene transcription. This in turn results in inhibition of ribosomal protein synthesis, decreased association of viral mRNA with polyribosomes and increased tolerance to the virus. Plant RNA quality control pathways have recently been proven to contribute to antiviral defense. UPF1, a key player in non-sense mediated decay (NMD), restricts *Potato Virus X* (PVX-GFP) by recognizing the internal termination codons and long 3' UTRs present in its subgenomic RNAs (Garcia *et al.*, 2014). UPF1 also restrains the accumulation of *Turnip Crinkle Virus* (TCV), and could constitute a limiting factor to all the RNA viruses that, because of their genomic organization and expression strategy, sport sequences recognized as aberrant by the NMD machinery. Finally, *A. thaliana* RTL1, an RNAse-III enzyme that processes dsRNA, has been shown to be strongly upregulated during viral infection and is likely to play a role in antiviral defense (Shamandi *et al.*, 2015). While the impossibility of obtaining a knock-out mutant of *RTL1* made it difficult for the authors to assess the exact implication of this factor in antiviral defense, they did show that its overexpression causes increased virus accumulation during infections by TVCV, but not TCV, CMV and TYMV. Though in the case of TVCV this result may seem counterintuitive, RTL1 was shown to act upstream of RNA interference, the main antiviral defense in plants. Therefore, RTL1 overexpression likely entails depletion of substrate for RNA interference and subsequent impairement of this pathway.

Since experimentally dissecting the molecular events characterizing each infection often represents a truly daunting challenge, it is very likely many offensive and defensive pathways remain to be uncovered.

With the exception of NMD and the case of RTL1, the defensive mechanisms listed above involve species-specific reactions, effectors or patterns, so it can be speculated that mutation

by a given virus may allow it to evade these defenses. It is a testimony to the brilliance of plant evolution that the main antiviral mechanism targets the universal and unavoidable product of RNA virus replication: double-stranded RNA. This conserved and multi-layered mechanism, that attacks double-stranded RNA engendered by viral genomic RNA replication or secondary structures and generates sequence-specific defense elicitors, is called RNA interference (RNAi), but is also known as RNA silencing or post-transcriptional gene silencing (PTGS).

II - RNA interference

Most eukaryotes possess RNA interference pathways that are remarkably similar across kingdoms. Although prokaryotes do not encode proteins analogous to eukaryotic silencing factors, they employ mechanisms that are functionally analogous. This structural and functional conservation coupled to frequent functional redundancy strongly suggests that tight control of RNA has been a priority since very early in the history of life. If we briefly allow ourselves to speculate on events in very ancient times, it is easy to infer how RNAi-like mechanisms may have represented a milestone in the evolution of complex life. According to the widely endorsed "RNA world" theory, at the dawn of life on Earth RNA used to be a dominant organic molecule, able to self-replicate and acting not only as vehicle of information but also as reaction catalyzer (ribozyme). These independent or semi-independent RNA molecules, that were presumably more or less structured, and possibly formed distinct populations of nearly identical individuals, may have been the main form of life for a very long time. In all likelihood these RNAs may have represented a significant obstruction for the rise of any new, more complex form of life possibly implementing proteins, if not DNA, in its molecular functioning. The development of machinery able to target replicating or structured RNA in a sequence-specific manner would have conferred a tremendous evolutionary advantage to its bearer. In this scenario, the emergence of proto-RNAi (and possibly other forms of RNA control) may have marked the beginning of the end for the "RNA world", causing the gradual yet inexorable extinction of most forms of independent RNA and issuing the beginning of a new world order in which RNA came to be merely one player in the intricate workings of a cell. This formidable evolutionary pressure

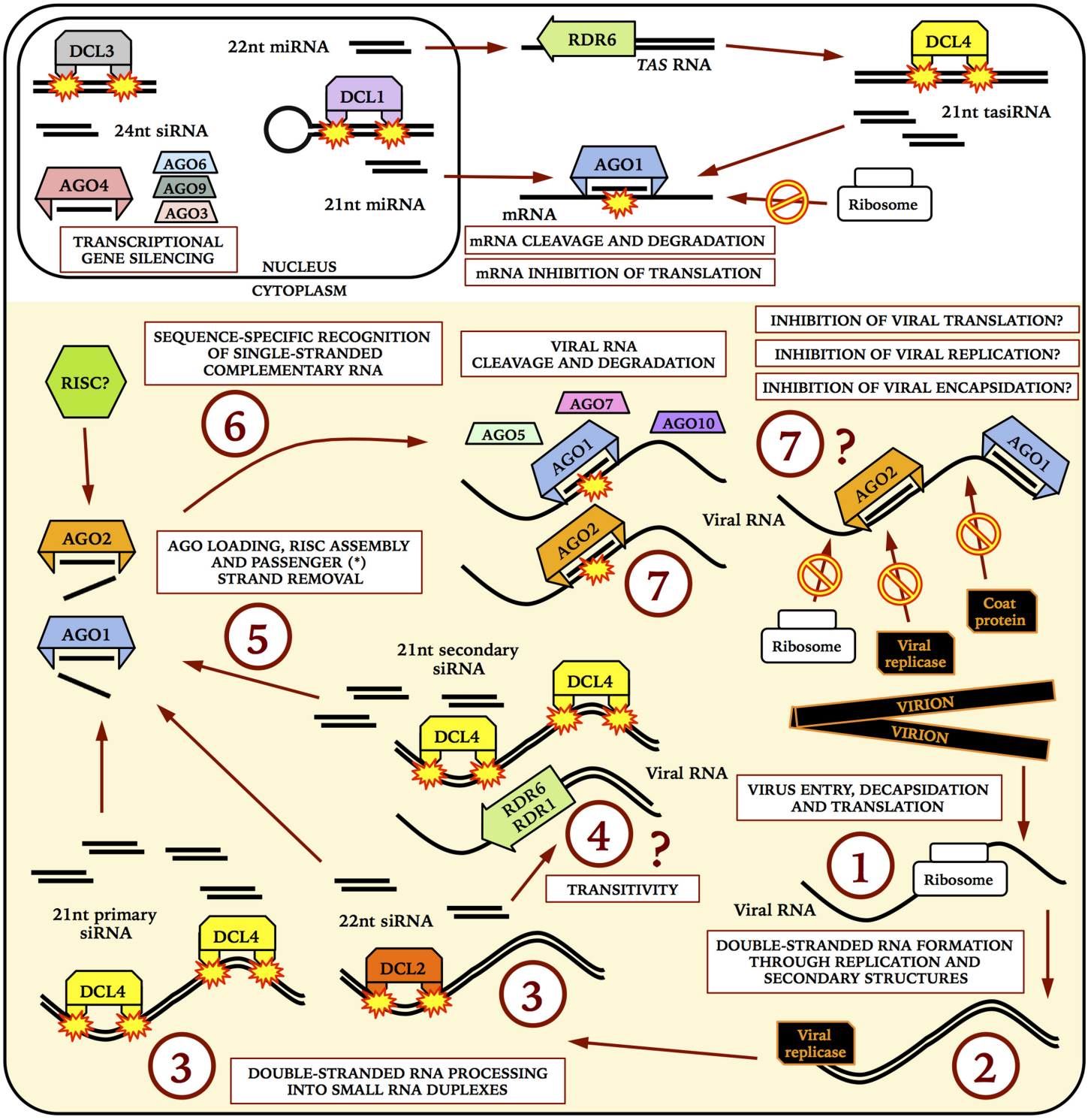

Figure II: Cell-autonomous antiviral RNAi in plants.
Schematic representation of cell-autonomous antiviral RNAi in plants. Upon entry into a cell, a ssRNA virus replicates, generating double-stranded RNA (1-2). This is processed by DCL enzymes into 21-22nt siRNAs (3-4), which are then incorporated into AGO proteins (5-6) to mediate the sequence-specific antiviral response (7). At the top is a schematic representation of the main endogenous RNAi pathways, such as genome maintenance and transcriptional regulation through 24nt siRNAs, or the regulation of mRNA accumulation and translation through 21-22nt miRNAs and ta-siRNAs.

would have only allowed the survival of those independent RNAs that managed to protect themselves with a shell of some kind and evade or counteract RNAi, learning at the same time how to take advantage of the increasingly complex machinery employed by the forms of life they inhabited. Testimony to this possible turn of events is the fact that viroids, the only known form of independent RNA that is non-coding and not encapsidated (excluding some active non-coding transposable elements), are present only in plants as a handful of species, perhaps an elusive reminder of what life was like in the very distant past.

RNAi was first observed by investigators working on plants, but it was Andrew Fire, Craig Mello and colleagues working on *C. elegans* that provided evidence that it is a reaction to the presence of double-stranded RNA and entails potent gene silencing (Fire *et al.*, 1998). In plants RNAi plays a key role in many aspects of life, from gene regulation to genome maintenance to the control of invading or aberrant RNA. In a nutshell, the long dsRNA trigger is processed by Dicer-like enzymes (DCLs) through endonucleolytic activity into 21-24nt small RNA (sRNA), one strand of which is loaded into an Argonaute (AGO) effector that uses it as a template to recognize complementary single-stranded RNAs and cleave them or inhibit their translation. In specific conditions, dsRNA can also be synthesized from ssRNA templates by RNA-dependent RNA-polymerases (RDRs), leading to further generation of sRNAs by DCLs and amplification of the silencing reaction in what is generally known as transitivity. This overview will outline the basic workings of RNAi in plants, focusing on its role in defense against RNA viruses (**Fig. II**).

IIa - Cell-autonomous RNAi: the dicing step

In the model plant specie *A. thaliana*, the four Dicer-like (DCL) enzymes and their products have been well characterized (reviewed in Bologna and Voinnet, 2014, Fukudome and Fukuhara, 2016), although it remains mostly unclear how they recognize/discriminate their substrates and if they are aided/chaperoned or inhibited by other proteins. DCL RNAse III enzymes possess several domains: a DExD-box, a helicase-C, a domain of unknown function, a PIWI/ARGONAUTE/ZWILLE (PAZ), two RNAse III domains and two dsRBDs (except DCL2 that has one)(Margis *et al.*, 2006). They process long dsRNA into sRNA duplexes with distinctive 2-nt overhangs and 5' monophosphates in an ATP-dependent

fashion (Tang *et al.*, 2003). The length of the α-helix separating the PAZ from the RNAse domains determines the length of the sRNA produced (MacRae *et al.*, 2007). Once generated, all sRNAs are 2'OH-methylated on their 3' end by HEN1 and thereby protected from degradation (Yu *et al.*, 2005). DCL proteins can generate two main types of sRNA: microRNA (miRNAs, mostly DCL1-dependent) and small interfering RNA (siRNAs, DCL2/DCL3/DCL4-dependent) (Henderson *et al.*, 2006; Xie *et al.*, 2004).

DCL1 processes genomic non-coding imperfectly paired foldback precursors into 21-22nt miRNAs (Park *et al.*, 2002; Reinhart *et al.*, 2002), and is mostly localized in the nucleus (Song *et al.*, 2007). DCL1-dependent miRNAs regulate many genes involved in housekeeping and development, which explains why knocking out DCL1 results in embryonic lethality. While the majority of miRNAs are 21nt long and regulate endogenous protein production mostly through AGO1 by cleaving (or "slicing") the corresponding mRNAs (German *et al.*, 2008) or inhibiting its translation (Brodersen *et al.*, 2008), a few miRNAs (22nt-long miR173 and miR828, 21nt-long miR390) are capable of triggering RDR6-dependent synthesis of dsRNA from non-coding *TAS* transcripts, which are then processed by DCL4 into precisely phased *trans*-acting siRNAs (ta-siRNAs) that proceed to mediate further gene silencing (Allen *et al.*, 2005; Vazquez *et al.*, 2004; Yoshikawa *et al.*, 2005).

DCL3 processes nearly perfectly complementary POLIV/POLV/RDR2-dependent dsRNA originating from transposons and repeats into 24nt siRNAs that mediate RNA-directed DNA methylation (RdDM) through AGO4 (Law *et al.*, 2010; Pontes *et al.*, 2006), that in turn leads to transcriptional gene silencing (TGS). This process is mostly nuclear and nucleolar. 24nt siRNAs generated by DCL3 are also capable through the same pathway of mediating antiviral defense against DNA viruses such as Geminiviruses (Raja *et al.*, 2010). DCL3 is able to process long dsRNA derived from exogenous hairpin constructs, but the 24nt products are not able to mediate effective PTGS (Dunoyer *et al.*, 2007). While DCL1 and DCL3 are capable of generating sRNAs from RNA viruses, to our knowledge their contribution to the defense against these viruses is negligible (Deleris *et al.*, 2006; Xie *et al.*, 2004).

While playing important roles in endogenous RNAi pathways and being able to take over in the establishment of TGS upon knock-out of DCL3 (Henderson *et al.*, 2006), DCL4 and DCL2 are the main dicers involved in defense against RNA viruses. They have been shown to act redundantly both in antiviral and endogenous RNAi, DCL2 taking over upon knockout of DCL4 (Deleris *et al.*, 2006). For this reason DCL2 is mostly considered to be a surrogate of DCL4. However, recently published results (Parent *et al.*, 2015) and results presented in this work suggest that DCL2, while undoubtedly serving as an alternate to DCL4, may have more complex roles in antiviral RNAi that have yet to be revealed.

DCL4 processes long perfectly or near-perfectly complementary dsRNA into 21nt siRNAs. It's responsible for the generation of the aforementioned RDR6-dependent ta-siRNAs, a few "young" miRNAs (e.g. miR822)(Rajagopalan *et al.*, 2006), the processing of endogenous inverted-repeats (IRs) (Zhang *et al.*, 2007), of transgenically delivered inverted-repeats (Dunoyer *et al.*, 2005) and, of greater interest here, the processing of viral RNA. DCL4 has been shown by many different independent studies to be the main DCL in RNAi against RNA viruses and the primary producer of antiviral siRNAs (Bouché *et al.*, 2006; Deleris *et al.*, 2006a; Garcia-Ruiz *et al.*, 2010; X.-B. Wang *et al.*, 2011). It has been shown *in vitro* to preferentially cleave long dsRNA, and to cleave blunt, 1nt- or 2nt-overhangs with similar efficiency (Nagano *et al.*, 2013). DCL4 has one known cofactor: DRB4. DRB4 is required for DCL4 activity *in vitro* (Fukudome *et al.*, 2011), while *in vivo* it strongly enhances, but is not mandatory for, DCL4-dependent processing of exogenous inverted-repeats and *TAS* dsRNA (Dunoyer *et al.*, 2007). While it assists DCL4 in defense against RNA viruses, it also plays antiviral roles through other pathways (Jakubiec *et al.*, 2012; Qu *et al.*, 2008; Zhu *et al.*, 2013).

DCL2 processes long perfectly complementary dsRNA into 22nt siRNAs. Compared to the other DCLs it has been far less extensively studied. It can act redundantly to DCL4 and downstream of RDR6 in the ta-siRNA pathways and in transgene-driven transitivity (Dunoyer *et al.*, 2007; Moissiard *et al.*, 2007). In phloem companion cells the processing of exogenous inverted repeats in the absence of DCL4 is carried out by DCL3, while DCL2 takes over only if both DCL3 and DCL4 are absent (Dunoyer *et al.*, 2007). When acting as surrogate to DCL4 in the processing of ta-siRNAs and exogenous IRs, DCL2 generates

significantly less siRNAs than DCL4 would, although this may simply be due to lower DCL2 accumulation. On the other hand, some endogenous IRs (e.g. IR71) are predominantly processed by DCL2 for unknown reasons. In the absence of DCL3 and DCL4, DCL2 acts in an antagonistic fashion toward DCL1 in the production of sRNAs, and has deleterious effects on development in the absence of DCL1 and DCL4 (Bouché *et al.*, 2006). As mentioned above, in the context of an RNA virus infection DCL2 has until now been reported to be activated mostly in *dcl4* knock-out conditions (Bouché *et al.*, 2006; Deleris *et al.*, 2006; Garcia-Ruiz *et al.*, 2010) or, as in the case of TCV infection, where accumulation of DCL4 and DCL3 are strongly reduced by the virus (Azevedo *et al.*, 2010; Qu *et al.*, 2008). In these cases, and in contrast with ta-siRNA and exogenous IR processing, DCL2 generates siRNAs in amounts comparable to DCL4. However, given that viral titer is increased, these 22nt siRNAs likely do not mediate RNAi as efficiently as 21nt siRNAs. No DCL2 cofactors are known.

IIb - Cell-autonomous RNAi: the amplification step

During a viral infection DCL4 and DCL2 can process not only double-stranded products of the viral RDRP but also products of host-encoded RDR proteins to produce more siRNAs, dubbed secondary siRNAs. This process, known as transitivity, is readily employed by plants on transgenes (Moissiard *et al.*, 2007; Voinnet, 2005) but tightly controlled when it comes to endogenous genes. Only three out of six *A. thaliana* RDR proteins have an experimentally proven biological role: RDR1, RDR2 and RDR6. RDR1 and RDR6 have been implicated in antiviral RNAi directed against RNA viruses (Wang *et al.*, 2010), and RDR6 has been shown to often play a pivotal role in it (Qu *et al.*, 2008; Wang *et al.*, 2011). Although the role of RDR6 in the amplification and spread of transgene-directed RNAi in reporter systems is well characterized (Moissiard *et al.*, 2007; Voinnet, 2005), the precise trigger, substrate and conditions of antiviral RDR1/RDR6 intervention are not clear. It is not clear, for example, whether RDR generation of viral dsRNA must be primed by a primary siRNA (as miRNAs prime endogenous ta-siRNA generation) or not. Although 21nt sRNAs can trigger RDR activity and transitivity (Moissiard *et al.*, 2007), recent studies suggest that both in endogenous and transgene-triggered RNAi the initiator of RDR amplification is mostly 22nt sRNAs (Chen *et al.*, 2010; Manavella *et al.*, 2012; Parent *et al.*,

2015). Consequently, DCL2-dependent 22nt siRNAs could initiate a putative RDR-dependent amplification step of antiviral reactions. On the other hand, one study has reported that siRNAs produced by DCL2 downstream of RDR6 were not proficient in mediating efficient antiviral RNAi (Wang *et al.*, 2011).

The evidence available today suggests that in *A. thaliana* there are some general trends in the generation of antiviral primary and secondary siRNAs, but also that there are likely many differences in the mode and timing of attack by DCLs and RDRs between one virus and the other. These differences could be due to intrinsic features of the silencing factors themselves, to the interaction of the virus with the cell machinery, or a combination of the two.

IIc - Cell-autonomous RNAi: the effector step

Although processing by DCL4 and DCL2 certainly reduces viral accumulation to a certain extent and possibly recruits other defensive factors onto the viral replication complexes, this first step of RNAi taken alone is not likely to have meaningful impact on viral accumulation. The fact that *A. thaliana* encodes ten often redundantly functioning AGO proteins that act downstream of DCLs makes it almost impossible to genetically isolate the contribution of DCL enzymes alone to the antiviral reaction. AGO proteins carry out the so-called effector step of RNAi, the sequence-specific recognition and attack of single-stranded RNAs that are complementary to the sRNAs generated by DCL enzymes. Our knowledge on plant AGO proteins and their links to other eukaryotic Argonautes is extensively reviewed in Poulsen *et al.*, 2013.

The key ability of AGO proteins is to bind sRNAs, since it allows them to recognize complementary target RNA in a sequence-specific manner. Of the sRNA duplex generated by DCLs, one strand is loaded into AGO (the guide strand), while the other is degraded (the passenger strand, or * strand). In one reported exception in plants, while the guide strand is loaded into AGO1, the passenger strand is loaded into AGO2 (Zhang *et al.*, 2011). In *Drosophila*, this last mechanism seems to be widespread (Okamura *et al.*, 2009). Little is known in plants about the precise cofactors (if any) that are involved in AGO loading and strand discrimination, or about how sRNAs pass from DCLs to AGOs.

Many AGOs possess RNAse H-like endonucleolytic activity that allows them to "slice", thereby destroying, RNA complementary to the sRNA they are carrying (Llave *et al.*, 2002). This RNAseH-like activity also allows AGO1 to remove the passenger strand of siRNA duplexes (Iki *et al.*, 2010) and to prime RDR activity and secondary siRNA generation (Carbonell *et al.*, 2012). All AGO proteins contain four common domains: an N-terminal domain, a PIWI/ARGONAUTE/ZWILLE (PAZ) domain, a middle MID domain and a PIWI domain. The sRNA is bound to the MID (5') and PAZ (3') domains (Ma *et al.*, 2004; Song *et al.*, 2003), while the PIWI domain carries the RNAse catalytic site (Song *et al.*, 2004). While in animals many proteins have been shown to interact with Ago to form the RNA-induced silencing complex (RISC), such a complex still evades detection in plants despite the considerable efforts made to identify it. In the wake of studies in animals and yeasts, though, some factors have been shown to interact with AGO proteins through the conserved GW motif (Azevedo *et al.*, 2010; El-Shami *et al.*, 2007; Till *et al.*, 2007). Other proteins that have been found to interact with AGO1 and mediate its functioning are TRN1, HSP90 and CYP40 (Cui *et al.*, 2016; Iki *et al.*, 2012; Iki *et al.*, 2010).

Different AGO proteins are loaded with different categories of sRNA, depending on the pathway involved and on the 5' base of the sRNA. AGO4, AGO3, AGO6 and AGO9 are loaded with DCL3-dependent 24nt siRNAs to mediate TGS (Havecker *et al.*, 2010; Zhang *et al.*, 2016). AGO7 is involved in *TAS3* processing (Montgomery *et al.*, 2008; Adenot *et al.*, 2006), while AGO10 is involved in specific meristematic miRNA-driven gene regulation and in AGO1 homeostasis (Mallory *et al.*, 2009; Zhu *et al.*, 2011). AGO7 and AGO10 have also been shown to play minor roles in antiviral RNAi (Garcia-Ruiz *et al.*, 2015; Qu *et al.*, 2008). While AGO5 has been associated to antiviral defense against *Potato Virus X* (PVX), *Turnip Mosaic Virus* (TuMV) and *Cucumber Mosaic Virus* (CMV) (Brosseau and Moffett, 2015; Garcia-Ruiz *et al.*, 2015; Takeda *et al.*, 2008) the main AGOs responsible for antiviral defense are AGO1 and AGO2 (Carbonell and Carrington, 2015; Pumplin and Voinnet, 2013). In a similar fashion to DCL4 and DCL2, AGO1 and AGO2 can act hierarchically and redundantly in antiviral RNAi, with AGO2 taking over defense in infections that suppress AGO1 function (Harvey *et al.*, 2011). However, several studies suggest that they can operate

independently and non-hierarchically, each one acting against a particular virus or in a particular tissue (Garcia-Ruiz *et al.*, 2015; Ma *et al.*, 2015; Wang *et al.*, 2011).

AGO1 is the most important and multifunctional AGO protein, so central to cellular gene regulation that its loss is lethal. AGO1 is by far the main effector in miRNA-mediated gene regulation, operating through both target slicing and translational inhibition. AGO1 also triggers the generation of phased ta-siRNAs through RDR6/DCL4 after being loaded with specific miRNAs (Vazquez *et al.*, 2004; Allen *et al.*, 2005; Yoshikawa *et al.*, 2005; Montgomery *et al.*, 2008). Through the use of an AGO-interacting suppressor of silencing, AGO1 has been shown to be present in two distinct pools, one loaded with miRNAs, the other with siRNAs (Schott *et al.*, 2012). AGO1 is a potent antiviral effector, and while it has been experimentally shown to be involved in defense against *Brome Mosaic Virus* (BMV), CMV, *Turnip Crinkle Virus* (TCV) and TuMV (Carbonell and Carrington, 2015; Garcia-Ruiz *et al.*, 2015; Morel *et al.*, 2002; Qu *et al.*, 2008), it can be assumed that it plays a role in most RNA virus infections. AGO1 was shown to be responsible for virus-induced gene silencing (VIGS) of endogenous genes in infections where AGO2 was attacking the virus (Ma *et al.*, 2015). One thing that is not clear is whether AGO1 slices viral RNAs or inhibits their translation, or both. AGO1 is predominantly loaded with sRNAs possessing a 5' terminal uridine (Mi *et al.*, 2008).

While mediating silencing by a few select miRNAs (Maunoury and Vaucheret, 2011; Zhang *et al.*, 2011) and being recruited to repair DNA double-strand break (Wei *et al.*, 2012), the preponderant function of AGO2 is thought to be antiviral. Evidence obtained in several labs confirms AGO2 involvement in infections by CMV, PVX, *Tobacco Rattle Virus* (TRV), TCV and TuMV on *A. thaliana* (Carbonell *et al.*, 2012; Garcia-Ruiz *et al.*, 2015; Harvey *et al.*, 2011; Jaubert *et al.*, 2011; Ma *et al.*, 2015; Wang *et al.*, 2011), and by *Tomato Bushy Stunt Virus* (TBSV) on *N. benthamiana* (Scholthof *et al.*, 2011). The slicing activity of AGO2 is crucial for defense against TuMV (Carbonell *et al.*, 2012), although it is not known if in infection by other viruses it can also act as a translational inhibitor. As for AGO1, given the number of infections in which AGO2 plays an active role, it can be reasonably assumed that it mediates RNAi against all or most RNA viruses. In addition to its direct role in the cleavage of viral

RNA, AGO2 mediates a boost in antiviral defense by mediating widespread silencing of endogenous genes, at least in the case of CMV and TuMV infection (Cao *et al.*, 2014), by means of the host-encoded, DCL4/RDR1-dependent virus-activated siRNAs (vasiRNAs). AGO2 is preferentially loaded with 5' adenosine sRNAs (Mi *et al.*, 2008).

From this summary of the cell-autonomous aspects of antiviral RNAi it is clear that most of the main players are (more or less) known. However, we are sorely missing a more detailed picture, and not because of lack of will but because of the technical challenge involved in observing the molecular details of a DCL/AGO assault on a viral RNA. The tools used in the last 20 years to unravel the functioning of RNAi are elegant inventions that allowed groundbreaking discoveries, but are not sufficient to answer some more specific questions. Investigators need to come up with new and subtler experimental tools and reporter systems to shed light on this next layer of complexity. Concerning antiviral RNAi many unanswered (and difficult to answer) questions come to mind. For example, (i) whether AGOs act as inhibitors of translation (as in the case of miRNA-targeted mRNA), and possibly of replication and encapsidation, (ii) whether DCLs and AGOs attack viruses together, with the aid of specific cofactors, and if there is any cross-talk between them to better coordinate defenses for the specific virus that is invading the plant, or (iii) different stages of the virus life cycle could correspond to different RNAi reactions. Additionally, it would be interesting to further characterize if and how RNAi is linked to other RNA quality control pathways, and what role RNAi plays in viral host range determination. Trying to answer these and many other questions will constitute a great challenge in the future.

IId - Cell-to-cell and systemic RNAi

Even before the precise factors involved in RNAi had been identified it was known that an RNA silencing trigger could move through the phloem from a silenced rootstock to a non-silenced scion, causing the latter to undergo PTGS (Palauqui *et al.*, 1997; Voinnet *et al.*, 1998). Moreover, it was clear that this silencing signal was capable of moving cell-to-cell, presumably through plasmodesmata (Himber *et al.*, 2003; Voinnet and Baulcombe, 1997). Taken together these works suggested that the sequence-specific silencing signal, once induced, moves out of the incipient cells through plasmodesmata, reaches the phloem and

enters it, and upon reaching distal parts of the plant it exits the phloem and triggers silencing in the recipient cells. As is logical, this signal follows a sink-source pattern reminiscent of that followed by moving viruses (Voinnet, 2005). The mobile silencing signal has been shown to be siRNAs in *N. benthamiana* (Hamilton *et al.*, 2002). Accordingly, sRNAs of all kinds have been found in phloem exudates of *B. napus* (Buhtz *et al.*, 2008). Rigorous genetic experiments in *A. thaliana* have shown that the transgene-driven mobile signal targeting an endogenous gene is DCL4-dependent 21nt siRNAs. These siRNAs move cell-to-cell not in complex with AGO1, but require AGO1 in the recipient cells to efficiently trigger silencing. Moreover, leaf bombardment with artificial siRNAs suggested that these move as duplexes (Dunoyer *et al.*, 2010). Also 24nt siRNAs are able to move cell-to-cell, but are not able to trigger PTGS (Dunoyer *et al.*, 2007, 2005). However, another study proved that 24nt siRNAs can move systemically and trigger TGS in distant tissues (Molnár *et al.*, 2010). Transgenic hairpin-driven DCL2-dependent 22nt siRNAs are able to move cell-to-cell and trigger PTGS (Dunoyer *et al.*, 2007), although it remains unclear whether they can do the same systemically or not. Since 21nt and 24nt siRNAs are able to move systemically it is reasonable to assume that 22nt siRNAs should be capable of systemic movement, though it isn't known to what extent they can mediate PTGS in systemic tissues. It has been shown that upon exiting the phloem, primary siRNAs can move up to 10-15 cells, after which they stop being able to mediate PTGS, either because movement entails a dilution effect or because of some intrinsic change in the siRNAs. However, in the presence of RDR6 and an siRNA-homologous template, the silencing signal can be amplified and move further (Himber *et al.*, 2003). What factors, if any, are needed for cell-to-cell and systemic movement of siRNA duplexes remains an open question.

Given the extensive data gathered through transgenic reporter systems on the movement of siRNAs and its consequences, it is logical to assume that during viral infection the antiviral siRNAs produced by DCLs at the site of infection would, in addition to mediating intracellular AGO and RDR activities, move cell-to-cell and systemically ahead of the virus. This way, the yet-uninfected tissues could employ the inbound virus-derived siRNAs to mount a preemptive sequence-specific defense to stop the virus upon arrival. It has been shown that CymRSV, a (+)ssRNA virus, lacking ability to neutralize 21nt siRNAs can leave the infected tissues to move systemically but can't exit the phloem once it reaches the

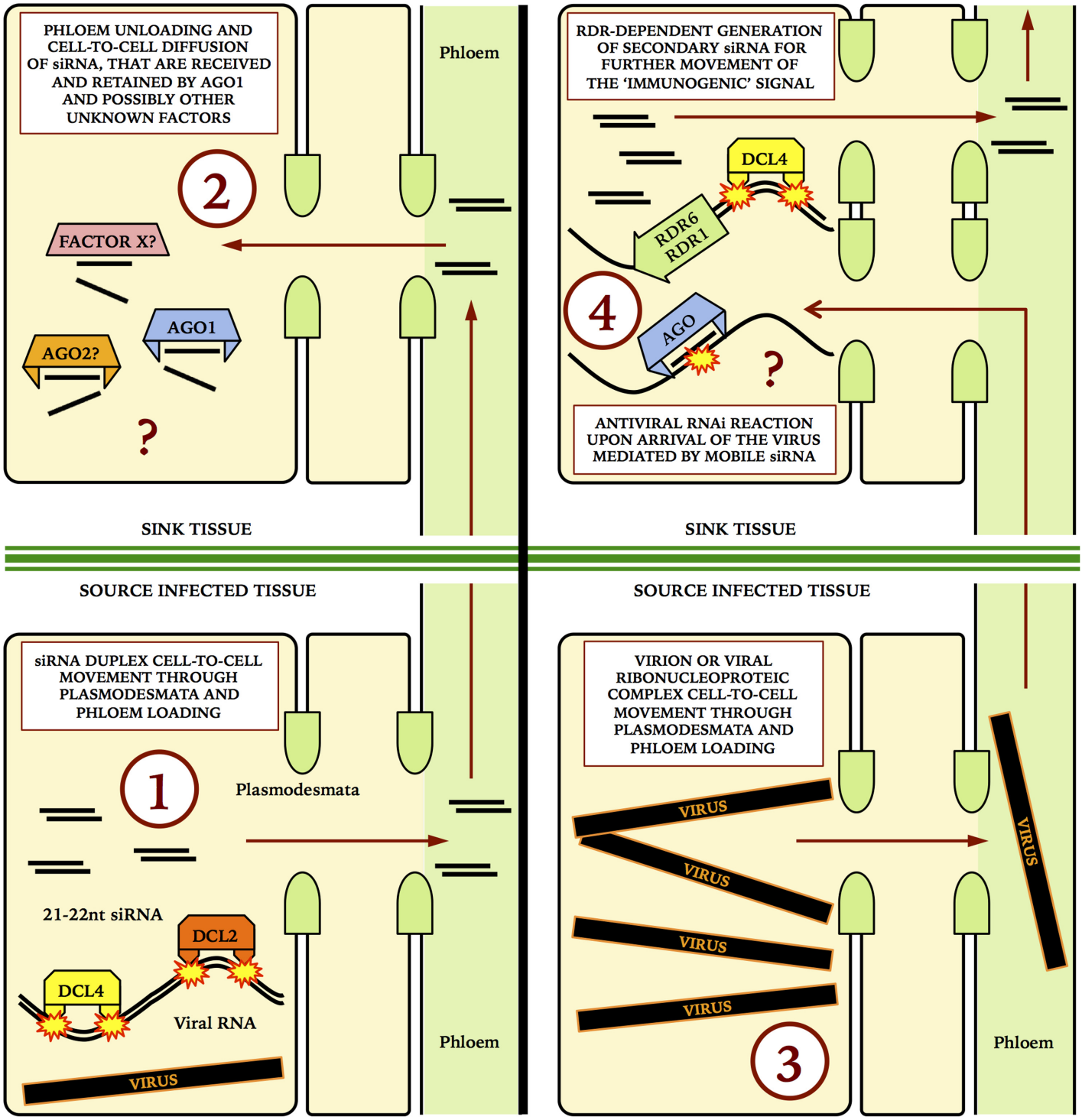

Figure III: Systemic antiviral RNAi in plants.
Schematic representation of non-cell autonomous, systemic antiviral RNAi. The primary RNAi response in infected tissues generates mobile siRNAs (1) which move cell-to-cell and systemically, priming a preemptive RNAi response in distant naïve tissues (2). Subsequently, when the virus exits the primarily infected tissues (3) and tries to colonise new ones, it faces a powerful and specific RNAi reaction (4).

systemic tissues (Havelda *et al.*, 2003), presumably because of the ability of 21nt siRNAs to prime effective defenses before or upon arrival of the virus. However, this could also be explained as an unprimed reaction to the virus, which is instantly stopped upon arrival because it lacks a VSR. Unfortunately this is the only reported example of an antiviral strategy that is presumably widely employed by plants, and leaves us not only wondering if and how much it is used during a genuine virus infection, but also which are the mechanisms and factors involved in the perception of this virus-specific "immunogenic" signal and its implementation in the preemptive defensive reaction (**Fig. III**).

While RDR6 is strongly involved in the perception of the systemically mobile silencing signal in transgenic systems (Himber *et al.*, 2003; Voinnet, 2005), presumably through its ability to amplify this signal in the recipient tissues, this cannot logically happen in viral infections. In fact, if the silencing signal moves ahead of the virus, the perceiving tissues have no template for RDR6-dependent generation of more siRNAs. However, upon arrival of the virus, RDR6 could use viral RNA to generate dsRNA for DCLs to make more antiviral siRNAs. These secondary siRNAs could mediate cell-autonomous silencing, "alert" the neighboring cells or, through further phloem loading, reach yet more systemic tissues. The factor/factors perceiving mobile antiviral siRNAs are not known, though it could be speculated that AGO1 is involved (Dunoyer *et al.*, 2010).

The difficulty in studying the antiviral aspect of mobile RNAi is mostly determined by the fact that in most viral infections it is not possible to experimentally untangle the virus' (i) ability to move, (ii) ability to block cell-autonomous RNA silencing and (iii) ability to block systemic mobile RNA silencing. In this work, thanks to a naturally occurring property of the viral protein P15, we managed to uncouple systemic from cell-autonomous RNAi in the context of a genuine viral infection. We hence provide evidence that mobile virus-derived 21nt siRNAs can strongly hinder viral systemic movement, at times completely abolishing it.

By now it is clear that a virus entering a cell is confronted with an adaptable, multi-layered, sequence-specific and aggressive defensive system, and that it cannot even hope to escape these defenses by moving to other cells and tissues, because it will be followed (or preceded!). In their struggle for survival viruses have come up with a myriad of tricks and

stratagems to neutralize RNAi, and scientists are barely starting to scratch the surface of this treasure trove.

III - Viral suppression of RNA silencing

Before going into the molecular details of viral suppression of silencing through especially adapted proteins, it is worth looking at the life cycle of a typical virus to identify some of the less specific and elaborate strategies through which it can evade RNAi.

The first and most obvious is the capsid. Whatever the number of strands and secondary structures of an RNA, a proteic shell will protect it from DCLs, AGOs and other nucleolytic enzymes. The second is the replication within membrane invaginations, forming partially enclosed viral factories that can act as protective alcoves, totally or partially inaccessible to the host's defensive machinery. A third strategy could be, so to speak, to "fly under the radar". Entailing low rates of replication to avoid full-blown RNAi reactions, this strategy could be employed by those viruses mentioned at the beginning of this chapter, that are present in low titers in their hosts but possibly over many generations. To state it differently, avoiding pathogenesis and an explosive rate of replication may be a valid means to evade RNA silencing. A fourth strategy could be to avoid triggering RNAi whenever possible by avoiding secondary RNA structures. From this point of view every secondary structure still present in a viral RNA genome after millennia of evolution (and many are described) could be presumed to be strictly necessary, or at least highly advantageous, to the viral life cycle. One case is reported where a non-coding secondary structure may act as a decoy for DCLs, diverting them away from the vital coding regions of the genome (Blevins *et al.*, 2011). Such "DCL-sponges" could be a widespread strategy. Additionally, although no such example has been specifically described, it would be of great advantage to the virus to be able to quickly separate the (+) and (-) RNA strands after replication to avoid triggering RNAi. The helicase domain present in many viral replicases could be responsible for this. A fifth possible strategy, despite being speculative and not confirmed by experimental data, is worth considering here. A fair number of virus species are phloem-limited. These viruses can be found in many different families and genera. It is certainly possible that these viruses actively avoid exiting the phloem, or are for some reason unable to move and replicate

outside this tissue. Another explanation could be that they are confined to the phloem because they lack the ability to sufficiently suppress plant defenses to exit this tissue. This hypothesis entails that the phloem would be somehow lacking in antiviral defenses, possibly antiviral RNAi. A few pieces of experimental evidence, while not directly addressing this question, may point toward a phloem-specific RNAi complement. Results obtained by Parent *et al.*, 2015 suggest that DCL2 is almost absent in companion cells. Some results presented in this work in Chapter 1 can be interpreted the same way. Parent and colleagues in the same study also show that transgenic phloem-generated 22nt siRNAs can induce RDR6/DCL4-dependent transitivity against an endogenous gene. Given the fact that the phloem is connected to the whole plant, mobile transitivity-inducing 22nt siRNAs could potentially have seriously detrimental plant-wide effects, so a strict control of DCL2 accumulation in this tissue wouldn't be surprising. Furthermore, the aforementioned study by Havelda and colleagues clearly shows that a virus lacking the ability to neutralize 21nt siRNAs can survive in the cells surrounding the sieve elements but cannot move further. One interpretation of these pieces of evidence combined is that in the phloem very little or no secondary RNAs are made because of the very low levels of DCL2 and transitivity-inducing 22nt siRNAs, so during a viral infection only primary DCL4-dependent 21nt siRNAs are available to mediate RNAi, leading to a reduced response and consequent survival of viruses with weak RNAi-suppressing ability. An additional evolutionary advantage of this state of affairs could be postulated: by keeping an RNAi-poor environment and therefore easing the selective pressure on viruses whose RNAi-suppression capacities are scarce, plants would greatly reduce the likelihood of these viruses developing strong suppressors of silencing.

While being hypothetical, these possibilities are worth experimental investigation. Nonetheless, if the phloem is indeed a low-RNAi haven, phloem restriction could be a way for viruses to avoid a full RNAi response, although this would be more an unwilling consequence than an active strategy. Confinement to the phloem could have the further advantage of facilitating transmission to new hosts by phloem-feeding vectors.

In addition to these more general strategies, viruses have evolved proteins that actively target specific steps of RNAi. These viral suppressors of RNA silencing (VSRs) have been

extensively studied, and the most significant results of these investigations are described in the following review.

Review

Cell PRESS

Feature Review

RNA silencing and its suppression: novel insights from *in planta* analyses

Marco Incarbone and Patrice Dunoyer

IBMP-CNRS, 12 rue du General Zimmer, 67084 Strasbourg Cedex, France

Plants employ multiple layers of innate immunity to fight pathogens. For both RNA and DNA viruses, RNA silencing plays a critical role in plant resistance. To escape this antiviral silencing-based immune response, viruses have evolved various counterdefense strategies, the most widespread being production of viral suppressors of RNA silencing (VSRs) that target various stages of the silencing mechanisms. Recent findings from *in planta* analyses have provided new insights into the mode of action of VSRs and revealed that plants react to the perturbation of the silencing pathways brought by viral infection by deploying a battery of counter-counter-defense measures. As well as discussing which experimental approaches have been most effective in delivering clear and unambiguous results, this review provides a detailed account of the surprising variety of offensive and defensive strategies set forth by both viruses and hosts in their struggle for survival.

RNA silencing pathways

RNA silencing is a paneukaryotic gene regulation mechanism with fundamental implications in many biological processes. It is triggered by double-stranded RNA (dsRNA) and causes a sequence-specific shut down of the expression of genes containing sequences identical or highly similar to the initiating dsRNA. In plants, RNA silencing acts at both the RNA and the DNA levels. Mechanisms of silencing at the RNA level include mRNA cleavage or translational repression, whereas at the DNA level they involve DNA and/or histone methylation and subsequent transcriptional gene silencing (TGS) through heterochromatin formation and maintenance [1,2].

All these manifestations of RNA silencing rely on the action of small RNA (sRNA) molecules of 21–24 nt that originate from the processing of the dsRNA trigger by RNaseIII-like enzymes called Dicer, or Dicer-like in plants. The model plant *Arabidopsis thaliana* encodes four Dicer-like proteins (DCL1, DCL2, DCL3, and DCL4), each with specialized functions [3]. DCL1 mainly contributes to the production of miRNAs [1], whereas DCL4, DCL2, and DCL3 generate populations of 21-, 22-, and 24-nt short-interfering RNAs (siRNAs), respectively [4,5].

Upon processing, one strand of the sRNA duplexes generated by DCLs is incorporated into an Argonaute (AGO)-containing RNA-induced silencing complex (RISC) to guide sequence-specific inactivation of targeted RNA or DNA. Most miRNAs and DCL4-dependent 21-nt siRNAs load into AGO1 to guide post-transcriptional gene silencing (PTGS) of target mRNAs [1]. These target mRNAs encode transcription factors required for plant development, as well as enzymes involved in various metabolic and hormonal pathways [1]. Upon their incorporation into AGO4, AGO6, or AGO9, DCL3-dependent 24-nt siRNAs act mostly in *cis*, to direct cytosine methylation and chromatin modifications at endogenous loci, including transposons and repetitive sequences, in a process known as RNA-directed DNA methylation (RdDM) [2].

Antiviral RNA silencing

Besides its roles in developmental patterning and maintenance of genome integrity, RNA silencing also constitutes the primary plant immune system against viruses. Antiviral RNA silencing is triggered by dsRNA replication intermediates or intramolecular fold-back structures within viral genomes [6–8]. These viral dsRNAs are mainly processed by DCL4 or its surrogate DCL2, to produce 21- or 22-nt virus-derived small RNAs (vsRNAs), respectively [9,10]. Optimal production of vsRNA also requires dsRNA- binding proteins (DRBs) such as DRB4, which facilitates the synthesis of DCL4-dependent vsRNA from RNA and DNA viruses [11,12]. vsRNAs are subsequently recruited, mainly by AGO1 and AGO2, to direct PTGS of viral RNA as part of antiviral RISCs (Figure 1) [12–19]. In DNA virus-infected plants (gemini- and pararetroviruses), a large amount of DCL3-dependent 24-nt vsRNAs is also produced [9,20]. These 24-nt vsRNAs direct cytosine methylation and chromatin condensation of nuclear viral episomes and minichromosomes to dampen viral transcription, most likely through AGO4 activity (Figure 1) [21–23]. The inverse correlation between the level of viral DNA methylation and the severity of viral symptoms suggests that plant defense against DNA viruses also relies on the RdDM pathway.

To cope with the high pace of virus replication and movement, plants have also evolved means to amplify the antiviral silencing response. This occurs through production of so-called secondary vsRNAs, as opposed to the primary vsRNAs which are generated directly from the structural features or replication intermediates of viral

Corresponding author: Dunoyer, P. (patrice.dunoyer@ibmp-cnrs.unistra.fr).

1360-1385/$ – see front matter
 http://dx.doi.org/10.1016/j.tplants.2013.04.001

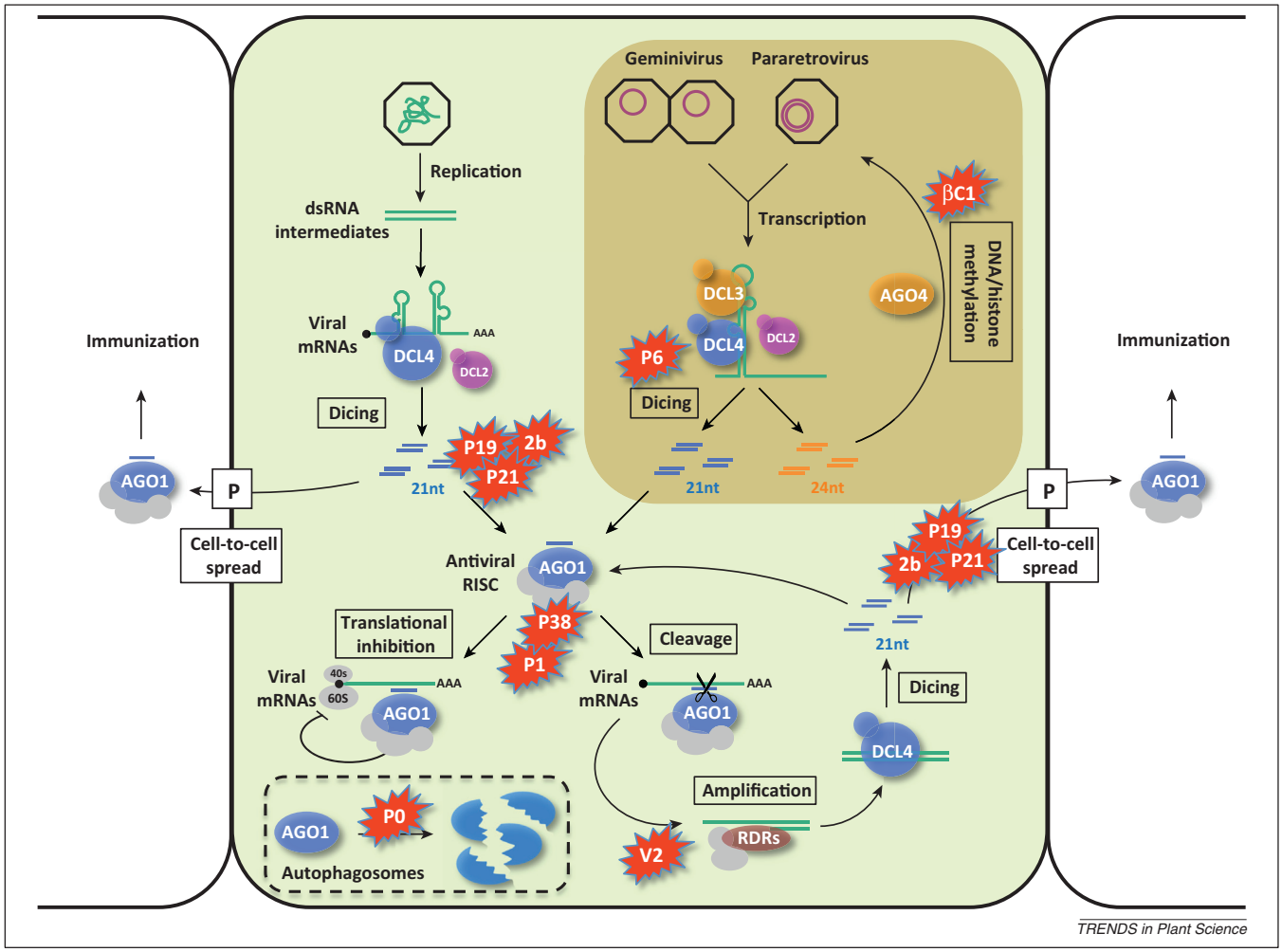

Figure 1. Antiviral RNA silencing and its suppression by virus-encoded silencing suppressors in plants. Antiviral RNA silencing is triggered by double-stranded RNA (dsRNA) replication intermediates or intramolecular fold-back structures within viral genomes that are processed into virus-derived small RNAs (vsRNAs) by RNaseIII-like enzymes called Dicer-like proteins (DCL4, DCL3, and DCL2). These vsRNAs are loaded into Argonaute (AGO)-containing RNA-induced silencing complexes (RISCs) to guide translational inhibition and/or slicing of viral RNA. Cleaved viral RNAs are also used by cellular RNA-dependent RNA polymerases (RDRs) and their cofactors to amplify the RNA silencing response through production of more dsRNA substrates for DCL processing. Both primary and secondary vsRNAs also have the potential to move to neighboring cells through plasmodesmata to prompt the antiviral silencing response. For DNA viruses, a large proportion of DCL3-dependent 24-nt vsRNAs are also produced. These 24-nt vsRNAs direct DNA and/or histone methylation of the viral DNA genomes. Viral suppressors of RNA silencing can inhibit various stages of this pathway, thereby preventing dicing, vsRNA loading, RISC formation or activity, amplification, and movement. The steps targeted by some of the VSRs discussed in this review (P19, P21, P38, P1, 2b, P0, P6, V2, and βC1) are depicted. Abbreviation: P, plasmodesmata.

RNA. These secondary vsRNAs are produced through the activity of cellular RNA-dependent RNA polymerases (RDRs), which convert single-stranded RNA (ssRNA) into new dsRNA substrate for processing by DCLs (Figure 1) [24]. In *Arabidopsis*, RDR1, RDR6, and, to a lesser extent, RDR2 have been implicated in this amplification step of vsRNA accumulation, which sometimes accounts for the largest bulk of the antiviral sRNA produced [12,25–29].

Moreover, antiviral RNA silencing can also spread from the site of initiation to the surrounding tissues [30,31]. In plants, the nature of the mobile silencing nucleic acids that convey sequence specificity has been unambiguously ascribed to siRNA [32–34]. This non-cell autonomous aspect of RNA silencing represents the systemic arm of this antiviral reaction, whereby transmission of mobile vsRNA ahead of the infection front primes antiviral silencing in cells that are yet to be infected (Figure 1). Consequently, replication or movement of the pathogen into those cells is delayed or precluded [35–37].

Viral suppressors of RNA silencing

One of the most compelling pieces of evidence supporting RNA silencing as a major antiviral defense mechanism in plants is the observation that most, if not all, phytoviruses have evolved means to counteract, attenuate, or escape this response [38]. Among these, the production of viral suppressors of RNA silencing (VSRs) is by far the most widespread viral counterdefense strategy employed. VSRs are highly diverse in sequence, structure, and activity within and across virus families, suggesting that their acquisition occurred through rapid evolutionary convergence as a mandatory adaptation to the RNA silencing-based immune response. In agreement with this, VSR expression is often a prerequisite for virus multiplication and systemic host infection in both plants and insects [10,27,28,39]. Although VSRs have been shown to target many stages of the antiviral silencing pathway (Figure 1), their modes of action are usually classified into three broad categories: (i) binding to long dsRNA resulting in inhibition

of Dicer processing; (ii) binding and sequestration of sRNA duplexes preventing RISC assembly; and (iii) direct targeting of effectors or processing factors leading to their inhibition or destabilization.

However, this rather simple classification has to be interpreted with caution in light of recent findings obtained from *in planta* analyses. This is particularly true for the first two categories, where the modes of action of VSRs are generally inferred from *in vitro* binding assays or transient heterologous expression systems. Indeed, in most cases, crucial controls such as adequate loss-of-function point-mutant VSR alleles are missing and, therefore, functional correlation between dsRNA or sRNA binding and silencing suppression activity is lacking. Moreover, VSRs are often multifunctional proteins that perform, in addition to their silencing suppression activity, other essential roles in the virus life cycle that require a close association with viral nucleic acids (such as replication, encapsidation, or movement). Consequently, whether binding observed *in vitro* is a genuine feature of silencing suppression or simply reflects these additional functions of VSR proteins frequently remains an open question.

VSRs targeting long dsRNA

This ambiguity is especially evident when RNA binding is nonspecific, as with P14 of *Pothos latent virus* (PoLV) and P38 of *Turnip crinkle virus* (TCV). Indeed, these two VSRs have been shown *in vitro* to bind dsRNA in a size-independent manner [40,41]. In the case of P38, binding to long dsRNA has been correlated with stabilization of inverted-repeat (IR) transcripts and a concomitant decrease of IR-derived 21- and 24-nt siRNA accumulation in transient agroinfiltration assays [41]. These results initially suggested that P38 suppresses silencing through sequestration or protection of long dsRNA from the processing activities of DCLs [41]. Subsequently, the use of wild type or a VSR-deficient mutant of TCV provided genetic evidence that P38 inhibits DCL4 activity during the antiviral silencing response in *Arabidopsis* [10]. However, the strong accumulation of DCL2-dependent 22-nt vsRNA in wild type TCV-infected plants [10] did not support the suggestion that dsRNA binding is the strategy that underlies P38 VSR activity, as it would imply that DCL2, as opposed to DCL4, is insensitive to P38-mediated sequestration of viral dsRNA substrates. Moreover, the use of P38 mutant derivatives revealed that dsRNA binding *in vitro* and silencing suppression *in vivo* can be uncoupled [42].

A plausible explanation for this apparent discrepancy was obtained when P38 VSR activity was characterized both genetically and biochemically *in planta* [43]. The authors of this study showed that P38 interacts directly and specifically with AGO1 by mimicking host-encoded glycine/tryptophan (GW/WG)-containing proteins normally required for RISC assembly or function in diverse organisms [44,45]. Importantly, point mutations of two GW residues are sufficient to abolish P38 VSR activity by preventing its association with AGO1 [43]. This binding of P38 to AGO1 strongly impairs siRNA- and miRNA-loaded AGO1 activity [43,46]. In particular, miR162-mediated regulation of DCL1 is suppressed by P38 in a GW motif-dependent manner, leading to a dramatic increase in DCL1 accumulation. This increase, in turn, promotes through as yet undefined mechanisms a drastic change in DCL homeostasis whereby accumulation of DCL3 and DCL4, but not DCL2, is strongly downregulated [43]. Therefore, the long dsRNA stabilization observed in agroinfiltration assays is likely to be explained by P38-mediated downregulation of DCL3 and DCL4 [41], the two DCLs that specifically process exogenous IR akin to that used in these assays [47]. This also explains the prominent contribution of DCL2 to antiviral silencing in wild type TCV-infected plants [10]. Interestingly, although DCL2 predominates in TCV-infected tissues, P38 has been shown to prevent the incorporation of 22-nt siRNA into AGO1 as efficiently as DCL4-dependent 21-nt siRNA [46]. Furthermore, expression of lower levels of P38 than those reached during transient agroinfiltration assays or TCV infection is sufficient to efficiently inhibit AGO1 activity without affecting IR processing [46]. Finally, although P38 has been shown *in vitro* to bind siRNA duplexes as well, cell-specific expression studies rule out a significant contribution of sRNA binding to the VSR activity of P38 *in planta* [46].

Collectively, these results suggest that P38 binding to dsRNA, as observed *in vitro*, most likely reflects only its need to interact with viral nucleic acids as a capsid protein (its other function in the virus life cycle) and is unrelated to its silencing suppression activity that largely, if not exclusively, relies on its direct and specific interaction with AGO1.

VSRs targeting sRNA duplexes

Binding and sequestration of sRNA has been proposed as one of the most common strategies employed by VSRs to inhibit RNA silencing [41,48]. The most compelling example of this mode of action was illustrated with the crystallization of the tombusvirus P19 protein in direct association with an siRNA duplex [49,50]. P19 acts as a head-to-tail homodimer that selectively binds to 21-bp siRNA duplexes with high affinity [49]. Importantly, based on its structure, point mutations designed to prevent binding of P19 to these siRNAs, without affecting its stability or dimerization, have been shown to abolish its silencing suppression activity *in vivo* [49]. sRNA binding by P19 was recently shown to quantitatively prevent both siRNA and miRNA incorporation into AGO1-containing RISCs, consistent with a silencing suppression strategy primarily based on sRNA sequestration [46]. In addition, cell-specific expression of this VSR showed that P19 specifically sequesters DCL4-dependent 21-nt siRNA *in planta* and prevents their cell-to-cell spread to neighboring recipient cells [32]. These observations agree with previous results obtained with the P19-producing *Cymbidium ringspot tombusvirus* (CymRSV), where P19 has been reported to be dispensable for virus accumulation within vascular bundles but required for further invasion of the leaf lamina. Lack of P19 is likely to allow movement outside the vasculature of mobile vsRNA, which immunizes neighboring cells and confers nucleotide sequence-specific resistance against CymRSV [37].

In the wake of this seminal example, several additional VSRs were suggested to suppress RNA silencing through sRNA binding. These include *Beet yellows virus* P21, Potyviral HC-Pro, *Peanut clump virus* (PCV) P15, and

TCV P38 [41,48]. However, these conclusions were mainly reached using *in vitro* binding assays, sometimes under non-physiological amounts of VSRs. In some instances, these observations were also supported by detection of sRNA in VSR immunoprecipitates [48,51,52] or by the stabilization of the otherwise labile miRNA* strand in infected plants or VSR-expressing transgenic plants [14,51–54]. Yet, these two lines of evidence neither fully support direct binding and sequestration of sRNA in vivo nor fully discriminate the contribution of sRNA binding, as opposed to other biochemical properties, to VSR action *in planta*. Indeed, the presence of siRNA in VSR immunoprecipitated fractions may merely reveal indirect interaction. Moreover, although it was previously used to extrapolate how VSRs prevent miRNA-mediated mRNA regulation, it was recently shown that stabilization of miRNA* strands cannot be reliably used as an indicator of sRNA duplex sequestration by VSRs *in vivo* [46]. Therefore, alternative approaches must be adopted to properly address these issues.

One such approach may rely on the systematic analysis of AGO1 sRNA-bound fractions in plants expressing VSRs. This approach has recently provided experimental evidence that TCV P38, *Turnip mosaic virus* (TuMV) HC-Pro, and PCV P15, like the tombusviral P19 used as a reference, prevent loading of siRNA into AGO1 [46]. However, and most importantly, this inhibition of siRNA loading does not always entail *in vivo* siRNA binding and sequestration as initially inferred from *in vitro* assays. For instance, TuMV and *Potato virus Y* HC-Pro display no or only weak siRNA-binding properties, respectively [41]. Yet, both proteins efficiently suppress silencing *in vivo* [51,55] and, at least in the case of TuMV, strongly prevent siRNA loading into AGO1 *in planta* [46]. HC-Pro from *Zucchini yellow mosaic virus*, another member of the Potyviridae family, exhibits strong siRNA binding *in vitro*. However, mutations within the highly conserved FRNK box, in the central region of the protein, nearly completely abolish this binding without affecting its silencing suppression activity [56]. Moreover, the findings that TCV P38, PCV P15, and TuMV HC-Pro, as opposed to P19, do not prevent loading of miRNA guide strands into AGO1, despite suppression of miRNA-mediated target regulation, bring further evidence against sRNA sequestration as the mechanism underlying the modes of action of these VSRs [46].

Cell-specific expression studies of VSR proteins could be another way of distinguishing the impact of sRNA binding and sequestration on the silencing suppression activity of VSRs *in planta*. Indeed, concomitant expression of the VSR and the silencing trigger in a given type of cell should result in reduced movement of the mobile siRNAs and, therefore, a reduced silencing phenotype in neighboring cells if the VSR sequesters those siRNAs. As previously alluded to, this approach, when performed with P19 or P21, confirmed that these two VSRs strongly rely on siRNA sequestration to suppress silencing, whereas it ruled out a prominent contribution of siRNA binding, as observed *in vitro*, to P38 VSR activity *in vivo* [32,46].

Alternatively, or perhaps in addition to the approaches described above, the generation of allelic series of VSR mutants can also be used to decipher which property underlies their silencing suppression strategies *in vivo*. This was recently illustrated with the *Cucumber mosaic virus* (CMV) 2b protein [57]. The CMV 2b protein was one of the first described VSRs shown to interact physically with AGO1 [14]. This interaction leads to inhibition of AGO1 slicing activity in a RISC *in vitro* reconstituted assay [14]. This VSR has also been shown to bind siRNA *in vitro* [58] and, accordingly, to prevent the spread of the systemic silencing signal when expressed in tissues through which the signal must travel to induce silencing in target cells [59]. Collectively, these results suggested that either: (i) CMV 2b possesses a dual mode of action entailing sequestration of siRNA on the one hand and inhibition of RISC activity through direct AGO interaction on the other; or (ii) these seemingly distinct biochemical properties are the two sides of the same coin, where interaction with AGO1 is a prerequisite for siRNA sequestration. The respective contribution of each property with respect to 2b-mediated silencing suppression activity *in vivo* was recently discriminated using 2b mutant derivatives [57]. Interestingly, binding of siRNA by 2b was shown to be essential and directly correlated with silencing suppression, whereas inhibition of the AGO1 slicer activity, or interaction between 2b and AGO1, were dispensable [57]. Therefore, these findings suggest that the silencing suppression strategy of 2b mainly relies on sRNA sequestration. Whether this sequestration similarly affects siRNA and miRNA loading into AGO1 and, if so, whether both depend on the same biochemical properties of 2b await characterization.

Bearing all these examples in mind, it is now clear that researchers need to adopt a combination of these different approaches to properly characterize the mode of action of their favorite VSR *in planta*.

VSRs targeting processing or effector proteins

As stated above, VSRs can also directly target other components of the antiviral silencing pathway, leading to their inhibition or destabilization. For instance, the VSR P6 of *Cauliflower mosaic virus* (CaMV), besides its role in translational transactivation of the viral 35S RNA, has been shown to interact physically with the dsRNA-binding protein DRB4, thereby inhibiting dsRNA processing by DCL4 [11]. Interestingly, this inhibition of DRB4 causes a dramatic increase in DCL3-dependent 24-nt siRNA accumulation that has the potential to trigger heterochromatin formation and TGS of CaMV minichromosomes [60], thereby dampening virus accumulation. Whether this is a deliberate strategy of the virus to somewhat preserve host cell integrity or rather suggests that P6, or another CaMV-encoded protein, is able to prevent the action of these 24-nt siRNAs on viral DNA, remains an open question. However, in line with the latter hypothesis, it has recently been shown that, although CaMV-infected *Arabidopsis* accumulates large amounts of 24-nt vsRNAs, few are loaded into AGO4 [61].

The V2 protein from *Tomato yellow leaf curl virus* directly interacts with SGS3, a factor involved in RDR6-mediated silencing amplification and virus resistance [62]. SGS3 and V2 are dsRNA-binding proteins that favor 5′-overhang-containing dsRNA as a substrate. Interestingly, V2, but not a V2 mutant lacking VSR activity *in vivo*,

efficiently outcompetes SGS3 for dsRNA binding [63]. Most likely this prevents SGS3 from accessing its substrate RNA, leading to inhibition of secondary vsRNA production.

In addition to P38 and 2b, which are discussed above, other VSRs have been shown to directly target AGO1 to inhibit its slicing activity. For instance, the P1 VSR of *Sweet potato mild mottle ipomovirus* uses the same strategy as P38 to mimic GW/WG motifs that hook up to AGOs. Like P38, P1 was shown to bind directly to AGO1 in a GW motif-dependent manner and inhibit siRNA/miRNA-programmed RISC activity [64]. This finding suggests that this GW motif-mimicking strategy may be a widespread approach to counteract the RNA silencing-based immune response. Through this interaction, these VSRs may outcompete, inactivate, or prevent the association of other AGO1 interactors required for functional RISC formation or action. Of note, analysis of AGO1 sRNA-bound fractions in various VSR-expressing plants revealed the existence of at least two distinct pools of AGO1 [46]. One pool seems preferentially loaded with siRNA, whereas the other seems preferentially loaded with miRNA, both being differentially affected by VSRs. For instance, as stated above, P38, P15, and HC-Pro, unlike P19, prevent siRNA but not miRNA loading into AGO1, yet they all efficiently inhibit both siRISC and miRISC activity [46]. A potential cofactor that may differentiate these two specific RISCs is the recently identified ethylene-inducible transcription factor RAV2/EDF2 [65]. RAV2 interacts with TuMV HC-Pro *in planta* and is required for HC-Pro-mediated inhibition of siRNA activity, but is dispensable for HC-Pro-mediated inhibition of miRNA activity [65]. These attributes make RAV2 a good candidate as a specific cofactor of the proposed AGO1–siRISC, whereby HC-Pro could sequester RAV2 and thereby deplete it from the siRISC.

Interaction of a VSR with AGO1 can also induce the degradation of this core component of the RISC. This strategy has been found with P0 proteins of phloem-restricted poleroviruses such as *Beet western yellows virus* [66–68] and in the enomovirus genus [69]. Unlike most VSRs studied to date, P0 displays no RNA-binding affinity *in vitro* [68]. Instead, P0 has been suggested to act as an F-box protein that interacts with and hijacks the host S-phase kinase-associated protein 1 (SKP1) of the Skp1-cullin-F-box (SCF) E3 ubiquitin-protein ligase complex to promote the degradation of AGO1 protein, thereby preventing antiviral RISC assembly [66,67,70]. Accordingly, mutation of its minimal F-box motif leads to the loss of P0 silencing suppression activity, and silencing of SKP1 in *Nicotiana benthamiana* increases resistance against polerovirus infection. Yet, P0-mediated AGO1 degradation is insensitive to proteasome inhibitors, arguing against a direct involvement of the ubiquitin-dependent proteasome pathway [67]. This apparent discrepancy was recently reconciled in a study which demonstrated that P0-induced AGO1 degradation was blocked by inhibition of the autophagy pathway and colocalized with autophagy-related proteins [71]. Collectively, these results support a model in which a viral SCF^{P0} E3 ligase promotes AGO1 turnover through autophagy. Interestingly, AGO1 is also degraded by the autophagy pathway in the absence of viral infection, in particular when miRNA production or stability is compromised [71], unraveling an additional component in the multilayered regulation of AGO1 homeostasis [72–75].

VSRs inhibiting the RdDM pathway

Unlike RNA viruses, which need to cope only with the RNA degradation pathway, DNA viruses are targeted by both the PTGS and the RdDM pathways [9,20–23]. Therefore, they have evolved VSRs able to inhibit both RNA silencing-based immune responses. One such VSR is the βC1 protein encoded by the β satellite of *Tomato yellow leaf curl China begomovirus* (TYLCCNV). Although the precise mode of action of βC1 in the suppression of PTGS remains unknown [76], a recent study provided insights regarding the strategy it employs to inhibit DNA methylation and TGS in the host. βC1 has been shown to interact with and inhibit the activity of S-adenosyl homocysteine hydrolase, a methyl cycle enzyme required for cytosine methylation, leading to reduced methylation of viral and host genomes [77]. Global inhibition of the methyl cycle seems to be the method of choice for DNA viruses to hinder the RdDM pathway, as both AL2 encoded by the *Tomato golden mosaic virus* and L2 of *Beet curly top virus* interact with and inactivate adenosine kinase (ADK), which is required for the efficient production of S-adenosyl methionine (SAM), an essential methyltransferase cofactor [78]. Additionally, the C2 protein of *Beet severe curly top virus* has been shown to dampen the 26S proteasome-mediated degradation of S-adenosyl-methionine decarboxylase (SAMDC1) through direct interaction [79]. SAMDC1 catalyzes the conversion of SAM to decarboxylated SAM (dcSAM), which can act as a competitive inhibitor against SAM for methyltransferases. Therefore, increased levels of SAMDC1 result in increased accumulation of dcSAM and inhibition of DNA methylation and TGS of the viral genome [79]. The findings that several DNA virus-encoded VSRs inhibit the RdDM pathway to minimize the methylation of their genome provide further evidence that this pathway is an important component of the host defense reaction against this type of virus.

An alternative or additional strategy for DNA viruses to protect their genome against antiviral RdDM is to encode a VSR that also impairs the miRNA pathway. miR402 has recently been shown to target efficient degradation of the mRNA of DNA glycosylase DEMETER-like 3 (DML3), which is involved in DNA demethylation through specific excision of 5-methylcytosine [80]. Therefore, inhibition of miRNA-mediated mRNA regulation by DNA virus-encoded VSRs would increase the accumulation of DML3 that could potentially trigger active DNA demethylation of the viral genome. The βC1 of the TYLCCNV β satellite may be one such VSR, because it has been shown to trigger developmental defects reminiscent of miRNA-deficient mutant plants and, accordingly, increased accumulation of miRNA targets [81]. Another protein that might fulfill these criteria is the AC4 VSR of *African cassava mosaic geminivirus*, which was reported to inhibit the miRNA pathway through binding of single-stranded miRNAs [82].

Surprisingly, the VSR 2b of CMV, an RNA virus with no DNA intermediates in its life cycle, was also shown to interfere with the RdDM pathway through binding of 24-nt siRNA in the nucleus, resulting in the inhibition of

AGO4 activities [57,83]. However, conflicting results have shown that 2b, rather than preventing, facilitates virus-induced TGS and DNA methylation of host gene promoter sequences [84], complicating the interpretation of these findings and their relevance in terms of antiviral defense.

Counter-counterdefense in plants

There is an increasing body of evidence indicating that plants have developed counter-counterdefense strategies to sense silencing suppression caused by VSRs and stimulate the enhancement of their defense reactions (Figure 2).

One such indication lies in the identification of additional antiviral AGOs. Several observations initially implicated AGO1 as the main AGO protein involved in the antiviral silencing response [13,14]. However, based on the massive amount and diversity of vsRNA produced during viral infection and on the loading rules of sRNA into AGOs [15,85,86], it was expected that other AGOs may participate in the antiviral silencing response. Accordingly, AGO2 and AGO5 immunoprecipitates have also been found to contain vsRNA [15,17]. In addition, several studies have recently revealed that AGO2 plays a major role in the antiviral silencing response [16–19]. Interestingly, this antiviral role of AGO2 is normally hidden or reduced in the presence of an active AGO1 through the action of miR403, which regulates the accumulation of AGO2 (Figure 2) [87]. Given that AGO1 is also the primary AGO in the plant miRNA silencing pathway and that VSRs frequently hinder its miRNA-mediated mRNA regulation, AGO2, upon infection, accumulates at much higher levels than in non-infected plants and acts in a cooperative manner in the antiviral silencing defense reaction. Therefore, plants, by placing antiviral effectors under the control of sRNAs whose actions are perturbed by viral infection, have found a way to counter or accommodate the detrimental effects of VSRs. This is also illustrated by the identification in *Medicago truncatula* and soybean (*Glycine max*) of miRNAs that target DCL2 and SGS3 [88], both proteins also being required for the antiviral silencing response (Figure 2) [10,89].

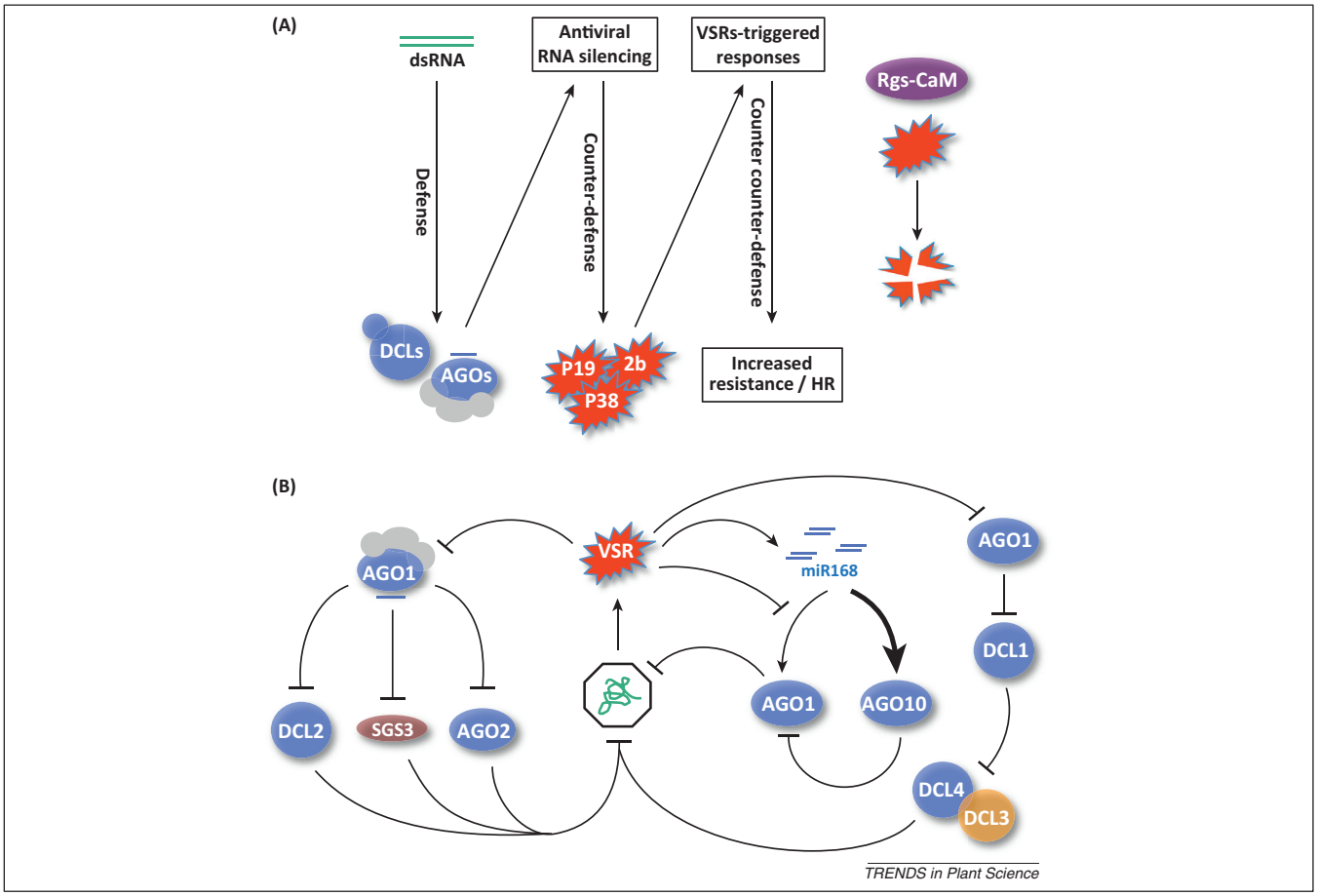

Figure 2. Illustration of the RNA silencing interplay during plant–virus interactions. (**A**) Upon viral infection, viral double-stranded RNAs (dsRNAs) are processed and effected by antiviral Dicer-like proteins (DCLs) and Argonautes (AGOs) to trigger the antiviral RNA silencing defense reaction of the plants. To counteract this response, viruses express viral suppressors of RNA silencing (VSRs) that inhibit various stages of this defense pathway, thereby enhancing their fitness in the host. To fight back, plants have evolved counter-counterdefense strategies that sense the VSRs, or their molecular consequences, to increase their resistance. One such strategy is depicted with the production of rgs-CaM, which triggers degradation of some VSRs by autophagy, allowing a more potent antiviral RNA silencing reaction. This zigzag model is similar in essence to the pathogen-associated molecular pattern (PAMP)-triggered immunity (PTI)–effector-triggered immunity (ETI) scheme observed during innate immune responses against bacteria. (**B**) Examples of how plants or viruses use perturbation of the miRNA pathway to increase resistance or viral fitness, respectively. Plants regulate the accumulation of several antiviral RNA silencing components (AGO2, DCL2, and SGS3) through miRNA-mediated regulation. VSRs, by preventing miRNA activity, promote the accumulation of these antiviral factors, leading to increased resistance. By contrast, VSRs can trigger increased accumulation of miR168 through an as yet undefined mechanism. The level of AGO1 is tightly regulated by miR168-mediated cleavage and translational repression of its mRNA by AGO1 and AGO10, respectively. VSRs, by inhibiting miR168 loading into AGO1, promote its incorporation into AGO10, thereby fostering translational inhibition of AGO1. In addition, VSRs by inhibiting miRNA-induced silencing complex (RISC) activity promote DCL1 accumulation which, in turn, leads to strong inhibition of DCL3 and DCL4 steady-state levels.

Box 1. Innate immunity during plant–bacteria interactions

Plants have two types of innate immunity against bacteria: PTI and ETI. PTI relies on detection by transmembrane receptors of highly conserved signature molecules called PAMPs [113]. PTI involves activation of mitogen-activated protein kinases, production of reactive oxygen species and stimulation of SA synthesis and signaling. To circumvent this first layer of defense, many host-adapted microbes produce effector proteins that suppress various steps of PTI [114]. In turn, host plants react to PTI suppression by deploying R proteins that may directly recognize pathogen virulence effectors or sense the molecular consequences of their action against PTI. The resulting ETI often culminates in the onset of cell death in a process known as the HR, which is thought to restrict pathogen growth and is accompanied by a potent SA-mediated systemic defense response. This interplay has been portrayed as the zigzag model [113] (Figure I).

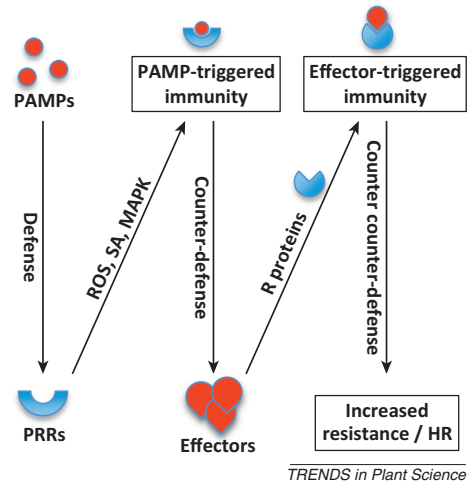

Figure I. Schematic representation of the innate immune response during plant–bacteria interactions. Pathogen-associated molecular patterns (PAMPs) are recognized by transmembrane pattern recognition receptors (PRRs) to trigger PAMP-triggered immunity (PTI). Successful pathogens deliver effectors that interfere with PTI, leading to increased susceptibility. Some effectors, or their molecular consequences, are recognized or sensed by disease resistance (R) proteins resulting in the onset of effector-triggered immunity (ETI), which corresponds to an accelerated and amplified PTI response. This results in disease resistance and, usually, a hypersensitive cell death response (HR) at the infection site. Abbreviations: ROS, reactive oxygen species; SA, salicylic acid; MAPK, mitogen-activated protein kinases.

Striking similarities can be seen between the general framework of antiviral silencing activation and its suppression by VSRs on the one hand and the classical pathogen-associated molecular pattern (PAMP)-triggered immunity (PTI)–effector-triggered immunity (ETI) zigzag scheme for resistance against bacteria on the other (Box 1) [90]. In this scenario, virus-derived dsRNA can be regarded as a PAMP, because this molecule is always associated with viral replication. Similar to PTI, this viral PAMP will be processed and effected by the DCLs and AGOs that mediate the antiviral silencing reaction. Again by analogy with the zigzag model, VSRs being, by definition, virulence effectors that perturb the cellular silencing machinery, it can be anticipated that plants have developed host-encoded functions, such as dedicated R genes, that either directly recognize VSRs or sense the damage or modifications triggered by them (Figure 2). Perception of these modifications will then, in turn, elicit responses similar to those observed during typical ETI, such as the hypersensitive response (HR). In support of this notion, there are at least three VSR proteins, namely TCV P38, TAV 2b, and TBSV P19, that are known to trigger HR-like lesions in a host-specific manner and, at least in the case of 2b, mutations that compromised its silencing suppression activity also compromised the HR [91–93]. Moreover, because ETI is associated with strong induction of salicylic acid (SA) production, a potential advantage of such a resistance (R) protein-based system in sensing VSR activity may rely on the stimulation of antiviral RNA silencing components, as seen with SA-dependent induction of RDR1 during defense [25,94].

Recent results obtained with the tobacco calmodulin-like protein rgs-CaM may potentially fit into this general framework. rgs-CaM has been reported to interact with HC-Pro and 2b [95]. Interestingly, overexpression of rgs-CaM strongly impairs HC-Pro protein accumulation without affecting HC-Pro mRNA levels [95]. An analogous, albeit milder effect was also observed with 2b. Similarly to what was observed for P0-induced AGO1 degradation [71], it has been shown that the rgs-Cam-mediated degradation mechanism of these VSRs, together with rgs-CaM itself, relies on the autophagy pathway rather than the 26S proteasome pathway [95]. Accordingly, both rgs-CaM and 2b have been found to be recruited to autolysosomes and silencing of *beclin1*, an autophagy-related gene, drastically increased the level of rgs-CaM. Of note, rgs-CaM transcription was increased upon viral infection and plants overexpressing rgs-CaM were less susceptible to viral infection, whereas plants knocked down for rgs-CaM were more susceptible [95]. Therefore, collectively these results support a model in which rgs-CaM is a defense factor whose expression is induced upon viral infection and that recognizes and binds specific VSRs. This binding leads to the degradation of the VSR–rgs-CaM complex, thereby weakening the viral counterdefense system and allowing the plant to mount a more vigorous antiviral response (Figure 2) [95].

Interestingly, intensive analyses of sRNA libraries obtained from tomato and *Medicago* have revealed the existence of a superfamily of miRNAs that target a high proportion of mRNAs encoding disease resistance genes with nucleotide-binding site (NBS) and leucine-rich repeat (LRR) motifs [88,96]. These miRNAs are 22 nt in length and, consistent with recent reports [97,98], are able to trigger production of so-called DCL4-dependent phased *trans*-acting siRNAs [87] from numerous and diverse members of the NBS-LRR class of disease resistance genes [88,96], thereby reinforcing the silencing of these targets. This observation is coherent with the finding that constitutive expression of disease resistance genes is, at least in some cases, detrimental to the host [99]. Maintaining these genes under reversible PTGS will therefore reduce the fitness cost of constitutive defense activation. Interestingly, infection by TCV, CMV, or the pathogenic *Pseudomonas syringae* DC3000, which also encodes suppressors of RNA silencing [100], alleviates the silencing of the targeted NBS-LRR mRNAs [96]. This, in turn, promotes increased accumulation of numerous NBS-LRR proteins that have, thereby, the potential to induce defense independently of the protein-based recognition mechanisms normally associated with the gene-for-gene relationship found in ETI [101]. The increase in NBS-LRR proteins in infected cells

enhances the level of immunity in the plant and is expected to potentiate ETI due to secondary infection, through accelerated activation of the defense pathways against secondary pathogens. This may explain why, for instance, tobacco (*Nicotiana tabacum*) plants that express a potyviral HC-Pro show enhanced resistance to a broad range of pathogens [102]. This may also be the basis of the near immunity observed in *dcl1* mutant and P19- or HC-Pro-expressing plants against wild type and tumor-inducing *Agrobacterium tumefaciens* [103].

Concluding remarks and future prospects

VSRs have been shaped by the neverending molecular arms race between hosts and pathogens, where pathogens need to efficiently thwart the RNA silencing-based immune response for efficient multiplication, whereas hosts must dampen the deleterious effects of these VSRs to survive. In general, viruses have a relatively narrow host range, but the mechanisms that determine such host specificities remain unclear. Because viruses are obligate parasites that transcribe, translate, and replicate their genetic material exclusively inside host cells, several incompatible interactions between host cellular factors that are normally hijacked by viral proteins in susceptible plants may be responsible for the inability of a virus to infect a given plant. These include host translational machinery factors and cellular proteins required for viral replication or movement [104–106]. Alternatively, recognition of viral factors by R proteins could also result in resistance [107]. However, the implication of RNA silencing in non-host resistance against viruses, whereby a plant is resistant to a given pathogen that is able to infect other plant species, has not been investigated in detail. Nevertheless, recent results obtained with Potato virus X (PVX) suggest that RNA silencing and the ability of a virus to efficiently suppresses the antiviral arm of this pathway play important roles in these specificities [18]. Indeed, *Arabidopsis* was previously considered as a non-host for PVX. However, genetic inactivation of the two main antiviral DCLs, DCL4 and DCL2, is sufficient to allow PVX to infect *Arabidopsis* [18] (P. Dunoyer, unpublished). Given that mutation of the antiviral AGO2 also alleviates the non-host resistance of *Arabidopsis* against wild type PVX [18], this strongly suggests that RNA silencing represents a crucial mechanism to restrict infection by non-host-adapted viruses and that the PVX P25 VSR is most likely not fully functional in this particular host.

The molecular bases of silencing suppression by VSRs are likely to be much more complex than initially anticipated. In addition, it is probably an oversimplified view to think that VSRs possess a single mode of action to fight host antiviral defense reactions. For instance, by targeting conserved core elements of RNA silencing pathways, VSR expression often results in the appearance of developmental phenotypes that have been assigned to the inhibition of the miRNA pathway [51,52,108]. The strong similarities between the morphological defects elicited by VSRs of various origin have led to the suggestion that inhibition of the miRNA pathway is unlikely to be a deliberate viral strategy to reprogram or alter host genome expression, but rather reflects a secondary consequence of inhibition of the antiviral silencing pathway at some steps shared with the miRNA pathway [51,52]. However, this may not be that straightforward and could instead reflect an alternative counterdefense strategy of the virus to promote its efficient accumulation. In line with this hypothesis is the observed change in DCLs homeostasy triggered by the inhibition of miR162-mediated regulation of DCL1 (Figure 2) [43]. It also fits with recent findings showing that several plant virus infections trigger specific induction of miR168 in a VSR-dependent manner [109]. AGO1 level is tightly regulated by miR168-mediated cleavage and translational repression of its mRNA by AGO1 and AGO10, respectively [72–74,110]. Inhibition of miRNA-loaded AGO1 activity in infected plants leads to increased accumulation of AGO1 mRNA, despite high levels of miR168 [109]. However, this overaccumulation of AGO1 mRNA was not accompanied by a concomitant increase in AGO1 protein level but by a decrease [109], supporting the notion that VSRs can promote AGO10-mediated translational inhibition of the antiviral AGO1 (Figure 2). Although the molecular basis of this VSR-dependent increase in miR168 accumulation remains unknown, one interesting possibility suggested by these findings is that VSRs may have evolved to avoid targeting specific AGOs such as AGO10 [43]. By doing so, VSRs have the potential to promote downregulation of negative regulators of virus accumulation. Therefore, to unravel the complex interplay occurring during plant–virus interactions, it may be as informative to determine which AGOs are targeted by VSRs as it is to identify the non-targeted ones.

One striking consequence of the inhibition of the miRNA pathway by VSRs is the stabilization of the normally rapidly degraded miRNA* strands. Although miRNAs* were once considered a useless byproduct of miRNA biogenesis, recent findings support the notion that they also possess intrinsic regulation properties like their miRNA guide strand counterparts [111,112]. Because miRNA* stabilization upon infection is not linked to their sequestration by VSRs in duplexed forms with their miRNA guide strand [46], their overaccumulation may potentially be beneficial to the virus for infection or to the plant for defense, through targeting of negative or positive regulators, respectively. In line with the latter hypothesis, it has recently been shown in *Arabidopsis* that miR393* loading onto AGO2 is induced by *Pseudomonas* infection [112]. This, in turn, promotes translational repression of the Golgi-localized SNARE gene MEMB12 mRNA and increased exocytosis of the antimicrobial pathogenesis-related protein PR1, thereby fostering innate immunity against this pathogen. Therefore, assessing where those stabilized miRNAs* are loaded in the presence of the VSRs and identifying their targets will undoubtedly unravel new interplays between defense, counterdefense, and counter-counterdefense mechanisms during virus infection. This ever-growing net of interactions further emphasizes the value of VSRs as molecular probes to study endogenous silencing pathways.

Acknowledgments

The authors apologize to colleagues whose work could not be cited because of space limitations. P.D. is supported by research grants from Agence National pour la Recherche (ANR-08-JCJC-0063 and ANR-10-LABX-36).

References

1 Voinnet, O. (2009) Origin, biogenesis, and activity of plant microRNAs. *Cell* 136, 669–687
2 Law, J.A. and Jacobsen, S.E. (2010) Establishing, maintaining and modifying DNA methylation patterns in plants and animals. *Nat. Rev. Genet.* 11, 204–220
3 Baulcombe, D. (2004) RNA silencing in plants. *Nature* 431, 356–363
4 Brodersen, P. and Voinnet, O. (2006) The diversity of RNA silencing pathways in plants. *Trends Genet.* 22, 268–280
5 Chapman, E.J. and Carrington, J.C. (2007) Specialization and evolution of endogenous small RNA pathways. *Nat. Rev. Genet.* 8, 884–896
6 Szittya, G. *et al.* (2010) Structural and functional analysis of viral siRNAs. *PLoS Pathog.* 6, e1000838
7 Qi, X. *et al.* (2009) Small RNA deep sequencing reveals role for *Arabidopsis thaliana* RNA-dependent RNA polymerases in viral siRNA biogenesis. *PLoS ONE* 4, e4971
8 Donaire, L. *et al.* (2009) Deep-sequencing of plant viral small RNAs reveals effective and widespread targeting of viral genomes. *Virology* 392, 203–214
9 Blevins, T. *et al.* (2006) Four plant Dicers mediate viral small RNA biogenesis and DNA virus induced silencing. *Nucleic Acids Res.* 34, 6233–6246
10 Deleris, A. *et al.* (2006) Hierarchical action and inhibition of plant Dicer-like proteins in antiviral defense. *Science* 313, 68–71
11 Haas, G. *et al.* (2008) Nuclear import of CaMV P6 is required for infection and suppression of the RNA silencing factor DRB4. *EMBO J.* 27, 2102–2112
12 Qu, F. *et al.* (2008) *Arabidopsis* DRB4, AGO1, AGO7, and RDR6 participate in a DCL4-initiated antiviral RNA silencing pathway negatively regulated by DCL1. *Proc. Natl. Acad. Sci. U.S.A* 105, 14732–14737
13 Morel, J-B. *et al.* (2002) Fertile hypomorphic *ARGONAUTE* (*ago1*) mutants impaired in post-transcriptional gene silencing and virus resistance. *Plant Cell* 14, 629–639
14 Zhang, X. *et al.* (2006) *Cucumber mosaic virus*-encoded 2b suppressor inhibits *Arabidopsis* Argonaute1 cleavage activity to counter plant defense. *Genes Dev.* 20, 3255–3268
15 Takeda, A. *et al.* (2008) The mechanism selecting the guide strand from small RNA duplexes is different among argonaute proteins. *Plant Cell Physiol.* 49, 493–500
16 Harvey, J.J. *et al.* (2011) An antiviral defense role of AGO2 in plants. *PLoS ONE* 6, e14639
17 Wang, X.B. *et al.* (2011) The 21-nucleotide, but not 22-nucleotide, viral secondary small interfering RNAs direct potent antiviral defense by two cooperative argonautes in *Arabidopsis thaliana*. *Plant Cell* 23, 1625–1638
18 Jaubert, M. *et al.* (2011) ARGONAUTE2 mediates RNA-silencing antiviral defenses against Potato virus X in *Arabidopsis*. *Plant Physiol.* 156, 1556–1564
19 Scholthof, H.B. *et al.* (2011) Identification of an ARGONAUTE for antiviral RNA silencing in *Nicotiana benthamiana*. *Plant Physiol.* 156, 1548–1555
20 Moissiard, G. and Voinnet, O. (2006) RNA silencing of host transcripts by *cauliflower mosaic virus* requires coordinated action of the four *Arabidopsis* Dicer-like proteins. *Proc. Natl. Acad. Sci. U.S.A.* 103, 19593–19598
21 Raja, P. *et al.* (2008) Viral genome methylation as an epigenetic defense against geminiviruses. *J. Virol.* 82, 8997–9007
22 Rodriguez-Negrete, E.A. *et al.* (2009) RNA silencing against geminivirus: complementary action of posttranscriptional gene silencing and transcriptional gene silencing in host recovery. *J. Virol.* 83, 1332–1340
23 Yadav, R.K. and Chattopadhyay, D. (2011) Enhanced viral intergenic region-specific short interfering RNA accumulation and DNA methylation correlates with resistance against a geminivirus. *Mol. Plant Microbe Interact.* 24, 1189–1197
24 Voinnet, O. (2008) Use, tolerance and avoidance of amplified RNA silencing by plants. *Trends Plant Sci.* 13, 317–328
25 Diaz-Pendon, J.A. *et al.* (2007) Suppression of antiviral silencing by *cucumber mosaic virus* 2b protein in *Arabidopsis* is associated with drastically reduced accumulation of three classes of viral small interfering RNAs. *Plant Cell* 19, 2053–2063
26 Donaire, L. *et al.* (2008) Structural and genetic requirements for the biogenesis of tobacco rattle virus-derived small interfering RNAs. *J. Virol.* 82, 5167–5177
27 Wang, X.B. *et al.* (2010) RNAi-mediated viral immunity requires amplification of virus-derived siRNAs in *Arabidopsis thaliana*. *Proc. Natl. Acad. Sci. U.S.A.* 107, 484–489
28 Garcia-Ruiz, H. *et al.* (2010) *Arabidopsis* RNA-dependent RNA polymerases and dicer-like proteins in antiviral defense and small interfering RNA biogenesis during *Turnip Mosaic Virus* infection. *Plant Cell* 22, 481–496
29 Qu, F. (2010) Antiviral role of plant-encoded RNA-dependent RNA polymerases revisited with deep sequencing of small interfering RNAs of virus origin. *Mol. Plant Microbe Interact.* 23, 1248–1252
30 Himber, C. *et al.* (2003) Transitivity-dependent and -independent cell-to-cell movement of RNA silencing. *EMBO J.* 22, 4523–4533
31 Dunoyer, P. *et al.* (2005) DICER-LIKE 4 is required for RNA interference and produces the 21-nucleotide small interfering RNA component of the plant cell-to-cell silencing signal. *Nat. Genet.* 37, 1356–1360
32 Dunoyer, P. *et al.* (2010) Small RNA duplexes function as mobile silencing signals between plant cells. *Science* 328, 912–916
33 Dunoyer, P. *et al.* (2010) An endogenous, systemic RNAi pathway in plants. *EMBO J.* 29, 1699–1712
34 Molnar, A. *et al.* (2010) Small silencing RNAs in plants are mobile and direct epigenetic modification in recipient cells. *Science* 328, 872–875
35 Voinnet, O. *et al.* (1998) Systemic spread of sequence-specific transgene RNA degradation is initiated by localised introduction of ectopic promoterless DNA. *Cell* 95, 177–187
36 Voinnet, O. *et al.* (2000) A viral movement protein prevents systemic spread of the gene silencing signal in *Nicotiana benthamiana*. *Cell* 103, 157–167
37 Havelda, Z. *et al.* (2003) In situ characterization of *Cymbidium Ringspot Tombusvirus* infection-induced posttranscriptional gene silencing in *Nicotiana benthamiana*. *J. Virol.* 77, 6082–6086
38 Ding, S.W. and Voinnet, O. (2007) Antiviral immunity directed by small RNAs. *Cell* 130, 413–426
39 Li, H. *et al.* (2002) Induction and suppression of RNA silencing by an animal virus. *Science* 296, 1319–1321
40 Merai, Z. *et al.* (2005) Aureusvirus P14 is an efficient RNA silencing suppressor that binds double-stranded RNAs without size specificity. *J. Virol.* 79, 7217–7226
41 Merai, Z. *et al.* (2006) Double-stranded RNA binding may be a general plant RNA viral strategy to suppress RNA silencing. *J. Virol.* 80, 5747–5756
42 Cao, M. *et al.* (2010) The capsid protein of *Turnip crinkle virus* overcomes two separate defense barriers to facilitate systemic movement of the virus in *Arabidopsis*. *J. Virol.* 84, 7793–7802
43 Azevedo, J. *et al.* (2010) Argonaute quenching and global changes in Dicer homeostasis caused by a pathogen-encoded GW repeat protein. *Genes Dev.* 24, 904–915
44 El-Shami, M. *et al.* (2007) Reiterated WG/GW motifs form functionally and evolutionarily conserved ARGONAUTE-binding platforms in RNAi-related components. *Genes Dev.* 21, 2539–2544
45 Till, S. *et al.* (2007) A conserved motif in Argonaute-interacting proteins mediates functional interactions through the Argonaute PIWI domain. *Nat. Struct. Mol. Biol.* 14, 897–903
46 Schott, G. *et al.* (2012) Differential effects of viral silencing suppressors on siRNA and miRNA loading support the existence of two distinct cellular pools of ARGONAUTE1. *EMBO J.* 31, 2553–2565
47 Dunoyer, P. *et al.* (2007) Intra- and intercellular RNA interference in *Arabidopsis thaliana* requires components of the microRNA and heterochromatic silencing pathways. *Nat. Genet.* 39, 848–856
48 Lakatos, L. *et al.* (2006) Small RNA binding is a common strategy to suppress RNA silencing by several viral suppressors. *EMBO J.* 25, 2768–2780
49 Vargason, J.M. *et al.* (2003) Size selective recognition of siRNA by an RNA silencing suppressor. *Cell* 115, 799–811
50 Ye, K. *et al.* (2003) Recognition of small interfering RNA by a viral suppressor of RNA silencing. *Nature* 426, 874–878
51 Dunoyer, P. *et al.* (2004) Probing the microRNA and small interfering RNA pathways with virus-encoded suppressors of RNA silencing. *Plant Cell* 16, 1235–1250

52 Chapman, E.J. *et al.* (2004) Viral RNA silencing suppressors inhibit the microRNA pathway at an intermediate step. *Genes Dev.* 18, 1179–1186
53 Yu, B. *et al.* (2006) Transgenically expressed viral RNA silencing suppressors interfere with microRNA methylation in *Arabidopsis*. *FEBS Lett.* 580, 3117–3120
54 Csorba, T. *et al.* (2007) The p122 subunit of *Tobacco Mosaic Virus* replicase is a potent silencing suppressor and compromises both small interfering RNA- and microRNA-mediated pathways. *J. Virol.* 81, 11768–11780
55 Brigneti, G. *et al.* (1998) Viral pathogenicity determinants are suppressors of transgene silencing in *Nicotiana benthamiana*. *EMBO J.* 17, 6739–6746
56 Shiboleth, Y.M. *et al.* (2007) The conserved FRNK box in HC-Pro, a plant viral suppressor of gene silencing, is required for small RNA binding and mediates symptom development. *J. Virol.* 81, 13135–13148
57 Duan, C.G. *et al.* (2012) Suppression of *Arabidopsis* ARGONAUTE1-mediated slicing, transgene-induced RNA silencing, and DNA methylation by distinct domains of the *Cucumber mosaic virus* 2b protein. *Plant Cell* 24, 259–274
58 Gonzalez, I. *et al.* (2010) *Cucumber mosaic virus* 2b protein subcellular targets and interactions: their significance to RNA silencing suppressor activity. *Mol. Plant Microbe Interact.* 23, 294–303
59 Guo, H.S. and Ding, S.W. (2002) A viral protein inhibits the long range signaling activity of the gene silencing signal. *EMBO J.* 21, 398–407
60 Al-Kaff, N.S. *et al.* (1998) Transcriptional and posttranscriptional plant gene silencing in response to a pathogen. *Science* 279, 2113–2115
61 Blevins, T. *et al.* (2011) Massive production of small RNAs from a non-coding region of *Cauliflower mosaic virus* in plant defense and viral counter-defense. *Nucleic Acids Res.* 39, 5003–5014
62 Glick, E. *et al.* (2008) Interaction with host SGS3 is required for suppression of RNA silencing by *tomato yellow leaf curl virus* V2 protein. *Proc. Natl. Acad. Sci. U.S.A.* 105, 157–161
63 Fukunaga, R. and Doudna, J.A. (2009) dsRNA with 5′ overhangs contributes to endogenous and antiviral RNA silencing pathways in plants. *EMBO J.* 28, 545–555
64 Giner, A. *et al.* (2010) Viral protein inhibits RISC activity by argonaute binding through conserved WG/GW motifs. *PLoS Pathog.* 6, e1000996
65 Endres, M.W. *et al.* (2010) Two plant viral suppressors of silencing require the ethylene-inducible host transcription factor RAV2 to block RNA silencing. *PLoS Pathog.* 6, e1000729
66 Bortolamiol, D. *et al.* (2007) The polerovirus F Box protein P0 targets ARGONAUTE1 to suppress RNA silencing. *Curr. Biol.* 17, 1615–1621
67 Baumberger, N. *et al.* (2007) The Polerovirus silencing suppresor P0 targets ARGONAUTE proteins for degradation. *Curr. Biol.* 17, 1609–1614
68 Csorba, T. *et al.* (2010) Polerovirus protein P0 prevents the assembly of small RNA-containing RISC complexes and leads to degradation of ARGONAUTE1. *Plant J.* 62, 463–472
69 Fusaro, A.F. *et al.* (2012) The Enamovirus P0 protein is a silencing suppressor which inhibits local and systemic RNA silencing through AGO1 degradation. *Virology* 426, 178–187
70 Pazhouhandeh, M. *et al.* (2006) F-box-like domain in the polerovirus protein P0 is required for silencing suppressor function. *Proc. Natl. Acad. Sci. U.S.A.* 103, 1994–1999
71 Derrien, B. *et al.* (2012) Degradation of the antiviral component ARGONAUTE1 by the autophagy pathway. *Proc. Natl. Acad. Sci. U.S.A.* 109, 15942–15946
72 Vaucheret, H. *et al.* (2006) AGO1 homeostasis entails coexpression of MIR168 and AGO1 and preferential stabilization of miR168 by AGO1. *Mol. Cell* 22, 129–136
73 Mallory, A.C. and Vaucheret, H. (2009) ARGONAUTE 1 homeostasis invokes the coordinate action of the microRNA and siRNA pathways. *EMBO Rep.* 10, 521–526
74 Mallory, A.C. *et al.* (2009) Redundant and specific roles of the ARGONAUTE proteins AGO1 and ZLL in development and small RNA-directed gene silencing. *PLoS Genet.* 5, e1000646
75 Earley, K. *et al.* (2010) An endogenous F-box protein regulates ARGONAUTE1 in *Arabidopsis thaliana*. *Silence* 1, 15
76 Cui, X. *et al.* (2005) A Begomovirus DNAbeta-encoded protein binds DNA, functions as a suppressor of RNA silencing, and targets the cell nucleus. *J. Virol.* 79, 10764–10775
77 Yang, X. *et al.* (2011) Suppression of methylation-mediated transcriptional gene silencing by betaC1-SAHH protein interaction during geminivirus-betasatellite infection. *PLoS Pathog.* 7, e1002329
78 Wang, H. *et al.* (2003) Adenosine kinase is inactivated by geminivirus AL2 and L2 proteins. *Plant Cell* 15, 3020–3032
79 Zhang, Z. *et al.* (2011) BSCTV C2 attenuates the degradation of SAMDC1 to suppress DNA methylation-mediated gene silencing in *Arabidopsis*. *Plant Cell* 23, 273–288
80 Kim, J.Y. *et al.* (2010) MicroRNA402 affects seed germination of *Arabidopsis thaliana* under stress conditions via targeting DEMETER-LIKE Protein3 mRNA. *Plant Cell Physiol.* 51, 1079–1083
81 Yang, J.Y. *et al.* (2008) betaC1, the pathogenicity factor of TYLCCNV, interacts with AS1 to alter leaf development and suppress selective jasmonic acid responses. *Genes Dev.* 22, 2564–2577
82 Chellappan, P. *et al.* (2005) MicroRNA-binding viral protein interferes with *Arabidopsis* development. *Proc. Natl. Acad. Sci. U.S.A* 102, 10381–10386
83 Hamera, S. *et al.* (2012) *Cucumber mosaic virus* suppressor 2b binds to AGO4-related small RNAs and impairs AGO4 activities. *Plant J.* 69, 104–115
84 Kanazawa, A. *et al.* (2011) Virus-mediated efficient induction of epigenetic modifications of endogenous genes with phenotypic changes in plants. *Plant J.* 65, 156–168
85 Mi, S. *et al.* (2008) Sorting of small RNAs into *Arabidopsis* argonaute complexes is directed by the 5′ terminal nucleotide. *Cell* 133, 116–127
86 Montgomery, T.A. *et al.* (2008) Specificity of ARGONAUTE7-miR390 interaction and dual functionality in TAS3 trans-acting siRNA formation. *Cell* 133, 128–141
87 Allen, E. *et al.* (2005) microRNA-directed phasing during trans-acting siRNA biogenesis in plants. *Cell* 121, 207–221
88 Zhai, J. *et al.* (2011) MicroRNAs as master regulators of the plant NB-LRR defense gene family via the production of phased, trans-acting siRNAs. *Genes Dev.* 25, 2540–2553
89 Mourrain, P. *et al.* (2000) *Arabidopsis SGS2* and *SGS3* genes are required for posttranscriptional gene silencing and natural virus resistance. *Cell* 101, 533–542
90 Ruiz-Ferrer, V. and Voinnet, O. (2009) Roles of plant small RNAs in biotic stress responses. *Annu. Rev. Plant Biol.* 60, 485–510
91 Li, H.W. *et al.* (1999) Strong host resistance targeted against a viral suppressor of the plant gene silencing defence mechanism. *EMBO J.* 18, 2683–2691
92 Scholthof, H.B. *et al.* (1995) Identification of tomato bushy stunt virus host-specific symptom determinants by expression of individual genes from a potato virus X vector. *Plant Cell* 7, 1157–1172
93 Chu, M. *et al.* (2000) Genetic dissection of tomato bushy stunt virus p19-protein-mediated host-dependent symptom induction and systemic invasion. *Virology* 266, 79–87
94 Pandey, S.P. and Baldwin, I.T. (2007) RNA-directed RNA polymerase 1 (RdR1) mediates the resistance of *Nicotiana attenuata* to herbivore attack in nature. *Plant J.* 50, 40–53
95 Nakahara, K.S. *et al.* (2012) Tobacco calmodulin-like protein provides secondary defense by binding to and directing degradation of virus RNA silencing suppressors. *Proc. Natl. Acad. Sci. U.S.A.* 109, 10113–10118
96 Shivaprasad, P.V. *et al.* (2012) A microRNA superfamily regulates nucleotide binding site-leucine-rich repeats and other mRNAs. *Plant Cell* 24, 859–874
97 Cuperus, J.T. *et al.* (2010) Unique functionality of 22-nt miRNAs in triggering RDR6-dependent siRNA biogenesis from target transcripts in *Arabidopsis*. *Nat. Struct. Mol. Biol.* 17, 997–1003
98 Chen, H.M. *et al.* (2010) 22-Nucleotide RNAs trigger secondary siRNA biogenesis in plants. *Proc. Natl. Acad. Sci. U.S.A.* 107, 15269–15274
99 Tian, D. *et al.* (2003) Fitness costs of R-gene-mediated resistance in *Arabidopsis thaliana*. *Nature* 423, 74–77
100 Navarro, L. *et al.* (2008) Suppression of the microRNA pathway by bacterial effector proteins. *Science* 321, 964–967
101 Bendahmane, A. *et al.* (1999) The *Rx* gene from potato controls separate virus resistance and cell death responses. *Plant Cell* 11, 781–791
102 Pruss, G.J. *et al.* (2004) The potyviral suppressor of RNA silencing confers enhanced resistance to multiple pathogens. *Virology* 320, 107–120

103 Dunoyer, P. *et al.* (2006) Induction, suppression and requirement of RNA silencing pathways in virulent *Agrobacterium tumefaciens* infections. *Nat. Genet.* 38, 258–263
104 Robaglia, C. and Caranta, C. (2006) Translation initiation factors: a weak link in plant RNA virus infection. *Trends Plant Sci.* 11, 40–45
105 Cosson, P. *et al.* (2010) RTM3, which controls long-distance movement of potyviruses, is a member of a new plant gene family encoding a meprin and TRAF homology domain-containing protein. *Plant Physiol.* 154, 222–232
106 Ishibashi, K. *et al.* (2009) An inhibitory interaction between viral and cellular proteins underlies the resistance of tomato to nonadapted tobamoviruses. *Proc. Natl. Acad. Sci. U.S.A.* 106, 8778–8783
107 Moffett, P. (2009) Mechanisms of recognition in dominant R gene mediated resistance. *Adv. Virus Res.* 75, 1–33
108 Kasschau, K.D. *et al.* (2003) P1/HC-Pro, a viral suppressor of RNA silencing, interferes with *Arabidopsis* development and miRNA function. *Dev. Cell* 4, 205–217
109 Varallyay, E. *et al.* (2010) Plant virus-mediated induction of miR168 is associated with repression of ARGONAUTE1 accumulation. *EMBO J.* 29, 3507–3519
110 Brodersen, P. *et al.* (2008) Widespread translational inhibition by plant miRNAs and siRNAs. *Science* 320, 1185–1190
111 Manavella, P. *et al.* (2013) Tissue-specific silencing of *Arabidopsis thaliana* SU(VAR)3-9 HOMOLOG8 by miR171a*. *Plant Physiol.* 161, 805–812
112 Zhang, X. *et al.* (2011) *Arabidopsis* Argonaute 2 regulates innate immunity via miRNA393(*)-mediated silencing of a Golgi-localized SNARE gene, MEMB12. *Mol. Cell* 42, 356–366
113 Jones, J.D. and Dangl, J.L. (2006) The plant immune system. *Nature* 444, 323–329
114 Dodds, P.N. and Rathjen, J.P. (2010) Plant immunity: towards an integrated view of plant-pathogen interactions. *Nat. Rev. Genet.* 11, 539–548

Since this review was written, two studies have been published that should be mentioned here. The first shows that HC-Pro during TuMV-GFP infection associates with 21nt antiviral siRNAs and prevents their loading into AGO1, AGO2 and AGO10 (Garcia-Ruiz *et al.*, 2015). Since a silencing suppression-deficient allele of HC-Pro containing two point mutations showed greatly reduced association to siRNAs, the authors conclude that HC-Pro suppresses RNAi mainly by binding and sequestering siRNAs. This topic will be taken up again in Chapter 2.

The second work shows that strong VSRs, such as P38 and 2b, are not only able to suppress RNAi, but also the action of RTL1 (Shamandi *et al.*, 2015). As mentioned previously (see section I), overexpression of RTL1 has been shown to degrade dsRNA upstream of DCL2, DCL3 and DCL4 and prevent antiviral RNAi, likely through dicer substrate depletion. In the same study, the authors showed through transient expression assays that the depletion of siRNAs caused by overexpression of RTL1 was completely abolished by VSRs P38, 2b and HC-Pro. The fact that several VSRs are able to inhibit RTL1 action further suggests the role of this protein in antiviral defense. How these strong VSRs can inhibit a pathway upstream of RNAi remains open to debate. Moreover, it seems unlikely that all three VSRs have developed distinct mechanisms to repress RTL1. In the case of P38, a point mutation deleting its ability to suppress RNAi also deletes its ability to inhibit RTL1, suggesting that P38 represses RNAi and RTL1 action through the same mechanism. This topic provides compelling work for the future, since its study could uncover novel interconnections between RNAi and other RNAse-based defense mechanisms, and could challenge our current perception of what is upstream and what is downstream in and around RNAi.

IV - *Peanut Clump Virus* (PCV) and P15, its VSR

Peanut Clump virus (PCV) was first described by Thouvenel and colleagues in 1974. Reported at first only in a few locations in Senegal and Burkina Faso, it has since then expanded and in the 90s could be found all around West Africa and India. It causes peanut clump disease on peanut (*Arachis hypogea*), which entails severely stunted growth, dark leaves and reduced fruit yield. However, symptoms can vary widely (www.icrisat.org). PCV has a wide host range, including peanut, wheat (*Triticum aestivum*), bean (*Phaseolus vulgaris*), *Nicotiana*

benthamiana and *Chenopodium amaranticolor* (www.dpvweb.net), among others. *A. thaliana* is not a listed host, but in this work we describe how efficient infection on this species can be achieved. PCV is transmitted by the soil-borne fungus *Polymyxa graminis* (Dieryck *et al.*, 2011).

PCV belongs to the family Virgaviridae, and together with its close relative *Indian peanut clump virus* (IPCV) forms the genus Pecluvirus. Closely related genera are Benyvirus and Pomovirus. PCV is a rod-shaped virus whose genome is made up by two genomic (+)-ssRNA molecules, and during infection several subgenomic RNAs are made. The two genomic RNAs (RNA1 is ≈5900nt long, RNA2 is ≈4500nt long) are 5' capped, while at the 3' end their sequence is highly homologous and can fold into a tRNA-like structure that is valylated. In contrast with *Turnip yellow mosaic virus* (TYMV), for which valylation of the 3' tRNA-like structure is mandatory for infectivity, in the case of PCV it increases replication but is not mandatory (Matsuda *et al.*, 2000). RNA1 possesses two ORFs: (i) a 131kDa helicase and its readthrough-generated alternative 191kDa replicase also containing a polymerase domain and (ii) a small 15 kDa cysteine-rich protein, P15, which is the object of this thesis. The latter is expressed through a subgenomic RNA. RNA2 possesses five ORFs: the coat protein (CP), which is not required for replication but is necessary for vascular movement (Herzog *et al.*, 1998), a 39kDa ORF that is thought to be involved in vector transmission (Hull, 2002) and a triple gene block (TGB) that, as for all viruses carrying it, is necessary for cell-to-cell and systemic movement of PCV (Herzog *et al.*, 1998). TGB1 protein has been shown to localize to plasmodesmata (Erhardt *et al.*, 1999). PCV replicates in membranous compartments derived from the endoplasmic reticulum and possibly the Golgi apparatus (Dunoyer *et al.*, 2002b).

The aforementioned second ORF of RNA1 encodes a cysteine-rich protein (CRP) that is essential for PCV replication (Herzog *et al.*, 1998), called P15. Early studies on this protein established that it is not localized at the site of replication during infection, a counter-intuitive feature for a protein presumably involved in replication (Dunoyer *et al.*, 2001). Small CRPs are encoded by the 3' terminal region of other virus genera, namely hordei-, furo-, tobra- and carlaviruses, and are sometimes associated to virus and viral protein accumulation (Dunoyer *et al.*, 2002; Herzog *et al.*, 1998). The most informative study on this

protein was carried out by Dunoyer, Pfeffer, *et al.*, 2002, establishing that P15 is a suppressor of RNAi, which explains its fundamental role in viral accumulation. Dimerization through its C-terminal putative coiled-coil is mandatory for silencing suppression. P15 possesses a C-terminal –SKL tripeptide that is a type 1 peroxisomal targeting signal (PTS1). Accordingly, GFP-fused P15 was observed through microscopy to localize in peroxisome-like microbodies. PCVΔN6, carrying an allele of P15 lacking the last coiled-coil heptad and the –SKL tripeptide (P15ΔN6) was able to replicate as efficiently as PCVwt in BY-2 cells, but was unable to move systemically in *N. benthamiana* plants. The authors concluded that peroxisomal localization of P15 is dispensable for suppression of RNAi, while it is mandatory for systemic movement of PCV (see some of these experiments repeated in **Fig. 2.1**). This duality is central to the work presented in this thesis. The means through which P15 suppresses RNAi are investigated in Chapter 1, while the role of its peroxisomal localization in PCV movement is investigated in Chapter 2.

V - Peroxisomes and peroxisomal protein import

Given the peroxisomal localization of P15 and its importance in PCV life cycle, a brief introduction on peroxisomes and the peroxisomal importomer is necessary for a better interpretation of the data presented in this work. We shall here focus on a few select aspects of plant peroxisome biology. For a more complete vision the reader is directed toward an excellent review by Kaur *et al.*, 2009. The authors describe peroxisomes as "…small eukaryotic organelles surrounded by a single membrane and specialized in oxidative metabolic reactions. They are devoid of nucleic acids and ribosomes and import their complement of proteins post-translationally from the cytosol". Among the functions performed by plant peroxisomes are lipid metabolism, photorespiration, nitrogen metabolism, detoxification, synthesis of some plant hormones, photomorphogenesis and plant-pathogen interactions. Many of the reactions happening in the peroxisome require exchange of metabolites with chloroplasts and mitochondria, leading to frequent physical association (Kaur *et al.*, 2009). Historically, according to their function peroxisomes can be classified as glyoxysomes in seedlings, gerontosomes in senescent tissues, leaf peroxisomes and unspecialized peroxisomes. Peroxisomes originate from the ER, are typically 0.1 to 1

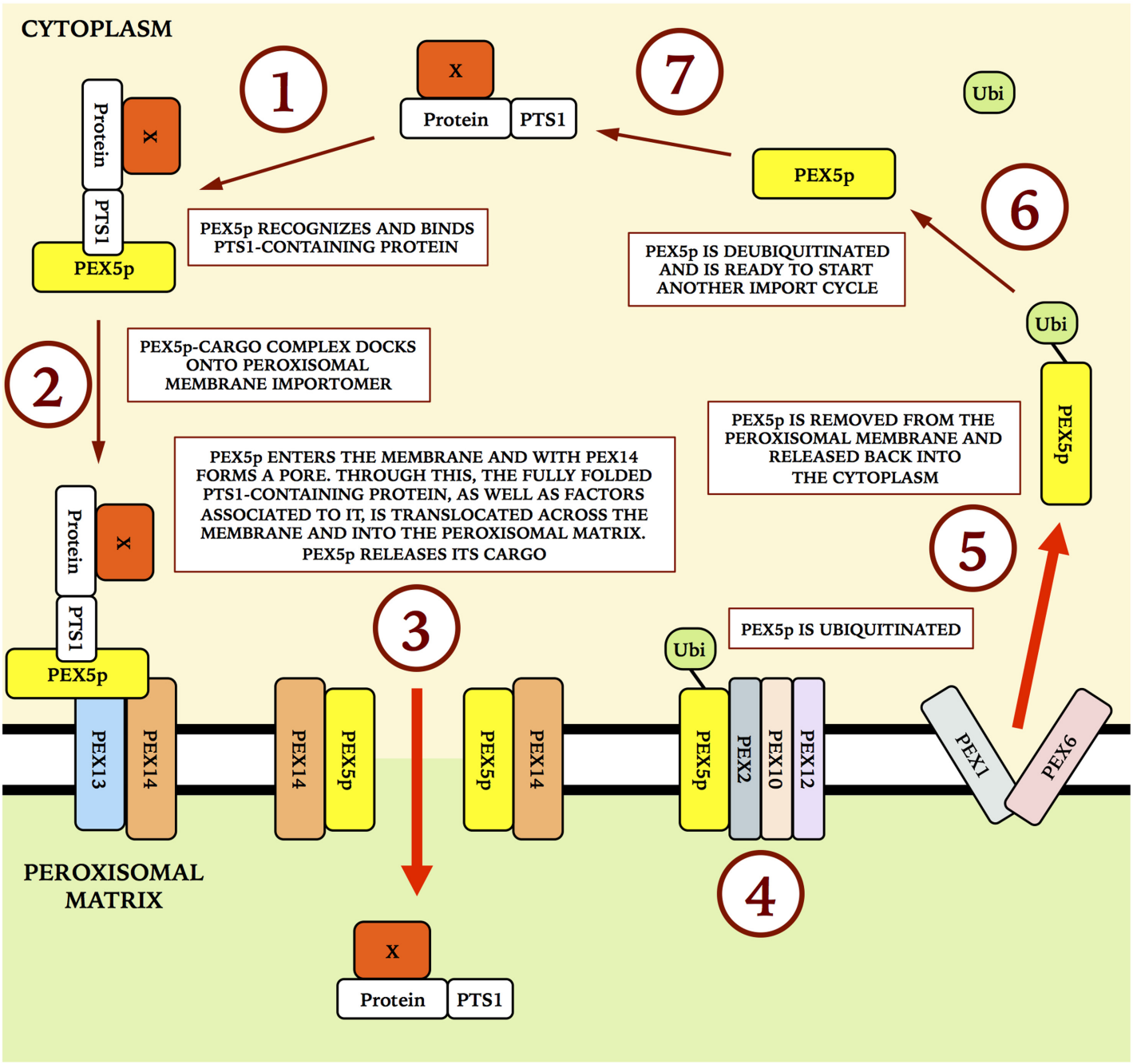

Figure IV: The peroxisomal importomer (adapted from Hasan *et al.*, 2013).
The PEX5p-mediated peroxisomal import cycle. PEX5p binds the PTS1 (Peroxisome Targeting Sequence 1) tripeptide (1) on a protein, shuttling this PTS1-containing protein and its potential cargo across the peroxisomal pore and into the organelle (2-3). PEX5p is then ubiquitinated (4) and re-exported back to the cytoplasm (5-6), where it can start another import cycle (7). X represents a cargo molecule that is bound to the PTS1-containing protein and is "piggybacked" into the peroxisome.

μm in diameter, move on the actin-myosin system in plants, and host a population of about one hundred different proteins, about double that of yeast and mammalian peroxisomes (Hasan *et al.*, 2013; Lanyon-Hogg *et al.*, 2010).

All peroxisomal proteins are synthesized by ribosomes in the cytoplasm and imported into the peroxisomal matrix by specialized receptors, PEX5 and PEX7, which recognize peroxisomal targeting motifs PTS1 and PTS2, respectively. However, the import does not take place as in other organelles, where the cargo protein is unfolded in order to pass the organellar pore and successively re-folded. The peroxisomal importomer is capable not only of importing folded proteins, but also oligomers of two or more associated proteins in what is known as "piggybacking" (Leon *et al.*, 2006). In fact, a subset of peroxisomal proteins is imported into peroxisomes not because they possess PTS motifs but because they are "piggybacked" by proteins that possess them. This extraordinary ability is of crucial importance in the present work.

Most peroxisomal matrix proteins harbor a C-terminal PTS1 targeting signal, defined by aminoacids SKL and variants (S/A/C - K/R/H - L/A) that is bound by import receptor PEX5 via tetratricopeptide repeats (TPR) present in its C-terminal half. PTS2-containing proteins are bound by import receptor PEX7, which in plants is then bound by PEX5. Peroxisomal import of receptor-cargo complexes can be divided into five stages: (1) cargo recognition by the import receptor in the cytosol, (2) docking of the receptor-cargo complex to the docking complex on the peroxisomal membrane, (3) cargo translocation across the membrane into the peroxisomal matrix, (4) release of the cargo and (5) recycling of the receptor for further rounds of import (Hasan *et al.*, 2013). Since PEX5 is the most important, best-characterized receptor and P15 possesses a PTS1, we shall here focus on this pathway (**Fig. IV**). PEX5 has been confirmed to be the PTS1 import receptor in plants (Kragler *et al.*, 1998). Most studies on peroxisomal import mechanics have been performed on yeast and mammalian cells, so while we cannot assign the exact same mechanisms to plants, since these pathways are quite conserved from yeast to human we can presume a certain amount of similarity in the general working and in the factors involved.

Upon binding its PTS1-bearing cargo, PEX5 has been shown to undergo significant conformational changes (Stanley *et al.*, 2006) that may be responsible for the fact that only

cargo-bound PEX5 is imported into peroxisomes (Gouveia *et al.*, 2003b). The PEX5-cargo complex then approaches the peroxisome membrane and PEX5 binds the so-called docking complex, made up of two transmembrane proteins that interact with each other, PEX13 and PEX14 (Pires *et al.*, 2003). After this, the cargo is translocated across the membrane through a mechanism that remains elusive. Several models have been proposed (Erdmann and Schliebs, 2005; Lanyon-Hogg *et al.*, 2010). The one that best explains the data collected in recent years is the transiently opened import pore (Hasan *et al.*, 2013). While the major members of this pore could be PEX13 and PEX14, the fact that PEX5 is able to bind lipids and effectively behave like an integral membrane protein suggests that it could indeed become part of the pore with PEX14 (Erdmann and Schliebs, 2005; Gouveia *et al.*, 2003a; Kerssen *et al.*, 2006). An experimentally reconstituted PEX5-PEX14 complex in a membrane is capable of acting as a channel when incubated with PEX5-cargo complexes, attaining a maximum diameter of 9nm (Meinecke *et al.*, 2010), that would indeed allow passage of folded proteins and possibly oligomers.

The next step is the release of the cargo from PEX5. Whether PEX5 completely or partially enters the peroxisomal matrix before doing this is not known. Also not clear is how exactly PEX5 releases its cargo. Some suggest the PEX5-cargo disassembly could be due to pH change (Wang *et al.*, 2003). Another study reports that release is mediated by the N-terminal part of PEX14 (Freitas *et al.*, 2011). After cargo release inside the peroxisome, PEX5 is monoubiquitinated by a RING-peroxin complex consisting of PEX2, PEX10 and PEX12 that has E3 activity (Kaur *et al.*, 2013). Once ubiquitinated, PEX5 is extracted from the membrane in an ATP-dependent manner by PEX6 and PEX1 and released back on the cytosolic side (Grimm *et al.*, 2012; Platta *et al.*, 2005), though again precisely how this unfolds remains an open question. Briefly after exit PEX5 is deubiquitinated and is ready to bind another cargo, starting the process over (Debelyy *et al.*, 2011; Hasan *et al.*, 2013).

Peroxisomes have been shown to play very important roles in plant-pathogen interactions. They are probably the main sites of accumulation of H_2O_2 and reactive oxygen species, which in turn play a pivotal role in incompatible reactions against pathogenic bacteria and fungi (Camejo *et al.*, 2016). Peroxisomal proteins of the GOX and PEN families have been shown to be responsible for many intra- and extracellular changes triggered by pathogen

detection. Moreover, several reactions in the synthesis of jasmonic acid (JA) and possibly of salicylic acid (SA) have been shown to take place within peroxisomes (Kaur *et al.*, 2009). These two hormones are known to stimulate defense reactions and to regulate each other. JA is involved in defense against bacteria, fungi, herbivores (Okada *et al.*, 2015) and incompatible virus interactions (Alazem and Lin, 2015).

Some examples are reported of interaction between viruses and peroxisomes. The best characterized example is the recruitment by tombusviruses of peroxisomal membranes as replication sites (Xu and Nagy, 2014). Although in yeast they are able to switch to other membranes if peroxisome biogenesis is compromised, most tombusviruses hijack the cellular membrane-deforming ESCRT machinery to create invaginations in the peroxisomal membrane that result in vesicles with small openings toward the cytosol where the virus can replicate (Barajas *et al.*, 2009). Protein VP4 of mammalian rotavirus possesses a very conserved PTS1 and is imported into peroxisomes, but the biological function of this localization is not known (Mohan *et al.*, 2002). Some plant viruses belonging to genus hordeivirus, closely related to PCV, encode small cysteine-rich proteins which possess PTS1 peptides (Savenkov *et al.*, 1998). While sequence similarity with P15 is low, the fact that the viruses are close relatives suggests that the function of peroxisomal localization of these proteins in viral infection, which is unknown, may resemble that of P15. However, unlike P15, the peroxisomal localization of γb protein of *Poa semilatent virus* was shown to be dispensable for viral systemic movement (Yelina *et al.*, 2005).

CHAPTER 1

EFFECT OF P15 ON CELL- AND NON-CELL AUTONOMOUS RNA SILENCING

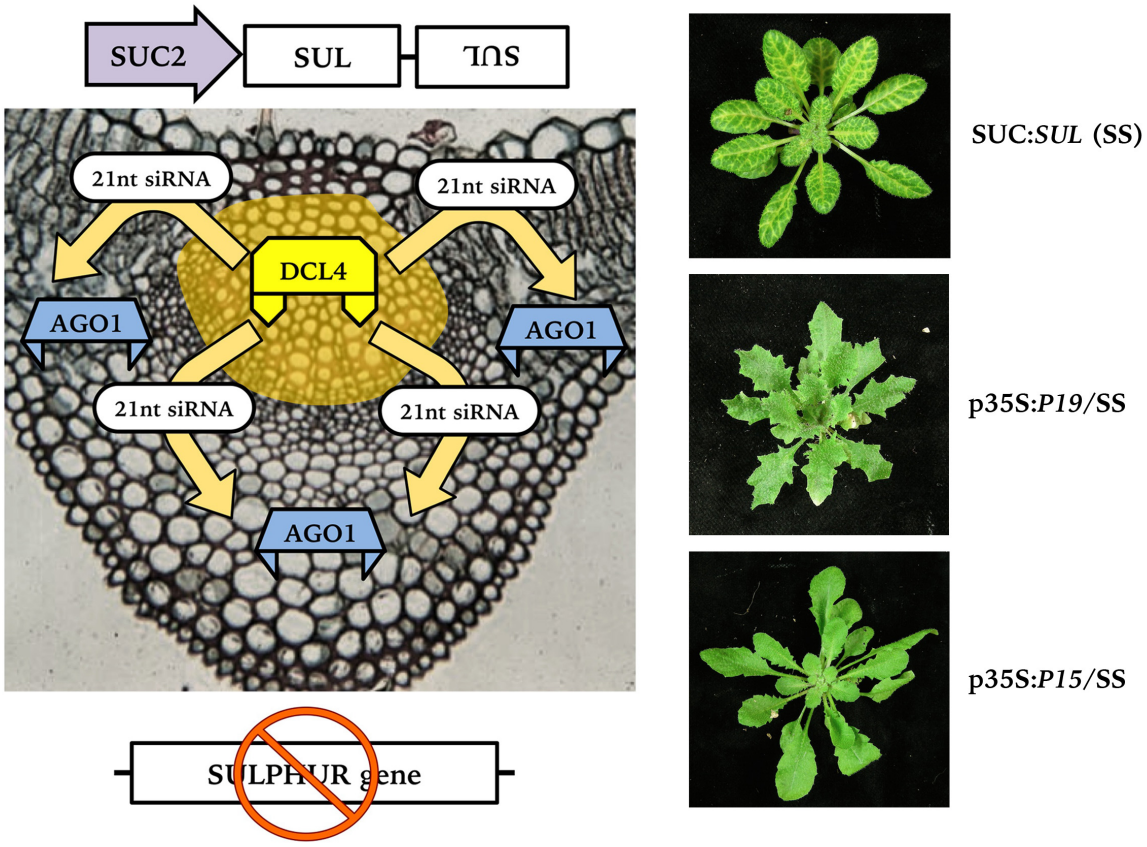

Figure 1.1: The SUC:*SUL* RNAi reporter system (SS).
Left: schematic representation on a leaf transversal section of the main events responsible for the yellow-vein SUC:*SUL* (SS) silencing phenotype, in which mobile DCL4-dependent, hairpin-derived siRNAs trigger the silencing of the endogenous *SULPHUR* gene through AGO1. Right: photos of a SS plant showing the characteristic phenotype (top) and of SS plants expressing VSRs P19 and P15 (middle and bottom) that abolish *SULPHUR* silencing.

During the last two decades many reporter systems have been devised to understand how RNA silencing operates at the molecular level. One of the most versatile and convenient to screen is the *A. thaliana* transgenic SUC:*SUL* system (pSUC:hp*SUL*, here abbreviated with SS) (Dunoyer *et al.*, 2010, 2007, 2005; Himber *et al.*, 2003). In this system, the companion cell-specific SUC2 promoter drives the transcription of an inverted repeat hairpin carrying the sequence of the endogenous *CH-42* gene (magnesium-chelatase subunit chlI – locus AT4G18480, here referred to as *SULPHUR*). This dsRNA hairpin is processed by DCL4 and DCL3 into siRNA of 21nt and 24nt, respectively. The DCL4-dependent 21nt siRNA move 10-15 cells outside the phloem companion cells and trigger AGO1-dependent PTGS of the *SULPHUR* gene in the recipient cells, that in turn leads to a yellow-vein phenotype (SS phenotype or *SUL*-silencing phenotype) (**Fig. 1.1**). The SS construct expressed in a *dcl4* knockout mutant is processed but does not lead to yellowing of veins, indicating that DCL3-dependent 24nt siRNAs are not able to mediate PTGS in this system.

For the *SUL*-silencing phenotype to appear the siRNAs need (i) to be generated, (ii) to be able to move cell-to-cell, (iii) to be loaded into AGO in recipient cells and (iv) to mediate PTGS. Every step in the mobile PTGS pathway can be monitored with this system. A specific experimental approach can be followed to investigate each of these steps: total RNA analysis to score generation of siRNAs, SUC2-driven expression of factors of interest to score their ability to promote or stop siRNA movement, AGO immunoprecipitation to score siRNA loading in recipient cells, and visual observation to score loaded AGO functionality. All these experimental approaches have been used in this work to answer specific questions concerning P15.

The SS system has been used in the past to conduct forward genetic screens through EMS mutagenesis to retrieve mutants in endogenous *A. thaliana* factors that are impaired in one or more of the RNAi steps mentioned above (Dunoyer *et al.*, 2007, 2005).

However, the SS system can also serve as a means to investigate how VSRs work (Dunoyer *et al.*, 2010; Schott *et al.*, 2012). As presented in detail further on, ubiquitous 35S-driven expression of a strong VSR abolishes the yellow vein *SUL*-silencing phenotype (**Fig. 1.1**) and can be used to probe the effect of a given suppressor on cell-autonomous RNA silencing. Furthermore, SUC2-driven expression of a VSR that is able to stop the cell-to-cell movement of siRNAs will also abolish the yellow vein phenotype, and can be used to probe

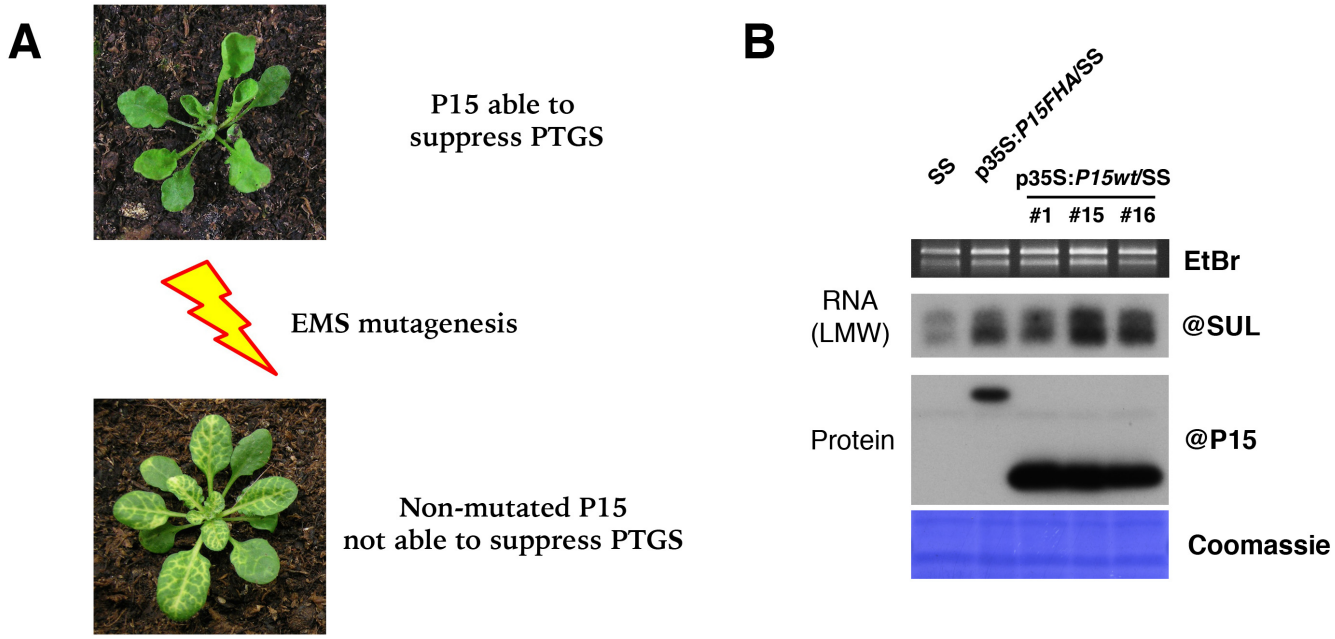

Figure 1.2: Mutagenesis of p35S:*P15*/SS to obtain SS phenotype revertants.
(A) schematic representation of the objective of the mutagenesis, the discovery of host factors necessary for P15 VSR activity. (B) anti-*SUL* siRNA and P15 protein accumulation in parental lines prior to EMS mutagenesis. p35S:*P15FHA*/SS was used for the first mutagenesis, p35S:*P15wt*/SS#16 for the second.

the effect of this suppressor on siRNA cell-to-cell movement. In this chapter, we present the results yielded by our experiments employing the SS system to determine how, and at what step, P15 suppresses RNA silencing.

1.1 - Characterization of the mode of action of P15 in the suppression of cell-autonomous RNA silencing

1.1a - Forward genetic screens via EMS mutagenesis

Since VSRs often act on stages of RNA silencing that are poorly understood, they can be used as genetic and biochemical tools to probe these pathways. P15 mode of action was not well characterized, so we used P15 as a reporter within the SS system in a forward genetic screen set up to investigate cell-autonomous RNA silencing. To identify gene products necessary for P15 suppression of RNA silencing we conducted EMS mutagenesis of p35S:*P15*/SS seeds. The objective was to obtain, through random mutagenesis, point mutants in which P15 suppression of silencing was abolished, leading to reversion of phenotype from green leaves (suppressed *SUL*-silencing) to yellow-veined leaves (functional *SUL*-silencing) (**Fig. 1.2**). Any mutation disrupting interaction of P15 with a partner mandatory for silencing suppression or disrupting the action of the partner itself, while maintaining functional RNAi, could lead to reversion of phenotype. While disruptive mutations within P15 would have been considered interesting, the focus here was on mutations in host factors leading to *SUL*-silencing phenotype restoration in the presence of non-mutated P15.

A first mutagenesis was carried out on a p35S:*P15FHA*/SS line expressing a Flag-HA (FHA) epitope-tagged P15 that is proficient in suppressing RNAi but not targeted to peroxisomes due to masking of PTS1 by the tag (**Fig. 2.2**). After germination and growth of the mutagenized seeds, the following generation was visually screened for revertant *SUL*-silencing phenotype. Molecular analysis of the few revertants obtained revealed that in all cases return of *SUL*-silencing phenotype was due to destabilization of P15FHA (**Fig. S1**,

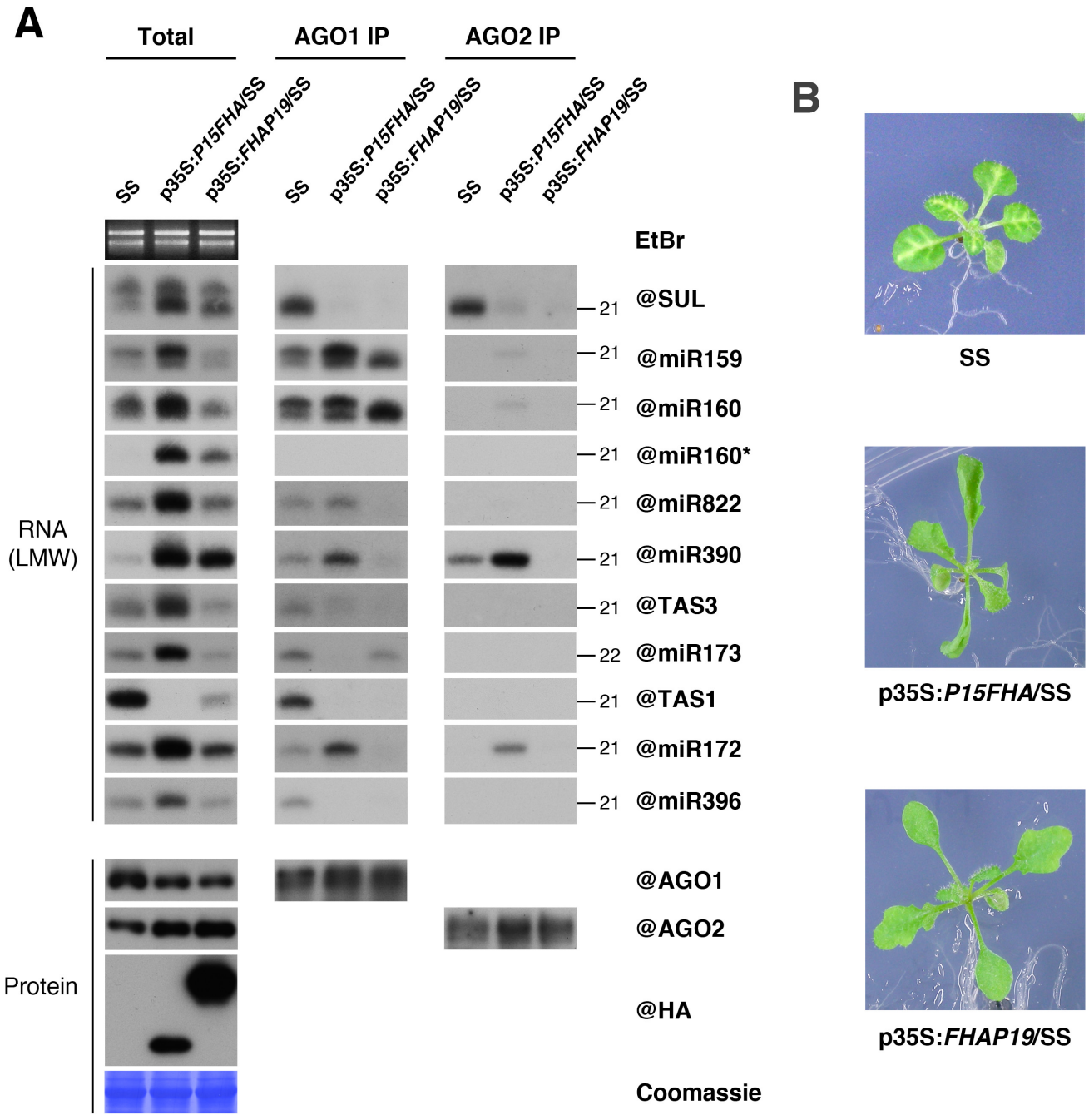

Figure 1.3: Effect of P15FHA on sRNA loading into AGO1 and AGO2.
Left: Northern blot analysis of low molecular weight (LMW) RNA (top) and western blot analysis of protein (bottom) from total seedling extracts and AGO1/AGO2 IPs. Right: photos of the seedlings at the moment of harvest. P15FHA prevents AGO loading of 21nt siRNAs and 22nt miRNAs, but not of 21nt miRNAs.

Annex1). Whether this was due to P15 mutation or secondary effects of EMS mutagenesis is not known. In one case anti-35S promoter siRNA were found, suggesting TGS of the P15FHA transgene. Consequently, the mutants were not further characterized. A second mutagenesis was performed on a p35S:*P15wt*/SS line expressing the wild-type allele of P15 (line #16, Fig. 1.2). Again, *SUL*-silencing phenotype return was sporadic and always due to significant decrease or complete disappearance of P15. The revertants were not further characterized. Given the absence of relevant results, the forward genetic approach was abandoned. At the same time, a biochemical approach was followed to identify P15 mode of action and cellular partners *in vivo*.

1.1b - AGO immunoprecipitation

sRNA loading into AGO effectors is a fundamental step in RNAi. Anti-*SUL* siRNA loading into AGO1 is necessary for *SULPHUR* gene silencing and the consequent *SUL*-silencing phenotype to appear (Dunoyer *et al.*, 2007; Schott *et al.*, 2012). Given that ubiquitous p35S:*P15FHA* expression abolishes *SULPHUR* gene silencing, we decided to biochemically assess the effect of P15FHA on sRNA loading into the main antiviral AGOs by performing immunoprecipitation (IP) of AGO1 and AGO2 and analyzing the co-immunoprecipitated (co-IPed) sRNA by PAGE low molecular weight (LMW) Northern blot (**Fig. 1.3A**). We performed the experiment on 3-week-old seedlings of SS, p35S:*P15FHA*/SS and p35S:*FHAP19*/SS. As seen in the introduction, P19 inhibits AGO1 loading through size-specific sequestration of 21nt sRNA duplexes (Schott *et al.*, 2012; Vargason *et al.*, 2003), and was thus here used as positive control.

In both P15FHA- and FHAP19-expressing lines the *SUL*-silencing phenotype was suppressed (**Fig. 1.3B**). Total RNA analysis showed that anti-*SUL* siRNAs were correctly generated, suggesting suppression of silencing downstream of the dicing step. Co-IPed RNA analysis revealed that P15FHA, as FHAP19, severely impaired the loading of both AGO1 and AGO2 with anti-*SUL* siRNAs. Given that steady state levels of AGO1 and AGO2 didn't show significant change in the presence of P15FHA, the cause of *SUL*-silencing phenotype disappearance can be ascribed to suppression of AGO1 loading with anti-*SUL* siRNAs. P15FHA also prevented AGO1 loading with ta-siRNA derived from *TAS3*.

On the other hand, AGO1 loading with endogenous DCL1-dependent 21nt miRNA (miR159, miR160, miR172) was not prevented by P15FHA, while it was prevented by FHAP19. One observed exception was miR396, whose loading into AGO1 was prevented. The complementary strands of miRNA (miRNA*), absent in SS total extracts as expected, were stabilized by P15FHA and FHAP19 (miR160*), although they were not found in association with AGO1 (see also **Fig. S2** – Annex 1). Loading of DCL4-dependent miR822 was not prevented. However, comparing the miR822 loading pattern into AGO1 with those of DCL1-dependent 21nt miRNA on one side, and with the pattern of miR822 steady-state levels on the other, it can be inferred that P15FHA may strongly inhibit DCL4-dependent miRNA loading into AGO1.

Conversely, AGO1 loading of 22nt-long miR173 was completely abolished. The same was observed for 22nt miR393 and miR472 (**Fig. S3** – Annex 1). Failed AGO1 loading of miR173 is very likely the cause of the absence of ta-siR255 in p35S:*P15FHA*/SS seedlings, as the AGO1-miR173 complex is responsible for DCL4-dependent production of this ta-siRNA from *TAS1* (Allen *et al.*, 2005; Xie *et al.*, 2005).

Interestingly, some miRNA (miR159, miR160, miR172, miR390) were found loaded into AGO2 exclusively in the presence P15FHA. Although further investigation on this topic is necessary, given P15FHA-dependent inhibition of siRNA loading, it can be hypothesized that failed loading with siRNA frees a pool of AGO2 that is subsequently loaded with miRNA. A similar pattern can be observed in the pattern of DCL1-dependent 21nt miRNA loading into AGO1. However, this phenomenon could also be ascribed to the increase in steady-state miRNA in seedlings expressing P15FHA.

From this experiment we conclude that P15 suppresses RNA silencing by preventing 21nt siRNA loading into AGO1. Although AGO2 is not an effector in SS silencing (Dunoyer *et al.*, 2010), P15-dependent inhibition of siRNA loading into AGO2 may be relevant in terms of antiviral defense. AGO1 loading of the vast majority of 21nt miRNAs was not affected, while loading of 22nt miRNA was abolished. This observation led us to postulate that P15FHA may show a bias toward 22nt sRNA in its suppression of AGO1 loading. We therefore proceeded to assess the effect of P15FHA on AGO1 loading with 22nt siRNA.

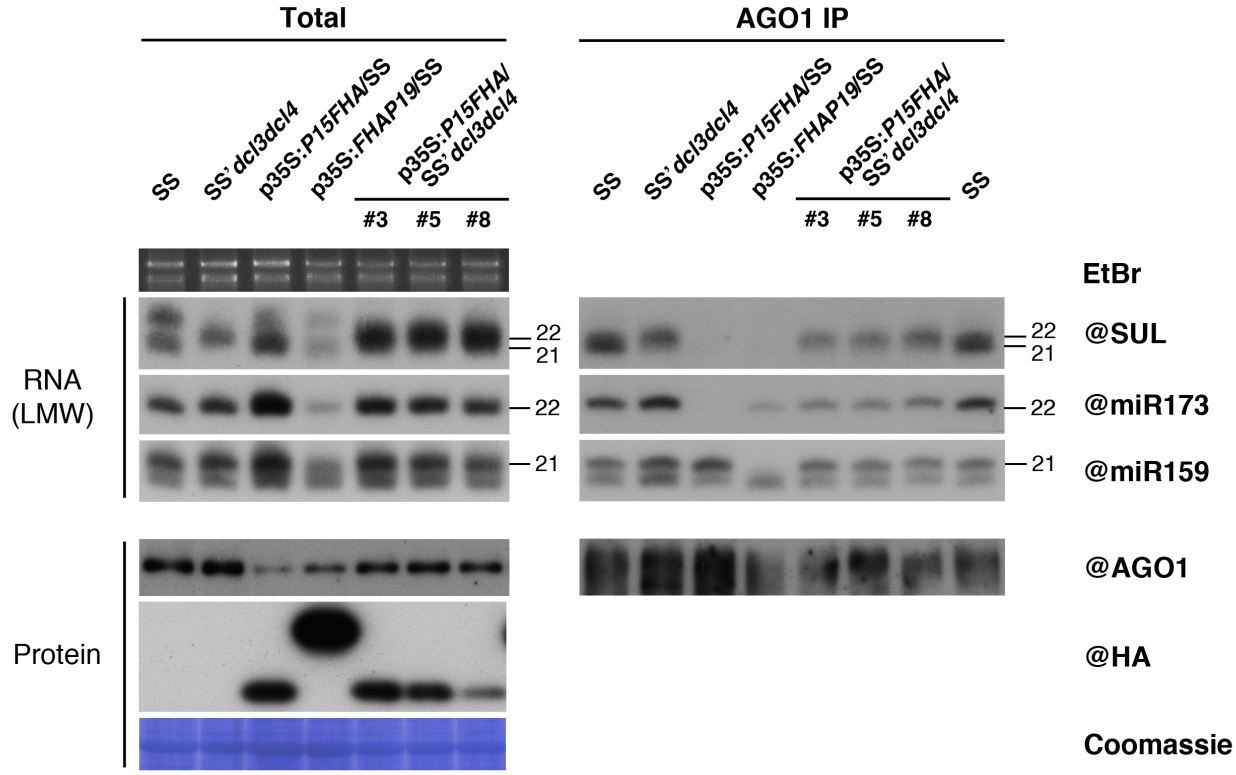

Figure 1.4: Effect of exclusive DCL2 siRNA generation on P15FHA VSR activity.
Left: Northern blot analysis of low molecular weight (LMW) RNA (top) and western blot analysis of protein (bottom) from total seedling extracts. Right: same analysis but on AGO1 IPs. A surge in 22nt siRNAs compromises efficient inhibition of AGO1 loading by P15FHA.

In the SS system the silencing phenotype trigger is DCL4-dependent 21nt siRNAs. Given that P15FHA efficiently inhibits AGO1 loading of 22nt miRNAs, we decided to test the effect of P15FHA on AGO1 loading with DCL2-dependent 22nt siRNAs. To this end we introduced p35S:*P15FHA* in a *dcl3dcl4* double knockout expressing the SS hairpin. In this system anti-*SUL* siRNAs, and in general all siRNAs, are generated by DCL2 and are consequently 22nt long (Dunoyer *et al.*, 2007). This line results from a separate SUC:*SUL* transformation event compared to the SS line, contains multiple transgene insertions, and will be referred to as SS'*dcl3dcl4*. Only if the SS transgene is present in multiple copies does DCL2 produce enough anti-*SUL* siRNAs for the *SUL*-silencing phenotype to appear, possibly due to low levels or low activity of DCL2 in companion cells. Again, we analyzed total RNA extracts and AGO1 co-IPed RNA from seedlings by Northern blot (**Fig. 1.4**).

The shift in anti-*SUL* siRNA size to 22nt could be clearly seen in SS'*dcl3dcl4*, and these siRNA increased in titer in the three p35S:*P15FHA*/SS'*dcl3dcl4* lines analyzed, although it cannot be said whether this was due to increased SS transgene transcription, siRNA stabilization, or both. AGO1 IP revealed that 22nt siRNA loading was only partially prevented by P15FHA. Accordingly, the *SUL*-silencing phenotype appeared in all p35S:*P15FHA*/SS'*dcl3dcl4* lines except in line #3, where it appeared only at later stages of growth. Furthermore, in SS'*dcl3dcl4* 22nt miR173 loading into AGO1 was only partially blocked by P15FHA, while in SS it was completely abolished. Considering the expected bias toward suppression of AGO1 loading with 22nt sRNA, these results were surprising. However, a possible explanation can be given by taking into account the nature of siRNA populations in the *dcl3dcl4* background. DCL3-dependent heterochromatic siRNAs represent the vast majority of the total siRNAs present in a plant at any given moment (Axtell, 2013). Considering the ability of DCL2 to act as surrogate to DCL3 and DCL4, it is probable that along with the anti-*SUL* siRNAs, a great deal of other DCL3- and DCL4-dependent siRNAs are generated by DCL2 and are therefore 22nt in length. In our experiment this surge in 22nt siRNAs may have overwhelmed the pool of P15FHA present in cells, dampening its ability to suppress AGO1 loading of 22nt anti-*SUL* siRNAs and 22nt miRNAs. Alternatively, in these lines the 35S:*P15FHA* transgene undergoes silencing in a localized manner, or in specific tissues, leading to release of silencing suppression in these tissues, but detection of

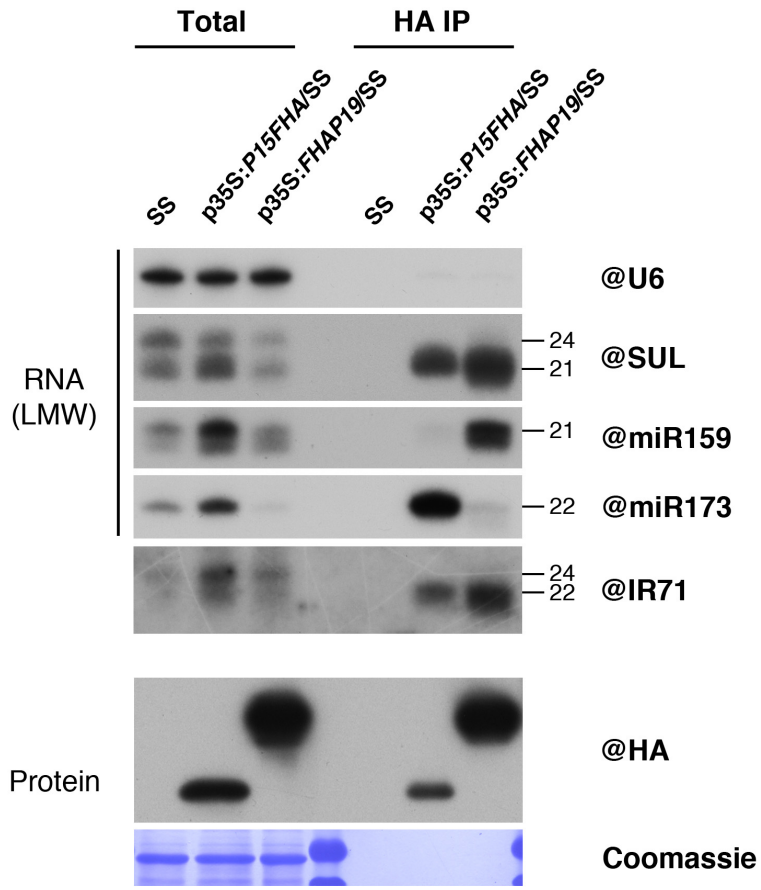

Figure 1.5: Association of P15FHA with sRNA.
Northern blot analysis of low molecular weight (LMW) RNA (top) and western blot analysis of protein (bottom) from total seedling extracts (left) and on HA IPs (right). P15FHA associates with 21nt siRNAs and 22nt miRNAs, but not with 21nt miRNAs.

the P15FHA in total extracts nonetheless. In fact, the 35S promoters present in the T-DNA insertion in many mutant collections (the SALK *dcl3-1* and *dcl4-2* here used originate from one of these) have been shown to drive the silencing of other transgenes driven by the 35S promoter (Daxinger et al., 2009). For this reason, the results obtained using SALK lines expressing 35S:*P15FHA* (see also following section) must not be considered conclusive. It would be interesting to perform these experiments using point mutants in the DCL genes, to avoid the presence of multiple 35S promoters.

Next, we wondered whether P15 associates with other molecules *in vivo*. To investigate whether P15 associates with sRNA, as well as possible association with *A. thaliana* proteins, we performed P15FHA IPs and analyzed co-IPed RNA and protein.

1.1c - P15FHA immunoprecipitation

To identify possible P15 protein interactors we immunoprecipitated P15FHA from both seedlings and flowers of p35S:*P15FHA*/SS. We used antibodies recognizing the Flag and HA epitopes in separate experiments. We then subjected the co-IPed proteins to mass spectrometry analysis, using SS co-IPed proteins as negative control. Despite numerous attempts involving two tissues and two different antibodies, no peptide was consistently found only in P15FHA samples, or with a consistent number of reads. We therefore focused our efforts on RNA co-IP and possible P15FHA association with sRNA. To this end we subjected RNA from HA co-IPs of SS, p35S:*P15FHA*/SS and p35S:*FHAP19*/SS seedlings to Northern blot (**Fig. 1.5**).

The results show that transgene-derived 21nt siRNAs and endogenous IR-derived 22nt siRNA were found associated to P15FHA in amounts comparable to FHAP19. Very little 21nt miRNA co-IP with P15FHA, at least in our experimental conditions, suggesting weak association. Moreover, 22nt miRNAs were found to strongly associate to P15FHA but not to FHAP19. An independent replicate of this experiment, where many miRNA were tested, is shown in **Fig. S3** – Annex 1. These results perfectly mirrored the AGO loading profile observed in the same lines and conditions (**Fig. 1.3A**), except for IR71, whose loading into AGO1 was not assessed. As for sRNA-sequestering FHAP19, the RNA species that were

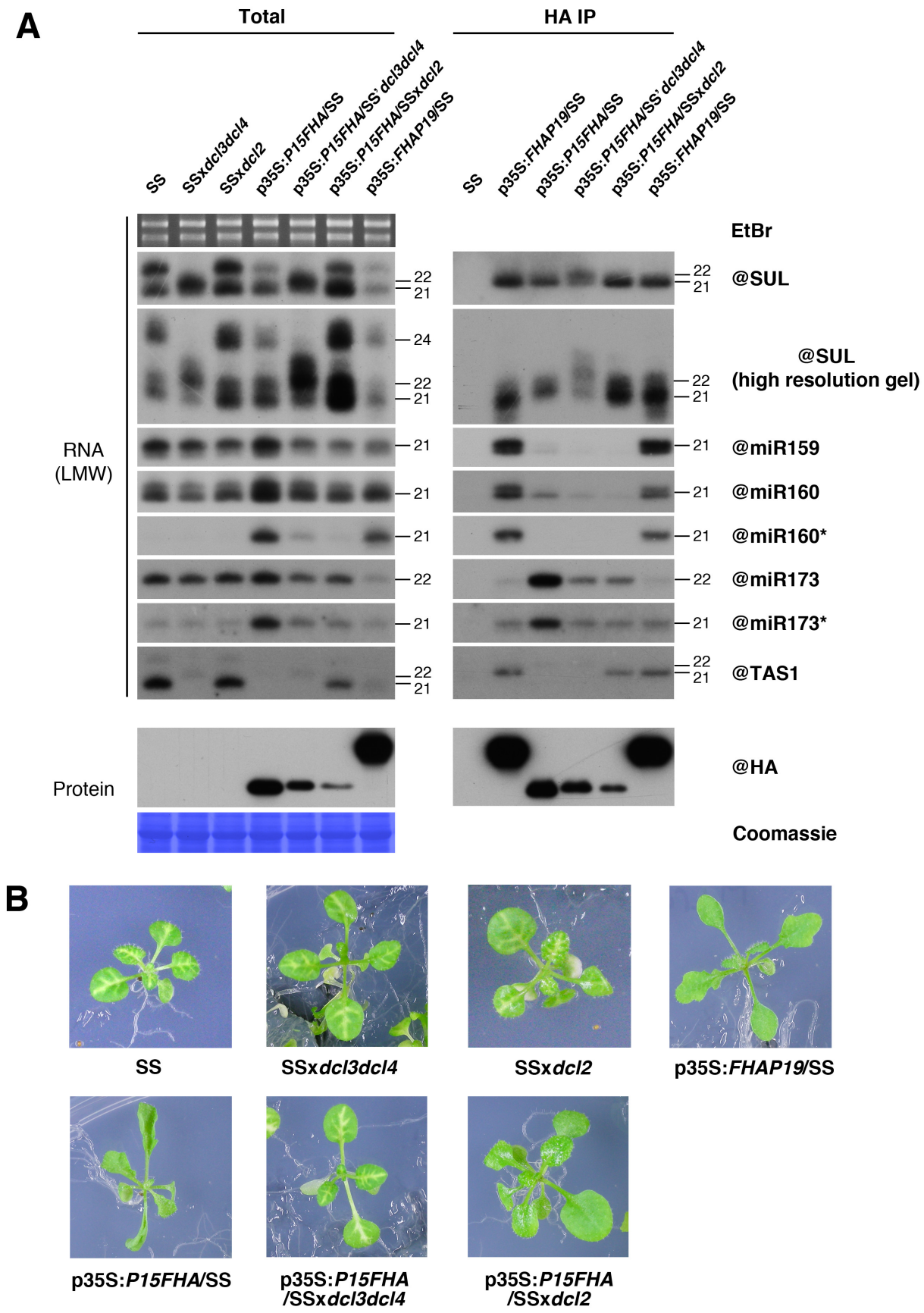

Figure 1.6: Effect of exclusive DCL2 activity versus DCL2 absence on P15FHA association with sRNA.

(A) Northern blot analysis of low molecular weight (LMW) RNA (top) and western blot analysis of protein (bottom) from total seedling extracts (left) and from HA IPs (right). A high resolution gel analysis is included to better assess anti-*SUL* siRNA size. (B) photos of the seedlings at the moment of harvest (SS, 35:*P15FHA*/SS and 35S:*FHAP19*/SS photos are the same as in Fig. 1.3B). P15FHA associates with 22nt siRNAs. When P15FHA is present in limited amounts, association with 22nt miRNAs is partially disrupted while association with 21nt siRNAs is not.

found associated with P15FHA were not loaded in AGO1/2. From this we conclude that P15FHA suppresses AGO loading of 21nt siRNAs and 22nt miRNAs, but not 21nt miRNAs, by associating with them. Furthermore, the fact that in identical tissues and IP conditions we easily found sRNA but no protein associated to P15FHA suggests that the P15FHA/RNA association is not mediated by other proteins. P15 can therefore be considered a case of *bona fide* sRNA binding protein.

Taking into account the strong association of P15FHA to 22nt miRNA versus the weak one to 21nt miRNA, coupled to the strong association to 21nt siRNA versus the weak one to 21nt miRNA, we hypothesized that P15FHA possesses two biases concerning association to sRNA. One concerns size and is a bias toward 22nt sRNA to the detriment of 21nt sRNA. The other concerns sRNA class and is a bias toward siRNA to the detriment of miRNA. To gain more insight on this matter *in vivo,* we analyzed P15FHA sRNA association and its effects on SS-silencing in a genetic background in which all siRNA are 22nt long (SS'*dcl3dcl4* – see previous section) and in one that is devoid of 22nt siRNA (SSx*dcl2*, a cross between SS and *dcl2-1* – see Materials and methods). The experimental approach was identical to that described in the previous paragraphs, and the results are shown in **Fig. 1.6**.

Several different aspects of these results need to be pointed out to draw the appropriate conclusions. First of all, as detailed in the previous section, the use of a 35S-driven transgene in SALK mutant backgrounds could trigger widespread or localized transgene silencing, so these results cannot be considered conclusive. For the sake of argument, these results will be commented upon nonetheless. In a *dcl3dcl4* background P15FHA is found associated to 22nt siRNAs. However, this association does not likely involve the whole anti-*SUL* siRNA pool and is therefore not sufficient to suppress the *SUL*-silencing phenotype. We ascribe this to the saturation of the P15FHA pool by the 22nt siRNAs produced by DCL2 acting as a surrogate to DCL3 and DCL4, as postulated in the previous section. The surge in 22nt siRNAs entailed by DCL3 and DCL4 knockout and its effect on P15FHA represents a disturbance in our experimental system that cannot be overlooked, and a serious limitation in the interpretation of the results. Furthermore, the high resolution gel shows anti-*SUL*

siRNA of 21nt. Although the source of these siRNA is not known, they could result from DCL1 activity.

Regarding p35S:*P15FHA*/SSx*dcl2*, the line we selected for this experiment produced enough P15FHA to efficiently suppress the *SUL*-silencing phenotype. Accordingly, 21nt anti-*SUL* siRNAs were found associated to P15FHA. On the other hand, the fact that siR255 was produced in this line suggests that the pool of miR173 was not completely sequestered and was therefore partially loaded into AGO1 to mediate ta-siR255 generation. This observation suggests that P15FHA more readily associates to 21nt siRNAs than to 22nt miRNAs. Additionally, in the same background P15FHA was found to associate with ta-siR255, showing it has affinity for this other class of siRNA. Finally, the observation that miR173* was detected in P15FHA IPed RNA strongly support that P15 binds sRNAs in a duplex rather than in a single-stranded form. Whether this is also the case for siRNAs remains to be formally addressed. Surprisingly, despite confirmation through PCR of DCL2 knockout, the high resolution gel shows a certain amount of anti-*SUL* siRNA of 22nt. While the origin of these siRNAs is not known, they could be (i) non-canonical size off-products of one of the three other DCL enzymes, (ii) a product of tailing activity or (iii) siRNA of 21nt which contain modifications that slow their electrophoretic migration, among other possibilities.

Given that these last results cannot be considered informative due to the presence of multiple 35S promoters, "preference" or "priority" in sRNA binding *in vivo* should be inferred from the IPs in a wild-type background (**Fig. 1.5**): 21nt siRNA over 21nt miRNA and 22nt miRNA over 21nt miRNA, as already stated above. Nothing can be said about 22nt siRNA at this point. The very generic and perhaps inappropriate words "preference" and "priority" are here used because the nature of P15FHA discriminative ability and selectivity is not known. For the sake of simplicity, the terms "affinity" and "binding capacity" will be used from now on.

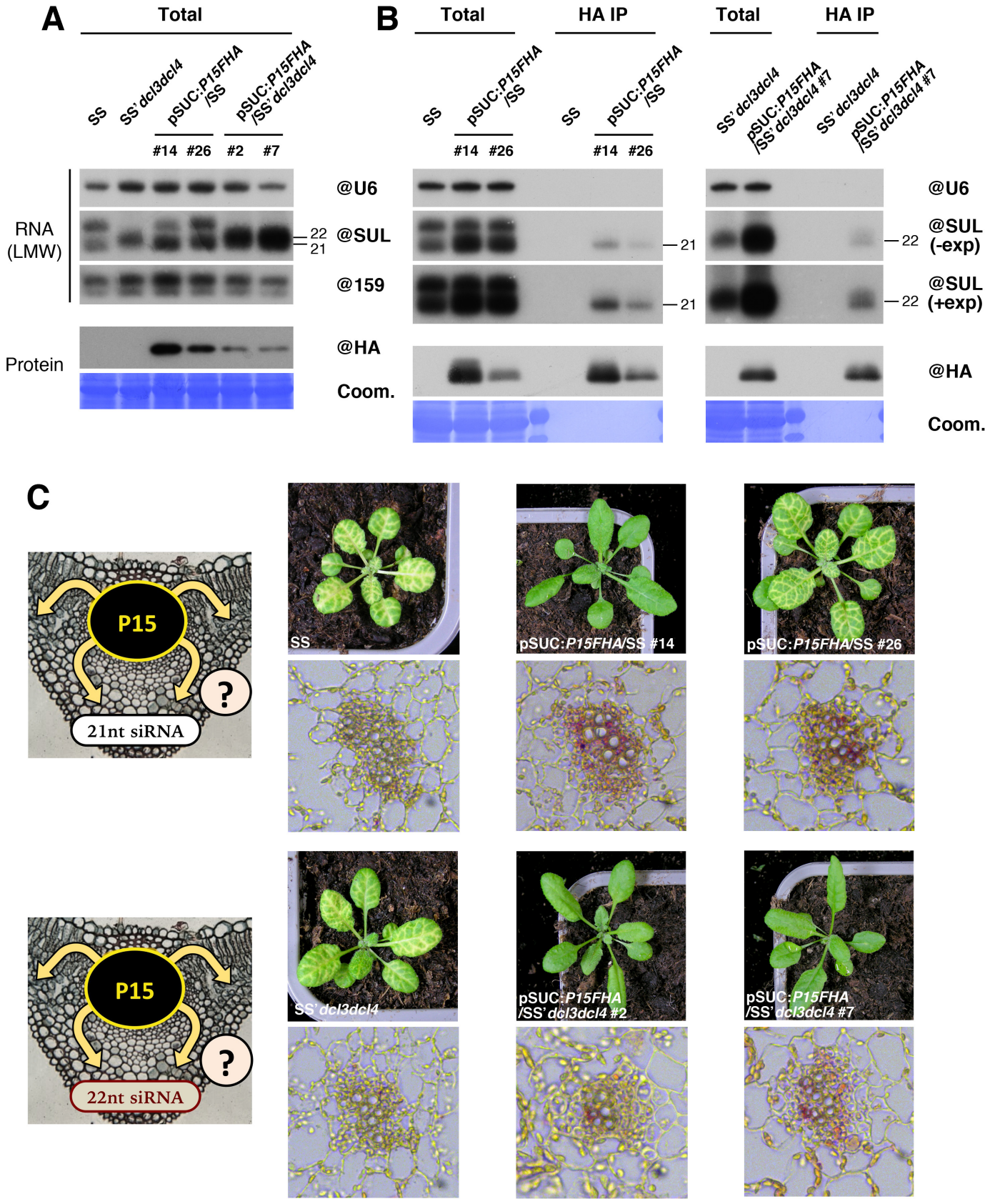

Figure 1.7: Effect of P15FHA on cell-to-cell movement of 21nt and 22nt siRNAs.
(A) Northern blot analysis of low molecular weight (LMW) RNA (top) and western blot analysis of protein (bottom) from total extracts of leaves from 6-week-old plants. (B) As in (A) but including HA IPs from the same tissues. (C) Left: schematic representation of the experimental system, consisting of P15FHA production in the same cells as the anti-*SUL* siRNAs and subsequent assessment of *SUL*-silencing phenotype. Right: photos of plants at the moment of harvest, and corresponding immunolocalization of the HA epitope. P15FHA is able to stop cell-to-cell movement of 21nt and 22nt siRNAs, but it stops 22nt siRNAs more efficiently

1.2 - Characterization of the mode of action of P15 in the suppression of non-cell autonomous RNA silencing

It has been shown that P19 of TBSV, when expressed in the same companion cells as the SS hairpin through the same SUC2 promoter, is able to stop cell-to-cell movement of anti-*SUL* siRNA, thereby preventing *SULPHUR* gene silencing and apparition of the *SUL*-silencing phenotype (Dunoyer *et al.*, 2010). P19 is therefore able to suppress non-cell autonomous RNA silencing. On the other hand, P38 of TCV, which suppresses RNA silencing by binding AGO1 and preventing its loading, is not able to stop cell-to-cell movement of siRNA when placed in the same experimental system (Schott *et al.*, 2012). This difference can be ascribed to the stage of RNA silencing with which a suppressor interferes. A suppressor that relies on direct siRNA binding and sequestration, such as P19, is capable of suppressing non cell-autonomous RNA silencing because it stops the mobile signal itself. On the other hand, a VSR acting on factors downstream of siRNA movement, such as P38 interacting with AGO1, is not likely to be able to block cell-to-cell movement of silencing.

To assess whether P15 is able to stop cell-to-cell movement of siRNAs, we expressed P15FHA under control of the SUC2 promoter (pSUC:*P15FHA*) in the SS system, thereby inducing P15FHA production in the same cells that produce the anti-*SUL* mobile trigger siRNAs. In this experimental system the disappearance of the *SUL*-silencing phenotype does not report the suppression of cell-autonomous RNA silencing as the p35S:*P15FHA*/SS experiments does, but rather the immobilization by P15FHA of siRNAs within their cells of origin. Since the results from IP experiments reported in the previous section established that P15FHA can associate with both 21nt and 22nt siRNAs *in vivo*, we introduced the pSUC:*P15FHA* transgene in both SS and SS'*dcl3dcl4* to establish the stopping power of P15FHA on these two classes of siRNAs. In pSUC:*P15FHA*/SS the mobile silencing trigger is DCL4-dependent 21nt siRNA, while in pSUC:*P15FHA*/SS'*dcl3dcl4* the mobile silencing trigger is DCL2-dependent 22nt siRNA (**Fig. 1.7C**).

Immunolocalisation of the HA epitope revealed strict limitation to the cells surrounding the sieve elements, in agreement with the companion cell-specificity of the SUC2 promoter

(**Fig. 1.7C**). Analysis of the molecular (**Fig. 1.7A**) and visual (**Fig. 1.7C**) phenotypes showed that P15FHA was able to stop movement of both 21nt and 22nt siRNAs. However, it is evident that P15FHA stopping power on the two classes of siRNAs was not at all the same. In fact, a relatively small amount of P15FHA efficiently stopped 22nt siRNAs in SSx*dcl3dcl4* (pSUC:*P15FHA*/SS'*dcl3dcl4*#2 and #7), while a considerably larger amount of P15FHA was needed to stop 21nt siRNAs in SS (pSUC:*P15FHA*/SS#14). A SS line producing less P15FHA (pSUC:*P15FHA*/SS#26), but still much more than pSUC:*P15FHA*/SS'*dcl3dcl4*#2 and #7, showed a marked *SUL*-silencing phenotype, indicating 21nt siRNA cell-to-cell movement. Assessment of the yellow vein phenotype, coupled with anti-*SUL* siRNA and P15FHA protein accumulation of primary transformants suggests that an analogous pattern can be observed in other lines with similar molecular phenotypes (**Fig. S4** – Annex 1). Interestingly, pSUC:*P15FHA* induced a consistent increase in 22nt anti-*SUL* siRNAs.

To establish whether the inhibition of siRNA movement by P15FHA was accompanied by P15FHA association to siRNAs, we performed HA-epitope IP and analyzed the co-IPed RNA (**Fig. 1.7B**). The results show association of P15FHA with both 21nt and 22nt siRNAs in the cells where their movement was arrested. This experiment confirmed the dose-dependent ability of P15FHA to stop movement of 21nt siRNAs.

These results shed light on two key traits of P15. First, it is able to stop siRNAs from exiting the cells where they are generated, which could potentially represent a feature of great importance in the context of a viral infection. Coupled to our results from the IP experiments, this ability strongly suggests that P15 suppresses RNA silencing by binding and sequestering siRNAs in a way analogous to P19. Second, its capacity to stop 22nt siRNAs greatly exceeds its capacity to stop 21nt siRNAs. This piece of information answers the question left open by the p35S:*P15FHA* IP experiments regarding P15FHA siRNA size binding bias. Taken together, our results confirm that *in vivo* P15 has two biases in sRNA binding: toward 22nt to the detriment of 21nt, and toward siRNAs to the detriment of miRNAs.

Given that DCL4-dependent 21nt siRNAs are considered the main mediators in *A. thaliana* defense against RNA viruses, the sequestration bias shown by P15 toward DCL2-dependent

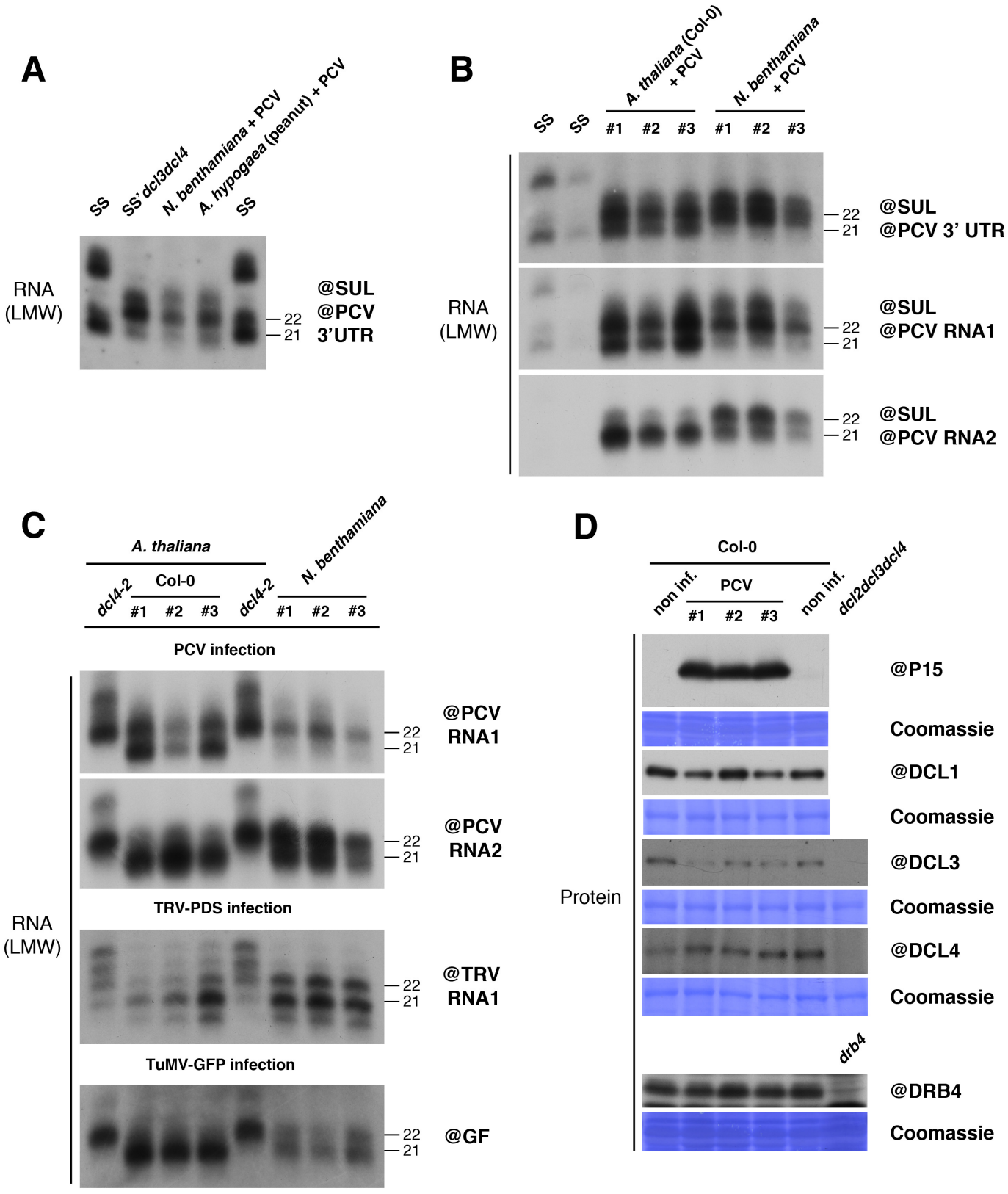

Figure 1.8: Antiviral siRNA population during PCV infection.
(A) Northern blot analysis on high resolution gel of low molecular weight (LMW) RNA of *N. benthamiana* and *A. hypogaea* leaves systemically infected with PCV. SS and SS*xdcl3dcl4* anti-*SUL* siRNAs are used as size references. (B) as in (A) but of three *A. thaliana* Col-0 and three *N. benthamiana* plants. SS loaded in two wells in different amounts. Three probes recognizing different regions of the PCV genome are used (3'UTR of RNA1 and RNA2, middle of RNA1, middle of RNA2). (C) as in (B) but including *dcl4-2* knockout mutant as siRNA size control (see Fig. 2.6 for viral genomic RNA accumulation), and parallel infection of the same lines with TRV-PDS and TuMV-GFP. (D) Western blot analysis of total proteins from non-infected and PCV-infected *A. thaliana* Col-0, to assess the accumulation of DCL proteins and DRB4. PCV infection triggers high DCL2 antiviral activity, which leads to a high proportion of 22nt siRNAs but does not correspond to

22nt siRNAs is puzzling and quite unique. We formulated two not mutually exclusive hypotheses to explain the functional significance of this bias. First, P15 could specifically prevent generation of secondary antiviral siRNAs by sequestering putative transitivity-triggering 22nt siRNAs. Since successful and repeatable PCV infection of *A. thaliana* was obtained relatively late in this project, we were not able to assess how RDR proteins, or the exclusive presence of 21nt versus 22nt siRNAs, affect PCV infection. Secondly, PCV could have evolved on a host or pathosystem in which a large proportion of anti-PCV siRNAs are 22nt long. PCV's RNA silencing suppressor P15 would have therefore evolved specific affinity for 22nt siRNAs in order to properly counter antiviral RNAi.

1.3 - Antiviral siRNA population generated during PCV infection

We decided to investigate the possibility that P15 may possess a binding and sequestration bias toward 22nt siRNAs because it evolved to suppress a largely 22nt siRNA-dependent RNA silencing response against PCV. To this end, we analyzed RNA from PCV-infected plants by high resolution PAGE Northern blot (**Fig. 1.8A, 1.8B and 1.8C**). First of all, we analyzed PCV infections on *N. benthamiana*, which is very sensitive to this virus, and on peanut (*A. hypogaea*), the species on which PCV causes most economic damage and with which it has presumably undergone a certain amount of co-evolution. As a size reference for 21/24nt and 22nt sRNA, SS and SS'*dcl3dcl4* leaf RNA extracts were used, respectively (**Fig. 1.8A**). The results clearly show very high incidence of 22nt anti-PCV siRNAs in both species. Unfortunately, the one peanut RNA analyzed belongs to the only infected plant we managed to obtain, so we abandoned this species in favor of *N. benthamiana* and, once we managed to efficiently infect it, *A. thaliana*.

The next step was to compare *N. benthamiana* and *A. thaliana* anti-PCV siRNA populations in systemically infected leaves by expanding the number of analyzed individuals to three per species and by using probes spanning different regions of the PCV genome (the 3'UTR common to RNA1 and RNA2, the middle portion of RNA1 and the middle portion of RNA2) (**Fig. 1.8B**).

The siRNA profiles of the three plants analyzed per species were highly homogeneous among each other. This analysis shows that anti-PCV siRNAs generated in *N. benthamiana* are mostly 22nt in length all across the PCV genome. The picture is quite different in *A. thaliana*. Surprisingly, in fact, siRNAs of different sizes are produced from different parts of the PCV genome, suggesting a major role for DCL2 in the processing of the 3' ends of the two viral RNAs, an equal contribution of DCL2 and DCL4 in the processing of the middle region of RNA1 and a preponderant role of DCL4 in the processing of the middle of RNA2.

We then proceeded to establish whether these 22nt siRNAs could be a product of DCL4 through a yet-unknown capacity of this enzyme to generate siRNAs of this length. We did so by infecting *A. thaliana dcl4* knock-out mutants, in this way also validating the size calibration provided by the SS lines in **Fig. 1.8A** and **1.8B**. In the same experiment, we carried out infections with TRV-PDS and TuMV-GFP, two well-known (+)ssRNA viruses, to compare their siRNA profiles with that of PCV (**Fig. 1.8C**).
Our analysis revealed that, as expected, in the absence of DCL4, 22nt siRNAs were present while 21nt siRNAs were not. This confirms the size of the PCV-derived 22nt siRNA population and its dependence on DCL2. Generation by DCL3 of these 22nt siRNAs can be excluded since in a *dcl2dcl4* double knockout both 21nt and 22nt anti-PCV siRNAs were absent (**Fig. S5** – Annex 1). Col-0 infection with TuMV-GFP showed exclusive production of DCL4-dependent 21nt antiviral siRNAs. TRV-PDS did trigger production of some 22nt antiviral siRNAs, but the majority was 21nt long. These results highlight that both *A. thaliana* and *N. benthamiana* produce a higher proportion of 22nt siRNAs in their defensive reaction against PCV than against TuMV or TRV. Of note, in the three viral infections analyzed, *N. benthamiana* showed a general propensity to generate a greater proportion of antiviral 22nt siRNAs than *A. thaliana*.

Since DCL2 can act as a surrogate of DCL4, we wondered whether this increased DCL2 activity against PCV could be due to DCL4 destabilisation, as happens during TCV infection (Azevedo *et al.*, 2010). We therefore analyzed DCL protein levels in non-infected and PCV-infected Col-0 by Western blot (**Fig. 1.8D**). Unfortunately we could not assess the accumulation of DCL2, the focus of this experiment, due to unavailability of an efficient

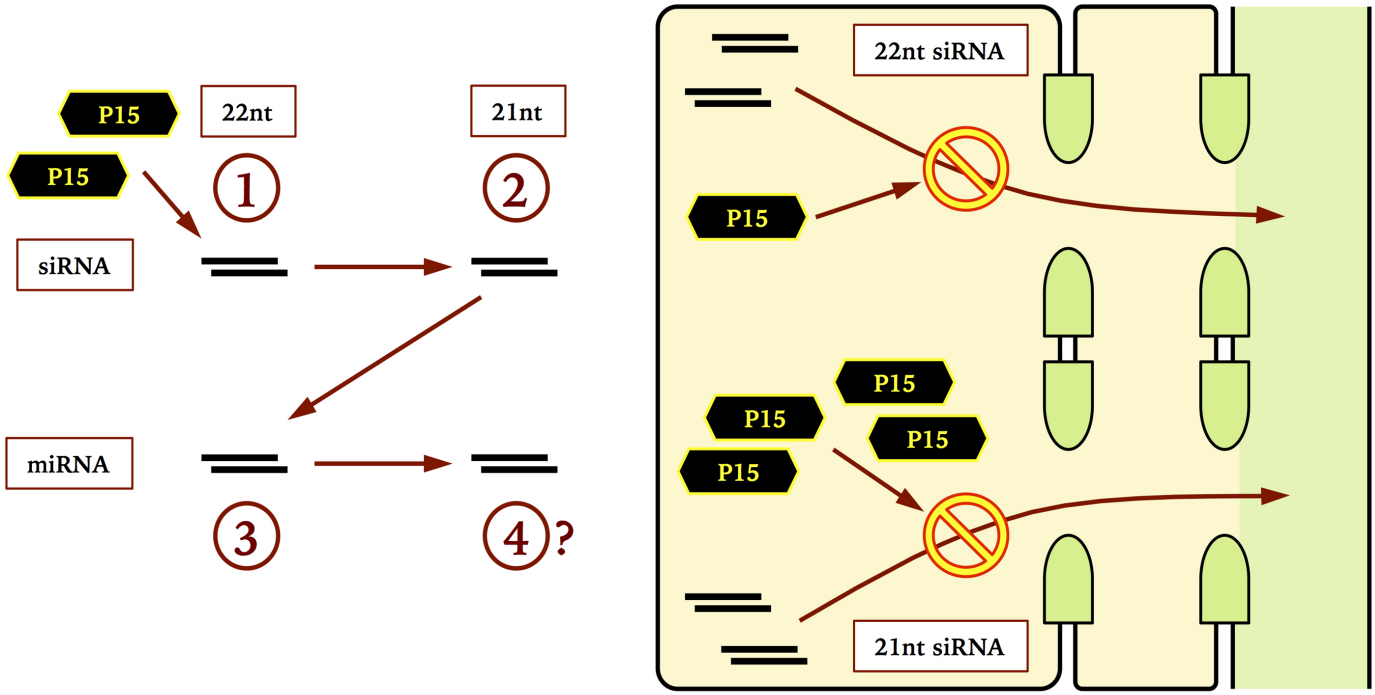

Figure 1.9: P15FHA sRNA sequestration hierarchy *in vivo*.
Schematic representation of (left) the hierarchy observed *in vivo* concerning P15FHA affinity for sRNA, from the highest (22nt siRNAs) to the lowest (21nt miRNAs), and (right) the dose-dependent ability of P15FHA to stop cell-to-cell movement of 21nt and 22nt siRNAs.

antibody. However, the accumulations of DCL4 and its cofactor DRB4 were not affected by PCV infection, ruling out a DCL4 destabilization similar to that observed for TCV. DCL1 is not affected either, while DCL3 is slightly less abundant in PCV-infected plants.

1.4 - Conclusion

By using the SS reporter system and several targeted experimental approaches, we established the mode of action of P15 in the suppression of cell-autonomous and mobile RNA silencing. P15, in a fashion similar to tombusviral P19, binds and sequesters siRNA, preventing both their loading into AGO effectors and their cell-to-cell movement. However, similarities with P19 end here, since P15 possesses several features that render it a unique VSR. Some of these features have been uncovered here in Chapter 1, while other perhaps even more compelling ones are unveiled in Chapter 2. Our experiments combined suggest that P15 shows two distinct biases in sRNA binding *in vivo* (**Fig. 1.9A**). Given the present data, the mechanisms and reasons behind these biases can merely be speculated upon.

One bias, toward 22nt-long sRNA to the detriment of 21nt-long sRNA, may likely involve structural features of P15, allowing it to optimally retain RNA of this specific length. Crystallization of P19, for example, revealed that it forms a dimer around an RNA duplex, acting as a molecular caliper that specifically binds 21nt RNA (Vargason *et al.*, 2003). Additional examples of structural determination of sRNA size are the DCL enzymes, each generating sRNAs of different and specific lengths. These differences have been suggested to depend, as for protozoan Dicer (MacRae *et al.*, 2007), on the distance between the PAZ and catalytic domains (Bologna and Voinnet, 2014).

Whatever the mechanism behind P15 size specificity, our analysis of PCV-derived siRNAs in several species provides a plausible (yet not at all final) explanation for the bias. In fact, compared to infections by TRV-PDS, TuMV-GFP and many cases reported in literature, during PCV infection a higher proportion of antiviral siRNAs are 22nt long. In a highly susceptible host, such as *N. benthamiana,* 22nt siRNAs represent the vast majority of anti-PCV siRNAs. In this context, evolution of a bias toward 22nt siRNAs would have allowed P15 to block antiviral RNA silencing more efficiently.

We show that anti-PCV 22nt siRNAs are generated by DCL2 in *A. thaliana*. Considering the minor role ascribed to DCL2 in antiviral defense, we can hypothesize two major scenarios leading to heightened DCL2 activity. The first presumes a surrogate role of DCL2 to DCL4, whereby DCL2 takes over upon loss of DCL4. Since our results establish that upon infection by PCV there is no change in steady-state levels of DCL4 protein or its co-factor DRB4, DCL2 would here compensate for loss of DCL4 activity, not stability. In this scenario, therefore, PCV would be able to somehow inactivate DCL4 while not destabilizing it. The second and possibly most appealing scenario presumes a specific DCL2 response to PCV, regardless of levels or activity of DCL4. What particular feature of PCV is responsible for the recruitment/activation of DCL2 in *A. thaliana* and its equivalent in *N. benthamiana* remains for the moment a matter of conjecture. Also not clear are the functions of these DCL2-dependent 22nt siRNAs, namely whether they act directly through AGO loading and viral RNA cleavage or if they trigger putative antiviral transitivity, and if their movement is significant in anti-PCV defense or not. PCV could therefore constitute a potent and unique tool to probe the poorly characterized biology of DCL2 during antiviral RNAi.

While P15 highest affinity is for 22nt siRNAs, it must not be forgotten that it also efficiently binds and sequesters 21nt siRNAs, inhibiting their loading into antiviral AGO proteins and stopping their cell-to-cell movement. P15 therefore possesses the remarkable ability to neutralize two separate antiviral siRNA species. However, its ability to stop cell-to-cell movement of 21nt siRNAs is considerably weaker than its ability to stop 22nt siRNAs (**Fig. 1.9B**). This potential limitation of P15 in RNA silencing suppression is evident for now only from experiments in a heterologous non-viral context. Yet, this limitation is of key importance in the interpretation of the results presented in Chapter 2 and must be kept in mind.

Regarding the second bias uncovered in this chapter, toward siRNAs to the detriment of miRNAs, it is more difficult to attempt an explanation. In fact, while 22nt and 21nt sRNA are physically different molecules, siRNAs and miRNAs of the same length are, to our knowledge, physically identical (except for the presence of bulges in most miRNA

duplexes). What distinguishes these two classes of sRNA are the enzymes that generate them and possibly other specific factors associated to them. Furthermore, these pathways could be active in different locations within the cell. The generation of miRNAs by DCL1 is believed to be a nuclear phenomenon (Song *et al.*, 2007). While localization of the SS hairpin processing by DCL4/DCL2 has not been well established, experiments performed in the lab indicate that the vast majority of DCL4 is located in the cytoplasm (Montavon *et al.*, submitted). In line with these observations, a P15FHA allele containing a nuclear localization sequence (NLS) was indeed imported into the nucleus but completely lost its SS-silencing suppression ability (**Fig. S6** – Annex 1). Conversely, a P15FHA allele with an NLS sequence containing mutations that disrupted nuclear import was proficient in suppression of SS silencing. The bias P15 shows toward siRNAs could therefore be due to a mostly cytoplasmic localization of DCL4/DCL2 siRNA-generating complexes as opposed to a nuclear localization of DCL1 miRNA-generating complexes. This could especially be true during PCV infection, since its replication is cytoplasmic and consequently DCL4/DCL2 likely process PCV dsRNA in the cytoplasm. Additionally, P15 could possess the ability to transiently bind DCL4/DCL2 or their cofactors, or to somehow remain in their vicinity, to more easily come into contact with 21-22nt siRNAs. As interesting as this possibility may be, our IP experiments revealed no strong and reproducible protein-protein interaction between P15FHA and *A. thaliana* factors. Another possibility for siRNA/miRNA discrimination by P15 could involve RNA modifications, but we are not aware of any modification differentiating siRNAs from miRNAs, and have gathered no data in this regard. From a functional point of view this bias seems a sound strategy for a VSR to adopt, since it is DCL4/DCL2-dependent siRNAs, and not miRNAs, that mediate antiviral RNAi.

Finally, some pieces of data resulting from these experiments, while granting insight on P15, also provide information about more general aspects of RNAi. Two of these results will be commented here. The first concerns the specific processing of different segments of the PCV genome by different DCLs in *A. thaliana*. Although DCL2 and DCL4 have been shown to be in some cases active in different tissues during TuMV-GFP infection in *A. thaliana* (DCL2 was able to limit the spread of a TuMV-GFP lacking VSR activity in flowers but not in inoculated or cauline leaves) (Garcia-Ruiz *et al.*, 2010), to our knowledge this is the first

description of "intra-genomic" specificity of antiviral DCL4 and DCL2 activity, and certainly merits further investigation. In literature there is quite an abundance of experiments involving deep sequencing of virus-derived siRNAs in different plant species infected by different viruses. However, to our knowledge in these studies the bioinformatic analysis of the sequencing data was not aimed at assessing intra-genome distribution of 21nt versus 22nt siRNAs (among others Kutnjak *et al.*, 2014; Miozzi *et al.*, 2013; Naveed *et al.*, 2014; Silva *et al.*, 2011). It would be interesting to perform a similar deep-sequencing experiment on different *dcl* knockout combinations of PCV-infected *A. thaliana*, appropriately focusing the bioinformatic analysis to identify respective DCL4 and DCL2 activity hotspots, and search for any common feature that might be responsible for specific DCL processing. Adding *rdr1* and *rdr6* knockouts could provide information on transitivity during PCV infection.

The second interesting result concerning a general aspect of RNAi uncovered by our experiments, already mentioned in the introduction, points toward low DCL2 abundance or activity in companion cells. In *dcl3dcl4* we observed that a 35S-driven P15FHA lost its ability to completely sequester 22nt siRNAs, which we interpreted as consequence of a ubiquitous surge in endogenous DCL2-dependent 22nt siRNAs, and subsequent saturation of the cellular pool of P15FHA with these siRNAs. However, in the same *dcl3dcl4* background a P15FHA driven by companion cell-specific SUC2 promoter was able to very efficiently sequester 22nt siRNAs, in spite of the loss of DCL3 and DCL4. One explanation could be that the SUC2 promoter leads to considerably higher production of P15FHA protein in the companion cells than the 35S promoter, thereby overcoming the postulated saturation effect. Another explanation could be that DCL2 is scarcely abundant or active in companion cells, so that within these a loss of DCL3 and DCL4 does not lead to a surge in endogenous 22nt siRNA sufficient to saturate P15FHA. The fact that for DCL2 to generate anti-*SUL* siRNAs the SS transgene has to be present in many copies, and that both DCL3 and DCL4 need to be absent (Dunoyer *et al.*, 2007), supports this hypothesis. Moreover, work done in another lab provides further support to this theory (Parent *et al.*, 2015). Here the authors, working on a similar system involving SUC2-driven expression of a hairpin targeting an endogenous gene (phytoene desaturase, or PDS), observed among other things that

p35S:*DCL2* expressed in a *dcl4* is able to rescue the mobile silencing phenotype absent in a simple *dcl4* (as in a SSx*dcl4* - Dunoyer *et al.,* 2007). While in a simple *dcl4* the hairpin is exclusively processed by DCL3, a p35S:*DCL2* transgene is enough to greatly reduce DCL3-dependent and promote DCL2-dependent exogenous hairpin processing, suggesting that DCL2 can compete with DCL3 in a dose-dependent manner. This would explain why in the SS system the loss of DCL4 entails processing by DCL3 and not DCL2: in incipient companion cells DCL3 activity is preponderant because DCL2 is barely present/active. As mentioned in the introduction, tight regulation of DCL2 and potential transitivity-inducing 22nt siRNAs around the vascular system is logical in terms of correct signaling within the plant.

In conclusion, probably both explanations hold some truth, since whatever the activity of DCL2 in incipient and recipient cells, in the same SSx*dcl3dcl4* background a pSUC:*P15FHA* was able to stop siRNA movement while a p35S:*P15FHA* was not, suggesting that more P15FHA is produced in companion cells when expression is driven by the SUC promoter.

After having defined the mechanisms through which P15 suppresses RNA silencing by using P15FHA, an allele that is not imported into peroxisomes (**Fig. 2.2C**), we investigated the fundamental role that peroxisomal localization of P15 plays in the establishment of systemic infection by PCV.

CHAPTER 2

ROLE OF P15 PEROXISOMAL LOCALIZATION IN PCV SYSTEMIC MOVEMENT

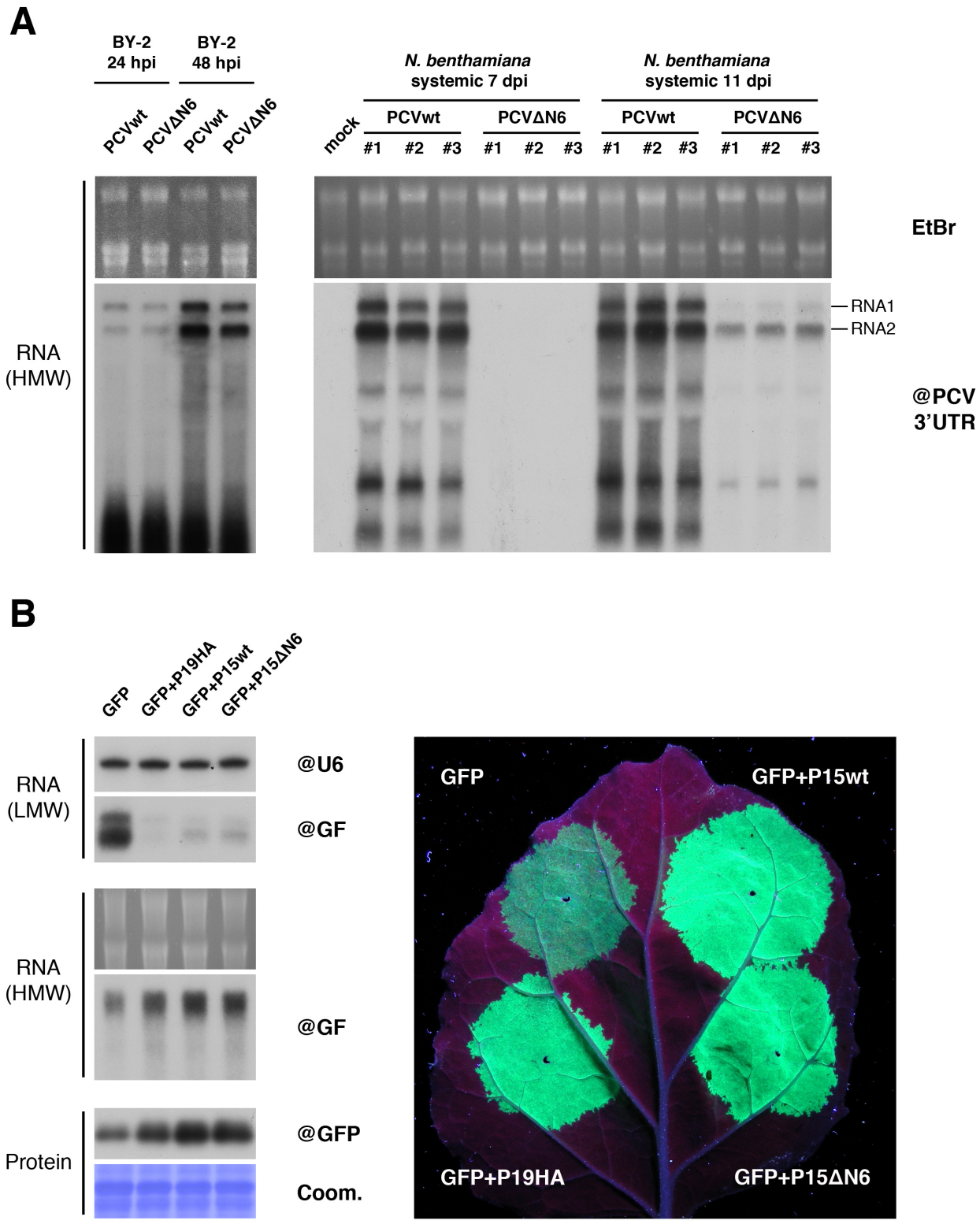

Figure 2.1: Effect of peroxisomal localization of P15 on PCV infection and on cell-autonomous RNAi. (A) Northern blot analysis of high molecular weight (HMW) RNA from PCVwt vs. PCVΔN6 infections. Left: BY-2 protoplasts 24 and 48 hours post-infection (hpi). Right: *N. benthamiana* systemically infected leaves 7 and 11 days post-infection (dpi). The probe recognizing the 3'UTR of PCV reveals the two genomic RNAs (RNA1 + RNA2) and the subgenomic RNA (sgRNA) encoding P15. (B) Inoculation of *N. benthamiana* leaves with *A. tumefaciens* expressing GFP alone or in combination with P19HA, P15wt and P15ΔN6, analyzed 5 dpi. Left: Northern blot analysis of corresponding high molecular weight (HMW) and low molecular weight (LMW) RNA, western blot analysis of proteins. Right: photo of an infiltrated leaf under UV light revealing GFP accumulation. Peroxisomal localization of P15 is dispensable in the suppression of cell-autonomous RNAi and the intracellular accumulation of PCV, but strongly bolsters PCV systemic movement.

The wild-type allele of P15 (P15wt) as found in PCV contains, as its last three C-terminal aminoacids, a serine-lysine-leucine (SKL) tripeptide. This is a typical PTS1 sequence, entailing peroxisomal import by PEX5 (see Introduction). In Dunoyer, Pfeffer, *et al.*, 2002 the authors, by infecting BY-2 protoplasts with PCVwt or PCVΔN6 (encoding P15ΔN6 lacking the PTS1), showed that intracellular replication and accumulation of PCV are not affected by the loss of PTS1 and P15 peroxisomal localization. The authors also showed that transiently expressed P15ΔN6 is as efficient as P15wt in suppressing RNAi. These results combined suggested that the two alleles are equally proficient in blocking cell-autonomous RNAi, thereby allowing equal accumulation of PCV in a system involving the infection of single cells such as BY-2 cell cultures. However, the situation was very different when PCV systemic infection was scored in a whole-plant context. Analysis of systemic leaves of *N. benthamiana* infected with the same *in vitro*-generated transcripts used on BY-2 cells revealed that while PCVwt was able to efficiently establish systemic infection, PCVΔN6 was not. The authors concluded that peroxisomal import of P15 is key to the movement of PCV while being dispensable for suppression of cell-autonomous RNA silencing.

As a primary approach toward the establishment of the function of P15 peroxisomal localization, we repeated the experiments reported above. When transiently expressed with GFP, P15wt and P15ΔN6 were able to inhibit silencing of GFP, as was P19HA (**Fig. 2.1B**). This is a sense-PTGS system that is highly prone to transitivity, so the greatly reduced amount of @GF siRNA seen in the presence of the suppressors very likely indicates that they prevented generation of secondary siRNA. In BY-2 protoplasts electroporated with *in vitro*-generated PCV RNA transcripts, both 24- and 48-hours post-infection (hpi) the two viruses encoding the two alleles of P15 accumulated in similar quantities (**Fig. 2.1A**). On the other hand, a two-point time course performed on *N. benthamiana* infected with purified virions indicated that PCVΔN6 requires significantly more time to establish systemic infection than PCVwt.

Of note, the first results we obtained with *in vitro* transcripts were similar to those obtained by Dunoyer and colleagues, namely that PCVΔN6 was completely unable to establish systemic infection. However, in a few sporadic cases PCVΔN6 did move systemically, and

when these systemically infected tissues were further used as inoculum, we observed that PCVΔN6 was indeed always able to establish systemic infection on *N. benthamiana*, but took several days more than PCVwt to do so. Consequently, plants infected in this fashion were used to obtain purified virions of PCVΔN6, which were used in parallel with purified virions of PCVwt as inoculum in all subsequent experiments shown in this chapter.

We hypothesized that P15 could improve systemic movement of PCV in two ways. First, it could enter peroxisomes and inhibit antiviral defense by interacting with, and preventing correct functioning of, a peroxisomal negative regulator of PCV movement. To this end we investigated whether P15wt caused any change in levels of the defensive hormone jasmonic acid, as its biosynthetic pathway partly takes place in peroxisomes. We observed no significant change in p35S:*P15wt*/SS compared to p35S:*P15ΔN6*/SS (**Fig. S7** – Annex 1), ruling out the possibility that P15 could promote PCV movement by dampening JA production and subsequent systemic antiviral signaling.

Second, P15 could bind a cytoplasmic host factor involved in negative regulation of PCV movement and, by taking advantage of the unique ability of the peroxisome import machinery to piggyback folded proteins and protein complexes into these organelles, confine it within peroxisomes. This way, the host factor hindering PCV systemic movement would be isolated from its site of action and therefore functionally inactive, in turn allowing efficient systemic movement of PCV.

We decided to investigate this possibility by isolating peroxisomes from *A. thaliana* plants expressing P15wt and P15ΔN6, searching for factors exclusively present (or at least highly enriched) in the peroxisomes of P15wt-expressing plants. Given our results showing binding of P15 to siRNAs and the ability of mobile siRNAs to trigger systemic RNAi, we focused our analysis on the possibility of siRNAs being piggybacked into peroxisomes.

2.1 - Isolation of peroxisomes from plants expressing p35S:*P15*

Peroxisome isolation is a technically demanding and time-consuming procedure, so we started a collaboration with Prof. Sigrun Reumann, an experienced investigator of plant

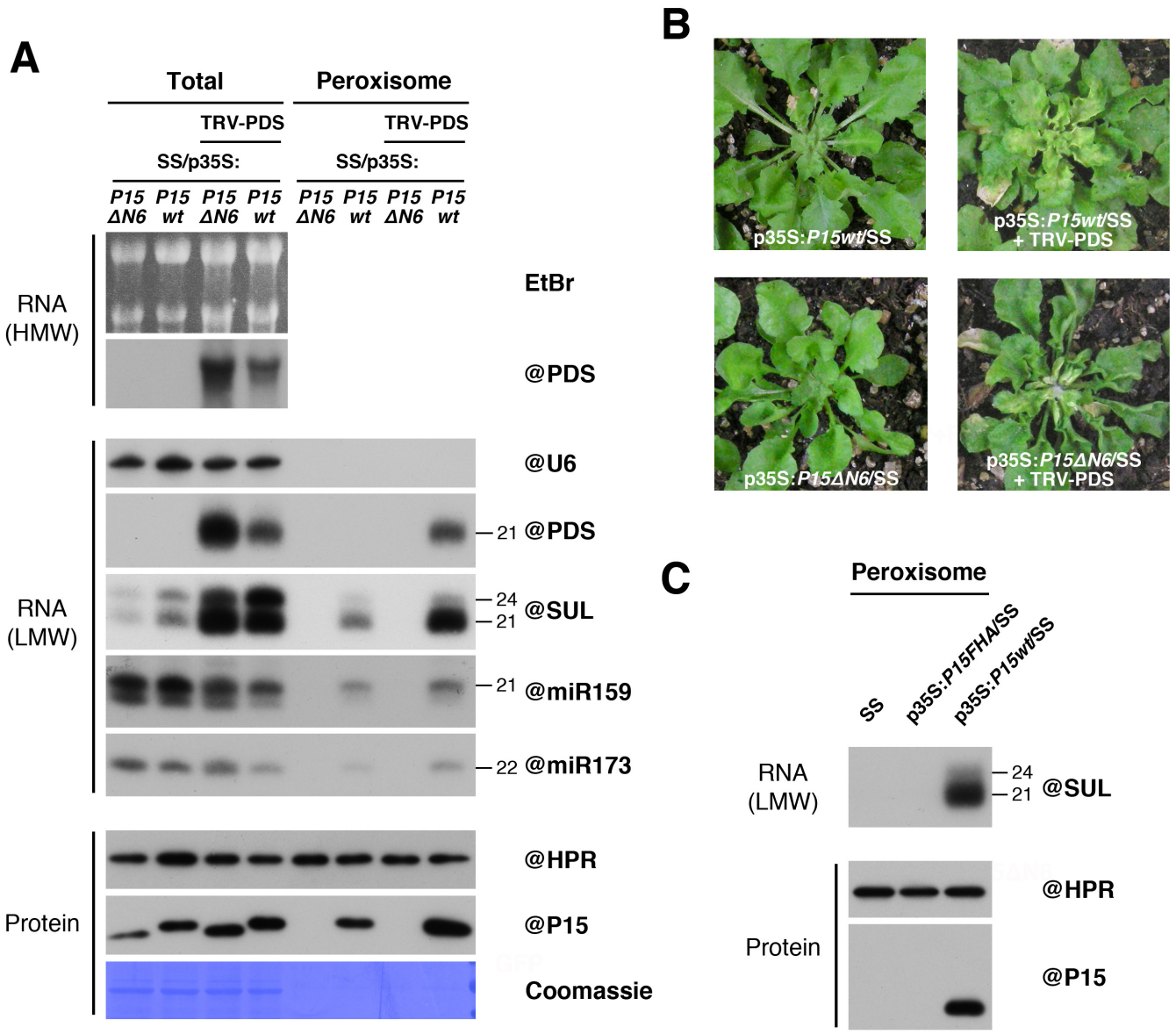

Figure 2.2: Analysis of peroxisomes isolated from P15-expressing plants.
(A) Northern blot analysis of high molecular weight (HMW) and low molecular weight (LMW) RNA (top), and western blot analysis of proteins (bottom) from total (left) and peroxisomal (right) fractions obtained from non-infected and TRV-PDS-infected SS plants expressing p35S:*P15ΔN6* or p35S:*P15wt*. (B) Photos of the plants analyzed in (A). (C) Northern blot analysis of low molecular weight (LMW) RNA (top) and western blot analysis of proteins (bottom) from peroxisomal fractions obtained from SS plants alone or expressing p35S:*P15FHA* and p35S:*P15wt*. P15wt is able to piggyback sRNAs into peroxisomes.

peroxisome biology, to learn how to correctly perform this experiment. After mastering the technique we carried out a first experiment to evaluate whether transgenically-expressed p35S:*P15wt* is imported into peroxisomes and whether it is able to transport sRNAs with it.

2.1a – Non-infected and TRV-PDS-infected plants

Using P15ΔN6 as negative control, we isolated peroxisomes from both non-infected and TRV-PDS-infected p35S:*P15wt*/SS and p35S:*P15ΔN6*/SS plants. We then analyzed proteins and LMW RNA extracted from the peroxisomal fractions obtained (**Fig. 2.2A**).
Consistent with their ability to suppress cell-autonomous RNAi, both P15 alleles were able to suppress the *SUL*-silencing phenotype and the TRV-induced PDS gene silencing (**Fig. 2.2B**). The efficiency of peroxisome isolations, when assessed through quantification of hydroxypiruvate reductase (HPR, a peroxisomal marker protein), was quite homogeneous between samples. P15wt was indeed found in peroxisomal extracts, while P15ΔN6 was absent, confirming specific P15wt import into peroxisomes. Moreover, import of P15wt did not significantly affect steady-state stability of HPR nor did it cause loss of peroxisome yield during isolations. Anti-*SUL* 21nt siRNAs could be readily and exclusively found in the peroxisomal fractions of P15wt-expressing plants. The same could be observed in TRV-PDS-infected plants. Most importantly, virus-derived siRNAs were found in the peroxisomal fraction exclusively in the presence of P15wt.

To simultaneously rule out the possibility that (i) siRNAs are normally present in peroxisomes as part of a yet undescribed pathway and (ii) are absent from peroxisomes of plants expressing P15ΔN6 because they are sequestered by this protein in the cytoplasm, we performed peroxisome isolation on SS plants. In this experiment, we tested the P15FHA protein to confirm that the FHA tag masking the PTS1 impedes peroxisomal import. The results (**Fig. 2.2C**) show that in SS plants anti-*SUL* siRNAs are absent from peroxisomes and that, as expected, P15FHA is not imported into these organelles.

We next wondered whether P15wt is also able to import proteins into peroxisomes. To this end, we extracted proteins from p35S:*P15wt*/SS and p35S:*P15ΔN6*/SS peroxisomal isolates (three biological replicates each) and analyzed them by mass spectrometry to assess their

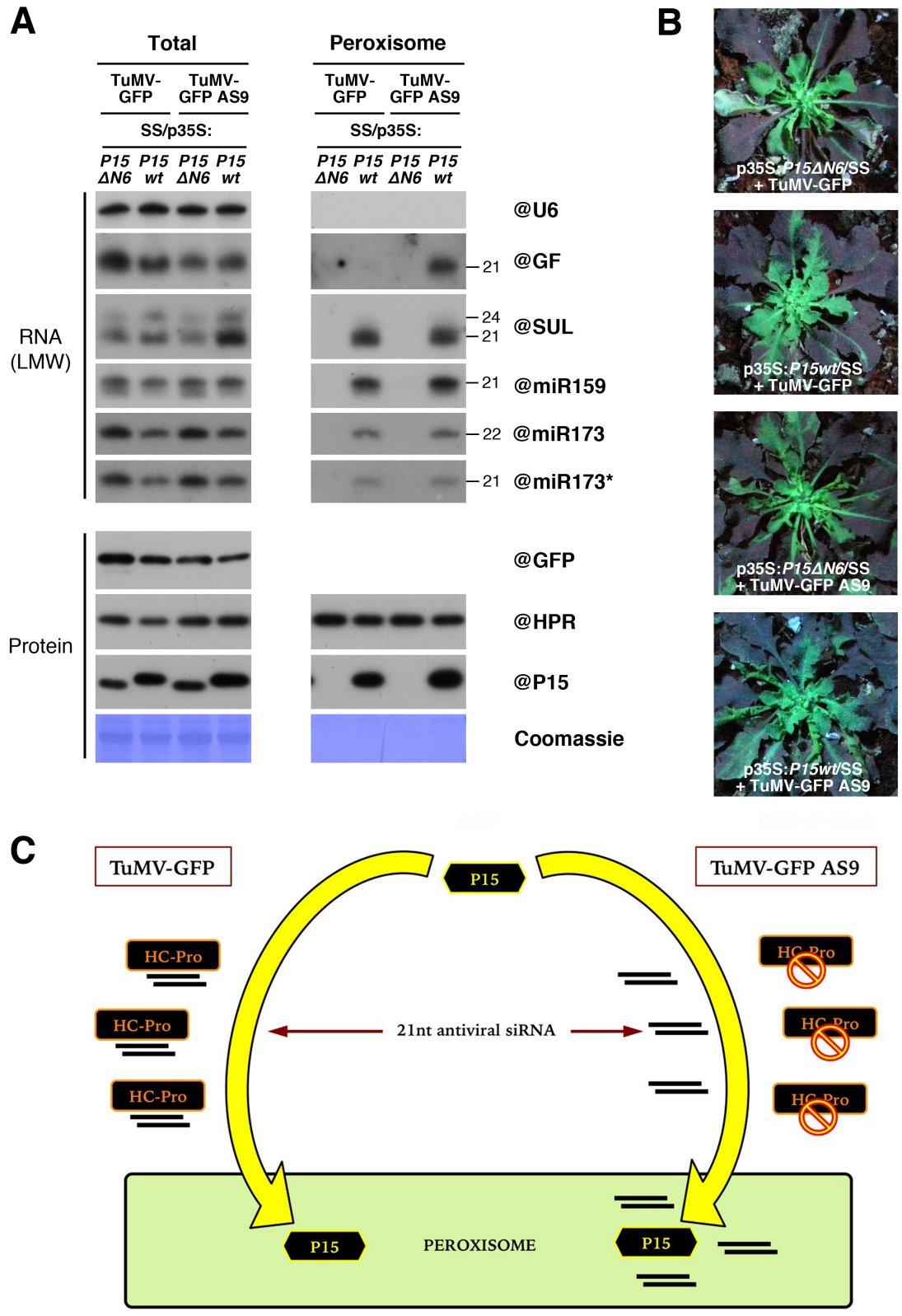

Figure 2.3: Effect of siRNA sequestration by another VSR on P15wt-dependent piggybacking of siRNAs into peroxisomes.

(A) Northern blot analysis of low molecular weight (LMW) RNA (top) and western blot analysis of proteins (bottom) from total (left) and peroxisomal (right) fractions obtained from TuMV-GFP- and TuMV-GFP AS9-infected SS plants expressing p35S:*P15ΔN6* or p35S:*P15wt*. Virus accumulation is assessed through quantification of GFP protein. (B) Photos under UV light of the plants analyzed in (A). (C) Schematic representation of the effect of a VSR-competent or a VSR-incompetent HC-Pro on peroxisomal import of siRNAs by P15wt. Sequestration of anti-TuMV siRNAs by HC-Pro precludes their piggybacking into peroxisomes by P15wt.

peroxisomal protein content. While all samples contained large amounts of peroxisomal proteins, only a handful of peptides were exclusively present or consistently enriched in P15wt-expressing plants, and in quantities barely above detection level. When we repeated the experiment with TRV-PDS- and TuMV-GFP-infected plants, the results were similar, albeit with different proteins enriched in P15wt peroxisomes. We therefore considered these low-count detection events as background noise. From this series of experiments we concluded that transgenically expressed P15wt most likely doesn't shuttle any host proteins into peroxisomes in significant amounts. However, it is still possible that a putative protein imported by P15 is quickly degraded within peroxisomes through an unknown mechanism, thereby escaping detection.

2.1b - TuMV-GFP-infected and TuMV-GFP AS9-infected plants

Next, we proceeded to perform a similar experiment with another RNA virus to confirm import of virus-derived siRNAs into peroxisomes by P15wt. We isolated peroxisomes from plants infected with TuMV-GFP, which encodes HC-Pro, a well-known VSR that binds and sequesters 21nt virus-derived siRNAs (Garcia-Ruiz *et al.*, 2015), and from plants infected with TuMV-GFP AS9, a mutant whose HC-Pro is not able to bind 21nt siRNAs and suppress silencing (Garcia-Ruiz *et al.*, 2015, 2010). While TuMV-GFP is capable of efficiently establishing systemic infection in Col-0 wild-type plants, TuMV-GFP AS9 can only do so when the host is impaired in antiviral RNAi, namely in *dcl2dcl4* and to a minor extent in *dcl4* mutant backgrounds (Garcia-Ruiz *et al.*, 2010). This experimental setting allowed us to test whether a functional siRNA-binding VSR (HC-Pro) can interfere with P15wt ability to import siRNAs into peroxisomes.

Our results show that both P15ΔN6 and P15wt, when ubiquitously expressed, were able to rescue systemic infectivity of a VSR-deficient TuMV (**Fig. 2.3B**). The similar amounts of GFP accumulated in systemic leaves of p35S:*P15wt*/SS and p35S:*P15ΔN6*/SS infected with TuMV-GFP AS9 confirm that these two alleles of P15 are equally proficient in suppressing cell-autonomous antiviral RNAi. Moreover, P15wt was able to import TuMV-GFP AS9-derived siRNAs into peroxisomes (**Fig. 2.3A**), further confirming the results obtained with TRV-PDS infection.

In stark contrast with TuMV-GFP AS9 infection, no TuMV-GFP-derived siRNA could be found in peroxisomes of plant expressing P15wt, despite efficient import of this protein into these organelles. Since to our knowledge the only difference between TuMV-GFP and TuMV-GFP AS9 is siRNA-binding and consequent silencing suppression ability of HC-Pro (Garcia-Ruiz *et al.*, 2015), we interpret this result as the direct consequence of antiviral siRNA sequestration by TuMV-GFP-encoded HC-Pro, and therefore competition between P15wt and HC-Pro for antiviral siRNA binding (**Fig. 2.3C**).

A first simple interpretation of this result could be that HC-Pro has higher affinity for 21nt siRNAs than P15wt. While this could indeed be true, a more detailed analysis is necessary to attempt a complete explanation. In fact, while wild-type HC-Pro completely abolished P15wt-dependent peroxisomal import of TuMV-derived siRNAs, it had no effect whatsoever on the import of anti-*SUL* siRNAs. This specific sequestration of TuMV-derived siRNAs by HC-Pro could be due to spatial separation (i) between virus- and transgenic-derived siRNAs, and/or (ii) between virus-encoded HC-Pro and transgene-encoded P15wt. This possibility is alluring, since RNA viruses normally replicate in spatially segregated viral factories and are likely processed by DCL enzymes in and around these factories. Given the key role that HC-Pro plays in potyvirus life cycle, not only as a VSR but also as a proteinase responsible for polyprotein cleavage (Carrington and Dougherty, 1987; Carrington *et al.*, 1990), we hypothesize that HC-Pro is abundant and sequesters siRNAs in and around TuMV replication enclaves. Consequently, we argue that a nuclear-encoded P15wt could be shuttled into peroxisomes without binding TuMV-GFP-derived siRNAs, which are sequestered by HC-Pro in or around viral factories. This assumption further entails that DCL enzymes process TuMV RNA in the vicinity of viral factories, that would in turn explain why most antiviral siRNAs are bound by HC-Pro and not by P15wt. Vice versa, a nuclear-transcribed hairpin such as SS is probably not significantly processed within viral factories, so HC-Pro does not sequester the siRNAs generated from it. As a result, P15wt ability to import these siRNAs into peroxisomes is not affected by the presence of a functional HC-Pro. To uncouple the possible spatial separation of P15wt and HC-Pro from their actual competition for siRNA binding, it would be interesting to assess the peroxisomal siRNA population of p35S:*P15wt*/SS expressing a transgenic p35S:*HC-Pro*.

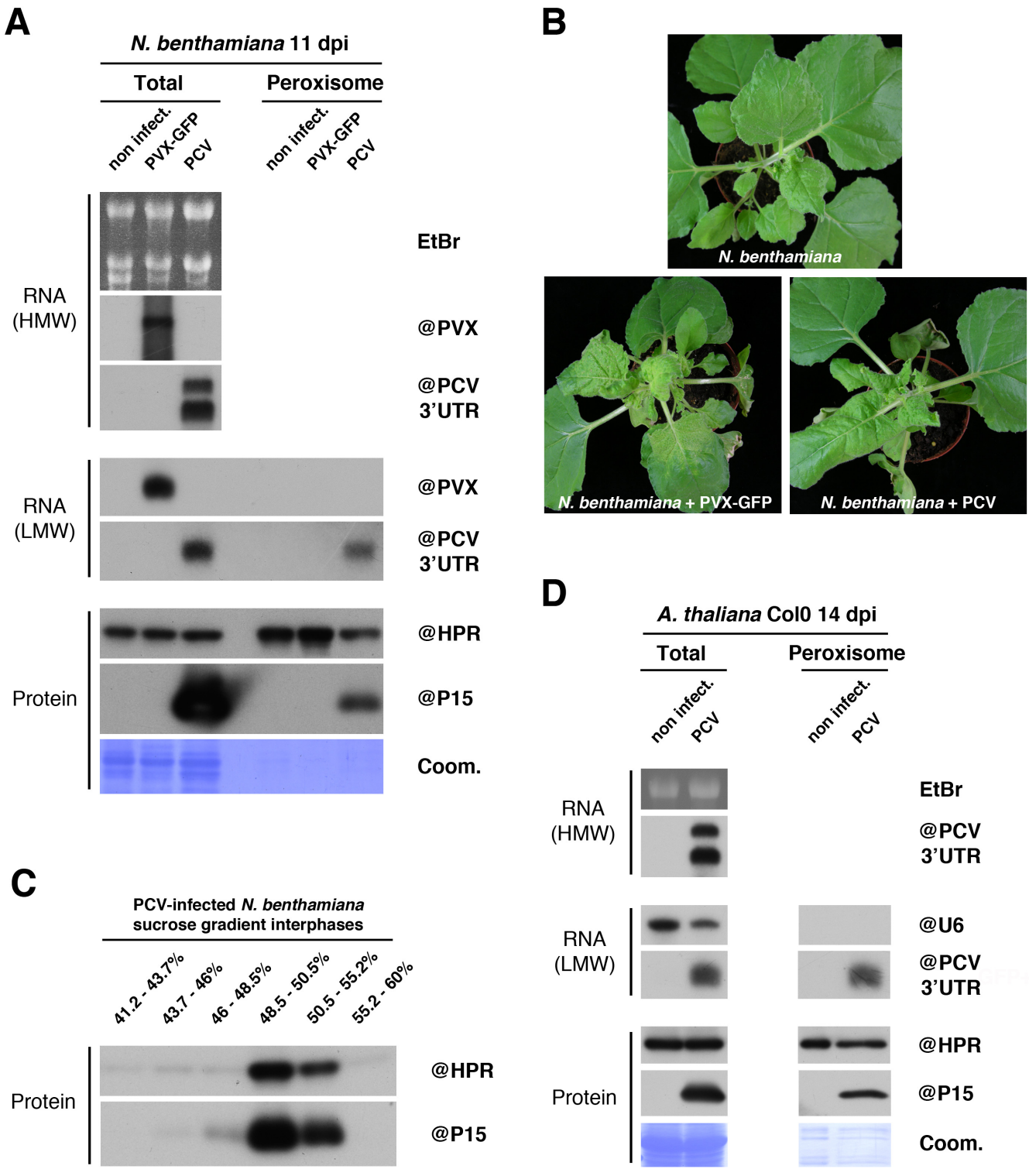

Figure 2.4: Analysis of peroxisomes isolated from PCV-infected plants.
(A) Northern blot analysis of high molecular weight (HMW) (top) and low molecular weight (LMW) (middle) RNA, and western blot analysis of proteins (bottom) from total (left) and peroxisomal (right) fractions from systemic leaves of non-infected, PVX-GFP- and PCV-infected *N. benthamiana*, harvested 11 dpi. (B) Photos of the plants analyzed in (A). (C) Western blot analysis of proteins extracted from six interphases collected from the discontinuous sucrose gradient after the final ultracentrifugation step of peroxisomal isolation. (D) as in (A), but on non-infected or PCV-infected *A. thaliana* systemic leaves, harvested 14 dpi. During genuine PCV infection in *N. benthamiana* and *A. thaliana*, P15 piggybacks anti-PCV siRNAs into peroxisomes.

Taken together, our results involving P15wt-expressing transgenic lines indicate that sRNAs, including virus-derived siRNAs, but no host proteins, are present with P15wt in peroxisomes. On the other hand, despite their presence in total extracts, both P15ΔN6 and sRNAs are absent in peroxisome isolates of plants expressing this allele. From this we infer that P15wt, after binding a sRNA, is able through its PTS1 to be imported into peroxisomes along with its cargo. These compelling results prompted us to verify whether this is the case during a genuine PCV infection.

2.2 - Isolation of peroxisomes from PCV-infected plants

To assess the presence of anti-PCV siRNAs in peroxisomes during PCV infection, we first performed peroxisome isolation from infected *N. benthamiana* plants, since this species is readily infected by PCV and at the time we had not yet developed an efficient infection protocol for *A. thaliana*. In this experiment we included two controls: non-infected plants and PVX-GFP-infected plants (**Fig. 2.4A, 2.4B**). PVX-GFP is a well-known RNA virus, and was included as a control to verify whether or not antiviral siRNAs can be detected in peroxisomes during infection by a virus other than PCV. To our knowledge no reports on peroxisome isolation from *N. benthamiana* leaves were available, so we proceeded to validate the use of the *A. thaliana* protocol by analyzing all the interphases from the sucrose gradient of PCV-infected *N. benthamiana* after the final ultracentrifugation (**Fig. 2.4C**). The results show that HPR accumulates at the expected sucrose density (50.5%), as does P15. While the HPR antibody was raised against *A. thaliana* HPR and not validated for *N. benthamiana*, the fact that by western blot we obtained a single band at the expected size and that this band was abundant in the 50.5% sucrose phase, supported that this antibody was also efficient in detecting *N. benthamiana* HPR.

The results of this experiment show that peroxisomes isolated from systemically infected leaves of PCV-infected plants indeed contained both P15 and anti-PCV siRNAs. On the other hand, peroxisomes isolated from PVX-GFP-infected plants did not contain anti-PVX siRNAs, suggesting that the presence of antiviral siRNAs is a peculiarity of PCV infection.

Once we established a protocol to obtain efficient and highly reproducible PCV systemic infection on *A. thaliana* (see Materials and Methods) we isolated peroxisomes from non-infected and PCV-infected Col-0 plants (**Fig. 2.4D**). PCVΔN6 was not included in this experiment as negative control because, as seen previously, it is severely impaired in systemic accumulation (**Fig. 2.5B**). The results show that also in *A. thaliana* anti-PCV siRNAs are present in the peroxisomal fraction along with P15.

At this point, a model can be hypothesized regarding the function of P15 peroxisomal localization in PCV systemic movement. Three facts must be considered: (i) P15FHA stops cell-to-cell movement of 21nt siRNAs much less efficiently than 22nt siRNAs (**Fig. 1.7**), suggesting a potential limitation in its ability to suppress non-cell autonomous RNAi, (ii) P15 is able to piggyback PCV-derived siRNAs into peroxisomes (**Fig. 2.4**) and (iii) peroxisomal localization of P15 strongly promotes PCV systemic infection (**Fig 2.1A**).
Thus, we hypothesized that during PCVwt infection P15 confines anti-PCV siRNAs within peroxisomes. Confinement within these organelles prevents siRNA systemic movement whether they stay bound to P15 or not, thereby allowing P15 to neutralize mobile siRNAs despite its lower affinity for 21nt siRNAs relative to 22nt siRNA. By blocking siRNA cell-to-cell and systemic movement, P15 in turn prevents the priming of systemic defenses ahead of the virus, so PCV faces little or no mobile siRNA-induced resistance upon its arrival into new tissues. On the other hand PCVΔN6, while efficiently suppressing intracellular RNAi, is not capable of confining anti-PCV siRNAs within peroxisomes and thus allows the movement of a critical amount of these siRNAs, which prime systemic defenses ahead of the virus and thereby significantly hamper the movement of PCV.

While this hypothesis is very compelling, we wanted to confirm it by ruling out the possibility that P15 allows movement of PCV independently from siRNA import into peroxisomes. In this scenario, P15 would piggyback siRNAs into peroxisomes as a consequence of its siRNA binding capacity but boost PCV movement through a separate peroxisomal function. To this end, we reasoned that if import by P15 of siRNA into peroxisomes is indeed what promotes PCV movement, removal of antiviral siRNA should restore PCVΔN6 ability to establish systemic infection (**Fig. 2.5A**). Since DCL4 and DCL2

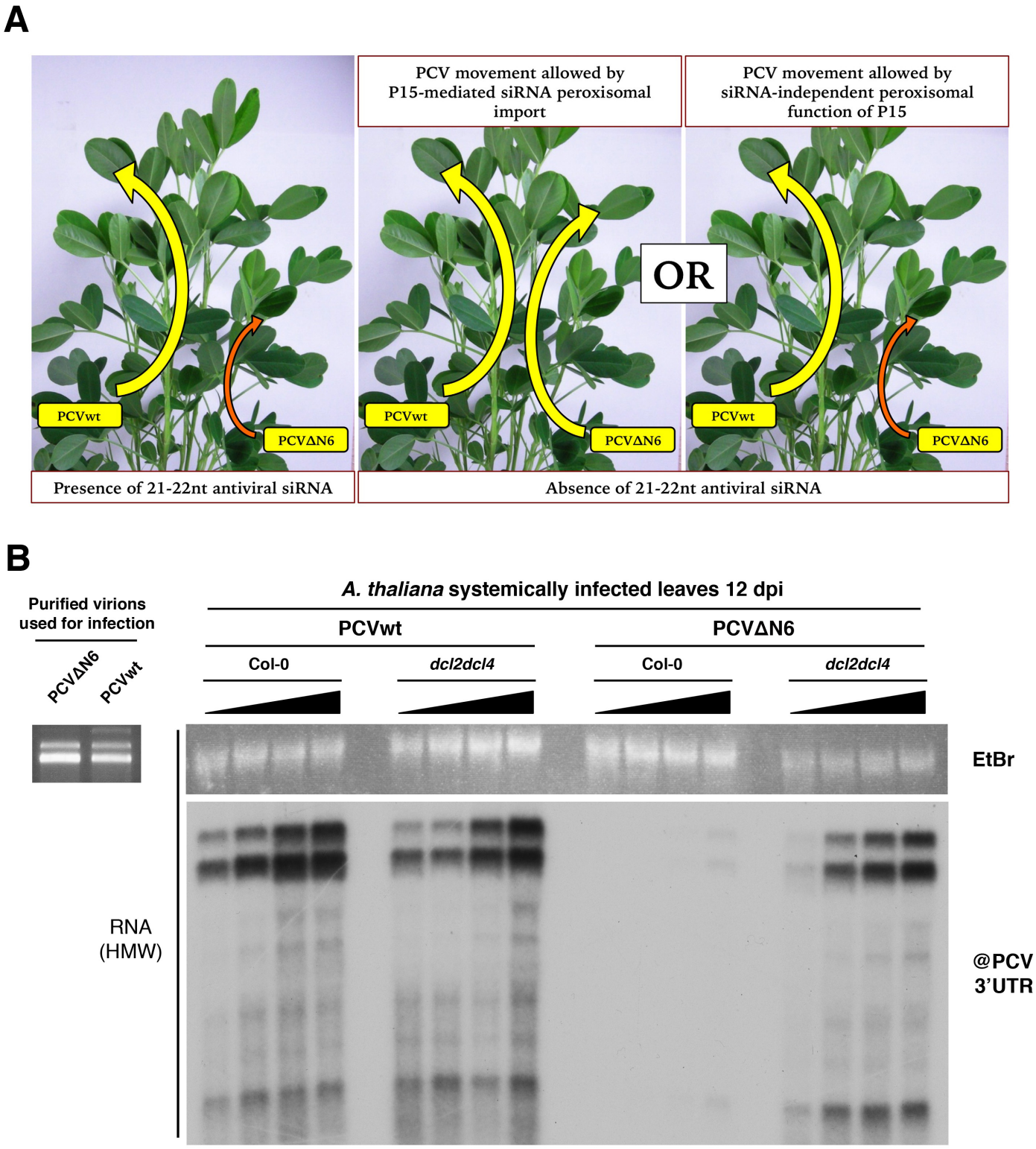

Figure 2.5: Relevance of P15wt-dependent siRNA peroxisomal import in PCV movement.
(A) Schematic representation of the possible outcomes of *dcl2dcl4* infection with PCVwt and PCVΔN6, depending on the relevance of siRNA peroxisomal import in PCV movement. (B) Left: verification of integrity and correct quantification of PCV virions used as inoculum, through agarose gel electrophoresis of virion RNA. Right: Northern blot analysis of high molecular weight (HMW) RNA from systemically infected leaves of Col-0 and *dcl2dcl4* plants infected with PCVwt or PCVΔN6, harvested 12 dpi. Out of the 20 plants infected per virus/genotype combination, 4 individuals are here shown spanning the range of viral titers observed during the preliminary molecular analysis of all plants. P15-dependent peroxisomal import of siRNAs allows PCV to efficiently establish systemic infection.

are the enzymes generating anti-PCV siRNAs (**Fig. 1.8**), if our model is correct PCVwt and PCVΔN6 should accumulate in similar amounts in a *dcl2dcl4* double knockout. We therefore used Col-0 and *dcl2dcl4* to genetically establish the significance of siRNA peroxisomal import by P15 in PCV systemic infection.

2.3 - Significance of siRNA peroxisomal import in PCV systemic movement

To verify whether or not PCVΔN6 ability to achieve systemic infection is restored upon removal of antiviral siRNAs, we infected *A. thaliana* Col-0 and *dcl2dcl4* mutants with equal amounts of PCVwt and PCVΔN6 purified virions. We infected 20 plants per combination, harvested systemic leaves 12 dpi and scored these for PCV genomic RNA accumulation by Northern blot. **Fig. 2.5B** shows 4 selected individuals per combination that span the range of PCV titers observed during the primary analysis of all plants.

In Col-0, as observed in *N. benthamiana*, PCVwt successfully established systemic infection while PCVΔN6 showed comparatively very little systemic accumulation, if any. On the other hand, in *dcl2dcl4* PCVΔN6 achieved systemic infection to a degree similar to PCVwt. We consider this result as genetic evidence that peroxisomal import of DCL4/DCL2-dependent siRNAs by P15wt, and not a distinct peroxisomal activity, enables PCV to establish efficient systemic infection.

We then decided to repeat the experiment while including an additional question. Since our pSUC:*P15FHA* results uncovered a potential limitation in the VSR activity of P15, namely a limitation in its capacity to stop intercellular movement of 21nt siRNAs, we wondered whether it is the movement of this specific size class of RNA that prevents efficient systemic infection by PCVΔN6. If this were the case, the specific removal of 21nt siRNAs would render peroxisomal localization of P15 dispensable for systemic movement. To address this point, we infected *A. thaliana* Col-0, *dcl4* and *dcl2dcl4* mutants with PCVwt and PCVΔN6, 15 plants per combination, and proceeded with analysis as described above (**Fig. 2.6**).

In this experiment, removal of DCL4 by genetic knockout restored PCVΔN6 systemic accumulation to near-PCVwt levels, further supporting that it is indeed the peroxisomal

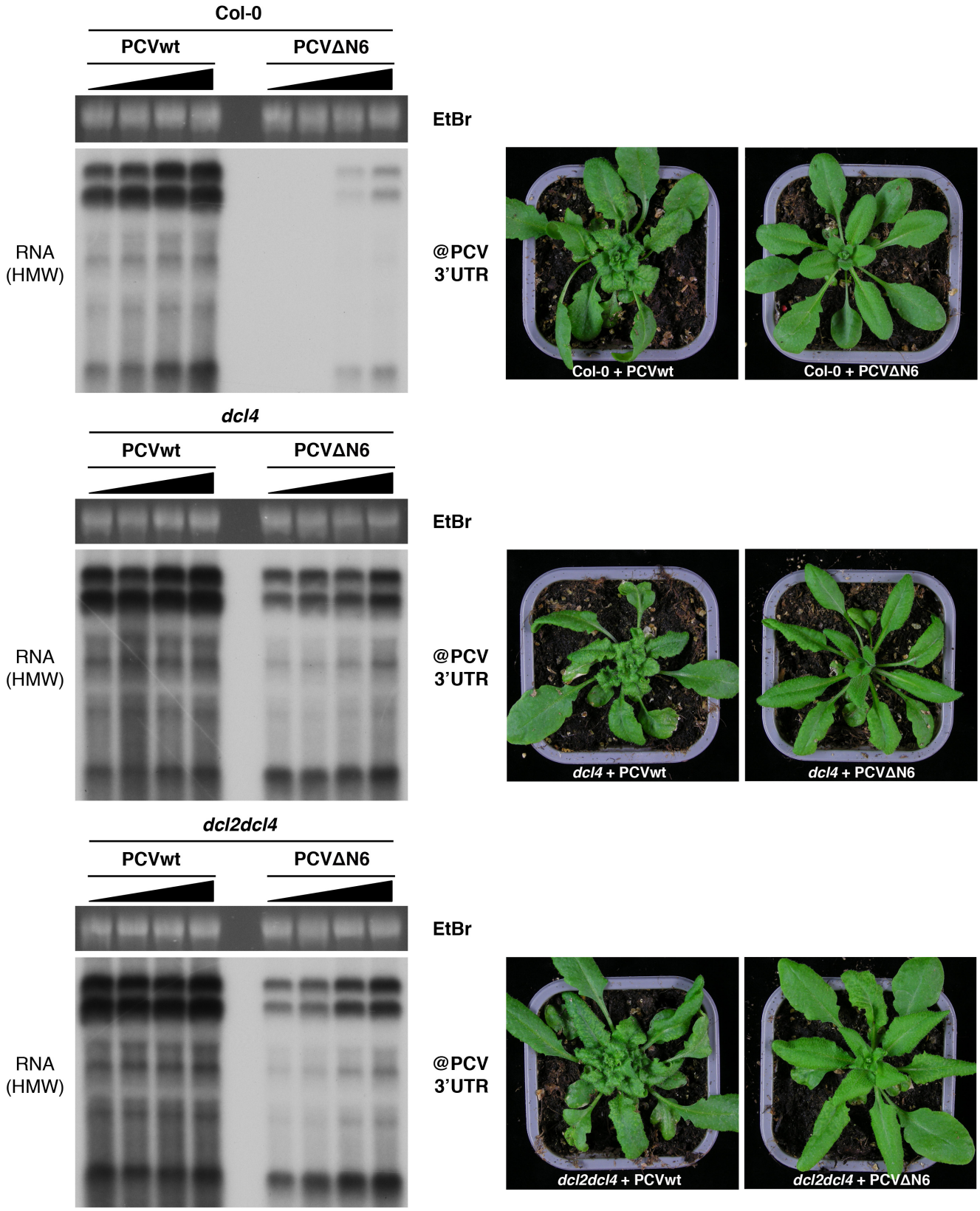

Figure 2.6: Relevance of 21nt versus 22nt siRNA peroxisomal import in PCV movement.
Left: Northern blot analysis of high molecular weight (HMW) RNA from systemically infected leaves of Col-0, *dcl4* and *dcl2dcl4* plants infected with PCVwt or PCVΔN6, harvested 12 dpi. Out of the 15 plants infected per virus/genotype combination, 4 individuals are here shown spanning the range of viral titers observed during a preliminary analysis of all plants. Right: photos of plants at the moment of harvest. Note that the samples shown on these Northern blots have been run in a different disposition (virus-wise as opposed to genotype-wise) and are shown in Figure 4 of the manuscript in Annex 4. Only the import of 21nt siRNAs into peroxisomes is relevant in PCV movement, the import of 22nt siRNAs is not.

import of 21nt siRNAs that enables PCVwt to greatly bolster its systemic infectivity. The very similar systemic accumulation of PCVΔN6 observed in *dcl4* and *dcl2dcl4* mutant backgrounds allows us to conclude that peroxisomal import of 22nt siRNAs is trivial in the establishment of systemic infection. While this result could be interpreted as a consequence of scarce or null ability of mobile 22nt siRNAs to prime systemic antiviral RNAi, it is tempting to ascribe this effect to the higher ability of P15 to bind 22nt siRNAs, which makes their peroxisomal confinement dispensable.

These experiments genetically showed that P15-mediated piggybacking of 21nt siRNAs into peroxisomes greatly increases the ability of PCV to establish systemic infection. Nevertheless, in plants devoid of 21-22nt siRNAs, PCVwt still accumulates in higher amounts than PCVΔN6. This observation suggests that peroxisomal localization of P15 brings an additional advantage to PCV, on top of siRNA neutralization. Moreover, the fact that in both experiments all plants infected with PCVΔN6 showed very mild and different symptoms compared to PCVwt, even on occasions where both viruses accumulated to similar viral titers, suggests that peroxisomal localization of P15 may be a determinant of symptom severity.

2.4 - Significance of phloem loading/unloading of siRNA in the systemic restriction of PCVΔN6

The results shown above suggest that PCVΔN6 is impaired in systemic accumulation because it is not able to efficiently stop systemic movement of antiviral siRNAs. Since antiviral siRNAs most likely move systemically through the phloem, we predicted that inhibition of siRNA phloem loading/unloading should restore PCVΔN6 movement to PCVwt levels, as happened upon removal of DCL4. To this end, we reasoned that if companion cell-specific expression of P15FHA is able to stop the movement of transgene-derived siRNAs out of this tissue (as in line pSUC:*P15FHA*/SS #14, see **Fig. 1.7**), it should also be able to stop antiviral siRNAs movement through the companion cells, in their journey from the surrounding infected tissue toward the actual sieve elements (**Fig. 2.7A**). In other words, mobile anti-PCV siRNAs moving ahead of the virus from infected cells

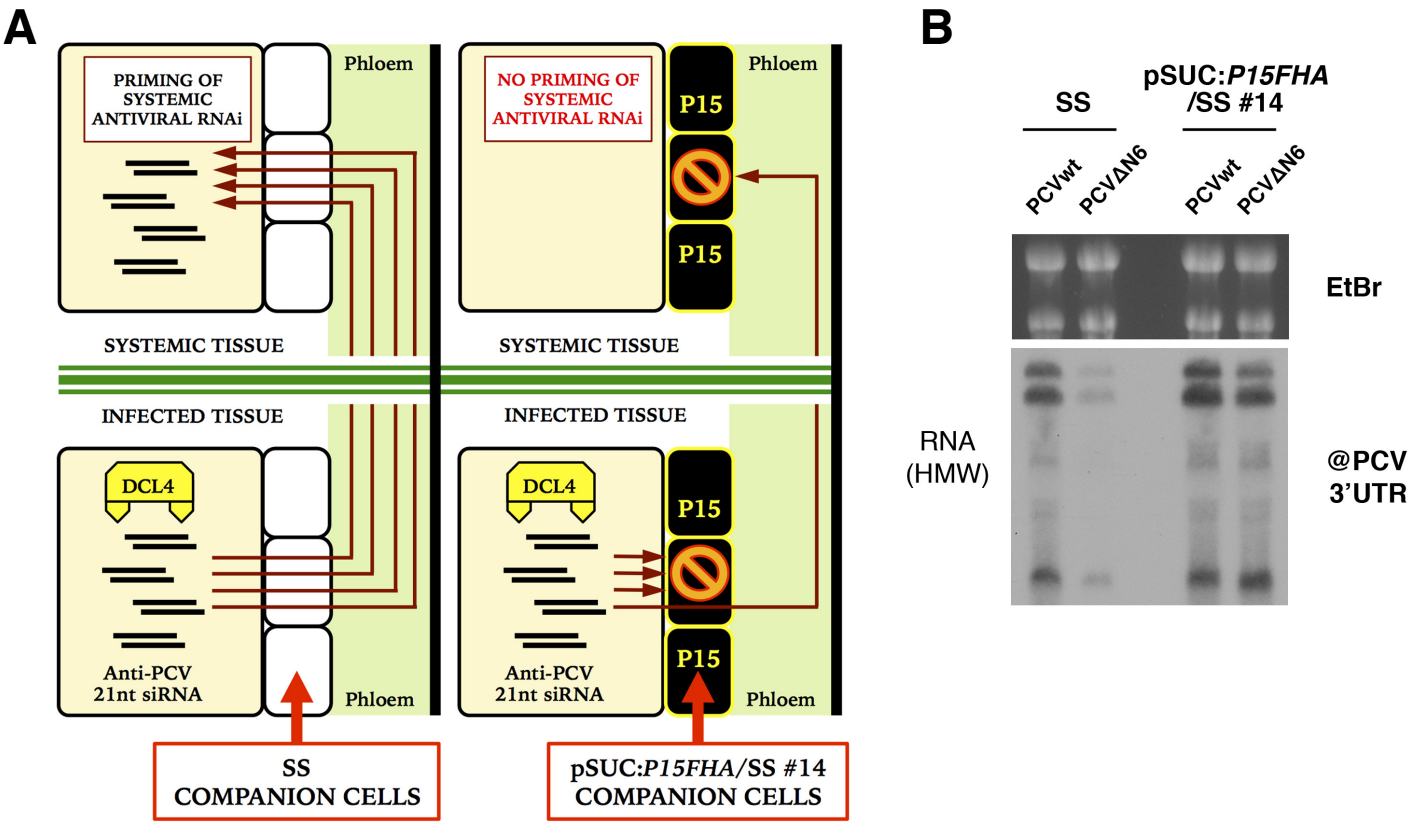

Figure 2.7: Relevance of antiviral siRNA phloem loading/unloading in PCVΔN6 systemic restriction. (A) Schematic representation of why pSUC:*P15FHA*/SS#14 plants were used to test the role of phloem antiviral siRNA trafficking in the impaired systemic accumulation of PCVΔN6. We postulate that P15FHA generates an "siRNA sponge" in companion cells that absorbs 21-22nt siRNAs moving to and from the sieve elements. (B) Northern blot analysis of high molecular weight (HMW) RNA from systemically infected leaves of SS and pSUC:*P15FHA*/SS#14 plants infected with PCVwt or PCVΔN6, harvested 11 dpi. Here each sample represents a pool of 4 plants. Blocking siRNA trafficking in companion cells rescues PCVΔN6 movement.

toward the phloem should be blocked by P15FHA in the cells surrounding it and prevented from entering the vasculature. This could also be true in recipient systemic leaves, since any siRNAs that manage to enter the phloem in infected tissues and move systemically would be stopped in companion cells on their way out. We therefore argue that the pSUC:*P15FHA*/SS #14 line described in Chapter 1 possesses two successive barriers against phloematic movement of 21-22nt siRNAs. This "siRNA sponge" may be able to sequester in- and outbound siRNAs and therefore shut down their phloem trafficking. If this is the case, in PCVΔN6 systemic accumulation should be rescued in pSUC:*P15FHA*/SS #14.

To test this hypothesis, we infected SS and pSUC:*P15FHA*/SS #14 with PCVwt and PCVΔN6, 4 plants per combination. At 11 dpi, systemic leaves were harvested, pooled and PCV accumulation was assessed by Northern blot (**Fig. 2.7B**). The reader is here reminded that in pSUC:*P15FHA*/SS#14 enough P15FHA is produced within companion cells to stop the movement of anti-*SUL* siRNA, despite peroxisomal exclusion of P15FHA. In this experiment the relevance of P15 peroxisomal import is assessed, as in the previous experiments, through the PCV-encoded P15, and not the transgenic P15FHA. The latter was used to sequester siRNA within companion cells, and other siRNA-sequestering VSRs (such as P19) could equally have been employed in this respect.

As expected, in SS plants PCVΔN6 accumulation was severely hampered compared to PCVwt. The difference in accumulation between the two viruses was not as pronounced as in Col-0 (**Fig. 2.5, 2.6**), which we attribute either to a SS-specific effect or to a casual fluctuation highlighted by the small number of plants used in this experiment. Nevertheless, in pSUC:*P15FHA*/SS #14 the systemic accumulation of PCVΔN6 and PCVwt was similar, indicating that companion cell-specific sequestration of 21-22nt siRNAs was able to rescue efficient systemic movement of PCVΔN6. Although this last experiment needs to be repeated on a larger sample population, the results presented in this chapter simultaneously (i) stress the relevance of peroxisomal import of P15 in the suppression of systemic RNAi, and (ii) provide compelling evidence that siRNAs that move through the phloem play a major role in antiviral defense. Additionally, since P15FHA was able to stop siRNAs transiting through companion cells but presumably generated elsewhere, it may be

speculated that these siRNAs do not travel in association to any proteins, or if they do, they remain accessible to P15FHA.

2.5 - Conclusions

By performing peroxisomal isolation in several experimental contexts and in two species we have shown that P15wt is able, through its C-terminal PTS1, to be imported into peroxisomes. Most importantly, thanks to the very particular ability of the peroxisome importomer to translocate cumbersome molecules such as folded proteins and protein complexes across the peroxisomal membrane, it is able to piggyback antiviral 21-22nt siRNAs into peroxisomes, most likely in the form of duplexes. We show that antiviral and hairpin-derived siRNAs are not normally present in peroxisomes as part of a yet undiscovered step of RNAi, but are present strictly as a consequence of P15 import.
This is the first report of a nucleic acid being piggybacked into these organelles, and a confirmation through different means of P15 binding to sRNAs observed in IP experiments. Interestingly, while 21nt miRNAs were not found in P15FHA IPs (**Fig. 1.5, 1.6**), they were easily detected in peroxisomal fractions of plants expressing P15wt (**Fig. 2.2, 2.3**), suggesting that this protein is indeed able to associate to a certain extent to this class of sRNA. While this difference could be due to the tag present in P15FHA, another explanation could be that the weak P15/miRNA interaction is preserved during peroxisomal import but disrupted during IP experimental procedures. More on this topic is presented in Chapter 3.

The exact fate of the sRNA upon arrival in the peroxisomal matrix is not clear. The fact that Northern blots show a sharp band at 21-22nt suggests that these RNA do not slowly lose nucleotides, but does not exclude rapid degradation of a certain amount of siRNAs. However, since peroxisomes are normally devoid of RNA and dedicated to specific metabolic reactions that do not directly involve nucleic acid, RNAse-driven RNA degradation within these organelles seems unlikely. Also the fate of P15 inside peroxisomes has yet to be elucidated. While peroxisomal proteases exist, their functioning and targets are not well known, and it is not very clear whether the exportomer responsible for PEX5

recycling is also capable of exporting other proteins (Platta *et al.*, 2014). On the other hand, the harsh chemical conditions found within peroxisomes could potentially trigger changes in both P15 and sRNA. Therefore, whether or not these "spurious" peroxisomal molecules remain within the peroxisomes until the end of the organelle's life cycle is at present a matter of conjecture.

One thing that can be safely assumed is that siRNAs within peroxisomes are isolated from intracellular RNAi machinery and from the rest of the plant, and thereby functionally inactive. Thus, by importing siRNAs into peroxisomes, P15 neutralizes and immobilizes them. Logically, once the importation has occurred, eventual loss of contact between P15 and its cargo siRNA should have no consequence on the inactive and immobile state of the siRNA.

By assessing PCVwt and PCVΔN6 systemic infectivity in different genetic backgrounds we have shown that by importing DCL4-dependent 21nt siRNAs into peroxisomes through P15, PCVwt prevents their systemic movement and thereby prevents the priming of systemic antiviral RNAi in naïve non-infected tissues. If these systemic defenses are activated by mobile siRNAs, as happens during PCVΔN6 infection, the virus is severely hampered in systemic movement, if it does manage to move at all. These observations fit with those concerning the ability of P15 to stop siRNA cell-to-cell movement in our pSUC:*P15FHA*/SS reporter systems. In fact, the evolution of a strong bias toward 22nt siRNAs may have entailed the relatively weak capacity P15 shows in preventing the cell-to-cell movement of 21nt siRNAs. Therefore, we propose that peroxisomal import of 21nt siRNAs is a very smart strategy that allows P15 to compensate for its poor binding to this class of sRNA, accomplishing their neutralization and immobilization while not requiring long-lasting sequestration through binding.

It is hard to tell what exactly determines the poor ability of P15 to stop movement of 21nt siRNAs *in vivo*. Yet, we argue that by resorting to peroxisomal confinement P15 needs to stay in contact with an siRNA merely the time to be recognized by PEX5 and shuttled into peroxisomes. Following this event, its job as a VSR is done, so to speak.

While our results allow us to conclude that peroxisomal import of DCL2-dependent 22nt siRNAs is completely dispensable in the systemic movement of PCV (**Fig. 2.6**), the reasons behind this fact remain unclear. On one hand, the binding bias shown by P15 toward this class of sRNA may ensure a more or less permanent sequestration and render neutralization through peroxisomal confinement superfluous. On the other hand, 22nt siRNAs may be much less efficient than 21nt siRNAs in priming systemic RNAi, so whether they move or not is irrelevant regarding PCV systemic infection. Of course, these two possibilities are not mutually exclusive. Although we have shown that plants react to PCV infection by generating consistent amounts of virus-derived 22nt siRNAs, their precise function in antiviral defense awaits elucidation. An appealing possibility would be that in other plant species, on which PCV has evolved, these 22nt siRNAs play a more prominent role during antiviral defense reactions.

PCVwt systemic accumulation in Col-0 and *dcl2dcl4* was very similar in our experiments, suggesting that this virus is able to very efficiently suppress DCL4/DCL2-dependent antiviral RNA silencing. It is interesting to note that even in the absence of DCL2 and DCL4, PCVwt still generally shows increased viral systemic titers and symptoms compared to PCVΔN6, suggesting that peroxisomal import of P15 confers an additional siRNA-independent advantage to PCV. Our mass spectrometry analysis experiments hint that this effect is likely not due to piggybacking by P15 of a host protein into peroxisomes. However, the import of P15 into peroxisomes in PCV-infected cells probably diverts a significant amount of PEX5, which becomes therefore unavailable for peroxisomal import of endogenous proteins. This could lead to indirect disruption of peroxisome biology in general, or of a specific peroxisomal antiviral mechanism, that would in turn favor PCV accumulation, movement and symptom manifestation. Disruption of peroxisome functionality could also derive from the accumulation of foreign material within these organelles. All in all it is plausible that peroxisomal localization of P15 bolsters PCV infection in more than one way.

Since PCVΔN6 is as proficient as PCVwt in suppressing cell-autonomous RNAi, the stark contrast between the systemic accumulation of PCVΔN6 in Col0 and that in a *dcl4* mutant

background can be ascribed to the sole action of mobile antiviral siRNA. To our knowledge, this is the first time that suppression of cell-autonomous and non-cell autonomous antiviral RNA silencing have been uncoupled in the frame of a genuine viral infection, allowing us to specifically assess the effect of 21nt siRNA movement on the establishment of viral systemic spread. Indeed, the effect of those siRNAs that are allowed to move by PCVΔN6 goes from a delay of days to complete prevention of viral systemic movement, depending on the species and the experiment. This proves that the systemic aspect of RNAi, which has been abundantly investigated in transgenic reporter systems and is assumed to have antiviral function, indeed constitutes a potent defensive barrier. We show here that, in the case of PCV, plants can exploit mobile siRNAs to immunize naïve tissues that, therefore, become able to efficiently target the virus upon arrival. However, it is not clear what proportion of mobile siRNAs, if any, are efficiently stopped by PCVΔN6, so this effect we observed may represent a mere fraction of the potential systemic defense that infected plants could mount ahead of an invading virus.

Finally, we showed that companion cell-specific sequestration of siRNA, and creation of an "siRNA sponge" around the sieve elements, was enough to abolish the detrimental effects that systemic antiviral RNAi had on PCVΔN6 movement. This result further suggests that piggybacking of siRNA into peroxisomes is specifically required to stop their systemic movement through the phloem. Furthermore, while this tissue has been the presumed vehicle of systemic antiviral RNAi for quite some time, this is the first report to confirm it through unbiased viral infection.

CHAPTER 3

PEROXISOMAL TARGETING AS A TOOL TO IDENTIFY NOVEL MOLECULAR INTERACTIONS

As described in the Introduction, the peroxisomal importomer is capable of translocating across the peroxisomal membrane not only PEX5 and its folded PTS1-containing cargo protein, but also protein oligomers (Leon *et al.*, 2006). We have shown here that 21-22nt sRNA duplexes bound to P15, a PTS1-containing protein, can also be imported through this pathway.

While the import of siRNAs by P15 has been abundantly discussed in the previous chapter, we will here focus on the results we obtained from the analysis of sRNA extracted from peroxisome isolates vis-à-vis the sRNA obtained from P15FHA IPs. While IPs showed virtually no binding of P15FHA to 21nt miRNAs such as miR159, this miRNA was clearly detectable in peroxisomes of plants expressing P15wt but absent in those expressing P15ΔN6. We interpreted this as *in vivo* binding of P15wt to a certain amount of miR159, resulting in the import of the P15wt/miRNA complex into peroxisomes and subsequent miRNA detection in peroxisome isolates.

Two theories can be put forth to explain this discrepancy between the results obtained by IP and those obtained by peroxisome isolation. First, the P15wt allele could be more proficient in binding miRNAs than the tagged P15FHA version. This possibility could be tested by performing peroxisome isolations on plants expressing a P15FHA allele containing a C-terminal PTS1 (P15FHA-SKL) and verifying whether miRNA are present or not in these organelles. Such lines have been generated but not yet tested.

A second hypothesis, on which the following experiments are based, is that the weak binding of P15 to 21nt miRNAs is disrupted during IP procedures (freezing, grinding, clarifying, incubating, washing and so on). Conversely, in P15wt-expressing plants the P15/miRNA contact is maintained during transport to peroxisomes, which takes place *in vivo* and is not subject to any *ex vivo* treatment or manipulation. When peroxisome isolation is finally carried out, the 21nt miRNAs that interacted with P15 are safely confined within peroxisomes, and their presence in the resulting isolates confirms interaction with P15 even if the interaction itself is somehow disrupted during the experiment.

3.1 – Experimental system design

Since peroxisomal import of P15 followed by molecular analysis of peroxisomal extracts allowed us to unveil interactions not revealed by IP (P15/21nt miRNAs), we considered the broader use of this experimental system as a novel tool to identify interactions that are perhaps not detected through other established methods such as immunoprecipitation. We reasoned that by placing a PTS1 at the C-terminal end of a protein of interest we would induce the cell machinery to shuttle it into peroxisomes along with factors associated to it, as was the case with P15. Peroxisomes would therefore serve as "interactor storage units" to be isolated and analyzed.

This way of searching for intermolecular interactions, through cell-driven compartimentalization of a protein of interest and its interactors, is to our knowledge conceptually quite novel (and untested). *A priori,* it possesses one chief advantage that was highlighted by our work on P15: the interaction is confirmed *in vivo* the moment the protein of interest and its interactor enter the peroxisome within a living cell, and doesn't have to withstand any exogenous disturbance. This is in stark contrast with immunoprecipitation, where interactions must withstand a fair amount of *ex vivo* manipulation. Another potential advantage is the diminutive size of the sequence that must be added to the protein of interest to perform this experiment, a mere SKL tripeptide. Other well-established techniques to identify interactions such as epitope tag immunoprecipitation, yeast two-hybrid and BiFC assays require the addition of bulky peptides to the protein of interest. Moreover, while the interactions detected through immunoprecipitation are only the ones taking place at the moment of tissue harvest, peroxisomal import could theoretically grant a cumulative effect, whereby peroxisome isolates contain the result of a great number of piggybacking events, depending on peroxisome physiological turnover and the efficiency of import.

However, several substantial potential limitations come to mind. First and foremost are the technical difficulty of peroxisome isolation, the small number of samples processed per isolation, the fragility and scarcity of peroxisomes, their frequent association to chloroplasts and mitochondria, the large amount of material required and the fact that tissue cannot be frozen prior to peroxisome isolation. Moreover, the protein of interest may be shuttled to

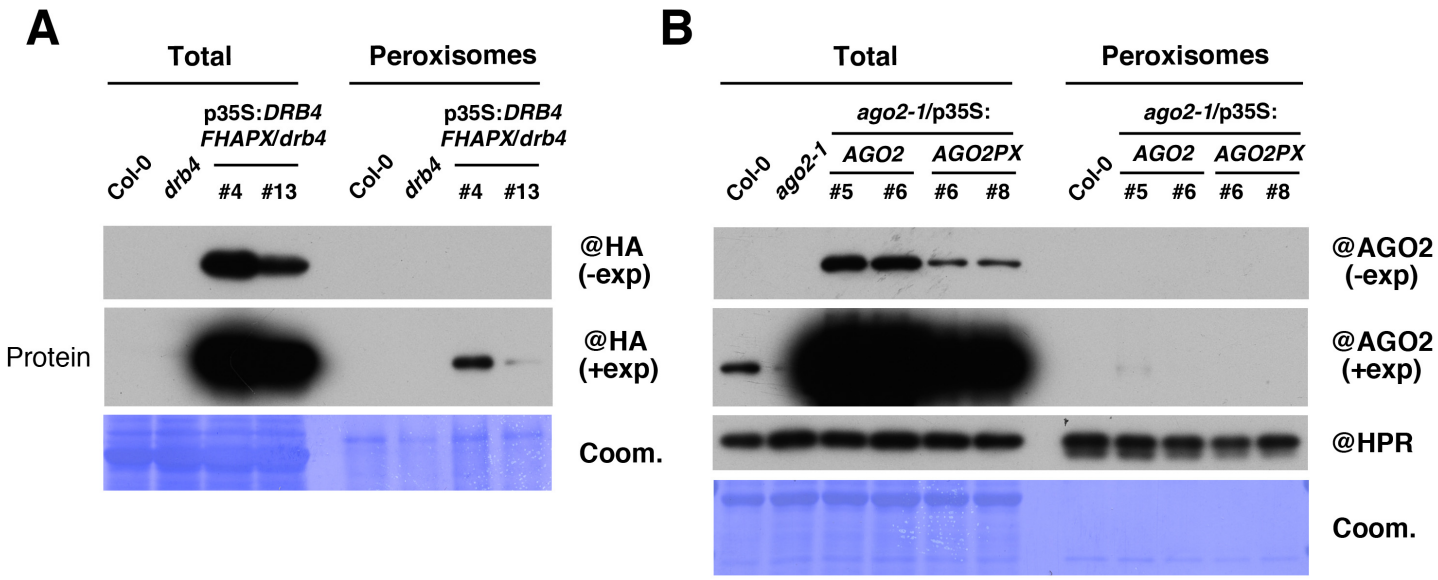

Figure 3.1: PTS1 addition to DRB4 and AGO2 to trigger peroxisomal targeting.
(A) Western blot analysis of proteins from total and peroxisomal fractions from plants expressing PTS1-containing DRB4FHA (DRB4FHAPX) and relative controls. (B) Same as in (A) but from plants expressing PTS1-containing AGO2 (AGO2PX). Despite the addition of a PTS1, DRB4 and AGO2 are not efficiently imported into peroxisomes.

peroxisomes before it comes into contact with its interactors. This also leads to the theoretic exclusion of all interactions that do not take place in the cytoplasm, where PEX5 is thought to come into contact with PTS1-containing proteins. In addition, the PTS1 must be on the C-terminal end of the protein of interest, and still be exposed on the surface of the protein so PEX5 can access it. It can also be argued that if the protein of interest is part of a large complex that is anchored to a specific structure within the cytoplasm, PEX5 may not be physically able to convey it to the peroxisomes. If the protein of interest is indeed shuttled to the peroxisome importomer with its interactors, the complex may be unable to cross the pore because of size constraints, or crossing the pore itself may cause loss of interactions. Finally, even if the protein of interest and interactors do make it into the peroxisomal matrix, they could be degraded within the organelle, thereby escaping detection.

Whatever its potential advantages and disadvantages, we were eager to test this system on some well known proteins involved in RNA silencing or its suppression by addressing them to peroxisomes, through the addition of a simple C-terminal SKL tripeptide, and subsequently analyzing the content of these peroxisomes.

3.2 - Peroxisomal targeting of endogenous RNAi factors: DRB4 and AGO2

As endogenous RNAi factors to target to peroxisomes we chose DRB4 and AGO2 (see Introduction). DRB4 was used as a possible proof of concept, as its interaction with DCL4 is well established and would ideally lead to DCL4 piggybacking into peroxisomes. We expressed DRB4FHAPX and AGO2PX encoding a C-terminal SKL PTS1, and DRB4FHA and AGO2 alleles to use as negative control, under a 35S promoter to ensure abundant production. To allow optimal detection of DRB4 by Western blot we used a FHA-tagged allele, while AGO2 was not tagged. *drb4-1* knock-out mutants were transformed with p35S:*DRB4FHA* or p35S:*DRB4FHAPX*, while *ago2-1* mutants were transformed with p35S:*AGO2* or p35S:*AGO2PX*. Strangely, none of the lines transformed with p35S:*DRB4FHA* accumulated any DRB4FHA protein, so in this experiment we used Col-0 and *drb4-1* as

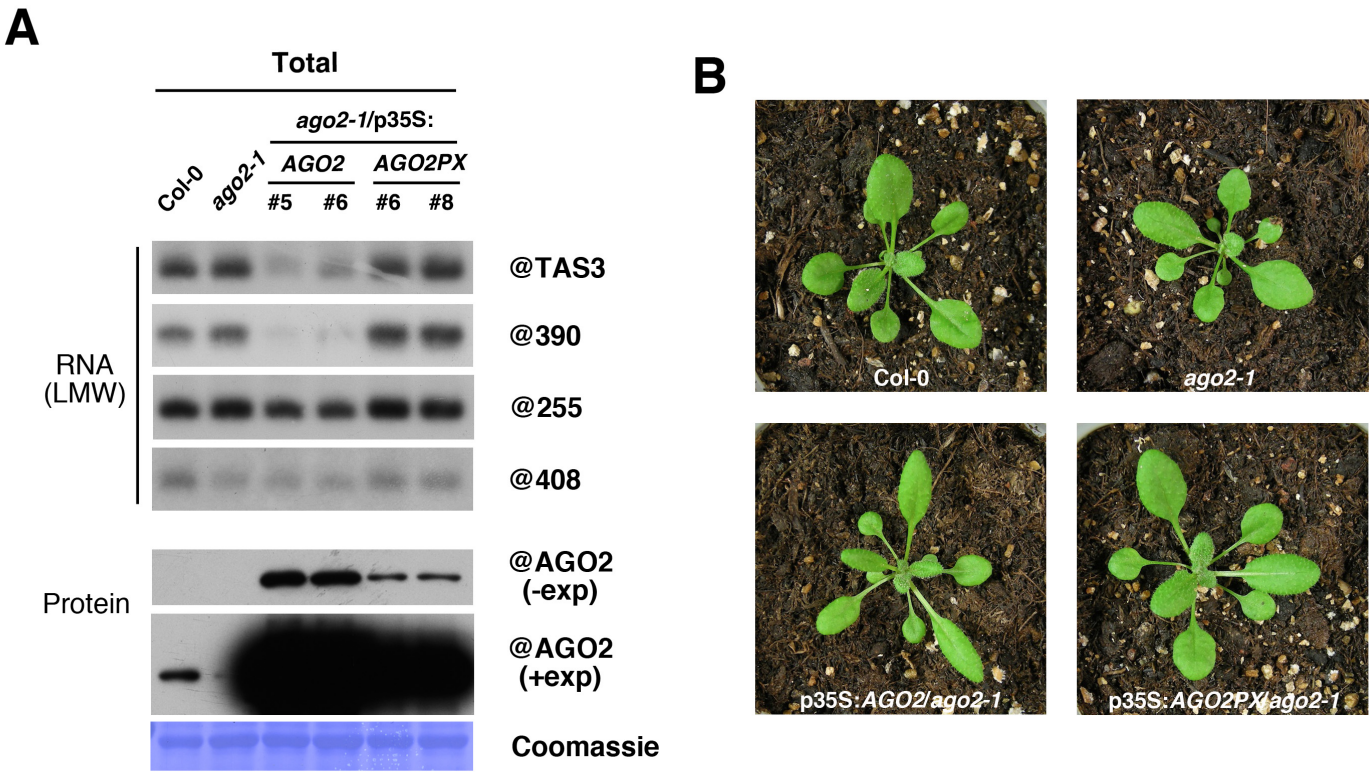

Figure 3.2: Effect of AGO2 overexpression on endogenous sRNA homeostasis.
(A) Northern blot analysis of low molecular weight (LMW) RNA (top) and western blot analysis of proteins (bottom) from the plants used for peroxisome extraction in Fig. 3.1. The western blot is the same as in Fig. 3.1. (B) Photos of the plants at the moment of harvest. AGO2 overexpression hampers accumulation of miR390 and downstream generation of *TAS3* ta-siRNAs, which probably leads to elongated leaves.

negative controls. To assess whether the PTS1-containing alleles were effectively imported into peroxisomes, we performed peroxisome isolation from plants expressing the constructs described and analyzed the proteins in these isolates to score for presence of DRB4FHAPX and AGO2PX (**Fig. 3.1**).

As can be observed from the results, AGO2PX was completely absent from peroxisomes (**Fig. 3.1B**) while DRB4FHAPX was present in very low amounts (**Fig. 3.1A**). Given the absence of AGO2 in the p35S:*AGO2PX/ago2-1* peroxisomes, we didn't proceed with mass spectrometry analysis. Since the crystal structures of human and yeast Argonautes reveal that the C-terminal end is not exposed on the surface but rather buried within the RNA binding cleft (Poulsen et al., 2013), failed import into peroxisomes of AGO2 is likely due to inaccessibility of the PTS1 by PEX5. Mass spectrometry analysis of p35S:*DRB4FHAPX/drb4-1* peroxisome isolates confirmed very low presence of DRB4FHAPX and no peptide corresponding to DCL4 could be detected (**Fig. S8** – Annex 1). Since in these experiments our endogenous proteins of interest weren't efficiently imported into peroxisomes as we hoped, we abandoned this line of enquiry.

However, it is necessary to briefly comment some unexpected results obtained with the p35S:*AGO2/ago2-1* lines, originally generated as a negative control for our AGO2PX peroxisomal import experiments. Interestingly, we observed that these plants consistently showed elongated leaves compared to Col-0 and *ago2-1* (**Fig. 3.2B**). This phenotype is typical of plants deficient in ta-siRNA generation, such as *dcl4* mutants, as *TAS3* ta-siRNAs are required for the regulation of proper leaf development and polarity (Adenot *et al.*, 2006; Garcia *et al.*, 2006). This observation prompted us to assess the steady-state accumulation of *TAS3*-derived ta-siRNAs in these transgenic lines. We observed that p35S:*AGO2*-expressing lines were severely impaired in the accumulation of *TAS3* ta-siRNAs (**Fig. 3.2A**), as was the accumulation of miR390, which is responsible for AGO7-mediated production of these ta-siRNAs (Montgomery et al., 2008). While low accumulation of *TAS3* ta-siRNAs could be due to low accumulation of miR390, this last observation is more difficult to explain. One possibility is that the very high amount of AGO2 causes competition for binding of miR390. Since miR390 carries a 5' adenosine, which is also the 5' nucleotide preferred by AGO2 (Mi et al., 2008), this option is plausible. Loading into AGO2 would somehow cause a

destabilization of miR390, hence the low accumulation observed. Alternatively, AGO2 could compete with AGO7 for miR390 loading, but be loaded with the passenger strand miR390* instead. This could lead to the processing of guide strand miR390 through the degradation pathway normally reserved to passenger miR390*, hence its low accumulation. Due to time limitations we were not able to test this hypothesis. AGO2PX overexpression didn't have any effect on the sRNAs we tested, suggesting that this allele of AGO2 may not be functional. More experimentation is needed to characterize this unexpected effect of AGO2 overexpression on endogenous sRNA homeostasis.

Next, we focused our attention on the possible use of peroxisomal targeting to identify interactors of two VSRs, P38 and P19.

3.3 - Peroxisomal targeting of viral suppressors of RNA silencing: P38 and P19

To test whether VSRs other than P15 are able to piggyback their interactors into peroxisomes, and hence enable us to use peroxisomal targeting as an alternative experimental system for interactome identification, we added a C-terminal SKL tripeptide to P38 from TCV and P19 from TBSV. These two VSRs, which have been already described in the previous chapters, were placed under control of a 35S promoter and introduced into the SS reporter line. These proteins were chosen because their interactors are well known: P38 interacts with and inhibits function of AGO1 (Azevedo *et al.*, 2010), while P19 (here tagged with HA epitope for purpose of detection) binds and sequesters 21nt sRNA duplexes (Dunoyer *et al.*, 2010; Vargason *et al.*, 2003).

To assess whether P38 is able to piggyback AGO1 into peroxisomes, after characterization of the transgenic lines we performed peroxisome isolations from SS (used as negative control) and p35S:*P38PX*/SS plants (three biological replicates each). Following quality control by Western blot, we subjected the proteins obtained to mass spectrometry analysis (**Fig. 3.3A**). First of all, it must be noted that, as opposed to p35S:*P38*/SS plants (Schott *et al.*, 2012), p35S:*P38PX*/SS plants showed the *SUL*-silencing phenotype, suggesting that the

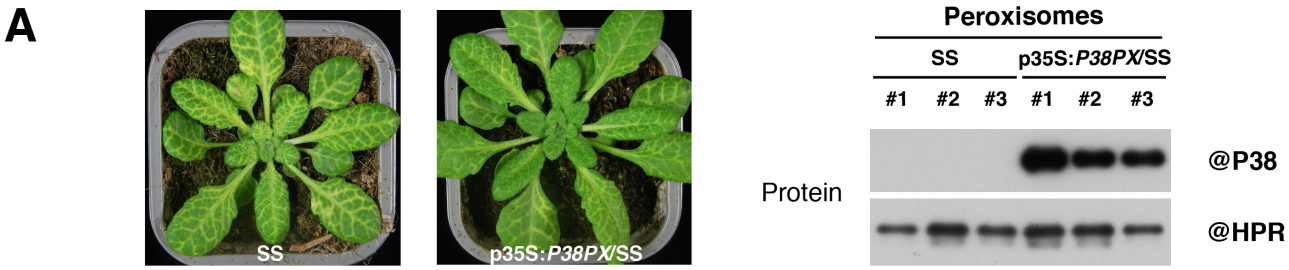

MS-MS mass spectrometry		SS			SS/35S::P38PX		
		1	2	3	1	2	3
Protein Set	Description	# Spectra	# Spectra	# Spectra	# Spectra	# Spectra	# Spectra
CAPSD_TCV = P38	CP Turnip crinkle virus (P38)				184	177	211
AT1G48410.2	Protein argonaute 1 (AGO1)					1	3
AT5G56290.1	Peroxin 5 (PEX5)	1			1		1
AT5G62810.1	Peroxin 14 (PEX14)	73	94	74	95	89	82
AT1G68010.2	Hydroxypyruvate reductase (HPR)	637	788	645	575	790	557
AT4G35090.1	Catalase 2 (CAT2)	813	1185	982	867	1018	743

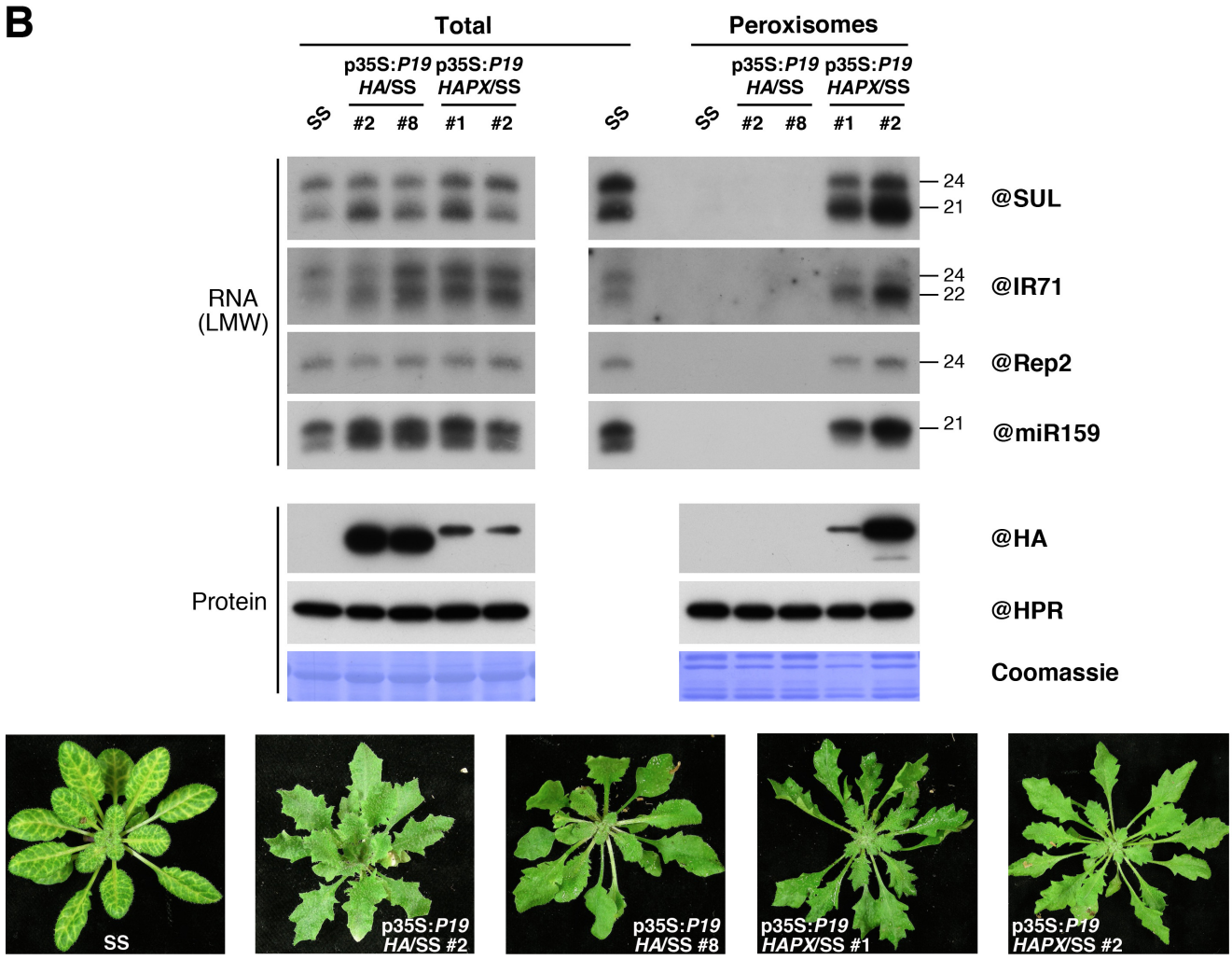

Figure 3.3: PTS1 addition to P38 and P19 to trigger peroxisomal targeting.
(A) Western blot analysis (top) and mass spectrometry MS-MS analysis (bottom) of proteins from peroxisomal fractions of SS plants expressing PTS1-containing P38 (p35S:*P38PX*/SS), and relative SS control. The MS-MS data shown represents a summary, relevant to the evaluation of this experimental approach. (B) Top: Northern blot analysis of low molecular weight (LMW) RNA and western blot analysis of proteins from total (left) and peroxisomal (right) fractions of SS plants expressing PTS1-containing P19HA (p35S:*P19HAPX*/SS), and relative SS and p35S:*P19HA*/SS controls. Bottom: photos of the plants at the moment of harvest. SS and p35S:*P19HA*/SS#2 are the same as in Fig. 1.1. Addition of a PTS1 to P19 and P38 triggers their peroxisomal import. P19 is able to abundantly piggyback into peroxisomes interactors that are not detected during IP and *in vitro* experiments.

addition of a PTS1 disrupts P38-mediated suppression of RNA silencing. The mass spectrometry results readily show presence in the peroxisomal isolates of typical peroxisomal proteins such as HPR and CAT2. The replicates are quite homogeneous among each other, as attested by spectral count. PEX14, the peroxisomal membrane protein that is part of the importomer, can also be easily detected in the isolates, suggesting that peroxisome membrane-bound proteins are not lost during the purification protocol. The fact that PEX5 is barely detectable (as it was in all the peroxisomal isolation experiments that we performed) supports its rapid and fleeting presence within peroxisomes. P38PX import into peroxisomes was confirmed by mass spectrometry. However, AGO1 peptides were barely above detection level suggesting that P38PX does not efficiently piggyback this protein into peroxisomes. This is either due to disruption of the P38/AGO1 interaction caused by the addition of the SKL tripeptide or to the rapid peroxisomal import of P38 prior to AGO1 binding.

To assess whether P19 is able to piggyback 21nt sRNAs into peroxisomes, we conducted peroxisome isolation on SS, p35S:*P19HA*/SS (used as negative controls) and p35S:*P19HAPX*/SS lines (where P19HA possesses a PTS1). We then analyzed the sRNAs from the peroxisomal isolates by Northern blot (**Fig. 3.3B**). The plant leaf phenotypes showed that, like our control P19HA, P19HAPX is proficient in suppressing the *SUL*-silencing phenotype, suggesting that the addition of a C-terminal SKL tripeptide does not disrupt sRNAs binding and the functionality of this VSR. Peroxisomal protein analysis by Western blot showed that P19HAPX was indeed imported into these organelles. Moreover, RNA analysis showed that P19HAPX was able to convey 21nt siRNAs and miRNAs into peroxisomes. More surprisingly, we also observed in the peroxisomes of P19HAPX-expressing plants the presence of a considerable amount of 22nt and 24nt sRNAs. This was unexpected based on (i) our *in vivo* IP results (**Fig. 1.5 and 1.6)** and (ii) published structural and *in vitro* data (Vargason *et al.*, 2003; Ye *et al.*, 2003).

Since mass spectrometry analysis of proteins from these same isolates revealed no protein enriched in p35S:*P19HAPX*/SS compared to p35S:P*19HA*/SS (**Fig. S9** – Annex 1), we interpret this result as evidence of 21nt, 22nt and 24nt sRNA piggybacking into peroxisomes through direct binding by P19. This in turn suggests that P19 is able to bind all

these sizes of sRNA, yet likely with different affinity. While this could be due to the use of differently tagged alleles (FHAP19 for IPs, P19HA for peroxisome experiments), it could also mean that peroxisomal import allows enrichment of interactors that are lost or undetected during IP or *in vitro* experiments.

3.4 - Conclusions

In the frame of its use as an alternative approach to interactor discovery, peroxisomal piggybacking of the factors we chose provided mixed results. In the case of DRB4 and AGO2, while we expected at least import into peroxisomes of these proteins, if not piggybacking of additional factors, the experiments clearly showed that these two proteins weren't efficiently shuttled to these organelles. Many possible explanations could be put forward, and mostly imply what has been already discussed in the introductive paragraph of this chapter. It is possible that in the folded forms of DRB4FHAPX and AGO2PX the PTS1 was not readily accessible to PEX5, or that PEX5 was for some reason unable to convey these proteins to peroxisomes. Even if PEX5 correctly bound the PTS1, the possible association of DRB4 and AGO2 with molecular complexes soon after their synthesis could have prevented PEX5-mediated translocation. Also, these two proteins could have been unable to cross the importomer pore and enter peroxisomes. However, given that P38PX was able to import AGO1 in small quantities, it is not likely that AGO2PX couldn't physically enter peroxisomes because of pore restrictions. Alternatively, these proteins could have been degraded once inside the peroxisomes. To this end, analysis of RNA from p35S:*AGO2PX/ago2-1* peroxisome isolates could reveal whether AGO2-loaded sRNAs are present, which could in turn constitute a "footprint" of AGO2PX import. Yet, total RNA analysis of p35S:*AGO2PX/ago2-1* and p35S:*AGO2/ago2-1* plants suggests that the AGO2PX allele may not be functional, so whether or not it's loaded with sRNAs remains an open question. These results suggest that, in the case of the proteins we chose, this approach in not able to provide any interesting or novel results. However, peroxisomal targeting of other proteins may yield more encouraging data.

Peroxisomal import of VSRs provided more interesting and promising results. A P19 allele possessing a PTS1 was, like P15, able to piggyback sRNAs into peroxisomes. Furthermore, and again similarly to what was observed with P15, peroxisomal piggybacking revealed interactions that were lost or not detected in IP experiments. A direct comparison can be made by confronting the anti-*SUL* siRNAs co-IPed with P19 (**Fig. 1.5 and 1.6**) (21nt long) to the anti-*SUL* siRNAs that colocalized with P19 in peroxisomes (**Fig. 3.3B**). While as expected most piggybacked anti-*SUL* siRNAs were 21nt long, the clear presence of a 24nt band is testimony to P19HAPX binding to siRNAs of this size *in vivo*. Moreover, P19HAPX was able to import Rep2 siRNA, which are DCL3-dependent heterochromatic 24nt siRNAs whose localization is presumed to be nuclear. This observation suggests that either some of these siRNAs exited the nucleus and were bound by P19HAPX, or that P19HAPX entered the nucleus, bound Rep2 siRNA and exited prior to recognition by PEX5. Results regarding miR159 show that while in total extracts it was present as two distinct species, only one of the two, presumably the one that is 21nt long, was piggybacked into peroxisomes. If this size assumption is correct, these observations suggest that while P19 can bind sRNAs longer than 21nt, it can't bind sRNAs that are shorter. An explanation for this could be that a 20nt sRNA is not long enough to be bound on both ends of the 21nt-long molecular caliper made up by two crucial tryptophane residues of P19 (Ye et al., 2003) so interaction is not established. On the other hand, it is also difficult to explain how 22nt and especially 24nt sRNAs can bind to this 21nt caliper. Assuming that these siRNAs are bound on both ends by P19, one explanation could be that the duplexes are bent to fit the 21nt-long caliper. This deformation could cause instability in the P19/sRNA interaction that causes it to be disrupted in IP or *in vitro* conditions.

Whatever the possible reasons behind P19-mediated import of 24nt siRNAs into peroxisomes, the experimental approach we devised did indeed provide us with precious information on *in vivo* P19 interactions that escaped detection during IP and *in vitro* experiments. As postulated in the first section of this chapter, this could be due to a combination of preservation of interactions during *in vivo* peroxisomal import and accumulation of interactors within these organelles. Whether or not these interactions are biologically relevant remains to be determined. Most importantly, the experiments need to

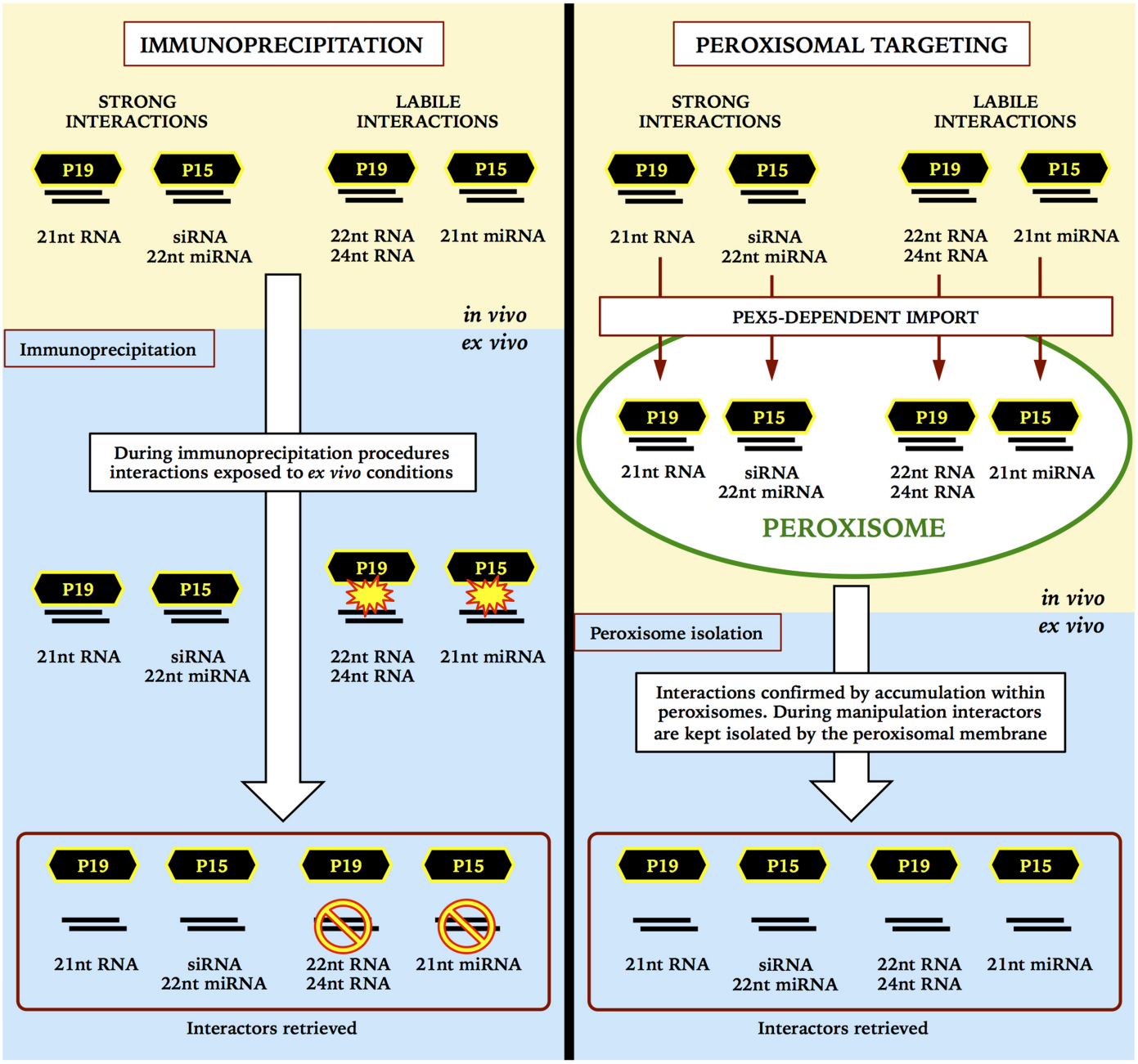

Figure 3.4: Advantages of P15 and P19 peroxisomal targeting in the identification of molecular interactions, compared to immunoprecipitation.
Schematic representation showing the potential advantages of peroxisomal targeting over immunoprecipitation, emerging from our preliminary experiments. Labile interactions may be disrupted during immunoprecipitation procedures. Conversely, peroxisomal import and piggybacking entails *in vivo* accumulation of interactors within a "container" (the peroxisome) that can be isolated and analyzed.

be repeated with the correct controls, performing IP and peroxisome isolation on the same alleles to be able to confidently compare the two techniques.

Considering the fact that this approach also uncovered P15 interactions that did not emerge from IP, we propose the use of targeted peroxisomal import as a powerful and very sensitive tool to investigate the interactomes of sRNA-binding proteins of viral origin such as P15 and P19 (**Fig. 3.4**). Results with P38 were less encouraging, since its activity was seriously compromised by the addition of a PTS1, and its import of AGO1 into peroxisomes was barely detectable. However, this could be an effect specific to P38, and peroxisomal targeting of other viral proteins interacting with host proteins could provide more promising results.

We have already discussed the many possible reasons behind the failure of this approach in providing interactors. Given the great complexity behind the efficient recruitment and piggybacking of a molecule into peroxisomes, it is very difficult, if not impossible, to determine exactly why DRB4 and AGO2 were not shuttled into peroxisomes, or why P38 was not able to abundantly piggyback AGO1. However, the compelling results we obtained through peroxisomal targeting of P19 suggest that this technique, when it works, allows detection of sensitive and labile interactions that are lost during immunoprecipitation. Therefore, provided the protein of interest escapes all the drawbacks postulated above, the use of this approach can be considered as a valid means to obtain potentially more sensitive and informative results. Since these drawbacks are not easily predictable for a given protein of interest, this technique must be tested empirically for each candidate, and evaluated in a case-by-case fashion.

DISCUSSION AND PERSPECTIVES

The objective of this experimental work was to provide a snapshot of a virus manipulating its host to fulfill its own agenda. In particular, the focus here was on PCV and its suppressor of RNA silencing, P15. The experiments performed to this end spanned a wide range of different approaches and techniques such as immunoprecipitation, tissue specific protein expression, peroxisome isolation and viral infection, performed *in vivo* and in different genetic backgrounds. While a number of questions remain unanswered, the data we gathered and presented in Chapter 1 and 2 is rather consistent and can be confidently assembled into a model describing how PCV neutralizes its host's local and systemic antiviral RNAi-based reaction by deploying a truly ingenious VSR.

4.1 – P15, a compelling example of viral evolution

Infection by PCV, a (+)ssRNA virus, faces a powerful and specific RNAi defensive reaction. As most or possibly all viruses, PCV has evolved one or more stratagems to block this defense. One of these stratagems comes in the form of P15, a small dimerizing protein that is absolutely necessary for successful establishment of infection (Dunoyer *et al.*, 2002a, 2001). This VSR, as a number of others, relies on binding and sequestration of antiviral siRNAs to disrupt (i) their loading into AGO proteins and the subsequent sequence-specific AGO-dependent attack on viral RNA, and (ii) their systemic movement and subsequent immunization of naïve tissues. P15 has evolved a binding bias toward siRNAs, the molecular bases of which remain to be determined. During PCV infection this bias likely allows P15 to preferentially sequester dangerous antiviral siRNAs rather than miRNAs, which are involved in endogenous pathways that are probably of little consequence to viral fitness.

However, sequestering antiviral siRNAs may be especially problematic during PCV infection. In fact, although during infection by many virus species antiviral RNAi relies heavily on DCL4-dependent 21nt siRNAs, PCV is efficiently processed by both DCL4 and DCL2. This leads to a mixed population of 21nt- and 22nt-long anti-PCV siRNAs. While the reasons behind this peculiar pattern and its functional significance remain obscure, it is reasonable to assume that P15 has had to evolve accordingly. In agreement with the observation that in a very susceptible species, such as *N. benthamiana*, anti-PCV siRNAs are

mostly 22nt long, P15 possesses higher affinity for 22nt- than for 21nt-long sRNAs. Consequently, P15 is able to efficiently sequester and neutralize 22nt siRNAs, preventing their use in both cell- and non-cell autonomous RNAi.

Despite the high rates of 22nt antiviral siRNAs produced, we found that anti-PCV 21nt siRNAs remain a force to be reckoned with, since they are able to move ahead of the virus to immunize naïve uninfected tissues. The lower binding capacity shown by P15 for this size of siRNAs, which may be the result of a molecular compromise in favor of 22nt siRNAs, constitutes a serious limitation in its ability to shut down the host's plant-wide RNAi response. In fact, while P15 binding to 21nt siRNAs is sufficient to inhibit AGO loading and cell-autonomous RNA silencing, the same cannot be said for non-cell autonomous, systemic RNA silencing. During PCV infection, if P15 relies only on direct binding to achieve siRNA neutralization, a critical amount of 21nt anti-PCV siRNA exits the infected tissues and is able to move systemically through the phloem ahead of the virus, reaching parts of the plant that have yet to be infected (**Fig. 4.1**). These siRNAs subsequently trigger a powerful antiviral response that, upon arrival of PCV, severely hampers its movement or blocks it altogether.

P15 developed a solution to this problem that is a testimony to the brilliance of viral evolution. Since sequestration through direct binding is not sufficient to stop systemic movement of 21nt siRNAs, P15 evolved the ability to confine them within peroxisomes, thereby neutralizing them (**Fig. 4.2**). In fact, once siRNAs are within these organelles, they are isolated from the symplasm and systemically immobile, whether they are bound to P15 or not. In other words peroxisomes, organelles of paramount importance in the correct functioning of a cell, serve as disposal units for antiviral siRNAs during PCV infection. This stratagem is only possible thanks to the peroxisome's very particular protein import machinery. As opposed to that of other organelles such as chloroplasts and mitochondria, the peroxisomal importomer is capable of translocating folded proteins and their cargos across the membrane and into the organelle.

The present study is the first report of peroxisomes being used in such a way, and in general of a pathogen using an organelle to neutralize molecules deployed against it by the host's defensive machinery. Moreover, it is an ingenious way for a viral protein to simultaneously deal with two antiviral molecules of different sizes, in a scenario in which development of

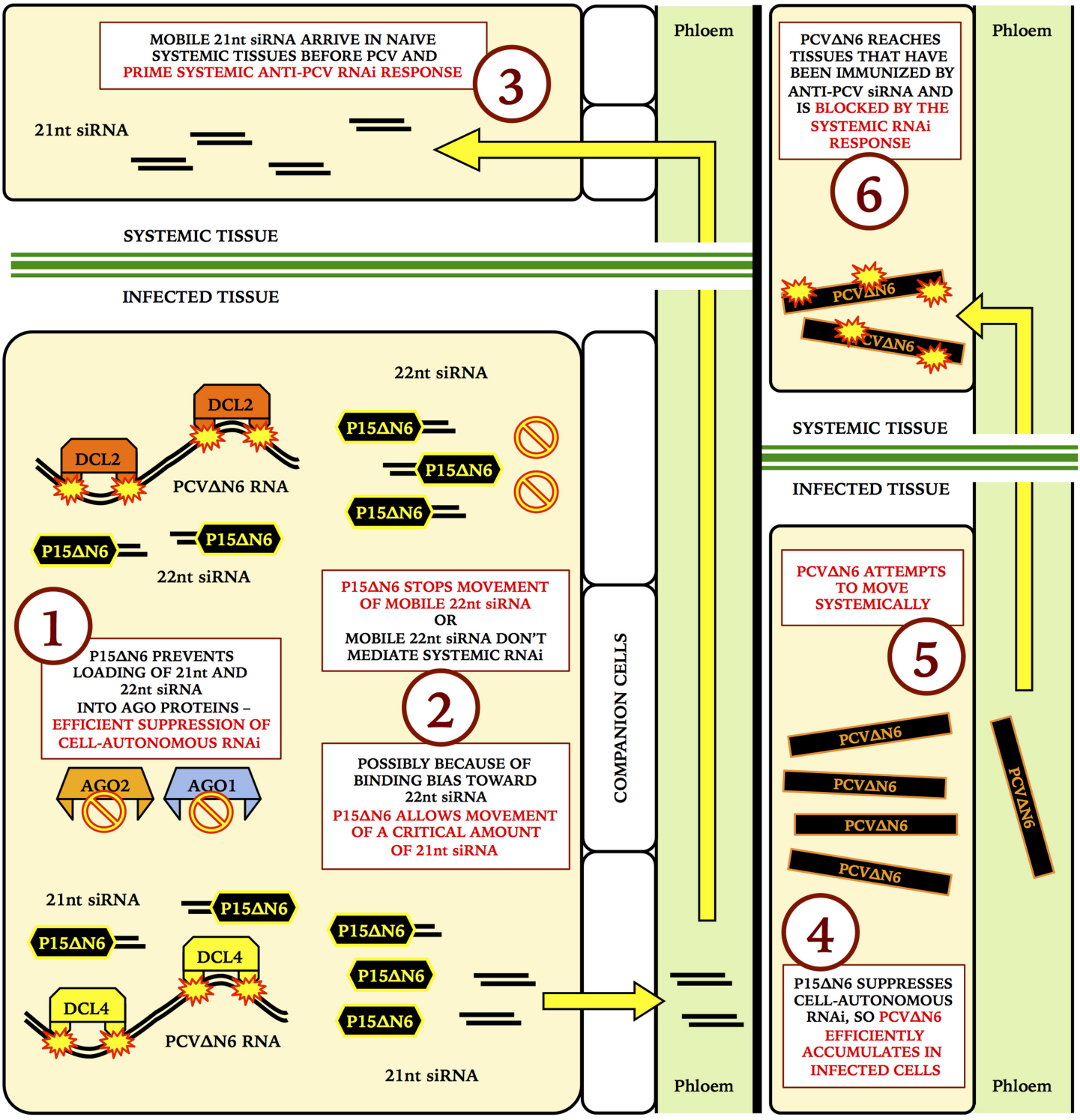

Figure 4.1: PCVΔN6 movement is blocked by systemic antiviral RNAi, which is triggered by phloematically mobile 21nt siRNAs.

Schematic representation of our model explaining why PCVΔN6 is scarcely or not able to establish systemic infection. "Leaky" sequestration of 21nt siRNAs by P15ΔN6 in infected tissues (1-2) allows the systemic movement of these siRNAs (3), which in turn trigger a powerful plant response in distant tissues that blocks PCVΔN6 upon arrival (6).

increased affinity for one size likely entails decreased affinity for the other. This discovery reiterates the truly manipulative nature of viral infection: in a way, PCV doesn't directly employ its own proteins to transport siRNAs within peroxisomes. Instead, by "placing" a PTS1 on antiviral siRNAs through P15, it tricks the plant into neutralizing its own defensive molecules.

4.2 – Peroxisomal confinement of host defense factors could be used by other pathogens

Although this could be a lonely and isolated case of such a strategy being used by a virus to dampen its host's defenses, the fact that other plant virus proteins are targeted to peroxisomes (Savenkov *et al.*, 1998) suggests otherwise. Furthermore, this strategy could be deployed by viruses infecting organisms other than plants. As mentioned in the introduction, protein VP4 of rotaviruses, causing some 600,000 deaths per year, possesses a PTS1 that is conserved in all 153 rotavirus species known (Mohan *et al.*, 2002). While it has been shown that VP4 does indeed localize to peroxisomes, the function of this localization remains unclear. We suggest that VP4 could, like P15, piggyback a negative regulator of the viral life cycle into these organelles, thereby neutralizing it. To this end, and similarly to the approach we followed in studying P15, it would be interesting to assess the importance of peroxisomal import in the rotavirus life cycle by removing the PTS1 from VP4 and verifying viral fitness. Most importantly, peroxisome isolation should be performed on cell cultures infected with rotavirus to score protein and RNA present in these isolates. Comparison of these with peroxisome isolates from healthy cells or cells infected with rotavirus lacking PTS1 could reveal whether or not VP4 is piggybacking molecules into these organelles.

It can also be envisaged that a viral protein binding a host's defensive factor but lacking a PTS could, in its quest to confine its cargo within peroxisomes, "hitch a ride" on a host protein possessing a PTS. Such a strategy would imply the import of a molecular complex comprising the import receptor, the host peroxisomal protein, the viral protein attached to it and the antiviral molecule to be disposed of. Although no experimental evidence exists suggesting this is the strategy they use, it has been shown that Nef protein of HIV and NS1 of influenza viruses interact with host peroxisomal proteins (Lazarow, 2011). Again, it

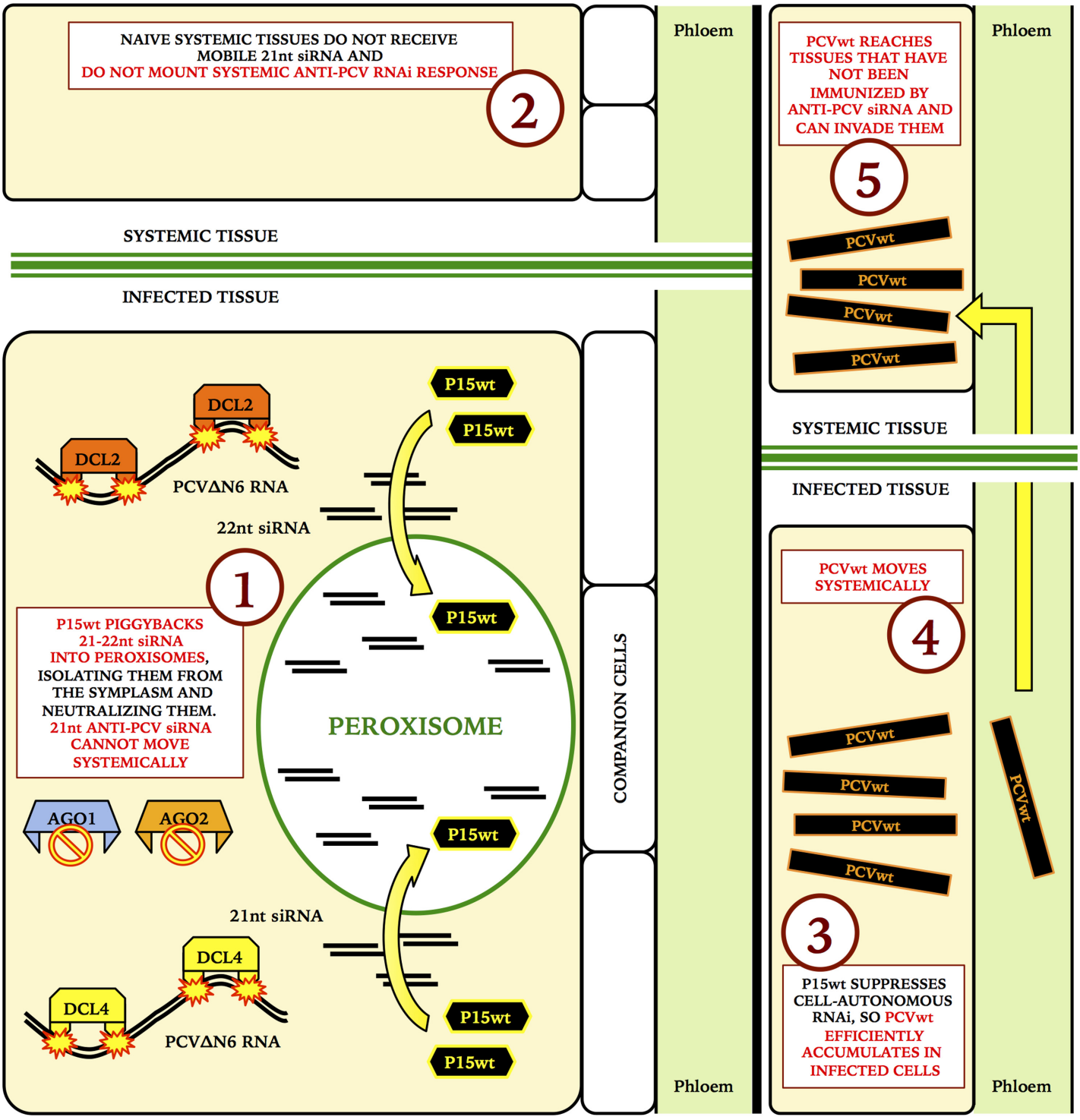

Figure 4.2: PCVwt prevents movement of siRNAs by confining them in peroxisomes.
Schematic representation of our model explaining how PCVwt achieves potent and rapid systemic infection. "Leaky" sequestration of 21nt siRNAs in infected tissues is compensated by peroxisomal localization of P15, that entails piggybacking of antiviral siRNA into peroxisomes and their subsequent neutralization (1). Systemic naïve tissues do not receive mobile anti-PCV siRNAs (2) and do not mount a preemptive response. PCVwt is therefore able to efficiently invade them (5).

would be interesting to isolate peroxisomes from cells infected with these viruses to score their molecular population for fingerprints of piggybacking events.

4.3 – Tools for future research

The results presented in this work also highlighted some very particular features of PCV that could be further used as tools to investigate uncharted territory in cell-autonomous and systemic antiviral defenses. Thanks to the very high efficiency and reproducibility of the protocol we developed to infect *A. thaliana* with PCV, several compelling avenues of enquiry lay open to scrutiny.

4.3a – DCL2 biology and DCL2/DCL4 interplay during antiviral defense

The major role DCL2 plays in anti-PCV RNAi surely requires more detailed investigation. Whether DCL2 recruitment is due to inactivation of DCL4 or to an undisclosed trait of PCV, inspecting the matter more closely may provide information on DCL2 biology and possibly a role for it that is not merely that of surrogate to DCL4. Furthermore, it remains to be determined whether or not these DCL2-dependent siRNAs trigger antiviral transitivity.

By probing different regions of the PCV genome we revealed what could be dynamic processing by DCL2 and DCL4 of specific sections of viral RNA. Further experiments on the nature of this differential processing may lead to the identification of particular patterns or features recognized by the two antiviral dicers. It would also be interesting to assess the eventual role of DRB proteins in the recruitment of specific DCLs upon the various regions of viral RNA. The identification of 21nt versus 22nt hotspots on the PCV genome, by high-throughput sequencing of PCV-infected DCL, RDR and DRB knockout mutants, may provide insight on these topics and pave the way for more targeted experiments.

4.3b – Uncoupling of systemic RNAi from cell-autonomous RNAi during unbiased viral infection

A very compelling feature of PCV uncovered in this study, is the possibility to assess, through removal of the PTS1 from P15, the effects of systemic RNAi independently from those of cell-autonomous RNAi during a genuine viral infection. Since these two aspects of RNAi are mediated by the same kinds of molecules and are tightly connected, functional separation in the context of viral infection is a very difficult goal to achieve. We could say that we got a lucky break by identifying, in the peroxisomal localization of P15, a naturally occurring discriminative trait, which we proceeded to characterize and validate. Factors suspected of taking part in the systemic movement of siRNA could be easily tested by infecting the corresponding mutants with PCVwt and PCVΔN6. Taking into account the results we obtained by infecting the *dcl4*, *dcl2dcl4* and pSUC:*P15FHA* lines, versus those obtained on BY-2 protoplasts, any factor whose knockout rescues systemic accumulation of PCVΔN6 could be quite confidently implicated in the movement of antiviral 21nt siRNA and further characterized through other approaches.

The observed rescue of PCVΔN6 systemic movement in the pSUC:*P15FHA*/SS transgenic lines provides a tentative "proof-of-concept" of the above-mentionned idea. Moreover, these results provide strong evidence backing the widely held belief that virus-derived siRNAs move systemically through the phloem, like their transgene-derived counterparts.
Additionaly, combining the use of this companion-cell specific "siRNA sponge" in various *dcl* mutant backgrounds with VSR-deficient viruses, could allow us to evaluate the impact of mobile 21nt versus 22nt siRNAs on systemic antiviral RNAi and the priming of preemptive antiviral responses in naïve tissues. We are currently performing experiments on wild-type and *dcl3dcl4* mutant background with TuMV-GFP and TuMV-AS9-GFP. This will hopefully shed some light on the unanswered question, that already emerged in Chapter 2, on whether or not mobile 22nt siRNAs are able to mediate efficient systemic antiviral RNAi.

4.3c – Peroxisomal isolation to uncover labile interactions and to investigate viral replication complexes

Some of the most exciting results we obtained emerged from peroxisome isolation experiments, regarding not only P15 but also the use of piggybacking to identify interactions that are not detected through other approaches. While our results are still preliminary and revealed many limits, the abundant detection of interactors previously described as poor targets, such as 24nt siRNAs (Vargason *et al.*, 2003; Ye *et al.*, 2003), suggests that this technique, as time-consuming and labor-intensive as it may be, could be advantageously used in parallel with other well-established protocols to shed light on the interactomes of small pathogen-encoded proteins. The fact that interactors are stored *in vivo* into peroxisomes, potentially accumulate over time and are not subjected to *ex vivo* manipulation, may allow for discovery of new and biologically relevant cytoplasmic intermolecular interactions (**Fig. 3.4**). However, the efficacy of the method must be evaluated in a case-by-case fashion.

Having validated the peroxisome isolation protocol on *N. benthamiana*, another path of enquiry lays open. In fact, many tombusviruses such as TBSV create their replication factories in membrane invaginations on peroxisomes (Barajas *et al.*, 2009; Xu and Nagy, 2014). Isolation of these organelles from TBSV-infected *N. benthamiana* plants, and subsequent mass spectrometry analysis, may allow identification of proteins that are present within the TBSV-generated alcoves. In addition to the tombusviral replicase, these could include host compatibility or restriction factors. Unfortunately, heavy plastid contamination and general "dirtiness" of peroxisome isolates from *N. benthamiana* give strong background noise, which when added to the plethora of peroxisomal proteins could significantly undermine the sensitivity of the experiment. Even if interesting candidate proteins do emerge, a further obstacle is constituted by the scarce annotation of the *N. benthamiana* genome and the unavailability of genetic tools in this species. Unfortunately, the ideal plant

species to perform this kind of experiment, *A. thaliana*, is not to our knowledge a host to TBSV. However, if these obstacles could be overcome, precious information may emerge from such an experiment.

MATERIALS & METHODS

5.1 - Cloning and transgene construction

Heat-shock competent *E. Coli* DH5α strain were used for all cloning procedures. After transformation, colonies were analysed by colony PCR for insert presence and orientation, positive colonies were grown in liquid culture, plasmid DNA was extracted by miniprep (Macherey-Nagel Plasmid Quickprep), and digested with appropriate restriction enzymes (not in the case of Gateway clones). Plasmids showing correct restriction profile were sequenced.

pSUC:*P15FHA* and p35S:*P15FHA*: P15 was amplified (using PCV1 containing pPC1wt as template – Herzog *et al.,* 1998) with primers designed to contain XmaI restriction sites and to abolish the stop codon. The resulting PCR product was purified, digested with XmaI and ligated into a pCTL (pCambia 1300 derivate) binary vector, between the SUC2 or 35S promoters and a double-FLAG double-HA epitope tag followed by a stop codon. pCTL carries bacterial resistance to kanamycin and plant resistance to hygromycin. p35S:*P15wt/ΔN6* have been previously generated in the lab by amplifying P15 from pPC1wt/ΔN6.

p35S:*P19HA/P19HAPX* and p35S:*P38/P38PX*: P19 and P38 were amplified (using plasmids present in the lab as templates) with primers designed to contain 5' SalI and 3' PstI restriction sites. P19HAPX and P38PX were obtained in the same way but adding to the 3' primer TCTAAACTG before the stop codon (the same peroxisomal targeting sequence found in P15 – SKL tripeptide). The resulting PCR products were purified, digested with SalI/PstI and ligated into a pCTL (pCambia 1300 derivate) binary vector containing a 35S promoter. pCTL carries bacterial resistance to kanamycin and plant resistance to hygromycin.

p35S:*DRB4FHA/DRB4FHAPX* and p35S:*AGO2/AGO2PX*: DRB4FHA and AGO2 were amplified with primers designed to contain attB sites for Gateway cloning (Invitrogen). Col-0 genomic DNA was used as template for AGO2, while a plasmid containing DRB4FHA was used to amplify the whole protein and tag (kindly provided by Dr. Marion Clavel). DRB4FHAPX and AGO2PX were obtained in the same way but adding to the 3' primer TCTAAACTG before the stop codon. The resulting PCR products were purified by PEG precipitation and inserted into pDONR221 through BP recombination. Plasmids with the

correct sequence were transferred through LR recombination into binary vector pH2GW7, containing a 35S promoter. pH2GW7 carries bacterial resistance to spectinomycin and plant resistance to hygromycin.

5.2 - *A. thaliana* stable transformation and transgenic line selection

Agrobacterium tumefaciens transformation: binary plasmids were electroporated into *A. tumefaciens* strain GV3101. After growth on kanamycin or spectinomycin LB agar and successive liquid culture, 50% glycerol stocks were made and used to start 24 hr 250ml liquid cultures. These were pelleted 10 min 5000 rpm (Beckman rotor F500) and resuspended in 250 ml 5% sucrose, 2.4 g/l MES, 0.05% Sylvett, 200 µM Acetosyringone (Bechtold and Pelletier, 1998). This was used for 30-second floral dip on *A. thaliana*, after which plants were put in a closed and dark portable greenhouse with high humidity for 24 hrs.

Transgenic line selection: primary transformant seeds were sown in vitro (see next paragraph) in the presence of hygromycin (20 mg/l). Resistant plants were transferred to soil 15 days after sowing, and transgenic protein accumulation was assessed 4-5 weeks after sowing by urea/Laemmli buffer protein extraction on one leaf per line followed by Western blot (see dedicated paragraph). Note that to detect peroxisomal proteins by this method, grinding in liquid nitrogen (using beads and a shaking device) before adding urea/Laemmli is mandatory.

5.3 - Plant germination and growth

A. thaliana knockout mutants used are all in a Col-0 background: *ago2-1* (SALK_003380)(Lobbes *et al.*, 2006), *drb4-1* (SALK_000736)(Curtin *et al.*, 2008), *dcl2-1* (SALK_064627), *dcl4-2* (GABI160G05), *dcl3-1* (SALK_005512)(Dunoyer *et al.*, 2007, Xie *et al.*, 2005). SUC:*SUL* was previously described (Dunoyer *et al.*, 2007, 2005)

In vitro A. thaliana seedlings for immunoprecipitation experiments: seeds were sterilized by washing 15 min in 70% ethanol 0.05% SDS, rinsed in 100% ethanol, air dried and sown on agar MS (5 g/l MS 255, 0.5 g/l MES, 1% sucrose, 0.8% agar, pH 5.7 and a selection antibiotic where necessary) petri dishes. Growth conditions were 22-18°C, 16h/8h

light/dark photoperiod, neon lighting. All plants photographed and harvested 21 days after sowing.

A. thaliana plants for pSUC:*P15FHA* experiments, viral infections and peroxisome isolations: plants for pSUC:*P15FHA* experiments were sown *in vitro* (see previous paragraph) on hygromycin and transferred to soil 15 days after sowing. Plants were harvested and pictures were taken at 5 weeks of age. Plants of this age were used in this experiment because the desired phenotype was more stable and consistent than in 3-week-old *in vitro* seedlings. *A. thaliana* for viral infections and peroxisome isolations were sown in soil without selection at 22-18°C, 12h/12h light/dark photoperiod and transferred to individual pots 15-18 days after sowing.

N. benthamiana plants: these were sown on soil following gibberellin treatment and grown at 22-18°C, 16h/8h light/dark photoperiod.

5.4 - Virus infection and patch assays

N. benthamiana patch assays: Liquid cultures of *A. tumefaciens* carrying binary plasmids encoding 35S-driven proteins of interest were grown 24 hrs at 28°C in liquid LB under kanamycin and rifampicin selection, pelleted, diluted to OD 0.5 in 10 mM MgCl2, 200 µM Acetosyringone and incubated 1 hr at room temperature. Infiltration in *N. benthamiana* leaves (5-6 week-old plants) was carried out with a neddle-less syringe (Hamilton et al., 2002). Leaves were analysed and harvested 5 dpi.

PCV *in vitro* transcript generation and BY-2 cell infection: capped (m7G cap analog) PCV1wt, PCV1ΔN6 and PCV2 RNAs were generated with Promega RiboMAX™ Large Scale RNA Production System – T7, according to manufacturer's indications. Plasmids pPC1 (wt or ΔN6) and pPC2 (Herzog *et al.*, 1998) containing a T7 promoter upstream of the viral genome were used as templates following MluI (pPC1) and HindIII (pPC2) linearization (Dunoyer *et al.*, 2002). After transcription RNAs were purified by Trizol extraction (see dedicated paragraph), resuspended in RNAse-free water, quantified and quality was assessed on a TBE agarose gel. *N. tabacum* BY-2 4-day-old liquid cultures were pelleted then resuspended in a sterile isotonic enzyme solution (0.45 M Mannitol, 0.7 g/l MES, 1% Cellulase, 0.1% Pectolyase) and incubated 2hrs at 30°C with gentle shake. Cells were then filtered, pelleted, washed twice in 0.45 M Mannitol 0.7 g/l MES, and their quantity was

estimated. 10^6 protoplasts in 500µl were electroporated with 5 µg of each RNA (100 Ω, 125 µF, 180 V), incubated 30 min at 4°C, pelleted and resuspended in BY-2 growth medium with 0.45 M Mannitol and 0.25 mg/ml Ampicillin. They were then incubated at 27°C for 24-48 hrs. PCV transcripts were also used to initially infect *N. benthamiana*. PCVwt moved systemically, and systemically infected leaves 11 dpi were used as inoculum for further infections (see next paragraph). *In vitro* generated PCVΔN6 RNA is mostly unable to establish systemic infection (Dunoyer *et al.*, 2002), although we observed that sporadically systemic infection was established. These systemically infected leaves 11 dpi were used as inoculum for further infections (see next paragraph).

Nicotiana benthamiana PCV and PVX-GFP infection: PCV and PVX-GFP infection for subsequent peroxisome extraction and PCVwt/PCVΔN6 infection to produce tissue for virus purification were carried out through sap rub-inoculation. The inoculum was prepared by grinding 0.4 g systemically infected *N. benthamiana* leaves (PCV) or agro-inoculated 4 dpi *N. benthamiana* leaves (PVX-GFP) (Garcia *et al.*, 2014) in liquid nitrogen, homogenizing in 2 ml 50 mM sodium phosphate pH 7.5 buffer, clarifying by spinning 2 min 1500 rpm and rub inoculating 3-4 leaves/plant with celite and 30 µl inoculum/leaf. PCVwt and PCVΔN6 infection to assess systemic movement and to produce tissue for further virus purification was performed using purified virus, approximately 300 ng/plant, resuspended in 50 mM sodium phosphate pH 7.5 buffer, rub inoculating 3-4 leaves/plant with celite and 30 µl inoculum/leaf. After infection plants were rinsed and kept at 22-18°C, 16h/8h light/dark photoperiod.

Arabidopsis thaliana TuMV-GFP and TRV-PDS agro-inoculation: plants were infected at 4 weeks of age. Liquid cultures of *A. tumefaciens* carrying pCB-TuMV-GFP/TuMV-AS9-GFP (Garcia-Ruiz *et al.*, 2010) TRV1 and TRV2-PDS (Liu *et al.*, 2002) were grown 24 hrs at 28°C in liquid LB under kanamycin and rifampicin selection. After pelleting by centrifuging 10 min 5000 rpm bacteria were induced by incubating 5-7 hours in induction media (10.5 g/l K_2HPO_4, 4.5 g/l KH_2PO_4, 1 g/l $(NH_4)_2SO_4$, 0.5 g/l sodium citrate, 0.1 g/l $MgSO_4$, 0.4% glycerol, 0.1 g/l MES, 200 µM Acetosyringone), then pelleting again and resuspending in 10 mM MES 10 mM $MgCl_2$. OD was brought to 0.5, then 3-4 leaves/plant were infiltrated with a syringe without needle. Plants were analysed 15 dpi (TuMV) or 18 dpi (TRV).

Arabidopsis thaliana PCV infection: *A. thaliana* does not appear on the list of PCV hosts. Every attempt at infecting *A. thaliana* with PCV using the methods used on *N. benthamiana* proved unsuccessful (see previous paragraphs), yielding very few infected plants, if any. Numerous attempts to obtain an infective agro-clone proved unsuccessful, possibly because of instability or toxicity of the RNA1 sequence in *E. coli*. We developed a procedure allowing PCV to establish rapid systemic infection in *A. thaliana*. While the very few plants systemically infected by PCV obtained through sap rub-inoculation showed symptoms 14-16 dpi, plants infected following our procedure started showing symptoms as early as 7 dpi, symptoms that were highly homogeneous among individuals, affecting 100% of the plants. Plants were 21-25 days old at the moment of infection. Inoculum was prepared in 50 mM sodium phosphate buffer pH 7.5 with freshly purified virus (see dedicated paragraph). Virus must not be frozen. 4 µg of virus were applied to each plant, in 40 µl, on 3-4 leaves. Leaves were sprinkled with celite, inoculum was applied and gently rubbed 3-4 times on each leaf with a cue tip. Right after infection plants were lightly rinsed with water and kept in the dark for 24 hrs. After this, plants were kept at 22-18°C, 16h/8h light/dark photoperiod. It is strongly advised to keep the plants under abundant light, favoring greenhouse over growth chamber, since we observed that fast vegetative growth significantly improves PCV movement.

5.5 - EMS mutagenesis

Prior to mutagenesis seeds were vernalized through 48-hour incubation at 4°C. Mutagenesis was performed on ≈15000 *A. thaliana* seeds, by incubating them 12 hrs in 0.25% EMS (methanesulfonic acid ethyl esther, Sigma-Aldrich). Seeds were then washed 4 times 15 mins in water, and sown in ≈3750 pots at an average density of 4-5 seeds/pot. Plant were grown at 22-18°C, 16h/8h light/dark photoperiod.

5.6 - Immunoprecipitation

All immunoprecipitations were performed on frozen 3-week-old *A. thaliana* seedlings grown *in vitro* (except for pSUC:*P15FHA* experiments, where leaves from 6-week old rosettes were used). All steps were performed at 4°C/on ice.

AGO immunoprepitation: the antibodies were previously described (Garcia *et al.*, 2012; Qi *et al.*, 2005) 0.3-0.4 g of frozen seedlings were ground in liquid nitrogen with 1ml lysis buffer (50 mM Tris-HCl pH 7.5, 150 mM NaCl, 10% glycerol, 0.1% Nonidet P-40, Roche Complete protease inhibitor cocktail) and homogenised 30 minutes on wheel. After 30 min centrifugation at 12000g, supernatant was transferred to a new tube and 50 ul Protein A agarose beads (Roche) were added. After incubation on wheel of 30 min, tubes were spinned 1 min 3000g, the supernatant transferred to a new tube, and the primary antibody added to supernatant (1:1000 dilution @AGO1, 1:500 dilution @AGO2). After 2 hours on wheel 80ul Protein A agarose beads were added, and tubes were incubated an additional 2 hours on wheel. Tubes were spinned 1 minute 3000g, the supernatant was discarded, 1ml lysis buffer was added, and after gentle resuspension incubation was allowed on wheel for 15 minutes. This wash was repeated twice. Finally, the beads were subjected to Trizol extraction (see dedicated paragraph).

HA-tagged and GFP-tagged protein immunoprecipitation: 0,4 g of frozen seedlings (p35S:*P15FHA* @HA IPs) or rosette leaves (pSUC:*P15FHA* @HA IPs) were ground in liquid nitrogen with 1 ml lysis buffer (50 mM Tris-HCl pH 8, 150 mM NaCl, 1% Triton X-100, Roche Complete protease inhibitor cocktail). After incubation 30 minutes on wheel, lysate was centrifuged at 13000 rpm 10 minutes and supernatant was transferred to a new tube. This step was repeated once. 50 ul of anti-HA micro-beads (MACS system, Myltenyi Biotec) were added and 30 min was allowed on wheel. After placing the magnetic column (MACS system, Myltenyi Biotec) on the magnetic stand, they were prepared by passing 200 µl lysis buffer through them. The lysate containing the beads was deposited on the column in 2x500 µl and allowed to flow through, washed with 2x500 µl lysis buffer then 100 µl 20 mM Tris-HCl pH 7.5. After excess liquid removal, column was removed from stand, and 1 ml Trizol passed through it (RNA analysis) or 150 ul 95°C 1X Laemmli buffer in 10% glycerol, 3% SDS, 62.3 mM Tris-HCl pH 8 was passed through (and directly sent for mass spectrometry analysis after 5 min 95°C denaturation).

5.7 - Peroxisome isolation

Peroxisome isolation was performed according to an adapted version of Reumann and Singhal, 2014. Isolations were performed on fresh tissue (do not use frozen tissue) of 6-7

week-old *A. thaliana*/5-6 week-old *N. benthamiana*, all steps were performed at 4°C/on ice. All solutions used were filter-sterilized after preparation and pH equilibration and stored at 4°C. The protocol describes the processing of one sample per extraction, but we found that by adapting the amount of starting tissue and grinding buffer, two samples at a time can be processed, while maintaining quality and yield.

Isolation procedure: before isolation, plants were kept in the dark for 16-20 hrs to favor dissociation of peroxisomes from plastids. After setting aside and freezing a small amount of tissue for total RNA and protein extraction, 20-30 g of entire rosettes (*A. thaliana* ≈30 plants) or leaves (*N. benthamiana*) were harvested and left on ice 2 hrs. Next, the plant tissue was minced as much as possible with a kitchen knife, then ground energetically in 120 ml grinding buffer with mortar and pestle (70 ml per sample if processing two samples)(170 mM Tricine pH 7.5, 1 M sucrose, 2 mM EDTA, 1% BSA, 10 mM KCl, 1 mM $MgCl_2$, plus 0.5% PVP-40, 5 mM DTT and Roche Complete protease inhibitor cocktail added just before use). The resulting pulp was filtered through Miracloth, the solid part in the filter discarded, the liquid divided into 4 tubes (3 tubes per sample if processing two samples) and centrifuged 1 min at 6700g (Beckman rotor JA25). The clarified supernatant was pooled and deposited on 8 freshly prepared and chilled Percoll/sucrose gradients (4 per sample if processing two samples). Refer to the section below for gradient composition. Gradients were centrifuged 12 min at 13200g, then without stop 20 min at 27000g, with medium brake. Top layers were carefully discarded by pipetting or vacuum pump (it is important to remove all the green material) while keeping bottom 2-3 ml containing peroxisomes. These bottom fractions were again pooled and diluted up to 80 ml in 36% sucrose (see next paragraph), divided in 4 tubes and centrifuged 30 minutes at 38700g. Next, the clearly visible organellar phase on the bottom of each tube (750 µl per tube) was directly harvested with a cut-tip pipette (plunge it directly, without removing the liquid on top) and transferred to a potter. The resulting 3 ml were gently homogenized by very slowly moving the piston up and down 4-5 times, and deposited on a sucrose 41.2% to 60% discontinuous gradient (see below). Gradients were then ultra-centrifuged 40 minutes at 110800g (Beckman rotor SW41 – 33500rpm), maximum acceleration and brake. 1.5 ml of visible white peroxisome fraction within the 50.5% sucrose phase were harvested and frozen at -80°C, then stored at -20°C. The peroxisomal fractions obtained were subjected to RNA

extraction or protein extraction (see dedicated paragraph). Note that when working on *A. thaliana*, after ultracentrifugation there will be no evident bands in the gradient except for the white peroxisomal fraction and the sediment on the bottom of the tube, while when working on *N. benthamiana* there will likely be green bands at every interphase, and the peroxisomal band itself, while containing peroxisomes, will be green, indicating high contamination by chloroplasts. The protocol should thus be optimized for further use on *N. benthamiana*.

Percoll/sucrose gradient: gradient is made starting from three stock solutions, 38% Percoll (38% Percoll, 750 mM sucrose, 20 mM tricine, 1 mM EDTA, 0.2% BSA), 15% Percoll (15% Percoll, 750 mM sucrose, 20 mM tricine, 1 mM EDTA, 0.2% BSA), 36% sucrose (36% sucrose w/w, 20 mM tricine, 1 mM EDTA). Gradient is made by gently depositing in a JA25 rotor tube, from bottom to top, 3 ml 36% sucrose, 2 ml of 1:2 38% Percoll:36% sucrose, 2ml of 2:1 38% Percoll:36% sucrose, 9 ml 38% Percoll, 3 ml 15% Percoll.

Sucrose discontinuous gradient: gradient is made directly in an ultracentrifuge tube in sterile conditions by gently depositing one on top of the other, from bottom to top, 0.8 ml 60% sucrose, 1.6 ml 55.2% sucrose (8:2 60% sucrose:36% sucrose), 0.5 ml 50.5% sucrose (7:3 60% sucrose:36% sucrose), 2.4 ml 48.5% sucrose (5:5 60% sucrose:36% sucrose), 1.6 ml 46% sucrose (4:6 60% sucrose:36% sucrose), 1.6 ml 43.7% sucrose (3:7 60% sucrose:36% sucrose), 0.8 ml 41.2% sucrose (2:8 60% sucrose:36% sucrose). These different sucrose phases were prepared beforehand by mixing different ratios (indicated in brackets) of two stock solutions: 36% sucrose (see previous paragraph) and 60% sucrose (60% sucrose w/w, 20 mM tricine, 1 mM EDTA). It is imperative that these solutions be kept sterile, since in our experience bacterial contamination leads to complete loss of peroxisomes.

5.8 - PCV purification

PCV purification was performed from frozen *N. benthamiana* systemic leaves infected with PCVwt and PCVΔN6 sap (harvested 28 dpi). All steps were performed at 4°C using sterile material.

50 g of frozen tissue were mixed with 120 ml borate buffer 100 mM ($Na_2B_4O_7$ pH 9, 1% Triton X-100, 0.2 % sodium sulfite - note that sodium sulfite in our experiment greatly

reduced the formation of aggregates) and 150 ml chloroform and blended abundantly in an electric mixer. The resulting solution was gently transferred to centrifuge 500 ml bottles (for Beckman rotor F500), centrifuged 15 min at 8670g, and the supernatant was filtered through sterile Miracloth into graduated cylinder. 1.2 g NaCl were added for each 100 ml, and after a gentle stir of a couple of minutes (magnetic stirrer – slow speed) 3 g PEG6000 for each 100 ml were added, allowed to dissolve, and precipitation was allowed O/N with gentle stir. Next, bottles were spinned 30 min at 14330g (F500 rotor) supernatant was removed (though kept for future use in case of purification failure) and pellet was resuspended in 100 ml borate buffer 40 mM, 0.2 % sodium sulfite (at least 1 hr with gentle stir). The resulting suspension was further clarified by centrifugation at 8670g 15 min, the supernatant was transferred to a new container and NaCl then PEG were added as before. A 4 hr precipitation with gentle stir was allowed. Next, samples were spinned 30 min at 14330g, supernatant was discarded and the pellet was gently resuspended in 20 ml borate buffer 40 mM, 0.2 % sodium sulfite. After clarification by spin 4420g 5 min, the supernatant (around 20 ml) was carefully deposed onto a 7 ml sucrose cushion (25% sucrose in 40 mM borate buffer, 0.2 % sodium sulfite) and ultracentrifuged 3 hr at 100000g, 6°C (Beckman rotor SW28), with medium acceleration and brake. After confirming the presence of the virus in the form of a white pellet on bottom of the tube, supernatant was discarded and 1ml borate buffer 40 mM, 0.2 % sodium sulfite was added to the pellet. The pellet was allowed to passively dissolve O/N on the bottom of the tube (no stir or shake), after which the resuspension was completed through delicate pipetting. One more clarification 5 minutes at 5000 rpm in 1,5 ml tubes was performed to remove remaining aggregates. To calculate virus concentration, OD260 was measured and the following formula was applied (Salah Bouzoubaa, personal communication):

Concentration (mg/ml) = (OD260 x dilution factor)/constant (3.2 for TMV and rod-shaped viruses)

Yield obtained was between 2 and 8 mg of virus from 50 g of tissue, the variation likely depending on the viral titer in the tissue used for extraction. A 50 µl aliquot was used for RNA extraction and agarose gel electrophoresis to assess viral RNA integrity. We observed

that both freezing the pure virus suspension at -20°C or freezing the virus suspension with 30% glycerol in liquid nitrogen resulted in a dramatic decrease in infectivity in *A. thaliana*. Therefore infection of *A. thaliana* must be performed with freshly purified virus. If these conditions are met and infection is performed according to the procedure we set up, 100% infection rate and high titer and symptom homogeneity can be achieved.

5.9 - RNA extraction

Total RNA extraction: all steps performed at 4°C/on ice. 0.1-0.25 g frozen tissue were ground in liquid nitrogen, then homogenized with 1 ml Trizol reagent (Sigma-Aldrich ref. T9424). Only when extracting from *N. benthamiana* the resulting homogenate was clarified through a 5 min 13000rpm spin (benchtop centrifuge). 500 µl chloroform were added, samples were vigorously shaken 2-3 min and centrifuged 10 min 13000rpm. The supernatant was transferred to a new tube, 1 vol. isopropanol was added, tubes were mixed by inversion and 1 hr precipitation was allowed on ice. Next, tubes were spinned 15 min 13000rpm, supernatant was discarded, ice-cold 80% ethanol was added, tubes were spinned 5 min, pellet was dried and resuspended in 50% formamide. RNA concentration and purity were assessed with a Nanodrop 2000 (Thermo Scientific), and quality was assessed on a TBE non-denaturing agarose gel.

Co-immunoprecipitated RNA extraction: all steps performed at 4°C/on ice. 500 µl chloroform were added to the 1 ml Trizol containing the agarose beads (AGO IPs) or the colloidal magnetic beads (HA and GFP IPs). After 2-3 min of vigorous shaking tubes were spinned 10 min 13000rpm, the supernatant was transferred to a new tube and 1 vol isopropanol + 1.5 µl glycogen were added, and precipitation was allowed O/N. After 30min 13000rpm centrifugation, supernatant was carefully discarded, the pellet was washed in 80% ethanol, dried and resuspended in 50% formamide (10 µl for AGO IPs, 20-40 µl for HA and GFP IPs). Protein was also isolated from the same IPs by collecting 350 µl of the phenolic phase after the phenol/chloroform extraction and centrifugation, adding 3-4 vol. of ice-cold acetone, mixing by inversion and allowing precipitation O/N at -20°C. After 15 min 13000rpm centrifugation supernatant was discarded, pellet was washed in 80% acetone, dried and resuspended in protein resuspension buffer (see X). Next, 1/3 vol. of 4X Laemmli

buffer was added and samples were denatured 5 min at 95°C, cooled on ice and stored at -20°C.

Peroxisomal RNA extraction: the 1.5 ml frozen sucrose solution containing the peroxisomes was divided into 4 tubes, and to each tube 1 ml of Trizol reagent was added. RNA extraction was performed as for co-immunoprecipitated RNA (see above paragraph), and pellets were resuspended in 10 µl 50% formamide then pooled. Protein from the same extracts was also isolated as detailed in the paragraph above.

5.10 - Protein extraction

Total protein extraction: according to Hurkman and Tanaka, 1986. 0.05-0.15 g of frozen tissue were ground in liquid nitrogen, 600 ul extraction buffer (0.7 M sucrose, 0.5 M Tris-HCl pH 8, 5 mM EDTA pH 8, 0.1 M NaCl, 2% 2-β-mercaptoethanol, Roche Complete protease inhibitor cocktail) and 600 µl saturated Biophenol pH 8 were added. After 5 min vigorous shake, samples were centrifuged 10 minutes 13000 rpm at 4°C, 5 volumes ice-cold methanol/0.1 M ammonium acetate were added and precipitation was allowed O/N at -20°C. After 15 min centrifugation 13000rpm 4°C, supernatant was discarded and pellet was washed once in methanol/0.1 M ammonium acetate (5 min centrifugation), dried and resuspended in resuspension buffer (10% glycerol, 3% SDS, 62.3 mM Tris-HCl pH 8). after Lowry quantification (BioRad) 4X Laemmli buffer added. 5 minutes at 95°C, 5 minutes on ice and stored at -20°C.

Peroxisomal protein extraction: the 1.5 ml frozen sucrose solution containing the peroxisomes was divided into 3 tubes, and to each tube 500 µl of saturated Biophenol pH8 was added. Extraction was then continued as for total protein. Each pellet was resuspended in 30 µl resuspension buffer, after which the samples were pooled, 1/3 vol. 4X Leammli was added and samples were denatured 5 min at 95°C. Extracts were then sent for mass spectrometry analysis.

5.11 - Northern blotting

Agarose denaturing Northern blot (high molecular weight RNA): 1X HEPES pH 7.4 (20 mM HEPES, 1 mM EDTA), 6% formaldehyde, 1% agarose gel was prepared. 5-10 µg RNA

were brought to 10 µl in 50% formamide, 30 µl loading buffer (12% HEPES 10X, 61% formamide, 20% formaldehyde 37%, bromophenol blue and ethidium bromide) was added and samples were denatured 10 min at 65°C. After 10 min on ice samples were loaded on the gel and run for 3 hrs at 130V in 1X HEPES. After checking RNA integrity and loading under UV, gel was set up for capillary transfer onto a neutral charge nylon Hybond™ NX filter membrane (GE Healthcare) in 20X SSC O/N. Membrane was then equilibrated on 2X SSC and RNA was fixed by UV crosslink.

Denaturing PAGE Northern blot (low molecular weight RNA): denaturing gel was prepared (7 M urea, 17.5% acrylamide/bisacrylamide 19/1, 0.5 TBE), polymerized by adding 1% ammonium persulfate and 0.1% TEMED, and cast into BioRad Mini Protean vertical plates (7 cm gel length). Gel was pre-run without samples for 30 min at 80 V in 0.5X TBE. RNA samples (10-30 µg in the case of total RNA) were brought to equal volume in 50% formamide, denatured at 95°C for 5 minutes, cooled on ice, and 1/3 vol of 4X loading buffer (50% glycerol, 50 mM Tris-HCl pH 7.7, 5 mM EDTA, bromophenol blue) was added. After cleaning the wells, samples were loaded and run was performed for 5 hr 30 min at 80 V (21nt RNA about 1 cm from the end of the gel). RNA was then electroblotted in 0.5 TBE for 1 hr 15 min at 300 mA onto a neutral charge nylon Hybond™ NX filter membrane (GE Healthcare) and chemically crosslinked by incubating 1 hr 30 min at 60°C on Whatmann paper imbibed with EDC solution, composed of 0.125 M 1-Methylimidazole (Sigma-Aldrich ref M5,083-4) and 3% N-(3-Dimethylaminopropyl)-N'-ethylcarbodiimide hydrochloride powder (Sigma-Aldrich ref E7750). Add 1% HCl 1 M to bring pH to 8.

Denaturing PAGE high resolution Northern blot (low molecular weight RNA): these blots were performed as described in the previous paragraph, except that they contained 15% acrylamide/bisacrylamide 19/1 and were cast and run in a CBS Scientific system featuring 20 cm gel length. Run was performed at 600 V, 15 W for around 3 hrs.

Northern blot probing and revealing: after at least 30 min pre-hybridization, all Northern blots were hybridized with radioactive P^{32} labelled γATP or αCTP DNA probes in PerfectHyb™ Plus (Sigma Aldrich ref H7033). High molecular weight Northern blots were hybridized for 2-4 hrs at 60°C then washed three times 20 min at 60°C in 2X SSC 0.1% SDS. Low molecular weight Northern blots were hybridized O/N at 42°C then washed 3 times at 50°C for 5-20 min (depending on probe) in 2X SSC 2% SDS. Once dry, the membranes were

put with FUJI autoradiographic film into reflective screen cassettes at -80°C. γATP was incorporated into DNA oligonucleotides by PNK according to manufacturer indication (Thermo Scientific), then unincorporated nucleotides were removed by G-25 Sepharose columns. αCTP was incorporated into purified PCR products by Klenow random priming according to manufacturer indication (Promega Prime-a-Gene) then unincorporated nucleotides were removed by G-50 Sepharose columns. Before use probes were denatured 5 min at 95°C, then 5 min on ice.

5.12 - Western blotting

Immunoblotting was carried out following standard SDS-PAGE separation on gels ranging from 6 to 15%. Protein extracts in Laemmli buffer were first stacked at 80 V in 4% acrylamide/bisacrylamide 37.5/1, 0.5% SDS, Tris pH 6.8 gel, then size-separated at 100-120 V in 6-15% acrylamide/bisacrylamide 37.5/1, 0.3% SDS, Tris pH 8.8 gel, all in 25 mM Tris, 200 mM Glycine, 0.1% SDS migration buffer. When desired separation was achieved, proteins were transferred by electroblot 90 min at 80 V in 20% ethanol, 25 mM Tris, 200 mM Glycine onto Immobilion-P membranes (Merck-Millipore). After blocking in 5% powdered milk, 1X PBS, 0.1% Tween, the primary antibody was added and membranes were incubated overnight. Membranes were then washed 4 times in 1X PBS, 0.1% Tween, incubated 1-2 hrs with the secondary antibody in 5% powdered milk, 1X PBS, 0.1% Tween at room temperature, and washed again 4 times in 1X PBS, 0.1% Tween. Incubation with the one-step peroxidase-coupled monoclonal HA antibody (Sigma-Aldrich ref H6533) was carried out 1-2 hrs at room temperature, and did not require secondary antibody. Revelation was performed with Roche LumiLight Plus (ref 1201519600) ECL kit, and exposed to FUJI autoradiographic film.

5.13 - Immunolocalisation

Leaves from 6-week-old plants were included in paraffin, sliced with a microtome and fixed to glass plates. Sections were rehydrated through serial washes (2x Histoclear, 2x EtOH 100%, EtOH 96%, EtOH 70% NaCl 0.85%, EtOH 50% NaCl 0.85%, NaCl 0.85%), washed twice in Tris-NaCl buffer (0.1 M Tris HCl pH 7.5, 0.15 M NaCl), saturated 45 minutes in

Tris-NaCl buffer + BSA 1%, then incubated O/N at 4°C in Tris-NaCl buffer + BSA 1% + 1:200 anti-HA antibody coupled to alkaline phosphatase (Sigma-Aldrich, ref. A-5477). After 3 washes in Tris-NaCl buffer, sections were equilibrated in Fast Red buffer, which was then removed and Fast Red added (SIGMAFAST FastRed TR/Naphthol AS-MX, ref. F4648) and incubated 3 hours at room temperature. The reaction was stopped by washing with water and the sections were prepared for microscopy by adding PBS 50% Glycerol 50%. Photos were taken with an E800 Nikon optical microscope and an IDS color camera.

5.14 - Mass spectrometry proteomic analysis

Mass spectrometry analysis was entirely performed by Philippe Hammann, Lauriane Kuhn and Johana Chicher at Plateforme Proteomique Strasbourg – Esplanade, IBMC (Institut de Biologie Moléculaire et Cellulaire), CNRS.

Protein digestion: proteins in resuspension buffer/Laemmli 1X were first precipitated with 100% Methanol / 0.1 M Ammonium Acetate (5 volumes). Protein pellets were then washed 2 times, vacuum dried and re-suspended in 50 mM ammonium bicarbonate. After reduction-alkylation step (5 mM DTT, 10 mM Iodoacetamide), proteins were digested overnight with 200 ng of sequencing-grade trypsin (Promega). After centrifugation at 12.000g, supernatant was collected in glass inserts and vacuum dried.

Nano-liquid Chromatography – electrospray Ionization TripleTOF MS/MS analysis:

before injection, dried peptides were re-suspended in 15 µL 0.1% FA (solvent A). One third of each sample was injected into a NanoLC-2DPlus system (nanoFlexChiP module; Eksigent, ABSciex, Concord, Ontario, Canada) coupled to a TripleTOF 5600 mass spectrometer (ABSciex) operating in positive mode. Peptides loaded on C18 reverse-phase columns (ChIP C-18 precolumn 300 µm ID x 5mm ChromXP and ChIP C-18 analytical column 75 µm ID x 15 cm ChromXP; Eksigent). Peptides eluted by using a 5%-40% gradient of solvent B (0.1 % FA in Acetonitrile) for 60 minutes at a 300 nL/min flow rate. The TripleTOF 5600 operated in high-sensitivity data-dependant acquisition mode with Analyst software (v1.6, ABSciex) on a 350-1250 m/z range. External calibration was performed before each sample by monitoring 10 peptides of a beta-galactosidase trypsic digest. Discovery "Top20" method was used: up to 20 of the most intense multiply-charged ions (2+ to 5+) were selected for CID fragmentation, cycle time 3.3s.

Database search and data analysis: raw data was converted to Mascot Generic File format (.mgf) and searched against the TAIR database supplemented by a decoy database (reverse sequences). The database search algorithm used was Mascot (version 2.2, Matrix Science, London, UK) through ProteinScape 3.1 package (Bruker Daltonics, Leipzig, Germany). The following peptide modifications were allowed during the search: N-acetyl (protein), carbamidomethylation(C) and oxidation (M). Mass tolerances in MS and MS/MS were set to 20 ppm and 0.5 Da, respectively. 2 trypsin missed cleavage sites were allowed. Peptide identifications obtained from Mascot were validated with a protein FDR of 1%, using Protein Assessment tool from ProteinScape. Identified proteins were assessed by total number of fragmented MS/MS spectra per protein, allowing a Spectral Count quantitative strategy.

TAIR accession numbers were identified in all samples aligned, allowing to cluster proteins, validated in either all conditions or in a specific condition. To remove aspecific interactions, first all proteins present in the triple negative controls (SS in IPs, p35S:*P15ΔN6*/SS in peroxisome isolates), including same-set and sub-set proteins, were discarded. Protein partners were considered only if present in all replicates. Second, for IPs a second filter was applied, consisting of a database of proteins emerging from negative controls in other HA co-IP experiments performed by colleagues on other occasions.

5.15 – Primers

Constructs and cloning:

P15-XmaI+: TATA-CCCGGG-ATGCCTAAGTCGGAGTTCTTTC

P15-XmaI-: TATA-CCCGGG-TTACAGTTTAGAACGAAGATTTTTAAACT

P15ΔN6-XmaI-: TATA-CCCGGG-TTATTTAAACTTTTCGCTAAGCAGC

P15nostop-XmaI- (P15-FHA fusion):

TATA-CCCGGG-CAGTTTAGAACGAAGATTTTTAAACTTTT

attB-AGO2+:

GGGGACAAGTTTGTACAAAAAAGCAGGCTATGGAGAGAGGTGGTTATCGAGGA

attB-AGO2-:

GGGGACCACTTTGTACAAGAAAGCTGGGTTCAGACGAAGAACATAACATTCTC

attB-AGO2PX-:

GGGGACCACTTTGTACAAGAAAGCTGGGTTCACAGTTTAGAGACGAAGAACATAACAT

TCTCAAGCTCTG

attB-DRB4+:

GGGGACAAGTTTGTACAAAAAAGCAGGCTATGGATCATGTATACAAAGGTCAAC

attB-HA-:

GGGGACCACTTTGTACAAGAAAGCTGGGTTCACGCGTAATCTGGAACAT

attB-HA-PX-

GGGGACCACTTTGTACAAGAAAGCTGGGTTCACAGTTTAGACGCGTAATCTGGAACAT

CGTA

SalI-P38+

TATATAGTCGACATGGAAAATGATCCTAGAGTCCG

P38-PstI-

TATATACTGCAGCTAAATTCTGAGTGCTTGCAATTTAC

P38-PX-PstI-

TATATACTGCAGTTACAGTTTAGAAATTCTGAGTGCTTGCAATTTACCC

SalI-P19+

TATATAGTCGACATGGAACGAGCTATACAAGGAAAC

P19-HA-PstI-

TATATACTGCAGTTAAGCGTAATCTGGAACATCGTATGGGTACTCGCTTTCTTTTTCGA

AGGTC

P19-HA-PX-PstI-

TATATACTGCAGTTACAGTTTAGAAGCGTAATCTGGAACATCGTATGGGTACTCGCTTT

CTTTTTCGAAGGTC

<u>Probes (primers to generate PCR products for Klenow labeling):</u>

SUL+

ATATCGAAAAGGCTTTGACAGAAG

SUL-

AATCTGGTCTTGAAGCTTGTCC

GFP1+

AGTAAAGGAGAAGAACTTTTCACT

GFP4-

TTCCGTCCTCCTTGAAATCGA

IR71+

AAATGACCGCTACACTGCTTATCT

IR71-

TCTCTCGTCAATGGACAATGAATC

PDS+

AGATTTGACTTCCCAGATGTC

PDS-

ACCATATATGAACATTAATAACTG

TRV1+

CAGAGAGAAATTTCTCGACAGAT

TRV1-

GCATAGCAGCATGAACCAC

PCV1mid+

ACAGAAGAAGATTCTGGAGATGTTG

PCV1mid-

GTCTTTATTACTAGCCAAGACGGC

PCV2mid+

GCTTGAGCTACAGAAACAAGTG

PCV2mid-

AGAGATACAACTGATCCGTCAGTTT

PCV-3'UTR+

CGAGCCATAGAGCACGGT

PCV-3'UTR-

GGAGCGATATCCGTCCCA

<u>Probes (oligonucleotides for PNK labeling):</u>

miR159

TAGAGCTCCCTTCAATCCAAA

miR160

TGGCATACAGGGAGCCAGGCA

miR160c*

CATGCTTGACTCCTTGTACGC

miR165

GGGGGATGAAGCCTGGTCCGA

mir165a*

CCTCGATCCAGACAACATTCC

miR172

ATGCAGCATCATCAAGATTCT

miR172b*

GTGAATCTTAATGGTGCTGC

miR173

GTGATTTCTCTCTGCAAGCGAA

mir173*

TTTCGCTTACACAGAGAATCA

miR390

GGCGCTATCCCTCCTGAGCTT

mir390a*

TGAAACTCAGGATGGATAGCG

miR393

GGATCAATGCGATCCCTTTGGA

mir393a*

AATCCAAAGAGATAGCATGAT

mir396

CAGTTCAAGAAAGCTGTGGAA

mir396a*

CTTCCCACAGCTTTATTGAAC

miR398

AAGGGGTGACCTGAGAACACA

miR408

GCCAGGGAAGAGGCAGTGCAT

miR472

GGTATGGGCGGAGTAGGAAAAA

mir472*

GATTTTGCCTACTTCGACCATACAT

miR822

CATGTGCAAATGCTTCCCGCA

miR822*

CTGTAGAAAGCATTTGCACA

TAS1-255

TACGCTATGTTGGACTTAGAA

TAS3

TGGGGTCTTACAAGGTCAAGA

Rep2

GCGGGACGGGTTTGGCAGGACGTTACTTAAT

U6

AGGGGCCATGCTAATCTTCTC

ACRONYMS & ABBREVIATIONS

AGO: Argonaute protein

BMV: Brome Mosaic Virus

CMV: Cucumber Mosaic Virus

CymRSV: Cymbidium Ringspot Virus

DCL: Dicer-Like protein

DRB: Double-stranded RNA binding protein

dsRNA: Double-stranded RNA

FHA: Flag HA epitope tag

GFP: Green fluorescent protein

HPR: Hydroxypyruvate reductase

miRNA: micro RNA

P15FHA: P15 carrying a C-terminal Flag HA epitope tag

P15wt: P15 as it is encoded by PCV

P15ΔN6: P15 missing the C-terminal last coiled-coil heptad and SKL tripeptide (PTS1)

PCV: Peanut Clump Virus

PCVwt: PCV encoding P15wt

PCVΔN6: PCV encoding P15ΔN6

PDS: Phytoene desaturase

PEX: Peroxin

PTGS: Post-transcriptional gene silencing

PTS1: Peroxisome targeting sequence 1

PVX: Potato Virus X

RDR: RNA-dependent RNA polymerase (host-encoded)

RDRP: RNA-dependent RNA polymerase (virus-encoded)

RNAi: RNA interference

siRNA: small interfering RNA

SKL: serine-lysine-leucine tripeptide, a PTS1

sRNA: small RNA

SS: SUC:*SUL* reporter *A. thaliana* line

ssRNA: Single-stranded RNA

ta-siRNA: *trans*-acting small interfering RNA

TBSV: Tomato Bushy Stunt Virus

TCV: Turnip Crinkle Virus

TGS: Transcriptional gene silencing

TRV: Tobacco Rattle Virus

TuMV: Turnip Mosaic Virus

TVCV: Turnip Vein Clearing Virus

TYMV: Turnip Yellow Mosaic Virus

UTR: Untranslated region

VSR: Viral suppressor of RNA silencing

REFERENCES

Adenot, X., Elmayan, T., Lauressergues, D., Boutet, S., Bouché, N., Gasciolli, V., Vaucheret, H., 2006. DRB4-Dependent TAS3 trans-Acting siRNAs Control Leaf Morphology through AGO7. Curr. Biol. *16*, 927–932.

Alazem, M., Lin, N.S., 2015. Roles of plant hormones in the regulation of host-virus interactions. Mol. Plant Pathol. *16*, 529–540.

Allen, E., Xie, Z., Gustafson, A.M., Carrington, J.C., 2005. microRNA-Directed Phasing during Trans-Acting siRNA Biogenesis in Plants. Cell *121*, 207–221.

Axtell, M.J., 2013. Classification and comparison of small RNAs from plants. Annu. Rev. Plant Biol. *64*, 137–159.

Azevedo, J., Garcia, D., Pontier, D., Ohnesorge, S., Yu, A., Garcia, S., Braun, L., Bergdoll, M., Hakimi, M.A., Lagrange, T., Voinnet, O., 2010. Argonaute quenching and global changes in Dicer homeostasis caused by a pathogen-encoded GW repeat protein. Genes Dev. *24*, 904–915.

Barajas, D., Jiang, Y., Nagy, P.D., 2009. A unique role for the host ESCRT proteins in replication of Tomato bushy stunt virus. PLoS Pathog. *5*, e1000705.

Blanc, S., Uzest, M., Drucker, M., 2011. New research horizons in vector-transmission of plant viruses. Curr. Opin. Microbiol. *14*, 483–491.

Blevins, T., Rajeswaran, R., Aregger, M., Borah, B.K., Schepetilnikov, M., Baerlocher, L., Farinelli, L., Meins Jr., F., Hohn, T., Pooggin, M.M., 2011. Massive production of small RNAs from a non-coding region of Cauliflower mosaic virus in plant defense and viral counter-defense. Nucleic Acids Res. *39*, 5003–5014.

Bologna, N.G., Voinnet, O., 2014. The diversity, biogenesis, and activities of endogenous silencing small RNAs in Arabidopsis. Annu. Rev. Plant Biol. *65*, 473–503.

Bouché, N., Lauressergues, D., Gasciolli, V., Vaucheret, H., 2006. An antagonistic function for Arabidopsis DCL2 in development and a new function for DCL4 in generating viral siRNAs. EMBO J. *25*, 3347–3356.

Brodersen, P., Sakvarelidze-Achard, L., Bruun-Rasmussen, M., Dunoyer, P., Yamamoto, Y.Y., Sieburth, L.E., Voinnet, O., 2008. Widespread Translational Inhibition by Plant miRNAs and siRNAs. Science *320*, 1185–1190.

Brosseau, C., Moffett, P., 2015. Functional and Genetic Analysis Identify a Role for Arabidopsis ARGONAUTE5 in Antiviral RNA Silencing. Plant Cell *27*, 1742–54.

Buhtz, A., Springer, F., Chappell, L., Baulcombe, D.C., Kehr, J., 2008. Identification and characterization of small RNAs from the phloem of Brassica napus. Plant J. 53, 739–749.

Camejo, D., Guzmán-Cedeño, Á., Moreno, A., 2016. Reactive oxygen species, essential molecules, during plant-pathogen interactions. Plant Physiol. Biochem. *103*, 10–23.

Cao, M., Du, P., Wang, X., Yu, Y.-Q., Qiu, Y.-H., Li, W., Gal-On, A., Zhou, C., Li, Y., Ding, S.-W., 2014. Virus infection triggers widespread silencing of host genes by a distinct class of endogenous siRNAs in Arabidopsis. Proc. Natl. Acad. Sci. U. S. A. *111*, 14613–8.

Carbonell, A., Carrington, J.C., 2015. Antiviral roles of plant ARGONAUTES. Curr. Opin. Plant Biol. *27*, 111–117.

Carbonell, A., Fahlgren, N., Garcia-Ruiz, H., Gilbert, K.B., Montgomery, T.A., Nguyen, T., Cuperus, J.T., Carrington, J.C., 2012. Functional Analysis of Three Arabidopsis ARGONAUTES Using Slicer-Defective Mutants. Plant Cell *24*, 3613–3629.

Carrington, J.C., Dougherty, W.G., 1987. Processing of the tobacco etch virus 49K protease requires autoproteolysis. Virology *160*, 355–362.

Carrington, J.C., Freed, D.D., Oh, C.-S., 1990. Expression of potyviral polyproteins in transgenic plants reveals three proteolytic activities required for complete processing. EMBO J. *9*, 1347–1353.

Chen, H.-M., Chen, L.-T., Patel, K., Li, Y.-H., Baulcombe, D.C., Wu, S.-H., 2010. 22-nucleotide RNAs trigger secondary siRNA biogenesis in plants. Proc. Natl. Acad. Sci. U.S.A. *107*, 15269–15274.

Chisholm, S.T., Mahajan, S.K., Whitham, S.A., Yamamoto, M.L., Carrington, J.C., 2000. Cloning of the Arabidopsis RTM1 gene, which controls restriction of long-distance movement of tobacco etch virus. Proc. Natl. Acad. Sci. U.S.A. *97*, 489–94.

Chisholm, S.T., Parra, M.A., Anderberg, R.J., Carrington, J.C., 2001. Arabidopsis RTM1 and RTM2 Genes Function in Phloem to Restrict Long-Distance Movement of Tobacco Etch Virus. Plant Physiol. *127*, 1667–1675.

Cui, Y., Fang, X., Qi, Y., 2016. TRANSPORTIN1 promotes the association of microRNA with ARGONAUTE1 in Arabidopsis. Plant Cell, Sep 23, tpc.00384.2016

Curtin, S.J., Watson, J.M., Smith, N.A., Eamens, A.L., Blanchard, C.L., Waterhouse, P.M., 2008. The roles of plant dsRNA-binding proteins in RNAi-like pathways. FEBS Lett. *582*, 2753–2760.

Daxinger, L., Kanno, T., Bucher, E., van der Winden, J., Naumann, U., Matzke, A.J.M., Matzke, M.A., 2009. A stepwise pathway for biogenesis of 24-nt secondary siRNAs and spreading of DNA methylation. EMBO J. *28*, 48–57.

de Ronde, D., Butterbach, P., Kormelink, R., 2014. Dominant resistance against plant viruses. Front. Plant Sci. 5, 307.

Debelyy, M.O., Platta, H.W., Saffian, D., Hensel, A., Thoms, S., Meyer, H.E., Warscheid, B., Girzalsky, W., Erdmann, R., 2011. Ubp15p, a ubiquitin hydrolase associated with the peroxisomal export machinery. J. Biol. Chem. *286*, 28223–28234.

Decroocq, V., Salvador, B., Sicard, O., Glasa, M., Cosson, P., Revers, F., García, J.A., Candresse, T., 2009. The Determinant of Potyvirus Ability to Overcome the RTM Resistance of Arabidopsis thaliana Maps to the N-Terminal Region of the Coat Protein. Mol. Plant-Microbe Int. *22*, 1302–1311.

Deleris, A., Gallego-Bartolome, J., Bao, J., Kasschau, K.D., Carrington, J.C., Voinnet, O., 2006a. Hierarchical action and inhibition of plant Dicer-like proteins in antiviral defense. Science *313*, 68–71.

Dieryck, B., Weyns, J., Doucet, D., Bragard, C., Legrève, A., 2011. Acquisition and Transmission of Peanut clump virus by Polymyxa graminis on Cereal Species. Phytopathology *101*, 1149–1158.

Dodds, P.N., Rathjen, J.P., 2010. Plant immunity: towards an integrated view of plant–pathogen interactions. Nat. Rev. Genet. *11*, 539–548.

Drugeon, G., Jupin, I., 2002. Stability in vitro of the 69K movement protein of Turnip yellow mosaic virus is regulated by the ubiquitin-mediated proteasome pathway. J. Gen. Virol. *83*, 3187–3197.

Dunoyer, P., Herzog, E., Hemmer, O., Ritzenthaler, C., Fritsch, C., 2001. Peanut clump virus RNA-1-encoded P15 regulates viral RNA accumulation but is not abundant at viral RNA replication sites. J. Virol. *75*, 1941–1948.

Dunoyer, P., Himber, C., Ruiz-Ferrer, V., Alioua, A., Voinnet, O., 2007. Intra- and intercellular RNA interference in Arabidopsis thaliana requires components of the microRNA and heterochromatic silencing pathways. Nat. Genet. *39*, 848–856.

Dunoyer, P., Himber, C., Voinnet, O., 2005. DICER-LIKE 4 is required for RNA interference and produces the 21-nucleotide small interfering RNA component of the plant cell-to-cell silencing signal. Nat. Genet. *37*, 1356–1360.

Dunoyer, P., Pfeffer, S., Fritsch, C., Hemmer, O., Voinnet, O., Richards, K.E., 2002a. Identification, subcellular localization and some properties of a cysteine-rich suppressor of gene silencing encoded by peanut clump virus. Plant J. *29*, 555–567.

Dunoyer, P., Ritzenthaler, C., Hemmer, O., Michler, P., Fritsch, C., 2002b. Intracellular Localization of the. Society 76, 865–874.

Dunoyer, P., Schott, G., Himber, C., Meyer, D., Takeda, A., Carrington, J.C., Voinnet, O., 2010. Small RNA Duplexes Function as Mobile Silencing Signals Between Plant Cells. Science *328*, 912–916.

El-Shami, M., Pontier, D., Lahmy, S., Braun, L., Picart, C., Vega, D., Hakimi, M.A., Jacobsen, S.E., Cooke, R., Lagrange, T., 2007. Reiterated WG/GW motifs form functionally and evolutionarily conserved ARGONAUTE-binding platforms in RNAi-related components. Genes Dev. *21*, 2539–2544.

Erdmann, R., Schliebs, W., 2005. Peroxisomal matrix protein import : the transient pore model. Nat. Rev. Mol. Cell Biol. *6*, 738–743.

Erhardt, M., Stussi-Garaud, C., Guilley, H., Richards, K.E., Jonard, G., Bouzoubaa, S., 1999. The first triple gene block protein of peanut clump virus localizes to the plasmodesmata during virus infection. Virology *264*, 220–229.

Fire, A., Xu, S., Montgomery, M.K., Kostas, S.A., Driver, S.E., Mello, C.C., 1998. Potent and specific genetic interference by double-stranded RNA in Caenorhabditis elegans. Nature *391*, 806–811.

Freitas, M.O., Francisco, T., Rodrigues, T.A., Alencastre, I.S., Pinto, M.P., Grou, C.P., Carvalho, A.F., Fransen, M., Sa-Miranda, C., Azevedo, J.E., 2011. PEX5 protein binds monomeric catalase blocking its tetramerization and releases it upon binding the N-terminal domain of PEX14. J. Biol. Chem. *286*, 40509–40519.

Fukudome, A., Fukuhara, T., 2016. Plant dicer-like proteins: double-stranded RNA-cleaving enzymes for small RNA biogenesis. J. Plant Res. doi:10.1007/s10265-016-0877-1

Fukudome, A., Kanaya, A., Egami, M., Nakazawa, Y., Hiraguri, A., Moriyama, H., Fukuhara, T., 2011. Specific requirement of DRB4, a dsRNA-binding protein, for the in vitro dsRNA-cleaving activity of Arabidopsis Dicer-like 4. RNA *17*, 750–760.

Garcia-Ruiz, H., Carbonell, A., Hoyer, J.S., Fahlgren, N., Gilbert, K.B., Takeda, A., Giampetruzzi, A., Garcia Ruiz, M.T., McGinn, M.G., Lowery, N., Martinez Baladejo, M.T., Carrington, J.C., 2015. Roles and Programming of Arabidopsis ARGONAUTE Proteins during Turnip Mosaic Virus Infection. PLoS Pathog. *11*, 1–27.

Garcia-Ruiz, H., Takeda, A., Chapman, E.J., Sullivan, C.M., Fahlgren, N., Brempelis, K.J., Carrington, J.C., 2010. Arabidopsis RNA-Dependent RNA Polymerases and Dicer-Like Proteins in Antiviral Defense and Small Interfering RNA Biogenesis during Turnip Mosaic Virus Infection. Plant Cell *22*, 481–496.

Garcia, D., Collier, S.A., Byrne, M.E., Martienssen, R.A., 2006. Specification of Leaf Polarity in Arabidopsis via the trans-Acting siRNA Pathway. Curr. Biol. *16*, 933–938.

Garcia, D., Garcia, S., Pontier, D., Marchais, A., Renou, J.P., Lagrange, T., Voinnet, O., 2012. Ago Hook and RNA Helicase Motifs Underpin Dual Roles for SDE3 in Antiviral Defense and Silencing of Nonconserved Intergenic Regions. Mol. Cell *48*, 109–120.

Garcia, D., Garcia, S., Voinnet, O., 2014. Nonsense-mediated decay serves as a general viral restriction mechanism in plants. Cell Host Microbe *16*, 391–402.

German, M.A., Pillay, M., Jeong, D.-H., Hetawal, A., Luo, S., Janardhanan, P., Kannan, V., Rymarquis, L.A., Nobuta, K., German, R., de Paoli, E., Lu, C., Schroth, G.P., Meyers, B.C., Green, P.J., 2008. Global identification of microRNA-target RNA pairs by parallel analysis of RNA ends. Nat. Biotech. *26(8)*, 941–946.

Golisz, A., Sikorski, P.J., Kruszka, K., Kufel, J., 2013. Arabidopsis thaliana LSM proteins function in mRNA splicing and degradation. Nucleic Acids Res. *41*, 6232-6249

Gouveia, A.M., Guimarães, C.P., Oliveira, M.E., Reguenga, C., Sá-Miranda, C., Azevedo, J.E., 2003a. Characterization of the peroxisomal cycling receptor, Pex5p, using a cell-free in vitro import system. J. Biol. Chem. *278*, 226–232.

Gouveia, A.M., Guimarães, C.P., Oliveira, M.E., Sá-Miranda, C., Azevedo, J.E., 2003b. Insertion of Pex5p into the peroxisomal membrane is cargo protein-dependent. J. Biol. Chem. *278*, 4389–4392.

Grangeon, R., Jiang, J., Laliberté, J.F., 2012. Host endomembrane recruitment for plant RNA virus replication. Curr. Opin. Virol. *2*, 677–684.

Grimm, I., Saffian, D., Platta, H.W., Erdmann, R., 2012. The AAA-type ATPases Pex1p and Pex6p and their role in peroxisomal matrix protein import in Saccharomyces cerevisiae. Biochim. Biophys. Acta - Mol. Cell Res. *1823*, 150–158.

Hamilton, A.J., Voinnet, O., Chappell, L., Baulcombe, D.C., 2002. Two classes of short interfering RNA in RNA silencing. EMBO J. *21*, 4671–4679.

Harvey, J.J.W., Lewsey, M.G., Patel, K., Westwood, J.H., Heimstädt, S., Carr, J.P., Ba,combe, D.C., 2011. An Antiviral Defense Role of AGO2 in Plants. PLoS One *6*, e14639.

Hasan, S., Platta, H.W., Erdmann, R., 2013. Import of proteins into the peroxisomal matrix. Front. Physiol. *4*, 1–12.

Havecker, E.R., Wallbridge, L.M., Hardcastle, T.J., Bush, M.S., Kelly, K.A., Dunn, R.M., Schwach, F., Doonan, J.H., Baulcombe, D.C., 2010. The Arabidopsis RNA-Directed DNA Methylation Argonautes Functionally Diverge Based on Their Expression and Interaction with Target Loci. Plant Cell *22*, 321–334.

Havelda, Z., Hornyik, C., Crescenzi, A., Burgyán, J., Burgyan, J., 2003. In Situ Characterization of Cymbidium Ringspot Tombusvirus Infection-Induced Posttranscriptional Gene Silencing in Nicotiana benthamiana. J Virol *77*, 6082–6.

Heinlein, M., 2015. Plant virus replication and movement. Virology 479-480, 657–671.

Heitz, T., Widemann, E., Lugan, R., Miesch, L., Ullmann, P., Désaubry, L., Holder, E., Grausem, B., Kandel, S., Miesch, M., Werck, D., Pinot, F., 2012. Cytochromes P450 CYP94C1 and CYP94B3 Catalyze Two Successive Oxidation Steps of Plant Hormone Jasmonoyl-isoleucine for Catabolic Turnover. J. Biol. Chem. *287*, 6296-6306

Henderson, I.R., Zhang, X., Lu, C., Johnson, L., Meyers, B.C., Green, P.J., Jacobsen, S.E., 2006. Dissecting Arabidopsis thaliana DICER function in small RNA processing, gene silencing and DNA methylation patterning. Nat. Genet. *38*, 721–725.

Herzog, E., Hemmer, O., Hauser, S., Meyer, G., Bouzoubaa, S., Fritsch, C., 1998. Identification of genes involved in replication and movement of peanut clump virus. Virology *248*, 312–22.

Himber, C., Dunoyer, P., Moissiard, G., Ritzenthaler, C., Voinnet, O., 2003. Transitivity-dependent and -independent cell-to-cell movement of RNA silencing. EMBO J. *22*, 4523–4533.

Hipper, C., Brault, V., Ziegler-Graff, V., Revers, F., 2013. Viral and cellular factors involved in Phloem transport of plant viruses. Front. Plant Sci. *4*, 154.

Hull, R., 2002. Plant Virology, 4th ed.

Hurkman, W.J., Tanaka, C.K., 1986. Solubilization of Plant Membrane Proteins for Analysis by Two-Dimensional Gel Electrophoresis. Plant Physiol. *81*, 802–806.

Hyodo, K., Kaido, M., Okuno, T., 2014. Host and viral RNA-binding proteins involved in membrane targeting, replication and intercellular movement of plant RNA virus genomes. Front. Plant Sci. *5*, 321.

Iki, T., Yoshikawa, M., Meshi, T., Ishikawa, M., 2012. Cyclophilin 40 facilitates HSP90-mediated RISC assembly in plants. EMBO J. *31*, 267-278.

Iki, T., Yoshikawa, M., Nishikiori, M., Jaudal, M.C., Matsumoto-Yokoyama, E., Mitsuhara, I., Meshi, T., Ishikawa, M., 2010. In Vitro Assembly of Plant RNA-Induced Silencing Complexes Facilitated by Molecular Chaperone HSP90. Mol. Cell *39*, 282–291.

Jakubiec, A., Yang, S.W., Chua, N.H., 2012. Arabidopsis DRB4 protein in antiviral defense against Turnip yellow mosaic virus infection. Plant J. *69*, 14–25.

Jaubert, M., Bhattacharjee, S., Mello, A.F.S., Perry, K.L., Moffett, P., 2011. ARGONAUTE2 mediates RNA-silencing antiviral defenses against Potato virus X in Arabidopsis. Plant Physiol. *156*, 1556–64.

Kaur, N., Reumann, S., Hu, J., 2009. Peroxisome biogenesis and function. Arab. B. *7*, e0123.

Kaur, N., Zhao, Q., Xie, Q., Hu, J., 2013. Arabidopsis RING Peroxins are E3 Ubiquitin Ligases that Interact with Two Homologous Ubiquitin Receptor Proteins. J. Integr. Plant Biol. *55*, 108–120.

Kerssen, D., Hambruch, E., Klaas, W., Platta, H.W., De Kruijff, B., Erdmann, R., Kunau, W.H., Schliebs, W., 2006. Membrane association of the cycling peroxisome import receptor Pex5p. J. Biol. Chem. *281*, 27003–27015.

Kragler, F., Lametschwandtner, G., Christmann, J., Hartig, a, Harada, J.J., 1998. Identification and analysis of the plant peroxisomal targeting signal 1 receptor NtPEX5. Proc. Natl. Acad. Sci. U. S. A. *95*, 13336–41.

Kutnjak, D., Silvestre, R., Cuellar, W., Perez, W., Müller, G., Ravnikar, M., Kreuze, J., 2014. Complete genome sequences of new divergent potato virus X isolates and discrimination between strains in a mixed infection using small RNAs sequencing approach. Virus Res. *191*, 45–50.

Leon, S., Goodman, J.M., Subramani, S., 2006. Uniqueness of the mechanism of protein import into the peroxisome matrix: Transport of folded, co-factor-bound and oligomeric proteins by shuttling receptors. Biochim. Biophys. Acta - Mol. Cell Res. *1763*, 1552–1564.

Lanyon-Hogg, T., Warriner, S.L., Baker, A., 2010. Getting a camel through the eye of a needle: the import of folded proteins by peroxisomes. Biol. Cell *102*, 245–263.

Law, J.A., Ausin, I., Johnson, L.M., Vashisht, A.A., Zhu, J.-K., Wohlschlegel, J.A., Jacobsen, S.E., 2010. A Protein Complex Required for Polymerase V Transcripts and RNA- Directed DNA Methylation in Arabidopsis. Curr. Biol. *20*, 951–956.

Lazarow, P.B., 2011. Viruses exploiting peroxisomes. Curr. Opin. Microbiol. *14,* 458–469.

Liu, Y.L., Schiff, M., Dinesh-Kumar, S.P., 2002. Virus-induced gene silencing in tomato. Plant J. *31*, 777–786.

Llave, C., Xie, Z., Kasschau, K.D., Carrington, J.C., 2002. Cleavage of Scarecrow-like mRNA Targets Directed by a Class of Arabidopsis miRNA. Science *297*, 2053–2056.

Lobbes, D., Rallapalli, G., Schmidt, D.D., Martin, C., Clarke, J., 2006. SERRATE: a new player on the plant microRNA scene. EMBO Rep. *7*, 1052–1058.

Ma, J.-B., Ye, K., Patel, D.J., 2004. Structural basis for overhang-specific small interfering RNA recognition by the PAZ domain. Nature *429*, 318–322.

Ma, X., Nicole, M.C., Meteignier, L.V., Hong, N., Wang, G., Moffett, P., 2015. Different roles for RNA silencing and RNA processing components in virus recovery and virus-induced gene silencing in plants. J. Exp. Bot. *66*, 919–932.

MacRae, I.J., Zhou, K., Doudna, J.A., 2007. Structural determinants of RNA recognition and cleavage by Dicer. Nat. Struct. Mol. Biol. *14 (10)*, 934-940.

Mallory, A.C., Hinze, A., Tucker, M.R., Bouché, N., Gasciolli, V., Elmayan, T., Lauressergues, D., Jauvion, V., Vaucheret, H., Laux, T., 2009. Redundant and Specific Roles

of the ARGONAUTE Proteins AGO1 and ZLL in Development and Small RNA-Directed Gene Silencing. PLoS Genet. *5*, e1000646.

Manavella, P. a, Koenig, D., Weigel, D., 2012. Plant secondary siRNA production determined by microRNA-duplex structure. Proc. Natl. Acad. Sci. U. S. A. *109*, 2461–6.

Mandadi, K.K., Scholthof, K.-B.G., 2013. Plant immune responses against viruses: how does a virus cause disease? Plant Cell *25*, 1489–505.

Margis, R., Fusaro, A.F., Smith, N.A., Curtin, S.J., Watson, J.M., Finnegan, E.J., Waterhouse, P.M., 2006. The evolution and diversification of Dicers in plants. FEBS Lett. *580*, 2442–2450.

Matsuda, D., Dunoyer, P., Hemmer, O., Fritsch, C., Dreher, T.W., 2000. The valine anticodon and valylatability of Peanut clump virus RNAs are not essential but provide a modest competitive advantage in plants. J. Virol. *74*, 8720–8725.

Maunoury, N., Vaucheret, H., 2011. AGO1 and AGO2 act redundantly in miR408-mediated Plantacyanin regulation. PLoS One *6*.

Meinecke, M., Cizmowski, C., Schliebs, W., Krüger, V., Beck, S., Wagner, R., Erdmann, R., 2010. The peroxisomal importomer constitutes a large and highly dynamic pore. Nat. Cell Biol. *12*, 273–277.

Mi, S., Cai, T., Hu, Y., Chen, Y., Hodges, E., Ni, F., Wu, L., Li, S., Zhou, H., Long, C., Chen, S., Hannon, G.J., Qi, Y., 2008. Sorting of Small RNAs into Arabidopsis Argonaute Complexes Is Directed by the 5' Terminal Nucleotide. Cell *133*, 116–127.

Miozzi, L., Pantaleo, V., Burgyán, J., Accotto, G.P., Noris, E., 2013. Analysis of small RNAs derived from tomato yellow leaf curl Sardinia virus reveals a cross reaction between the major viral hotspot and the plant host genome. Virus Res. *178*, 287–296.

Mohan, K.V.K., Som, I., Atreya, C.D., 2002. Identification of a type 1 peroxisomal targeting signal in a viral protein and demonstration of its targeting to the organelle. J. Virol. *76*, 2543–2547.

Moissiard, G., Parizotto, E.A., Himber, C., Voinnet, O., 2007. Transitivity in Arabidopsis can be primed, requires the redundant action of the antiviral Dicer-like 4 and Dicer-like 2, and is compromised by viral-encoded suppressor proteins. RNA *13*, 1268–78.

Molnár, A., Melnyk, C., Bassett, A., Hardcastle, T., Dunn, R.M., Baulcombe, D.C., 2010. Small Silencing RNAs in Plants Are Mobile and Direct Epigenetic Modification in Recipient Cells. Science *328*, 872–875.

Montgomery, T.A., Howell, M.D., Cuperus, J.T., Li, D., Hansen, J.E., Alexander, A.L., Chapman, E.J., Fahlgren, N., Allen, E., Carrington, J.C., 2008. Specificity of ARGONAUTE7-miR390 Interaction and Dual Functionality in TAS3 Trans-Acting siRNA Formation. Cell *133*, 128–141.

Morel, J., Godon, C., Mourrain, P., Béclin, C., Boutet, S., Feuerbach, F., Proux, F., Vaucheret, H., 2002. Fertile Hypomorphic *ARGONAUTE* (*ago1*) mutants impaired in post-transcriptional gene silencing and virus resistance. Plant Cell 14, 629–639.

Nagano, H., Fukudome, A., Hiraguri, A., Moriyama, H., Fukuhara, T., 2013. Distinct substrate specificities of Arabidopsis DCL3 and DCL4. Nucleic Acids Res. *42*, 1845-1856.

Naveed, K., Mitter, N., Harper, A., Dhingra, A., Pappu, H.R., 2014. Comparative analysis of virus-specific small RNA profiles of three biologically distinct strains of Potato virus Y in infected potato (Solanum tuberosum) cv. Russet Burbank. Virus Res. *191*, 153–160.

Okada, K., Abe, H., Arimura, G.I., 2015. Jasmonates induce both defense responses and communication in monocotyledonous and dicotyledonous plants. Plant Cell Physiol. *56*, 16–27.

Okamura, K., Liu, N., Lai, E.C., 2009. Distinct mechanisms for microRNA strand selection by Drosophila Argonautes. Mol. Cell *36*, 431-444.

Palauqui, J.C., Elmayan, T., Pollien, J.M., Vaucheret, H., 1997. Systemic acquired silencing: Transgene-specific post-transcriptional silencing is transmitted by grafting from silenced stocks to non-silenced scions. EMBO J. *16*, 4738–4745.

Pallas, V., García, J.A., 2011. How do plant viruses induce disease? Interactions and interference with host components. J. Gen. Virol. *92*, 2691–2705.

Parent, J.S., Bouteiller, N., Elmayan, T., Vaucheret, H., 2015. Respective contributions of Arabidopsis DCL2 and DCL4 to RNA silencing. Plant J. *81*, 223–232.

Park, W., Li, J., Song, R., Messing, J., Chen, X., 2002. CARPEL FACTORY, a Dicer Homolog, and HEN1, a Novel Protein, Act in microRNA Metabolism in Arabidopsis thaliana. Curr. Biol. *12*, 1484–1495.

Pires, J.R., Hong, X., Brockmann, C., Volkmer-Engert, R., Schneider-Mergener, J., Oschkinat, H., Erdmann, R., 2003. The ScPex13p SH3 domain exposes two distinct binding sites for Pex5p and Pex14p. J. Mol. Biol. *326*, 1427–1435.

Platta, H.W., Grunau, S., Rosenkranz, K., Girzalsky, W., Erdmann, R., 2005. Functional role of the AAA peroxins in dislocation of the cycling PTS1 receptor back to the cytosol. Nat. Cell Biol. *7*, 817–822.

Platta, H.W., Hagen, S., Reidick, C., Erdmann, R., 2014. The peroxisomal receptor dislocation pathway: To the exportomer and beyond. Biochimie *98*, 16–28.

Pontes, O., Li, C.F., Nunes, P.C., Haag, J., Ream, T., Vitins, A., Jacobsen, S.E., Pikaard, C.S., 2006. The Arabidopsis Chromatin-Modifying Nuclear siRNA Pathway Involves a Nucleolar RNA Processing Center. Cell *126*, 79–92.

Poulsen, C., Vaucheret, H., Brodersen, P., 2013. Lessons on RNA silencing mechanisms in plants from eukaryotic argonaute structures. Plant Cell *25*, 22–37.

Pumplin, N., Voinnet, O., 2013. RNA silencing suppression by plant pathogens: defence, counter-defence and counter-counter-defence. Nat. Rev. Microbiol. *11*, 745–60.

Qi, Y., Denli, A.M., Hannon, G.J., 2005. Biochemical specialization within Arabidopsis RNA silencing pathways. Mol. Cell *19*, 421–428.

Qu, F., Ye, X., Morris, T.J., 2008. Arabidopsis DRB4, AGO1, AGO7, and RDR6 participate in a DCL4-initiated antiviral RNA silencing pathway negatively regulated by DCL1. Proc. Natl. Acad. Sci. U. S. A. *105*, 14732–7.

Raja, P., Wolf, J.N., Bisaro, D.M., 2010. RNA silencing directed against geminiviruses: Post-transcriptional and epigenetic components. Biochim. Biophys. Acta - Gene Regul. Mech. *1799*, 337–351.

Rajagopalan, R., Vaucheret, H., Trejo, J., Bartel, D.P., 2006. A diverse and evolutionarily fluid set of microRNAs in Arabidopsis thaliana. Genes Dev. *20*, 3407–3425.

Reichel, C., Beachy, R.N., 2000. Degradation of Tobacco mosaic virus movement protein by the 26S proteasome. J. Virol. *74*, 3330–3337.

Reinhart, B.J., Weinstein, E.G., Rhoades, M.W., Bartel, B., Bartel, D.P., 2002. MicroRNAs in plants. Genes Dev. *16*, 1616–1626.

Reumann, S., Singhal, R., 2014. Isolation of leaf peroxisomes from arabidopsis for organelle proteome analyses. Methods Mol. Biol. *1072*, 541–552.

Roossinck, M.J., 2011. The good viruses: viral mutualistic symbioses. Nat. Rev. Microbiol. *9*, 99–108.

Savenkov, E.I., Solovyev, A.G., Morozov, S.Y., 1998. Genome sequences of poa semilatent and lychnis ringspot hordeiviruses. Arch. Virol. *143*, 1379–1393.

Scholthof, H.B., Alvarado, V.Y., Vega-Arreguin, J.C., Ciomperlik, J., Odokonyero, D., Brosseau, C., Jaubert, M., Zamora, A., Moffett, P., 2011. Identification of an ARGONAUTE for antiviral RNA silencing in Nicotiana benthamiana. Plant Physiol. *156*, 1548–1555.

Schott, G., Mari-Ordonez, A., Himber, C., Alioua, A., Voinnet, O., Dunoyer, P., 2012b. Differential effects of viral silencing suppressors on siRNA and miRNA loading support the existence of two distinct cellular pools of ARGONAUTE1. EMBO J. *31*, 2553–65.

Shamandi, N., Zytnicki, M., Charbonnel, C., Elvira-Matelot, E., Bochnakian, A., Comella, P., Mallory, A.C., Lepère, G., Sáez-Vásquez, J., Vaucheret, H., 2015. Plants Encode a General siRNA Suppressor That Is Induced and Suppressed by Viruses. PLoS Biol. *13*, 1–28.

Silva, T.F., Romanel, E.A.C., Andrade, R.R.S., Farinelli, L., Østerås, M., Deluen, C., Corrêa, R.L., Schrago, C.E.G., Vaslin, M.F.S., 2011. Profile of small interfering RNAs from cotton plants infected with the polerovirus Cotton leafroll dwarf virus. BMC Plant Mol. Biol. *12*:40

Song, J.-J., Liu, J., Tolia, N.H., Schneiderman, J., Smith, S.K., Martienssen, R.A., Hannon, G.J., Joshua-Tor, L., 2003. The crystal structure of the Argonaute2 PAZ domain reveals an RNA binding motif in RNAi effector complexes. Nat Struct Biol *10*, 1026–1032.

Song, J.-J., Smith, S.K., Hannon, G.J., Joshua-Tor, L., 2004. Crystal structure of Argonaute and its implications for RISC slicer activity. Science *305*, 1434–1437.

Song, L., Han, M.-H., Lesicka, J., Fedoroff, N., 2007. Arabidopsis primary microRNA processing proteins HYL1 and DCL1 define a nuclear body distinct from the Cajal body. Proc. Natl. Acad. Sci. U.S.A. *104*, 5437–5442.

Stanley, W.A., Filipp, F. V., Kursula, P., Schüller, N., Erdmann, R., Schliebs, W., Sattler, M., Wilmanns, M., 2006. Recognition of a Functional Peroxisome Type 1 Target by the Dynamic Import Receptor Pex5p. Mol. Cell *24*, 653–663.

Takeda, A., Iwasaki, S., Watanabe, T., Utsumi, M., Watanabe, Y., 2008. The Mechanism Selecting the Guide Strand from Small RNA Duplexes is Different Among Argonaute Proteins. Plant Cell Physiol. *49*, 493–500.

Tang, G., Reinhart, B.J., Bartel, D.P., Zamore, P.D., 2003. A biochemical framework for RNA silencing in plants A biochemical framework for RNA silencing in plant. Genes Dev. *17*, 49–63.

Till, S., Lejeune, E., Thermann, R., Bortfeld, M., Hothorn, M., Enderle, D., Heinrich, C., Hentze, M.W., Ladurner, A.G., 2007. A conserved motif in Argonaute-interacting proteins mediates functional interactions through the Argonaute PIWI domain. Nat. Struct. Mol. Biol. *14*, 897–903.

Vargason, J.M., Szittya, G., Burgyán, J., Hall, T.M.T., 2003. Size Selective Recognition of siRNA by an RNA Silencing Suppressor. Cell *115*, 799–811.

Vazquez, F., Vaucheret, H., Rajagopalan, R., Lepers, C., Gasciolli, V., Mallory, A.C., Hilbert, J.-L., Bartel, D.P., Crété, P., 2004. Endogenous trans-Acting siRNAs Regulate the Accumulation of Arabidopsis mRNAs. Mol. Cell *16*, 69–79.

Voinnet, O., 2005. Non-cell autonomous RNA silencing. FEBS Lett. *579*, 5858-5871.

Voinnet, O., Baulcombe, D.C., 1997. Systemic signalling in gene silencing. Nature *389*, 553.

Voinnet, O., Vain, P., Angell, S., Baulcombe, D.C., 1998. Systemic spread of sequence-specific transgene RNA degradation in plants is initiated by localized introduction of ectopic promoterless DNA. Cell *95*, 177–187.

Wang, A., 2014. Dissecting the Molecular Network of Virus-Plant Interactions: The Complex Roles of Host Factors. Annu. Rev. Phytopathol. *53*.

Wang, D., Visser, N. V, Veenhuis, M., van der Klei, I.J., 2003. Physical interactions of the peroxisomal targeting signal 1 receptor pex5p, studied by fluorescence correlation spectroscopy. J. Biol. Chem. *278*, 43340–43345.

Wang, X.-B., Jovel, J., Udomporn, P., Wang, Y., Wu, Q., Li, W.-X., Gasciolli, V., Vaucheret, H., Ding, S.-W., 2011. The 21-nucleotide, but not 22-nucleotide, viral secondary small interfering RNAs direct potent antiviral defense by two cooperative argonautes in Arabidopsis thaliana. Plant Cell *23*, 1625–38.

Wang, X.B., Wu, Q., Ito, T., Cillo, F., Li, W.X., Chen, X., Yu, J.L., Ding, S.-W., 2010. RNAi-mediated viral immunity requires amplification of virus-derived siRNAs in Arabidopsis thaliana. Proc. Natl. Acad. Sci. U.S.A. *107*, 484–489.

Wei, W., Ba, Z., Gao, M., Wu, Y., Ma, Y., Amiard, S., White, C.I., Michaela, J., Danielsen, R., Yang, Y., Qi, Y., 2012. A Role for Small RNAs in DNA Double-Strand Break Repair. Cell *149*, 101–112.

Xie, Z., Allen, E., Wilken, A., Carrington, J.C., 2005. DICER-LIKE 4 functions in trans-acting small interfering RNA biogenesis and vegetative phase change in Arabidopsis thaliana. Proc. Natl. Acad. Sci. U.S.A. *102,* 12984–12989.

Xie, Z., Johansen, L.K., Gustafson, A.M., Kasschau, K.D., Lellis, A.D., Zilberman, D., Jacobsen, S.E., Carrington, J.C., 2004. Genetic and Functional Diversification of Small RNA Pathways in Plants. PLoS Biol *2*, e104.

Xu, K., Nagy, P.D., 2014. Expanding use of multi-origin subcellular membranes by positive-strand RNA viruses during replication. Curr. Opin. Virol. *9*, 119–126.

Yamaji, Y., Maejima, K., Komatsu, K., Shiraishi, T., Okano, Y., Himeno, M., Sugawara, K., Neriya, Y., Minato, N., Miura, C., Hashimoto, M., Namba, S., 2012. Lectin-Mediated Resistance Impairs Plant Virus Infection at the Cellular Level. Plant Cell *24*, 778–793.

Ye, K., Malinina, L., Patel, D.J., 2003. Recognition of small interfering RNA by a viral suppressor of RNA silencing. Nature *426*, 0–4.

Yelina, N.E., Erokhina, T.N., Lukhovitskaya, N.I., Minina, E.A., Schepetilnikov, M. V, Lesemann, D., Schiemann, J., Solovyev, A.G., Morozov, S.Y., 2005. Localization of Poa semilatent virus cysteine-rich protein in peroxisomes is dispensable for its ability to suppress RNA silencing. J. Gen. Virol. *86*, 479–489.

Yoshikawa, M., Peragine, A., Park, M.Y., Poethig, R.S., 2005. A pathway for the biogenesis of trans-acting siRNAs in Arabidopsis. Genes Dev. *19*, 2164–2175.

Yu, B., Yang, Z., Li, J., Minakhina, S., Yang, M., Padgett, R.W., Steward, R., Chen, X., 2005. Methylation as a Crucial Step in Plant microRNA Biogenesis. Science *307*, 932–935.

Zhang, X., Henderson, I.R., Lu, C., Green, P.J., Jacobsen, S.E., 2007. Role of RNA polymerase IV in plant small RNA metabolism. Proc. Natl. Acad. Sci. U. S. A. *104*, 4536–41.

Zhang, X., Zhao, H., Gao, S., Wang, W.-C., Katiyar-Agarwal, S., Huang, H.-D., Raikhel, N., Jin, H., 2011. Arabidopsis Argonaute 2 Regulates Innate Immunity via miRNA393*-Mediated Silencing of a Golgi-Localized SNARE Gene, MEMB12. Mol. Cell *42*, 356–366.

Zhang, Z., Liu, X., Guo, X., Wang, X.-J., Zhang, X., 2016. Arabidopsis AGO3 predominantly recruits 24-nt small RNAs to regulate epigenetic silencing. Nat. Plants *2*, 16049.

Zhu, H., Hu, F., Wang, R., Zhou, X., Sze, S.-H., Liou, L., Barefoot, A., Dickman, M., Zhang, X., 2011. Arabidopsis Argonaute10 Specifically Sequesters miR166/165 to Regulate Shoot Apical Meristem Development. Cell *145*, 242–256.

Zhu, S., Jeong, R.D., Lim, G.H., Yu, K., Wang, C., Chandra-Shekara, A.C., Navarre, D., Klessig, D.F., Kachroo, A., Kachroo, P., 2013. Double-Stranded RNA-Binding Protein 4 Is Required for Resistance Signaling against Viral and Bacterial Pathogens. Cell Rep. *4 (6)*,1168-8.

Zorzatto, C., Machado, J.P.B., Lopes, K.V.G., Nascimento, K.J.T., Pereira, W.A., Brustolini, O.J.B., Reis, P.A.B., Calil, I.P., Deguchi, M., Sachetto-Martins, G., Gouveia, B.C., Loriato, V.A.P., Silva, M. a. C., Silva, F.F., Santos, A.A., Chory, J., Fontes, E.P.B., 2015. NIK1-mediated translation suppression functions as a plant antiviral immunity mechanism. Nature 520 (7549), 679-82.

ANNEXES

Annex 1

Supplementary Figures S1 to S9, with corresponding legends.

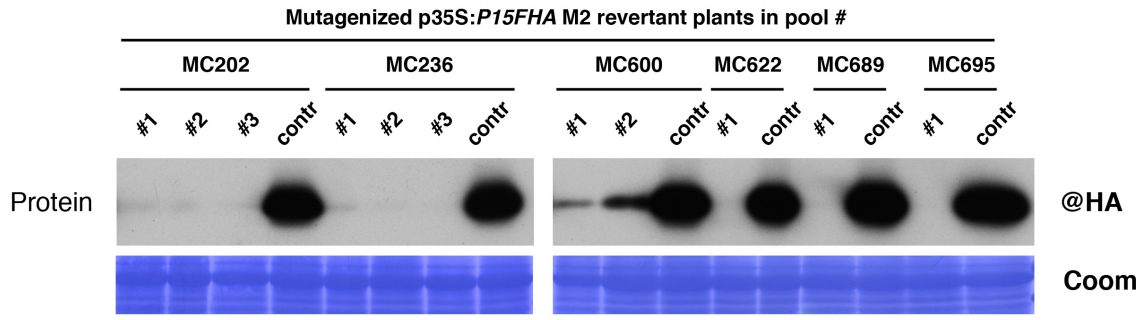

Figure S1: accumulation of P15FHA protein in revertant plants.
Western blot analysis of proteins from a sample of M2 revertant plants (showing a SS yellow vein phenotype) after EMS mutagenesis. Where more than one revertant appeared in each pool, all were analysed. "Contr." are plants within the same pool showing no yellow vein phenotype.

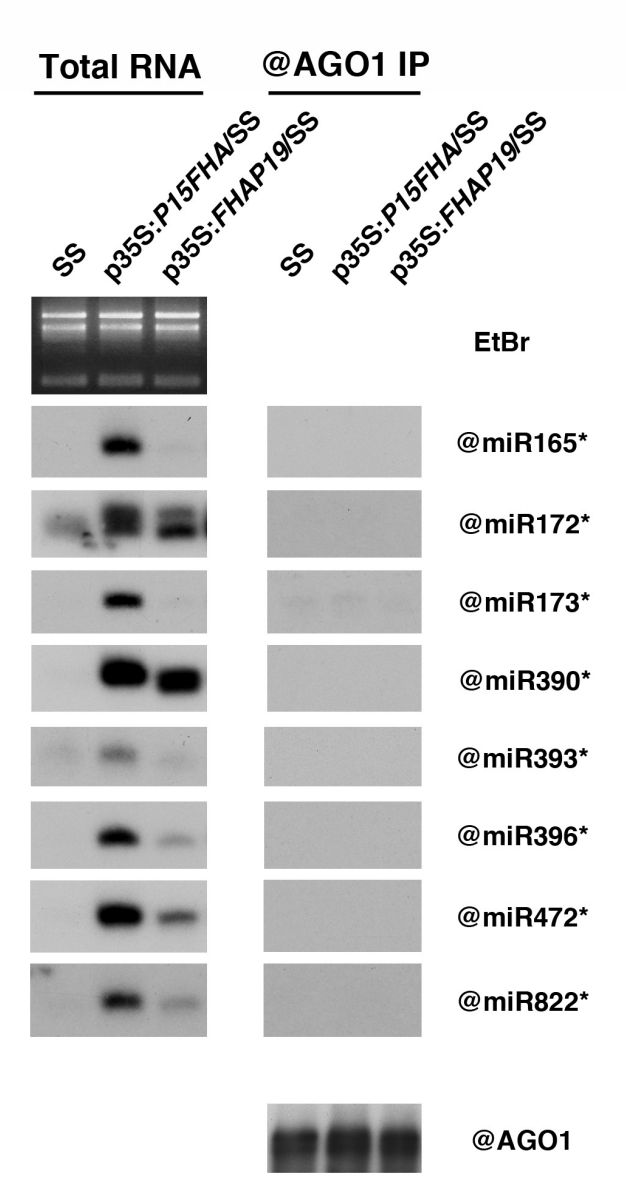

Figure S2: accumulation of miRNA star (*) strands in total and AGO1 co-IPed RNA.
Further probing of the Northern blots shown in Fig. 1.3 to reveal the accumulation of miRNA passenger strands. See Fig. 1.3 for protein analysis. Note that total RNA blots and EtBr, as well as western blot of IPed protein, are the same as in Fig. 1.3 and/or S3.

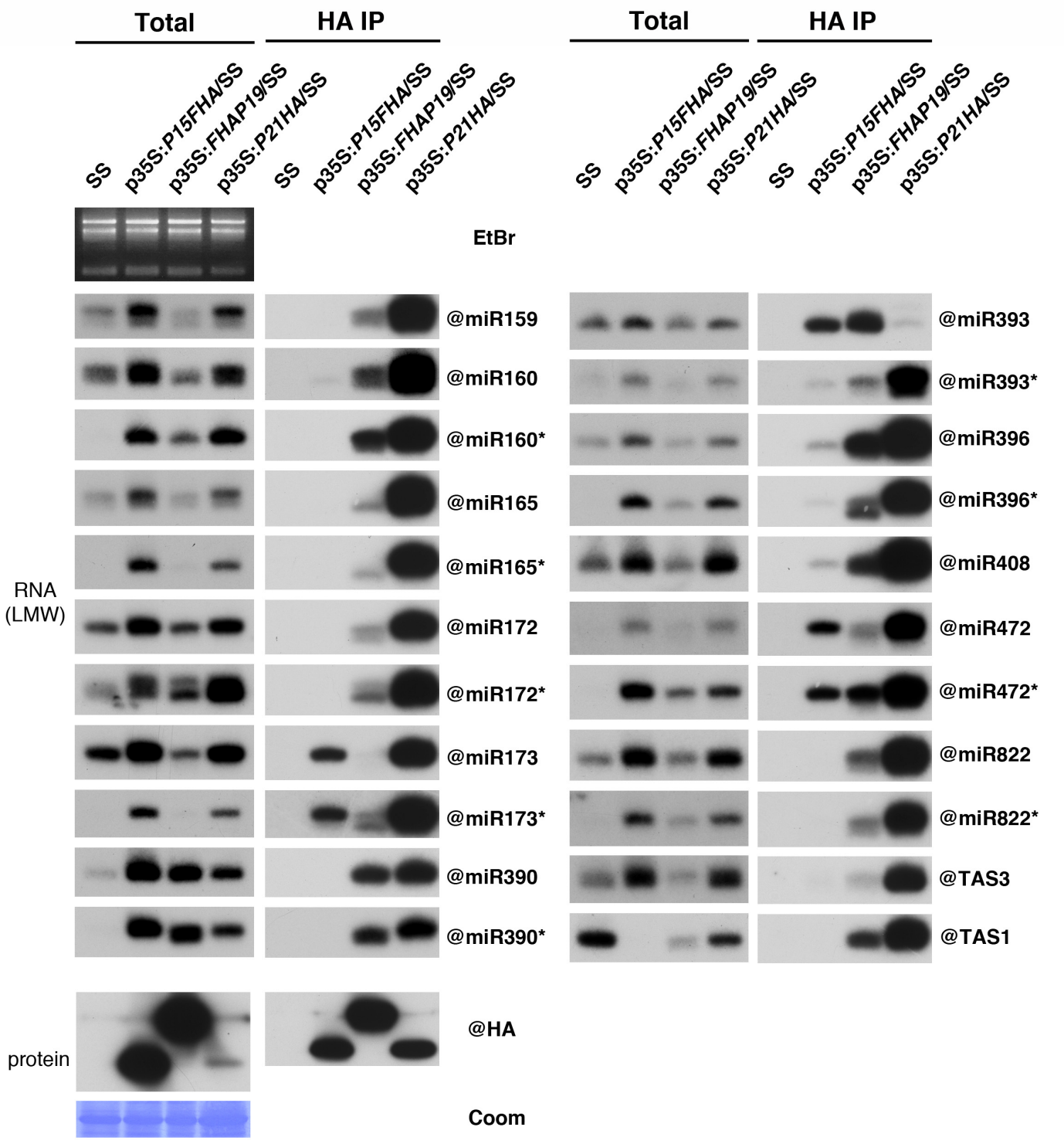

Figure S3: association of P15FHA to different small RNAs and their passenger strands.
Total: further probing of the Northern blots shown in Fig. 1.3 to reveal the accumulation of various small RNA and their passenger strands in total extracts. Note that the blots shown for total RNA, as the protein analysis, are the same as Fig.1.3 and/or Fig. S2, with additions. See Fig. 1.3 for total protein analysis. The p35S:*P21HA*/SS lane here present was not included in Fig. 1.3 for the sake of simplicity. HA IP: co-IPed RNA from IP performed on the same seedlings used in Fig. 1.3 and the total RNA of this figure. This experiment is independent from the @HA IPed RNA shown in Fig. 1.5.

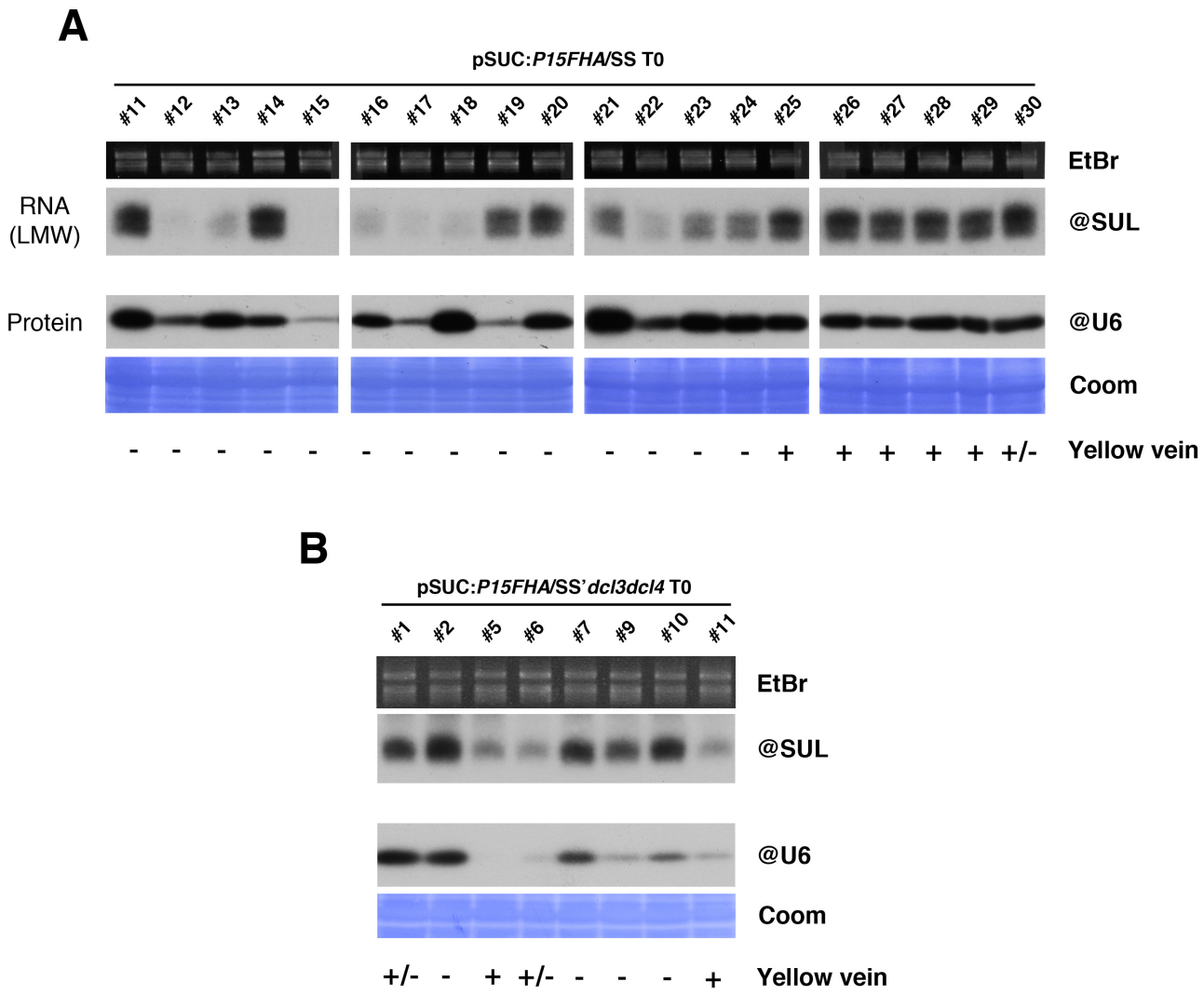

Figure S4: P15FHA protein accumulation, anti-*SUL* siRNA accumulation and presence/absence of yellow vein phenotype in pSUC:*P15FHA* primary transformants (T0).
(A) LMW Northern blot analysis (top) and western blot protein analysis (bottom) of leaves harvested from rosettes of pSUC:*P15FHA* primary transformants. Below the proteins, it is indicated whether the plants showed a SS yellow vein phenotype (+), a very light phenotype (+/-), or normal green leaves (-). Note that plants #11 to #20 are on different gels than plants #21 to #30, so the apparent higher accumulation of the P15FHA protein in plants #21 to #30 is likely an artifact. The following generation of lines #14 and #26 were used for further experiments (Fig. 1.7). (B) same as in (A) but on transformed SS'*dcl3dcl4* plants. The following generation of lines #2 and #7 were used for further experiments (Fig. 1.7).

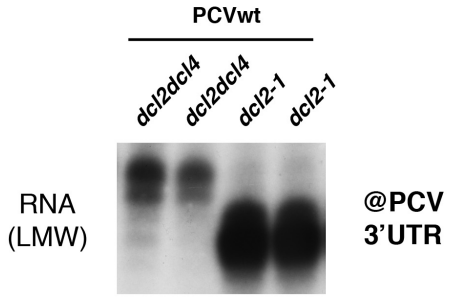

Figure S5: anti-PCV siRNA size in *dcl* knockout mutants.
LMW Northern blot analysis of total RNA from systemic leaves of PCVwt-infected plants.

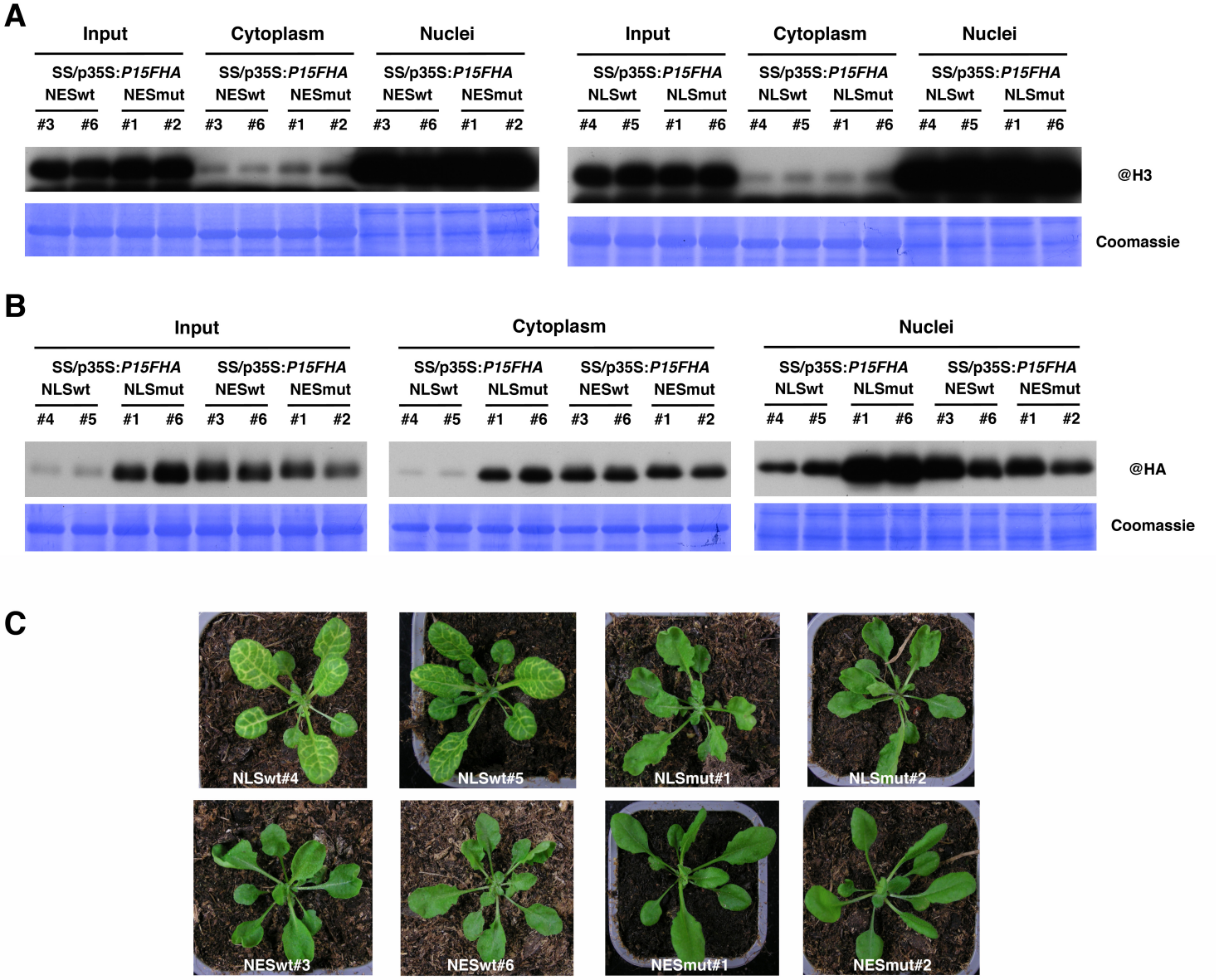

Figure S6: nuclear fractionation (performed according to Golisz *et al.*, 2013) on SS plants expressing P15FHA with NLS/NES.

(A) Western blot analysis of H3 accumulation in total, cytoplasmic and nuclear fractions. NLSwt is a functional nuclear localization signal, NLSmut is a non-functional one. NESwt is a functional nuclear exclusion signal, NESmut is non-functional. (B) As in (A), but to reveal the accumulation of P15FHANLS/NES.

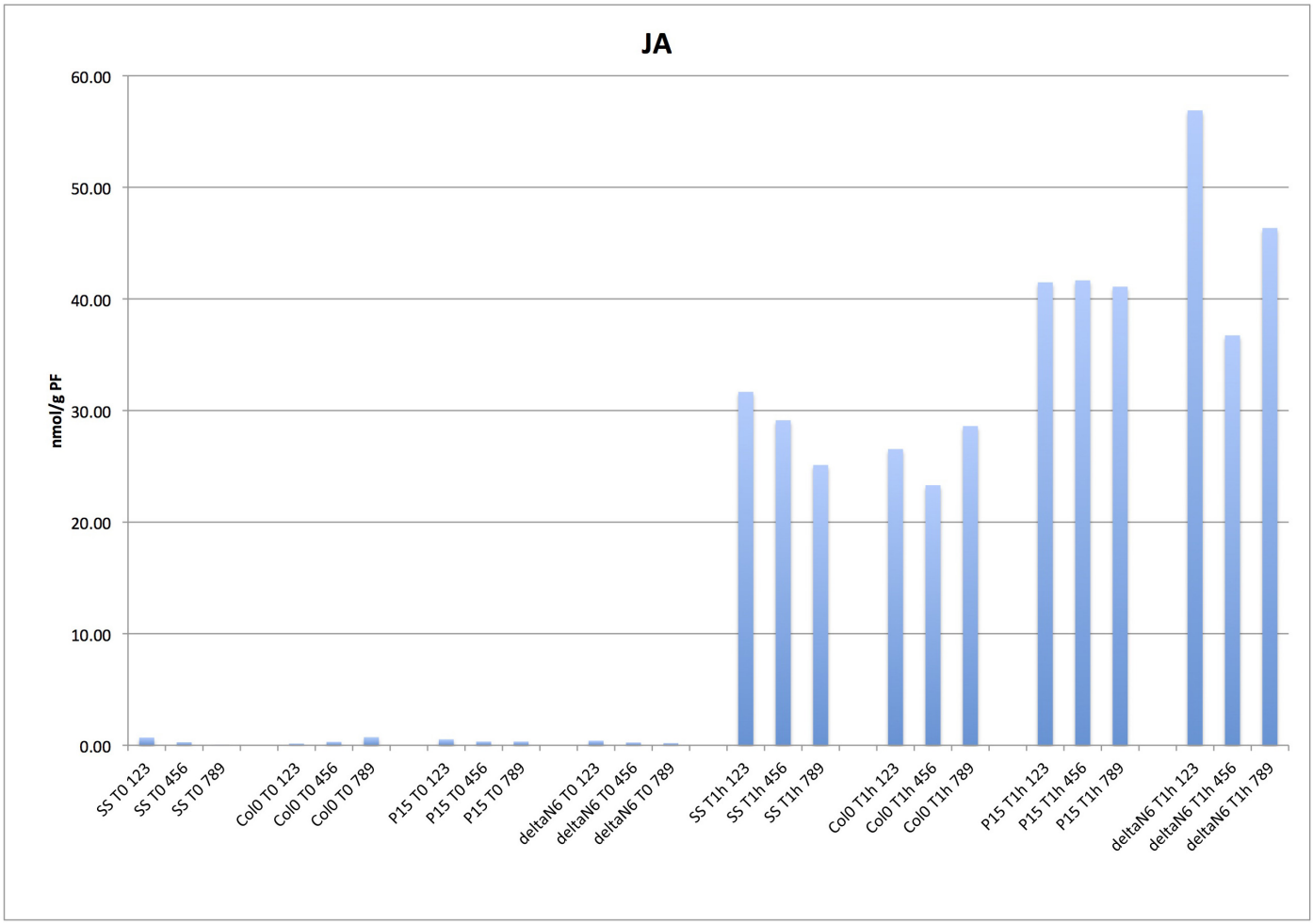

Figure S7: Jasmonic acid quantification before and after wounding, performed according to Heitz *et al.*, 2012.

Accumulation of jasmonic acid (JA) before (left) and one hour after wounding (right) of Col0, SS, p35S:*P15wt*/SS and p35S:*P15ΔN6*/SS. Expressed in nmol/g of fresh weight.

			Col0	drb4-1	DRB4FHAPX#4	DRB4FHAPX#13
EntryName	Description	MW [kDa]	# Spectra	# Spectra	# Spectra	# Spectra
AT3G62800.1	double-stranded-RNA-binding protei...	38,4			26	13
AT5G27770.1	Ribosomal L22e protein family	14			3	1
AT3G56490.1	HIS triad family protein 3, Symbol...	16			3	1
AT4G03205.2	Coproporphyrinogen III oxidase, Sy...	26,9			2	
AT1G50940.1	electron transfer flavoprotein alp...	38,4			4	2
AT3G24830.1	Ribosomal protein L13 family protein	23,4			4	3
AT5G07350.2	TUDOR-SN protein 1, Symbols: Tudor..	110			4	5
AT1G65540.1	LETM1-like protein	83,5			3	2
AT1G80230.1	Rubredoxin-like superfamily protein	18,6			3	1
AT2G18110.1	Translation elongation factor EF1...	25,3			3	2
AT3G20050.1	T-complex protein 1 alpha subunit,...	59,2			3	3
AT3G22110.1	20S proteasome alpha subunit C1, S...	27,5			3	3
AT3G26450.1	Polyketide cyclase/dehydrase and l...	17,8			3	1
AT4G17520.1	Hyaluronan / mRNA binding family	38,9			3	3
AT4G34450.1	coatomer gamma-2 subunit, putative..	98,4			3	3
AT5G53350.1	CLP protease regulatory subunit X,...	61,9			3	1
AT1G11650.2	RNA-binding (RRM/RBD/RNP motifs) f.	44,1			2	2
AT1G24360.1	NAD(P)-binding Rossmann-fold super..	33,5			2	2
AT3G15000.1	cobalt ion binding	42,8			2	1
AT3G22330.1	putative mitochondrial RNA helicas...	65,3			2	1
AT3G27430.2	N-terminal nucleophile aminohydrol...	29,5			2	1
AT3G53740.2	Ribosomal protein L36e family protein	12,7			2	1
AT3G54110.1	plant uncoupling mitochondrial pro...	32,6			2	3
AT3G54360.1	zinc ion binding	44,5			2	3
AT4G05020.2	NAD(P)H dehydrogenase B2, Symbols:	69,2			2	1
AT4G14160.1	Sec23/Sec24 protein transport fami...	85,3			2	2
AT4G26780.1	Co-chaperone GrpE family protein, ...	36,1			2	2
AT4G31300.2	N-terminal nucleophile aminohydrol...	25,3			2	1
AT5G02450.1	Ribosomal protein L36e family protein	12,2			2	1
AT5G23140.1	nuclear-encoded CLP protease P7, S...	26,3			2	2
AT5G23740.1	ribosomal protein S11-beta, Symbol...	17,7			2	1
AT5G40770.1	prohibitin 3, Symbols: ATPHB3, PHB3	30,4			2	1
AT5G66040.1	sulfurtransferase protein 16, Symb...	12,7			2	1
ATCG00770.1	ribosomal protein S8, Symbols: RPS8	15,5			2	1
AT1G01800.1	NAD(P)-binding Rossmann-fold super..	31,6			1	1
AT1G04420.1	NAD(P)-linked oxidoreductase super...	46,4			1	1
AT1G14610.1	valyl-tRNA synthetase / valine--tR...	125,8			1	3
AT1G16700.1	Alpha-helical ferredoxin	25,4			1	1
AT1G26880.1	Ribosomal protein L34e superfamily...	13,7			1	2
AT1G30630.1	Coatomer epsilon subunit	32,6			1	1
AT1G42550.1	plastid movement impaired1, Symbol.	93,8			1	1
AT1G51390.1	NFU domain protein 5, Symbols: NFU..	30			1	1
AT1G69620.1	ribosomal protein L34, Symbols: RPL34	13,6			1	1
AT1G80380.2	P-loop containing nucleoside triph...	51			1	2
AT2G18040.1	peptidylprolyl cis/trans isomerase...	13			1	1
AT2G25450.1	2-oxoglutarate (2OG) and Fe(II)-de...	40,3			1	2
AT2G41100.1	Calcium-binding EF hand family pro...	36,8			1	1
AT3G15450.1	Aluminium induced protein with YGL...	27,7			1	2
AT3G51160.1	NAD(P)-binding Rossmann-fold super..	41,9			1	3
AT3G53990.1	Adenine nucleotide alpha hydrolase...	17,8			1	1
AT3G54210.1	Ribosomal protein L17 family protein	23,5			1	1
AT4G02450.1	HSP20-like chaperones superfamily ...	25,5			1	2
AT4G17100.2	unknown protein	49,9			1	1
AT4G39460.1	S-adenosylmethionine carrier 1, Sy...	34,8			1	1
AT5G12040.1	Nitrilase/cyanide hydratase and ap...	40,3			1	1
AT5G23540.1	Mov34/MPN/PAD-1 family protein	34,3			1	1
AT5G44730.2	Haloacid dehalogenase-like hydrola...	28,8			1	1
AT5G47770.1	farnesyl diphosphate synthase 1, S...	44,2			1	1
AT5G56710.1	Ribosomal protein L31e family protein	13,8			1	2
AT5G65400.1	alpha/beta-Hydrolases superfamily ...	28,1			1	1
ATCG00380.1	chloroplast ribosomal protein S4, ...	23,2			1	1
ATCG00750.1	ribosomal protein S11, Symbols: RPS11	15			1	1

Figure S8: mass spectrometry analysis of proteins from peroxisome isolates of p35S:*DRB4FHAPX/drb4-1* plants.

List of peptides retrieved only in peroxisomes of plants expressing DRB4FHAPX (see Fig. 3.1 for western analysis).

		SS/P19#2	SS/P19#8	SS/P19PX#2
EntryName	Description	# Spectra	# Spectra	# Spectra
P19PX	P19PX			18
AT3G08530.1	Clathrin, heavy chain			4
AT5G20070.1	nudix hydrolase homolog 19, Symbol...			4
AT5G59880.1	actin depolymerizing factor 3, Sym...			4
AT4G02520.1	glutathione S-transferase PHI 2, S...			3
AT3G03250.1	UDP-GLUCOSE PYROPHOSPHORYLASE 1, S...			3
AT3G48730.1	glutamate-1-semialdehyde 2,1-amino...			3
AT2G27530.1	Ribosomal protein L1p/L10e family,...			3
AT2G40010.1	Ribosomal protein L10 family protein			3
AT3G22110.1	20S proteasome alpha subunit C1, S...			2
AT3G45030.1-AT5G62300.1	Ribosomal protein S10p...			2
AT5G65010.2	asparagine synthetase 2, Symbols: ...			2
ATCG00350.1	Photosystem I, PsaA/PsaB protein, ...			2
AT4G20890.1	tubulin beta-9 chain, Symbols: TUB9			2
AT3G48990.1	AMP-dependent synthetase and ligas...			2
AT1G17290.1	alanine aminotransferas, Symbols: ...			2
AT5G44340.1	tubulin beta chain 4, Symbols: TUB4			2
AT5G25590.1	Protein of unknown function (DUF63...			2
AT2G42600.2	phosphoenolpyruvate carboxylase 2,...			2
AT1G30520.1	acyl-activating enzyme 14, Symbols...			2
AT5G48545.1	histidine triad nucleotide-binding...			2
AT1G79810.1	Pex2/Pex12 N-terminal domain-conta...			2
AT1G07770.1-AT5G59850.1	ribosomal protein S15A...			2
AT1G19550.1	Glutathione S-transferase family p...			2
AT1G78380.1	glutathione S-transferase TAU 19, ...			2
AT1G55860.1	ubiquitin-protein ligase 1, Symbol...			2
AT1G78680.1	gamma-glutamyl hydrolase 2, Symbol...			1
AT1G04480.1-AT2G33370.1-AT3G04400.1	Ribosomal ...			1
AT1G79040.1	photosystem II subunit R, Symbols:...			1
AT1G17260.1	autoinhibited H(+)-ATPase isoform ...			1
AT5G51150.1	Mitochondrial import inner membran...			1
AT4G34150.1	Calcium-dependent lipid-binding (C...			1
AT1G65520.1	delta(3), delta(2)-enoyl CoA isome...			1
AT2G37170.1	plasma membrane intrinsic protein ...			1
AT1G56410.1	heat shock protein 70 (Hsp 70) fam...			1

Figure S9: mass spectrometry analysis of proteins from peroxisome isolates of p35S:*P19HAPX*/SS plants.

List of peptides retrieved only in peroxisomes of plants expressing P19HAPX (see Fig. 3.3 for western and Norhtern analysis). The small amount of P19PX detected in peroxisomal isolates, coupled to the relative abundance of small RNA, suggests that P19PX may degraded following peroxisomal import.

Annex 2

Summary of the thesis in French.

Résumé de la thèse en français.

Résumé de these

Chez les plantes et les invertébrés, le RNA silencing, tout en jouant un rôle crucial dans la régulation des gènes au cours du développement et dans la maintenance de l'intégrité du génome, est le principal mécanisme de défense antivirale. La séquence-spécificité de ce mécanisme est opérée par de petites molécules d'ARN de 21 à 24nt (short-interfering ARN, siARN) qui sont produites par l'action d'enzymes de type RNaseIII appelées Dicer, ou Dicer-like chez les plantes, à partir de substrats ARN double brin (ARNdb). La grande majorité des virus qui infectent ces organismes possèdant un génome à ARN, les ARNdb responsable de l'activation de la machinerie cellulaire du RNA silencing antiviral proviennent soit d'intermédiaire de réplication du génome viral, soit de structures intramoléculaires arborant un haut degré de complémentarité qui sont présentes intrinsèquement dans les ARN viraux. Parmi les quatre DCLs codées par le génome de la plante modèle *Arabidopsis thaliana*, DCL4 est le Dicer antiviral principal et produit les siARN de 21nt dérivant des génomes viraux (virus-derived siARN, vdsiARN), qui s'accumulent majoritairement au cours de l'infection d'une plante sauvage. En réponse à l'inactivation de DCL4, DCL2 prend en charge le silencing antiviral en produisant des vdsiARN de 22nt, qui sont normalement sous le seuil de détection, indiquant son rôle de substitution à DCL4 dans la défense antivirale. Une fois produit, les vdsiARN vont être incorporés dans un complexe multi-protéique nommé RISC (RNA-induced silencing complex), contenant AGO1 ou AGO2, les deux protéines ARGONAUTE antivirales principales chez *Arabidopsis*, et serviront de guide à ce complexe pour lui permettre d'induire le clivage ou l'inhibition de traduction de tout ARN homologue à l'ARN viral initiateur. De plus, les plantes ont développé un mécanisme permettant l'amplification de cette réponse antivirale. Cette amplification repose sur l'action d'ARN polymérase ARN-dépendante (RDR) qui vont convertir de l'ARN viral simple brin en ARNdb, entrainant la production par DCL4 de vdsiARN dit secondaires, qui pourront également être incorporés dans AGO1/AGO2 entrainant un renforcement des réactions de défense. En plus de cet aspect dit « cellule-autonome » ou intracellulaire, un aspect spectaculaire du RNA silencing chez les plantes est sa nature systémique. Activé localement dans une feuille, il peut se propager à travers toute

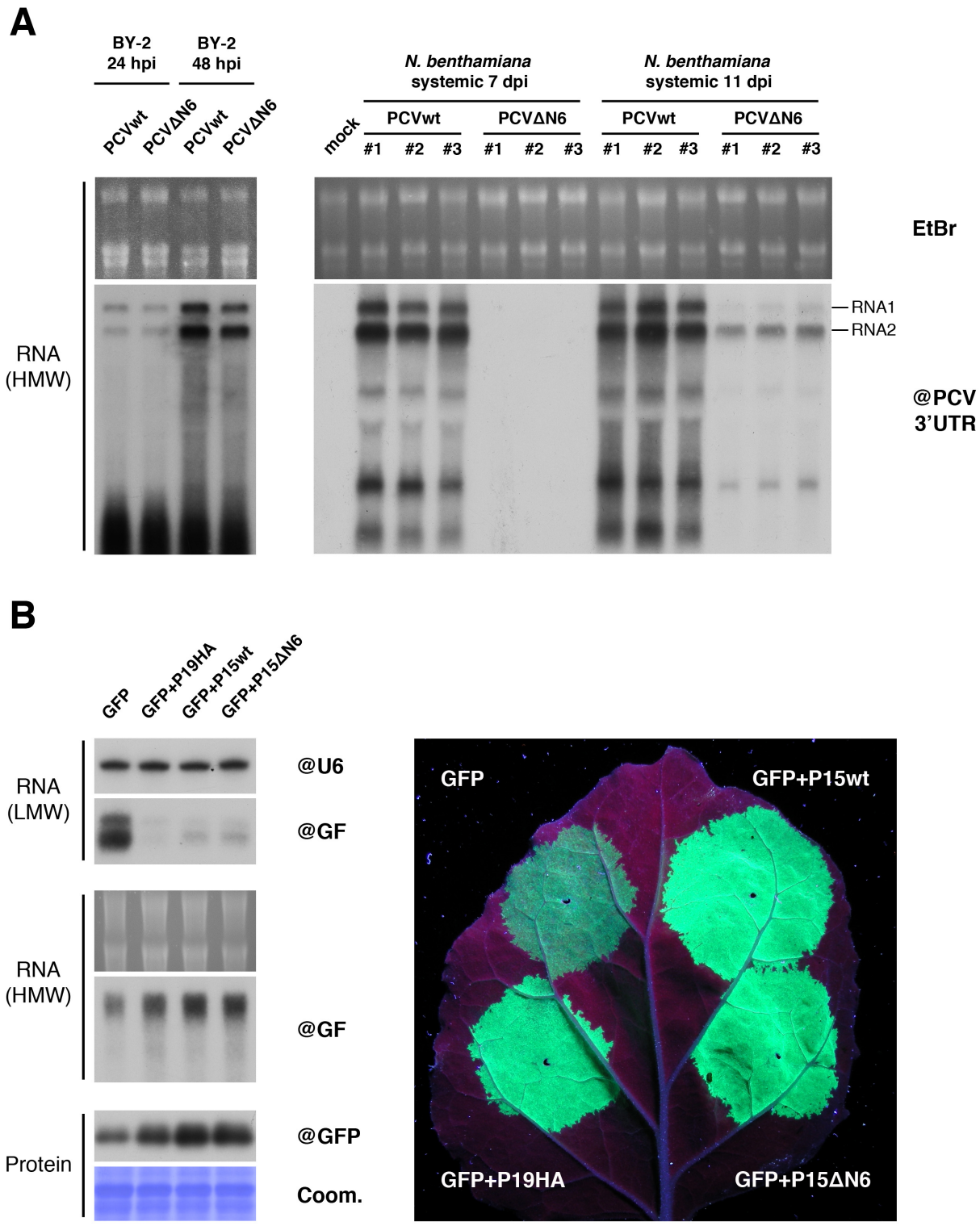

Figure 1: Effet de la localisation peroxysomale de P15 sur l'efficacité de l'infection par le PCV et la suppression du RNAi intracellulaire. Figure 2.1 de la thèse.
(A) Analyse de l'accumulation des ARN viraux dans des protoplastes de BY-2 (cellules isolées) ou des feuilles systémiques après infection par le PCV sauvage (wt) ou le PCVΔN6. hpi: hours post-infection; dpi: days post-infection. La sonde PCV 3'UTR révèle les deux ARN génomiques (RNA1 et RNA2) et les ARN sub-génomiques (sgRNA). (B) Expression transitoire dans N. benthamiana d'un transgène codant pour la GFP, seul ou en combinaison avec P19HA, P15wt ou P15ΔN6. A gauche: analyse par Northern blot de l'accumulation de l''ARNm GFP (HMW: High molecular weight) ou des siARN GFP (LMW: Low molecular weight) extraits des tissus agroinfiltrés, et analyse par western blot des protéines correspondantes. A droite: photo d'une feuille agroinfiltrée sous lumière UV pour révéler l'accumulation de la GFP.

la plante en empruntant les plasmodesmes pour son transport intercellulaire et les canaux du phloème pour son mouvement à longue distance. La molécule signal assurant la propagation « non-cellule autonome » du RNA silencing est constituée de siARN qui confèrent la spécificité de séquence de ce mécanisme. Cette composante systémique fait probablement partie intégrante de la fonction antivirale du RNA silencing. En effet, produit dans une lésion locale au cours de la réplication du virus, les vdsiARN vont pouvoir se propager dans des tissus éloignés des zones virosées, les prémunissant ainsi contre l'infection à venir. Cependant, bien que le mouvement des siARN soit clairement établi, les expériences démontrant de manière non-ambiguë l'importance de cet aspect non-cellule autonome, au cours de la défense antivirale, demeurent rares.

Afin de se prémunir contre cette réaction de défense, les virus codent pour des protéines capables de supprimer le RNA silencing à des étapes très variées. Le mode d'action de ces suppresseurs viraux du RNA silencing (Viral Suppressor of RNA silencing, VSR) varie de la séquestration des siARN, empêchant ainsi leur incorporation dans le complexe RISC, à l'inhibition ou la déstabilisation de facteurs clés du RNA silencing antiviral (revue dans Incarbone & Dunoyer, 2013, Trends in Plant Science). Caractériser le mode d'action de ces VSR est une étape cruciale pour notre compréhension global du cycle viral ainsi que pour permettre le développement de moyens de lutte adaptés contre les différents phytovirus. Au cours de ma thèse, je me suis intéressé à la protéine P15 du Peanut clump virus (PCV), dont le mode d'action en tant que VSR était totalement inconnu. De plus cette protéine possède un signal fonctionnel d'adressage aux peroxysomes (Peroxysomal targeting signal 1, PTS1) qui, bien que non requis à sa fonction de suppresseur de RNA silencing intracellulaire, semble nécéssaire au mouvement systémique du PCV (Figure 1). L'objectif de cette thèse était donc, d'une part, de caractériser la stratégie de suppression du RNA silencing de P15 (chapitre 1), et d'autre part de déterminer en quoi sa localisation peroxysomale autorisait la propagation systémique du PCV (chapitre 2).

Afin d'étudier le mode d'action de P15 comme suppresseur de silencing, nous avons dans un premier temps généré des plantes transgéniques exprimant sous contrôle d'un promoteur ubiquitaire (35S) une version étiquetée fonctionnelle de cette protéine (P15HA),

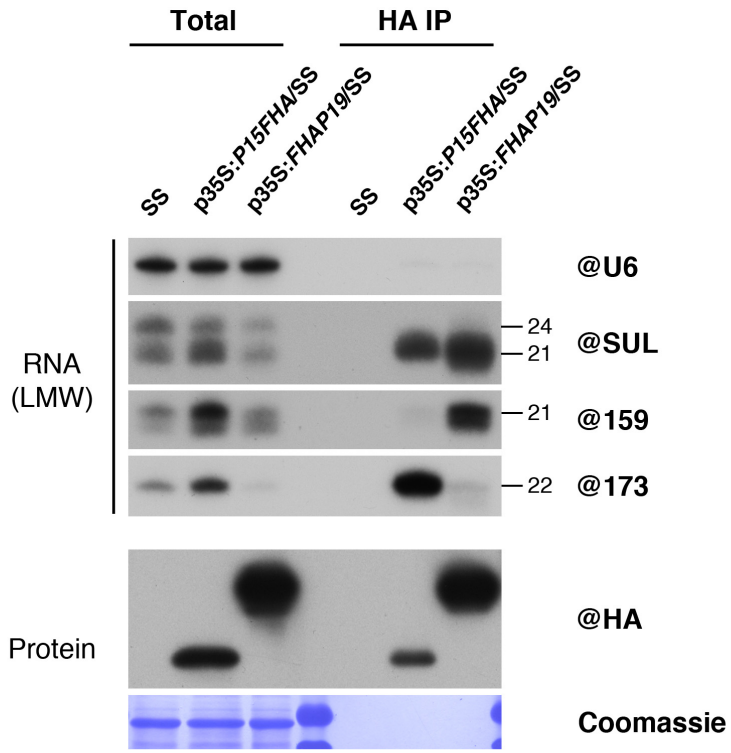

Figure 2: Association de P15FHA aux petits ARNs. Figure 1.5 de la these.
Analyse de l'accumulation de différentes espèces de petits ARN (en haut) dans les extraits totaux (gauche) de plantules transgéniques ou provenant des immunoprecipitations de la P15FHA ou de la FHAP19 (droite). L'analyse par Western blot (en bas) révèle la présence des protéines immunoprécipitées à partir des extraits totaux.

dans le système rapporteur SUC-SUL. Dans ce système, un transgène induit le silencing d'un gène endogène (SUL), qui se traduit par l'apparition d'une chlorose au niveau des cellules compagnes du phloème (où il est exprimé par le promoteur SUC), ainsi que dans les 10-15 cellules adjacentes (grâce au mouvement des siARN). L'analyse moléculaires par northern blot de ces plantes transgéniques (35S-P15HA/SUC-SUL) a permis de mettre en évidence que l'expression de P15 inhibait complétement l'apparition de la chlorose, sans pour autant avoir un impact sur l'accumulation des siARN SUL, écartant l'hypothèse d'un effet de P15 sur la biogénèse ou la stabilté des siARN comme stratégie de suppression du RNA silencing. A l'inverse, des expériences d'immunoprécipitation de P15 (Figure 2), ou des protéines AGO1 et AGO2, ont permis de révéler que P15 supprimait le RNA silencing intracellulaire en séquestrant les siARN, empêchant ainsi leur incorporation dans les deux protéines ARGONAUTE antivirales principales d'*Arabidopsis*. Une analyse moléculaire plus exhaustive dans différents fonds mutants a également permis de mettre en évidence que, bien que capable de fixer les siARN de 21nt produit de DCL4, P15 semble avoir une bien meilleure affinité pour les siARN de 22nt produit par DCL2.

Nous nous sommes ensuite demandé si P15 était également capable de bloquer le mouvement de cellule-à-cellule des siARN. Pour répondre à cette question *in planta*, nous avons réalisé des expériences de suppression du RNA silencing cellule-spécifique en exprimant P15HA sous contrôle du promoteur SUC (SUC-P15HA/SUC-SUL). L'expression de P15 spécifiquement au niveau des cellules compagnes (CC) du phloème, comme cela a pu être vérifié par immunolocalisation, a, là aussi, conduit à la disparition du phénotype chlorotique. Ces mêmes expériences réalisées dans différents fonds mutants, couplées à l'analyse des niveaux de P15 présent dans ces lignées transgéniques et des siARN immunoprécipités par ce VSR, a permis de mettre en évidence que, comme dans le cas du RNA silencing intracellulaire, P15 était capable d'inhiber de manière dose-dépendant le RNA silencing non-cellule autonome en séquestrant les siARN produit dans les CC du phloème, empêchant ainsi leur propagation aux cellules adjacentes (Figure 3). Une fois de plus, ces expériences ont révélé que P15 présentait une meilleure affinité pour les siARN de 22nt par rapport à ceux de 21nt. Afin de comprendre la raison de cette plus forte affinité de P15 pour les siARN de 22nt, nous avons voulu déterminer la taille des vdsiARN s'accumulant au cours d'une infection par le PCV. Après avoir établi les conditions

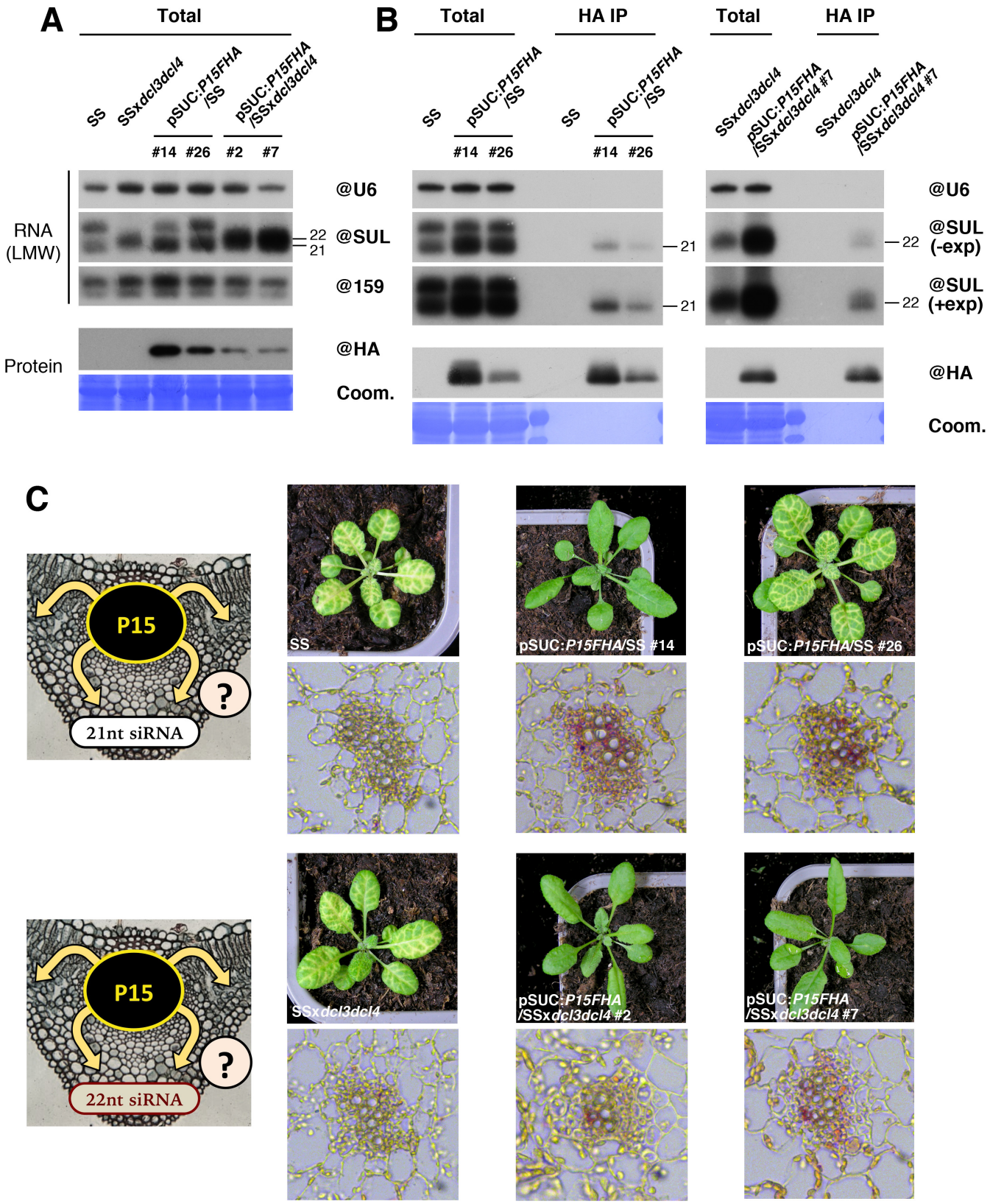

Figure 3: Effet de P15FHA sur le movement cellule-à-cellule des siARN de 21nt et 22nt. Figure 1.7 de la these.

(A) Analyse par Northern blot de l'accumulation de différentes espèces de petits ARN (haut) et par Western blot de la protéine P15FHA (bas), à partir d'extraits totaux de feuilles provenant des lignées transgéniques indiquées. (B) Comme dans (A) mais incluant les IP anti-HA réalisées à partir des tissus correspondants. (C) A gauche: représentation schématique du système expérimental, consistant en la production de P15FHA dans les mêmes cellules où sont produits les siARN anti-*SUL*. A droite: photos des plantes au moment de la récolte, et immunolocalisation de la P15FHA dans des coupes transversale de feuilles provenant de ces mêmes plantes

optimales d'infection de ce virus sur *Arabidopsis thaliana*, nous avons pu constater que, contrairement à ce que l'on pouvait observer au cours d'infection par d'autres types de phytovirus, où la vaste majorité des vdsiARN étaient de 21nt, l'infection par le PCV conduit à une très grande proportion de vdsiARN de 22nt, malgré des niveaux de DCL4 inchangé. Bien que les raisons de ce pattern d'accumulation particulier de vdsiARN restent à déterminer, ces observations suggèrent fortement une adaptation évolutive de P15 pour fixer plus efficacement les siARN majoritairement produit au cours de l'infection par le PCV. Pour conclure ce chapitre, nous avons également cherché à identifier les interacteurs protéiques potentiels de P15 au sein de la cellule. Pour cela des expériences d'immunoprécipitation (IP) de ce VSR, couplées à une analyse par spectrométrie de masse ont été réalisées en collaboration avec P. Hammann (Plateforme protéomique de l'Esplanade, IBMC), mais n'ont malheureusement pas permis de mettre en évidence des candidats fiables, présents de manière reproductible, dans les fractions IP.

Dans un deuxième temps, nous nous sommes intéressés au rôle de la localisation peroxysomale de P15 dans l'infection systémique des plantes par le PCV. Les peroxysomes sont des organites intracellulaires qui jouent un rôle clé dans de nombreuses voies enzymatiques cellulaires. Ne possèdant ni génome, ni machinerie de traduction, l'ensemble des protéines peroxysomales sont importées à partir du cytoplasme grâce à des récepteurs spécialisés (PEX5p dans le cas des protéines possédant un PTS1). Contrairement aux autres organites (mitochondries, chloroplastes) les peroxysomes ont la capacité d'importer, dans leur matrice, des protéines et des oligomères sous forme native. De plus, des protéines possédant un signal d'adressage aux peroxysomes peuvent emmener avec elle les facteurs qui lui sont associés. Au vue de ces propriétés, nous nous sommes alors demandé si l'effet de la localisation peroxysomale de P15 sur le mouvement systémique du PCV n'était pas lié à l'import dans la matrice des peroxysomes d'un facteur de défense de la plante interagissant avec P15. Une fois importée dans les peroxysomes, ce facteur deviendrait incapable de remplir sa fonction, permettant ainsi le mouvement du virus. Pour répondre à cette question, nous avons dans un premier temps dû acquérir la technique de purification des peroxysomes auprès d'un expert dans ce domaine, le Pr. Sigrun Reumann de l'université de Stavanger (Norvège). Une fois cette technique maitrisée, les peroxysomes de plantes

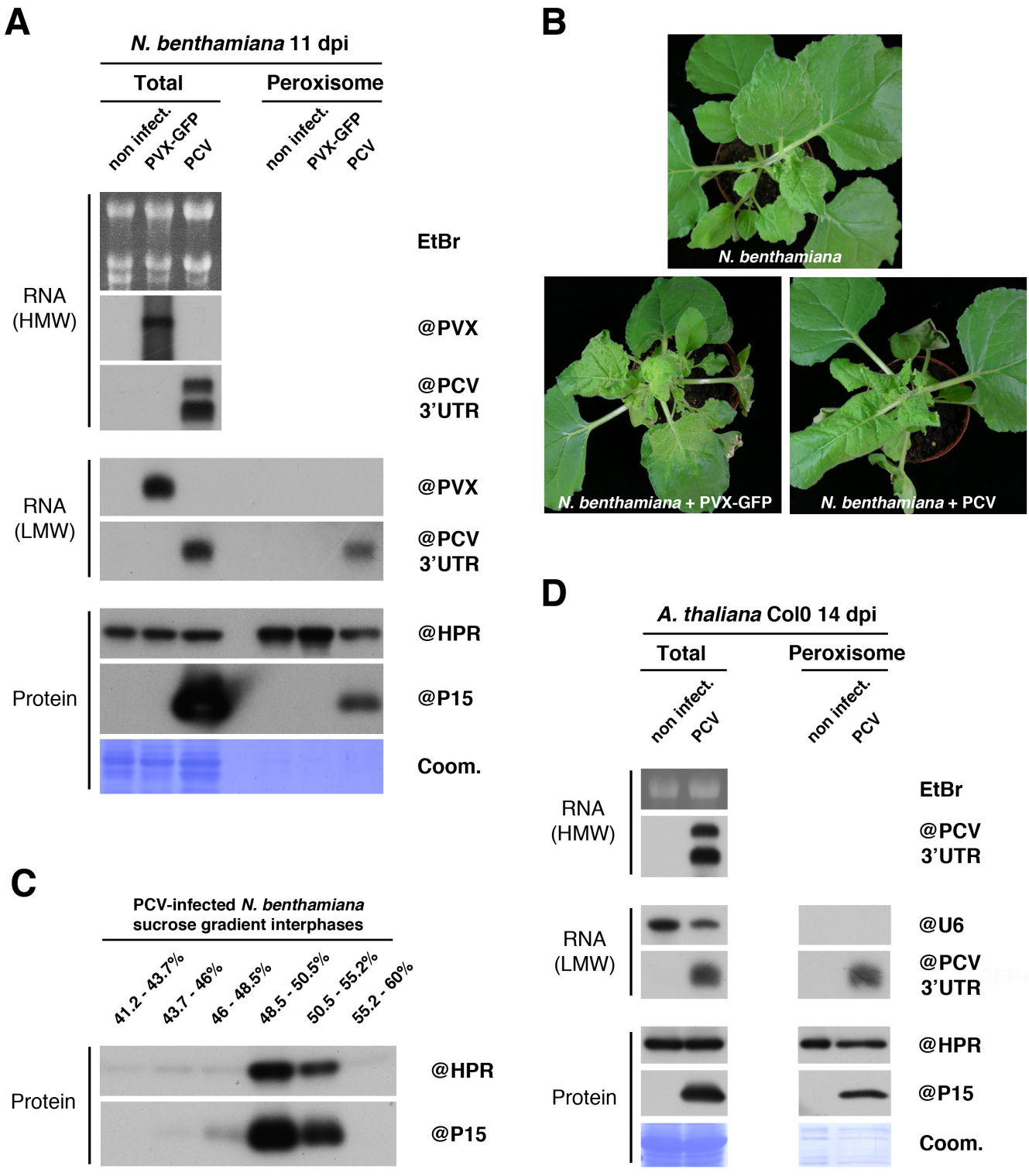

Figure 4: Analyse des peroxisomes isolés à partir de plantes infectées par le PCV. (Figure 2.4 de la these)

(A) Analyse de l'accumulation des ARN viraux, des petits ARN antiviraux et des protéines à partir de fractions totale (gauche) et peroxisomale (droite) extraits des feuilles systemiques de *N. benthamiana* infectées par PVX-GFP, par PCV, ou non infectées. (B) Photos des plantes analysées en (A). (C) Analyse par Western blot de protéines extraites de six interphases collectées du gradient discontinu de saccharose après l'étape d'ultracentrifugation finale d'isolation de peroxisomes. (D) comme dans (A), mais sur feuilles systémiques d'*A. thaliana* non infectées ou infectées par le PCV.

transgéniques exprimant constitutivement la protéine P15 sauvage (P15wt), ou muté dans son signal d'adressage aux peroxysomes (P15ΔN6), ont été isolés et leurs contenus protéiques analysés par spectrométrie de masse. Bien que cette analyse ait permis de mettre en évidence l'import dans la matrice des peroxysomes uniquement de la version sauvage de P15, elle n'a pas permis de révéler l'enrichissement (ou la présence exclusive) d'un facteur cellulaire spécifique, corrélé à la présence de ce VSR. Ces résultats excluant la possibilité d'un facteur de défense protéique importé dans les peroxysomes par P15, nous avons alors cherché à déterminer si ce facteur ne pouvait pas être de nature nucléique. L'analyse par northern blot des ARN extrait des peroxysomes a permis de mettre en évidence l'import de vdsiARN uniquement en présence de P15wt. Ces résultats ont également pu être confirmé en contexte naturel d'infection par le PCV, suggérant qu'au cours de l'infection P15 importe dans la matrice des peroxysomes les vdsiARN auquels elle est fixé (Figure 4). En les isolant ainsi du symplasme, P15 empêche ces siARN de se propager aux cellules adjacentes et, de ce fait, inhibe la mise en place du silencing antiviral non-cellule autonome permettant ainsi le mouvement systémique optimal du PCV. Cette stratégie de séquestration des vdsiARN dans un organite pourrait permettre à ce VSR de compenser son affinité plus faible pour les siARN de 21nt produit par DCL4, en arrêtant efficacement leur mouvement. Afin de tester cette hypothèse, des plantes mutées pour DCL4 ont été infectées par le PCV codant soit pour la P15 sauvage soit pour la P15ΔN6 (PCVΔN6, incapable de se propager systémiquement). L'analyse moléculaire de ces plantes a permis de mettre en évidence que le mouvement systémique de PCVΔN6 était restauré, à un niveau proche du PCV sauvage, dans les plantes incapables de produire les siARN de 21nt, confirmant ainsi notre hypothèse. Des expériences complémentaires ont également permis de montrer que l'import dans les peroxysomes des vdsiARN de 22nt (pour lesquels P15 a une forte affinité) n'était, lui, pas nécessaire au mouvement systémique du PCV (Figure 5).

Collectivement, ces résultats démontrent une stratégie nouvelle de suppression du RNA silencing définie par la P15 du PCV qui, d'une part séquestre efficacement les vdsiARN de 22nt de part sa forte affinité pour cette taille de siARN et, d'autre part, empêche le RNA silencing non-cellule autonome opéré par les siARN de 21nt en utilisant sa capacité à les importer au sein des peroxysomes. L'ensemble de ces résultats a été réuni au sein d'un

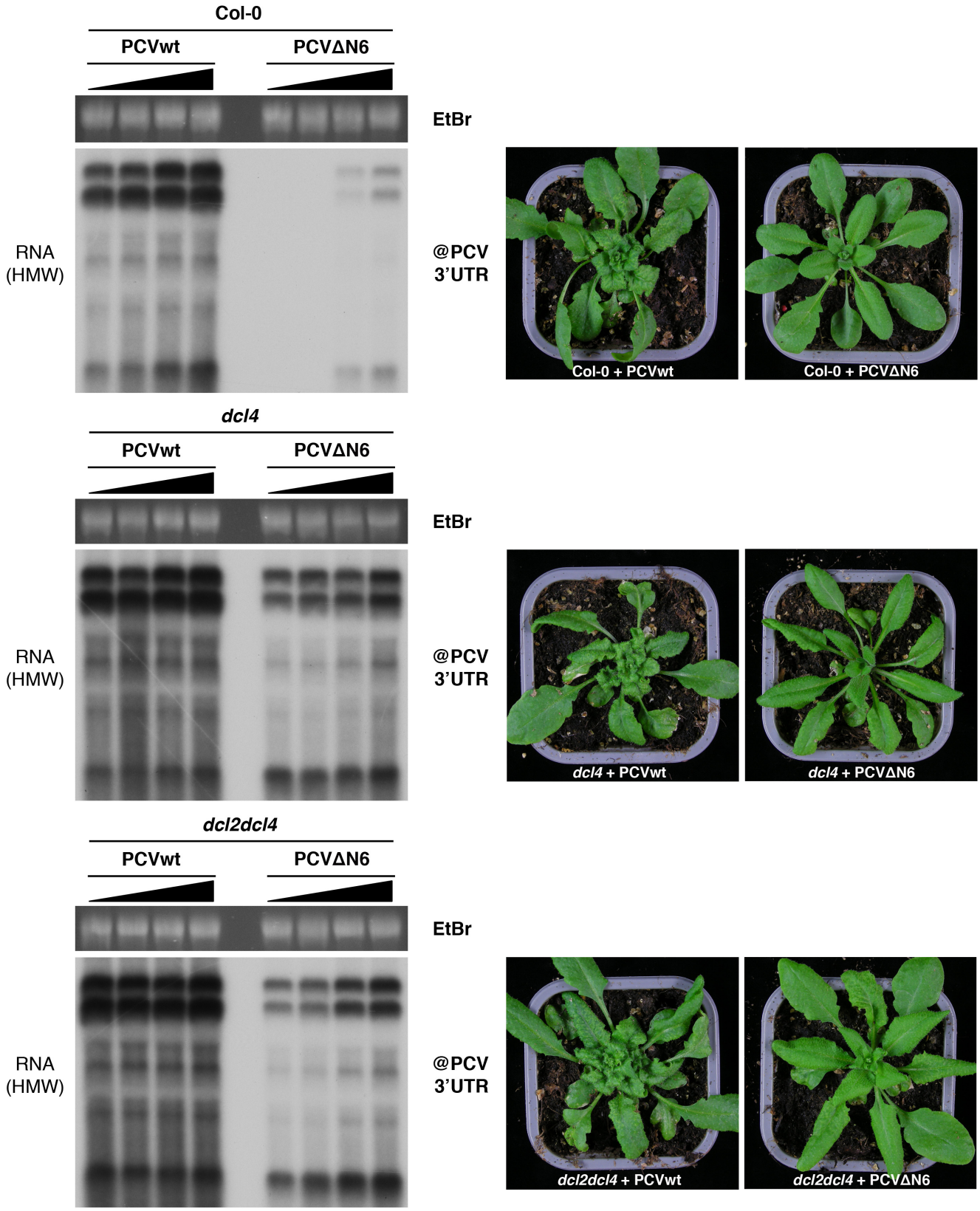

Figure 5: Impact sur le mouvement systémique du PCV de l'import des siARN dans les peroxisomes. (Figure 2.6 de la thèse)

A gauche: Analyse par Northern blot de l'accumulation des ARN viraux du PCV dans des feuilles systémiques de Col-0, *dcl4* et *dcl2dcl4* infectées par le PCVwt ou le PCVΔN6. Sur les 15 plantes infectées pour chaque combinaison virus/génotype, 4 individus sont ici montrés couvrant la gamme des titres viraux observés lors d'une analyse préliminaire de l'ensemble de ces plantes. A droite: photos des plantes au moment de la récolte. Les échantillons présentés sur ces Northern blots ont été chargés dans une disposition différente sur la Figure 4 du manuscrit présenté en Annexe 4.

manuscrit qui va être soumis fin Juin 2016 pour publication et ont également fait l'objet d'une communication lors d'un congrès.

Alors que les expériences d'immunoprécipitation ont exclu une interaction significative entre les miARN de 21nt et P15, les expériences d'isolement des peroxysomes ont clairement révélé que P15 est capable d'importer les miARN de 21nt au sein de ces organites. Cette observation suggère que l'interaction entre les miARN de 21nt et P15 est conservée pendant le processus de transport vers les peroxysomes, et à travers leurs membranes, et que cette interaction est largement perturbée ou éliminée au cours de la procédure d'immunoprécipitation. Par conséquent, l'analyse des ARN importés par P15 dans les peroxysomes a fourni plus d'information comparée à l'analyse des ARN associés à P15FHA lors d'une immunoprécipitation. Nous avons décidé d'explorer la possibilité d'utiliser l'envoi d'une protéine d'intérêt dans les peroxysomes *in planta*, suivi par une analyse moléculaire des peroxysomes isolés à partir de ces plantes, comme un outil expérimental pour découvrir les interactions qui peuvent être perdus au cours des expériences d'immunoprécipitation. Pour ce faire, nous avons ajouté un PTS1 à deux protéines endogènes (DRB4 et AGO2) ainsi qu'à deux suppresseurs de silencing (P38 et P19). Bien que les expériences avec DRB4, AGO2 et P38 n'ont pas donné des résultats prometteurs, l'analyse moléculaire des peroxysomes isolés à partir des plantes exprimant P19 avec un PTS1, ont fourni des résultats très intéressants. De nombreuses expériences dans plusieurs laboratoires ont montré une affinité forte et specifique de cette protéine pour les petites ARN de 21nt. En accord avec celles-ci, des nombreuses expériences d'immunoprécipitation réalisées au cours de cette thèse ont montré une interaction entre P19 et des petits ARN de 21-22nt. Cependant, notre nouvelle approche expérimentale d'analyse des peroxysomes a révélé que P19 est capable d'importer dans ces organites non seulement les petits ARNs de 21-22nt, mais aussi d'importantes quantités de petits ARN de 24nt. Ces résultats suggèrent que P19 est capable d'interagir *in vivo* avec des petits ARN de 24nt, et que cette approche expérimentale peut permettre l'identification d'interactions qui peuvent être perdues au cours d'expériences d'immunoprécipitation.

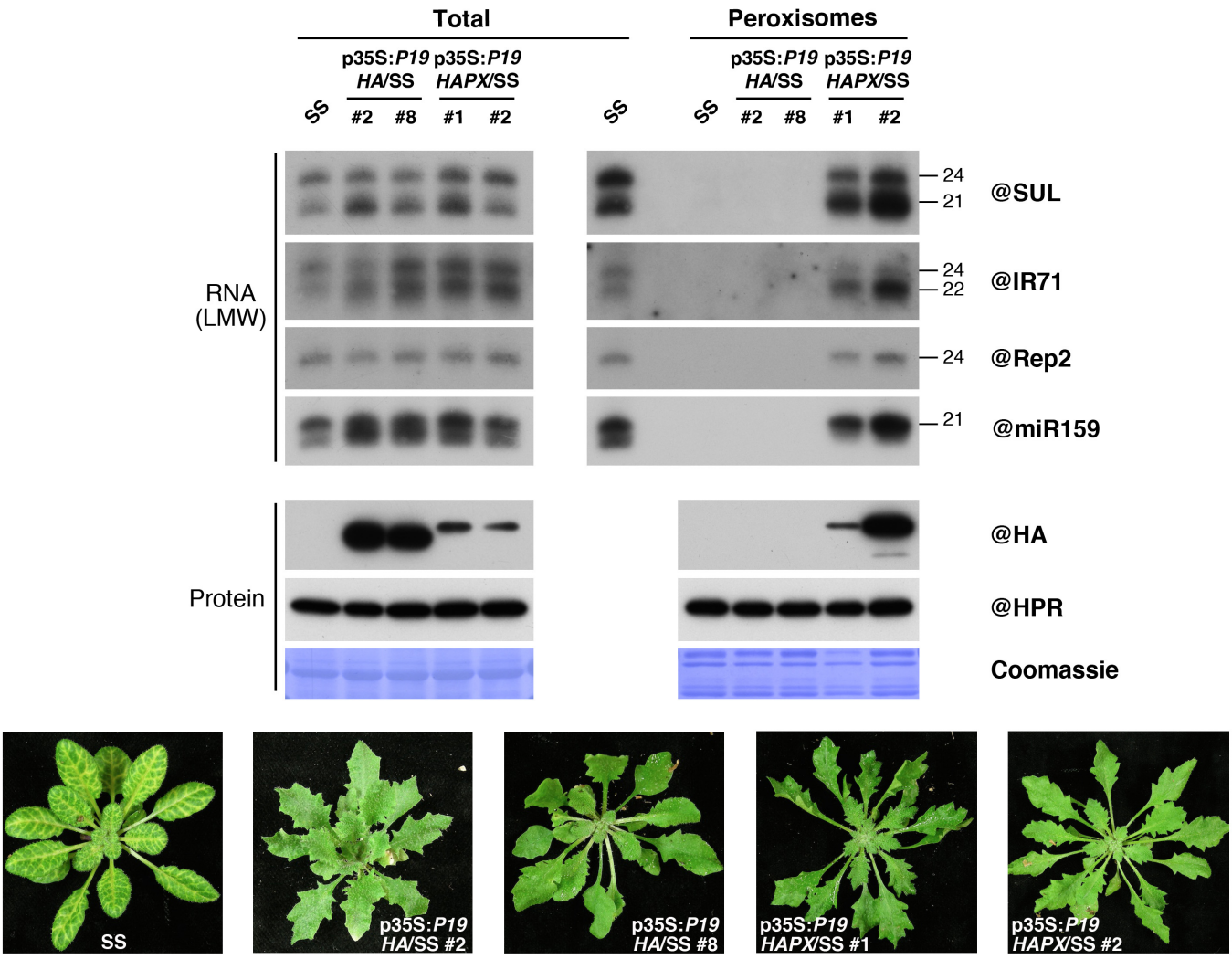

Figure 6: Importation de P19 dans les peroxysomes par l'ajout d'un PTS1 à son extrémité C-terminale. (Figure 3.3 de la these)

En haut: analyse par Northern blot de l'accumulation de différents types de petits ARN et par Western blot des protéines P19 provenant des fractions totales (à gauche) et peroxisomales (à droite) de plantes SS exprimant P19HA fusionnée (p35S:*P19HAPX*/SS) ou non (p35S:*P19HA*/SS) à un PTS1. En bas: photos des plantes au moment de la récolte.

Publication acceptée:

Incarbone M & Dunoyer P (2013). “RNA silencing and its suppression: novel insights from *in planta* analyses.” Trends in Plant Science 18; 382-392.

Publication soumise:

Incarbone M, Zimmermann A, Hammann P, Erhardt M, Reumann S, Michel F & Dunoyer P. “Neutralization of mobile antiviral small RNA through peroxisomal import.”

Communication lors d’un congrès :

Incarbone M & Dunoyer P. “P15: new insights into viral suppression of RNA silencing.” Advances in plant virology – AAB congress, Birmingham, UK, 31/3 - 2/4/2015

Annex 3

The abstract of a talk given on 1st April 2015 at the Advances in Plant Virology congress in Birmingham, UK. The congress was organized by the Association of Applied Biologists (AAB). The presentation was awarded the Bryan Harrison prize.

P15: new insights into viral suppression of RNA silencing

MARCO INCARBONE and PATRICE DUNOYER

Institut de Biologie Moleculaire des Plantes, CNRS, 12 rue du General Zimmer, 67084 Strasbourg Cedex, France

ABSTRACT

RNA silencing is the primary antiviral defence deployed by plants. It is mediated mainly by 21 and 22 nt-long siRNAs (small interfering RNAs), generated from viral double-stranded RNA by DCL4 and DCL2, respectively (in *A. thaliana*). These virus-derived siRNA are then loaded into AGO proteins, that use them as guides to recognize complementary viral RNAs and degrade them. SiRNAs have also been shown to move from cell to cell and systemically to prime a sequence-specific defence ahead of the invading virus. While the bulk of virus-derived siRNA in *A. thaliana* are DCL4-dependent 21nt-long siRNA, the smaller pool of DCL2-dependent 22nt siRNA has been suggested to be responsible for transitivity, the putative RDR-dependent amplification of the antiviral silencing reaction. Viruses have evolved a fascinating array of strategies to counter these defences, from the sequestration of siRNA to the interference with effector AGO proteins (reviewed in Incarbone and Dunoyer, 2013).

P15 is a strong suppressor of RNA silencing encoded by *Peanut Clump Virus* (PCV), a (+) polarity ssRNA virus. Interestingly, it possesses a peroxisomal localisation signal that is not required for the suppression of intracellular RNA silencing, but is indispensable for the systemic movement of the virus.

Our recent work on P15 has revealed several key facts regarding its mode of operation. P15 has highest affinity for 22 nt-long RNAs, suggesting that it may be able to suppress a putative antiviral transitivity pathway. Although P15's affinity for 21 nt RNAs is significantly lower, it still prevents the loading of these into the two main antiviral AGOs. Accordingly, P15 stops the cell to cell movement of 22 nt siRNA much more efficiently than the movement of 21 nt siRNA. These results, obtained using a peroxisome-excluded allele, suggest that an only partial block of cell to cell movement of 21 nt-long siRNA may indeed constitute P15's crucial shortcoming. Interestingly, peroxisome isolation experiments have revealed that P15 is able to import both 21 and 22 nt-long RNAs into these organelles. Given the key role of peroxisomal localization in the movement of PCV, although further experimentation is needed, we suggest that by importing virus-derived siRNA into peroxisomes P15 is able to neutralize them and prevent them from triggering a systemic response without being permanently bound to them, thereby overcoming its main shortcoming.

References

Incarbone M and Dunoyer P. 2013. *Trends in Plant Science*, Jul 18 (7):382-92

Annex 4

The manuscript of the article “Neutralization of mobile antiviral small RNA through peroxisomal import”, comprising the results shown in Chapter 1 and 2 of this thesis, was submitted for publication as a Short Article in *Cell Host & Microbe*.

Neutralization of mobile antiviral small RNA through peroxisomal import

M. Incarbone[1], A. Zimmermann[1], P. Hammann[2], M. Erhardt[1], F. Michel[1], Patrice Dunoyer[1]*

Affiliations:

[1]Institut de Biologie Moléculaire des Plantes du CNRS, UPR2357, Université de Strasbourg, France

[2]Institut de Biologie Moléculaire et Cellulaire du CNRS, Plateforme Protéomique Strasbourg – Esplanade, FRC1589, Strasbourg, France

***Correspondence to:** patrice.dunoyer@ibmp-cnrs.unistra.fr

ABSTRACT

In animals, certain viral proteins are targeted to peroxisomes to dampen the antiviral immune response mediated by these organelles. In plants, RNA interference (RNAi) is the main antiviral defense mechanism. To protect themselves against the cell- and non-cell autonomous effects of RNAi, viruses produce suppressors of RNA silencing (VSR). By combining biochemical approaches, cell-specific inhibition of RNAi movement and peroxisome isolation, we show here that one such VSR exploits these organelles to prevent spread of antiviral small interfering RNA (siRNA) by delivering them into the peroxisomal matrix. Piggybacking of these VSR-bound nucleic acids into peroxisomes potentiates viral systemic infection and highlights a novel pathogenic strategy that may have its direct counterpart in animals. Our results also emphasize the powerful antiviral effect of non-cell autonomous RNAi during genuine viral infection.

INTRODUCTION

In mammalian cells, peroxisomes are not only metabolic organelles but also serve as signaling platforms to orchestrate an early antiviral immune response mediated by mitochondrial antiviral signaling adaptors (MAVS) anchored to the surface of peroxisomal membranes (Dixit et al., 2010). In turn, viruses have developed mechanisms to inhibit the peroxisomal MAVS-dependent antiviral signaling by targeting viral proteins to the membrane of these organelles (Bender et al., 2015; Ferreira et al., 2016; Magalhaes et al., 2016). For instance, in the case of the cytomegalovirus protein vMIA, this targeting occurs through its interaction with the peroxin protein PEX19 (Magalhaes et al., 2016). Although it is not entirely clear how vMIA inhibits peroxisomal MAVS-dependent signaling, the Hepatitis C virus NS3-4A protease was shown to do so through MAVS cleavage (Bender et al., 2015; Ferreira et al., 2016). Moreover, specific animal viruses have evolved to convey viral proteins into peroxisomes. While Nef protein of HIV is thought to enter peroxisomes through interaction with a peroxisomal thioesterase (Cohen et al., 2000), rotavirus VP4 is imported through a peroxisomal targeting signal (PTS1) (Mohan et al., 2002), a C-terminal tripeptide which is recognized by the import receptor PEX5 (Leon et al., 2006). These examples further support an important, yet in these latter cases uncharacterized, role of these organelles in viral pathogenesis and/or disease manifestation.

In plants, RNA interference (RNAi) is the main antiviral defense mechanism. It relies on the production by the RNaseIII Dicer-like 4 (DCL4), or its surrogate DCL2, of 21- and 22-nucleotide (nt) virus-derived (v)siRNAs, respectively (Deleris et al., 2006). These vsiRNA are mainly loaded into Argonaute 1 (AGO1) and AGO2, which then target single-stranded viral RNA for cleavage (Carbonell et al., 2012; Wang et al., 2011), in what is known as cell-autonomous RNAi. Moreover, in plants, the effect of RNAi can extend beyond the sites of its initiation, owing to the movement of siRNAs (Chitwood et al., 2009; Dunoyer et al., 2010; Molnár et al., 2010). Transgene-derived siRNAs have been shown to move cell-to-cell through plasmodesmata and systemically through the phloem, triggering RNA cleavage in remote tissues (Voinnet et al., 2000; Voinnet et al., 1998). During viral infection, the spread of vsiRNAs most likely immunizes cells that are yet to be infected, thereby delaying or precluding accumulation of the pathogen in these cells (Deleris et al., 2006; Havelda et al., 2003). However, the cell-autonomous and mobile aspects of antiviral RNAi are tightly connected and factors specifically involved in non-cell autonomous RNAi still await identification. Therefore, experimental evidence supporting an important defensive role of systemic RNAi in the context of genuine viral infection is rather scarce.

To escape these cell- and non-cell autonomous RNAi-based immune responses, viruses produce suppressors of RNAi (VSR), which have been shown to work through various strategies, from sequestration of siRNA to inhibition of AGO stability (Incarbone and Dunoyer, 2013). The in-depth

study of these proteins is crucial to properly understand the biological cycle of plant viruses and potentially find new solutions to control these pathogens. One such VSR, the *Peanut clump virus* (PCV)-encoded P15, possesses a C-terminal PTS1 that entails its peroxisomal localization, which is dispensable for suppression of cell-autonomous RNAi (**Figure S1, A and B)**, but potentiates viral movement (**Figure S1C**), through a yet undefined process (Dunoyer et al., 2002; Schott et al., 2012). Here, we characterize *in vivo* the mode of action of P15 in the suppression of cell- and non-cell autonomous RNAi, and reveal the function of its peroxisomal localization in the establishment of successful PCV systemic infection. We find that P15 is able to bind both 21-nt and 22-nt siRNAs, but shows a markedly superior capacity to stop cell-to-cell movement of the latter. To compensate for its poor ability to stop movement of 21-nt siRNA, and subsequent systemic immunization, PCV has evolved a novel pathogenic strategy consisting in P15-mediated piggybaking of these antiviral molecules into the peroxisomal matrix.

RESULTS

P15 prevents 21-22nt small RNA loading into AGO proteins through binding and sequestration

As a first step to determine the silencing suppression strategy of P15 *in vivo*, we introduced a 35S:*P15FHA* transgene into SUC:*SUL* plants, in which an IR construct, driven by the phloem-companion cell-specific AtSUC2 promoter, triggers RNAi of the ubiquitously expressed endogenous *SULPHUR* (*SUL*) mRNA. Processing of the phloem-specific *SUL* dsRNA generates 21- and 24-nt siRNAs and causes RNAi spread manifested by a chlorotic phenotype expanding 10–15 cells beyond the vasculature (**Figure 1A**). Of the two siRNA species, only 21-nt siRNAs are required for *SUL* RNAi in both incipient and recipient cells, through their incorporation into AGO1 (Dunoyer et al., 2007; Dunoyer et al., 2010). As expected, 35S:*P15FHA/*SUC:*SUL* transgenic lines displayed no *SUL*-silencing phenotype (**Figure 1A**), despite accumulating similar, or even higher, amount of the 21-nt *SUL* siRNA species than the one found in our SUC:*SUL* reference line (**Figure 1B**). AGO1 immunoprecipitation (IP) experiments performed on these transgenic lines showed that P15 efficiently prevented the incorporation of 21-nt *SUL* siRNAs into this protein (**Figure 1B**). Similar observations were made in AGO2 IP (**Figure S2**). In parallel, immunoprecipitation analyses of the epitope-tagged P15 revealed that, out of the two *SUL* siRNA species, P15 only binds the 21-nt *SUL* siRNAs (**Figure 1C**). Similar results were obtained with our 35S:*FHAP19/*SUC:*SUL* transgenic line used here as control (**Figure 1B-C and Figure S2)**, indicating that P15, akin to the tombusviral P19 (Vargason et al., 2003), sequesters 21-nt siRNAs, thereby preventing their incorporation into the two major antiviral AGOs.

P15 stops cell-to-cell movement of 22nt siRNA more efficiently than that of 21nt siRNA

Next, to assess the ability of P15 to prevent movement of siRNAs, we expressed this VSR in a companion cells-specific manner by introducing a SUC:*P15FHA* transgene into SUC:*SUL* plants. Highly expressing SUC:*P15FHA* transgenic lines (#14) displayed no *SUL*-silencing movement, whereas movement remained unaltered in lower-expressing lines (#26) (**Figure 2A-B**). In both high- and low-expressing plants, immunostaining confirmed that P15FHA accumulation was strictly confined within phloem-companion cells (**Figure S3**). Immunoprecipitation of epitope-tagged P15 in these transgenic lines revealed that *SUL*-silencing suppression was correlated with the amount of 21-nt *SUL* siRNAs sequestered by P15 (**Figure 2C**) indicating that suppression of non-cell autonomous RNAi relies on the dose-dependent capacity of P15 to sequester DCL4-dependent 21-nt *SUL* siRNAs in incipient cells. Interestingly, similar experiments performed in a *dcl3/dcl4* mutant background, where non-cell autonomous *SUL*-RNAi is mediated by DCL2-dependent 22-nt *SUL* siRNAs (Dunoyer et al., 2007), revealed that movement of this specific size class of small RNA is efficiently impaired by significantly less P15 than in a wild-type background (**Figure 2A-B and D**), suggesting that P15 has stronger binding capacity for 22-nt than for 21-nt small RNAs. Assessing microRNA accumulation in P15FHA IP fraction further supported this hypothesis. Indeed, we found that P15 strongly binds to, and impairs AGO1 loading of, 22-nt but not 21-nt miRNAs whereas P19, in agreement with its documented size-specificity (Vargason et al., 2003) showed efficient sequestration of 21-nt but not 22-nt miRNAs (**Figure 1B-C**). Collectively, these results indicate that P15 suppresses both cell- and non-cell autonomous RNAi through sequestration of 21-nt and 22-nt siRNAs and is more efficient in preventing movement of the latter due to an apparent higher affinity for this specific size class.

The existence of such dual binding capacity of siRNAs by P15 might be explained by the observation that, as opposed to other plant RNA viruses (such as the *Turnip mosaic virus*, TuMV) which trigger predominant accumulation of DCL4-dependent 21-nt vsiRNAs (**Figure S4A**) (Garcia-Ruiz et al., 2015), processing of PCV-derived dsRNAs results in a high proportion of both 21-nt and 22-nt vsiRNAs (**Figure S4B**). Although the reason for the high proportion of DCL2-dependent vsiRNAs in PCV-infected tissues is unknown, it does not result from a strong decrease in DCL4 accumulation (**Figure S5**), as opposed to what was previously observed during *Turnip crinkle virus* infection (Azevedo et al., 2010).

P15 is able to import small RNA into peroxisomes

The above findings prompted us to investigate how P15 could efficiently prevent movement of 21-nt siRNA despite its apparent lower binding capacity to this specific size class and, in turn, potentially optimize PCV systemic infection. Based on the observation that (i) P15 peroxisomal localization potentiates PCV cell-to-cell and long distance movement (**Figure S1C**) while being dispensable for cell-autonomous RNAi suppression (**Figure S1A-B)** (Dunoyer et al., 2002), and (ii) given that, as opposed to mitochondria or chloroplasts, peroxisomes have the unique property to import folded

proteins, oligomers and protein complexes (Leon et al., 2006), we hypothesized that P15 could isolate siRNAs from the symplasm and thereby impair their movement to adjacent cells by delivering them into peroxisomes. To address this possibility, we first performed peroxisome isolations to near homogeneity on SUC-*SUL* plants expressing 35S:*P15wt* or 35S:*P15ΔN6*, a C-terminal truncated version of P15 lacking its PTS1 and peroxisomal localization (Dunoyer et al., 2002). Efficient suppression of the *SUL*-silencing phenotype in both lines (**Figure 3A**) further supports the notion that P15 peroxisomal localization is dispensable for intracellular silencing suppression (**Figure S1A**). As expected, analysis of peroxisomal proteins in these transgenic lines revealed that P15, but not P15ΔN6, was imported into peroxisomes (**Figure 3B**). In parallel, RNA analyses showed that 21-nt *SUL* siRNAs were detected in the peroxisomal fraction only in presence of P15 (**Figure 3C**). In addition, upon infection of these transgenic lines with a modified *Tobacco rattle virus* (TRV) containing a fragment of the *Arabidopsis* phytoene desaturase (*PDS*) gene, detection of TRV-PDS-derived 21-nt vsiRNAs in the peroxisomal fraction was also strictly correlated with the import of P15 (**Figure 3B-C**). Similar results were obtained upon infection with a GFP-tagged VSR-deficient TuMV (TuMV-AS9-GFP; **Figure 3D-F**) (Garcia-Ruiz et al., 2010), indicating that P15, but not P15ΔN6, is indeed able to efficiently import 21-nt siRNAs in the peroxisomal matrix. Of note, P15-mediated peroxisomal import of TuMV-derived 21-nt vsiRNAs was inhibited during wild-type TuMV-GFP infection (**Figure 3F**), most likely as a result of competition for vsiRNA binding between P15 and the functional TuMV-encoded VSR HC-Pro (Garcia-Ruiz et al., 2015).

Import of 21nt siRNA into peroxisomes by P15 strongly bolsters PCV systemic infection

We then investigated whether P15-mediated peroxisomal import of vsiRNAs also occurs in the context of PCV infection. P15 and PCV-derived vsiRNAs were indeed detected in purified peroxisomes of PCV-infected *Arabidopsis thaliana* (**Figure 4A-C**) and *Nicotiana benthamiana* (**Figure 4D-F**), while *Potato virus X* (PVX)-derived vsiRNAs were absent from peroxisomes of PVX-GFP-infected plants (**Figure 4D-F**). Together with the observation that systemic spread (**Figure S1C**), but not intracellular accumulation (**Figure S1B**), of PCV-ΔN6 is highly impaired, these experiments (**Figure 3 and 4**) strongly suggested that the efficiency of PCV cell-to-cell and long distance movement is directly correlated to the ability of P15 to deliver vsiRNAs into peroxisomes. Consequently, we reasoned that spread of PCV-ΔN6 should be restored in plants impaired in vsiRNA production, chiefly the DCL4-dependent 21-nt vsiRNAs that are less tightly bound by P15. To address this, wild-type Col-0, *dcl4* or *dcl2/dcl4* mutant plants were infected with equal amounts of either PCV-wt or PCV-ΔN6 purified virions. Similarly to what was observed in *Nicotiana benthamiana* (**Figure S1C**), PCV-ΔN6 was in most cases absent or barely detectable in systemic leaves of Col-0-infected plants, whereas PCV-wt accumulated to high levels (**Figure 4, G and H, and Figure S6**). By contrast, systemic movement of PCV-ΔN6 in *dcl4* or *dcl2/dcl4* was restored to near PCV-wt levels (**Figure 4 G**

and H, and Figure S6). These observations strongly support that compromised spread of PCV-ΔN6 in wild-type plants mainly results from impaired delivery of DCL4-dependent 21-nt vsiRNAs into peroxisomes. In addition, the similar amount of PCV-ΔN6 detected in *dcl4* and *dcl2/dcl4* mutant backgrounds suggests that either (i) mobile 22-nt siRNAs are not able to significantly undermine systemic movement of PCV or (ii) that P15 stronger affinity for 22-nt siRNAs renders their peroxisomal import dispensable.

DISCUSSION

We have provided genetic and biochemical evidence that P15 suppresses cell- and non-cell autonomous RNAi through sequestration of siRNAs of two distinct size classes. Similarly to the high affinity of P19 for 21-nt siRNA, P15 has a stronger binding capacity for 22-nt siRNA, which are abundantly produced during PCV infection (**Figure S4**). This high proportion of DCL2-dependent vsiRNAs does not result from a change in the homeostasis of DCL4, nor of its cofactor DRB4 (**Figure S5**), suggesting that, in the context of PCV infection, either DCL4 activity is compromised or DCL2 is not merely the surrogate of DCL4. If the second scenario proved to be true, this virus could become a means to investigate the unexplored biology of DCL2 during antiviral defense.

While the molecular mechanism behind this observation remains an open question, PCV must neutralize two abundant and distinct size classes of antiviral siRNA. Although P15 affinity for DCL4-dependent 21-nt siRNAs is sufficient to impair their incorporation into the main antiviral AGOs, and therefore suppress cell-autonomous RNAi, in the absence of peroxisomal import (P15FHA, **Figure S7**), spread of these siRNAs, as opposed to 22-nt siRNAs, is poorly inhibited by this VSR (**Figure 2A-B**). To compensate for its reduced ability to stop 21-nt siRNAs from exiting incipient cells, PCV has evolved a novel pathogenic strategy, whereby an organelle is used to isolate these vsiRNAs from the symplasm, thus preventing their cell-to-cell and long-distance movement. This is achieved through P15-mediated piggybacking of siRNAs into the peroxisomal matrix. In the absence of such import (e.g. in the presence of P15ΔN6), DCL4-dependent 21nt vsiRNAs are not efficiently sequestered and become able to move systemically, priming antiviral RNAi in naïve cells and strongly delaying PCV systemic infection (**Figure 4**).

Although some tombusviruses hijack peroxisomal membranes to form viral replication complexes (Laliberte and Zheng, 2014), this is, to our knowledge, the first report of a VSR exploiting an organelle to suppress an aspect of the RNAi-based antiviral immune response and, thereby, to potentiate its silencing suppression capacity. In this respect, peroxisomes are particularly well suited for the confinement of host defensive molecules, as they import folded PTS-containing proteins (Leon et al., 2006), preserving potential protein-protein or protein-RNA interactions. In the case of PTS1-

containing proteins, this import is mediated by PEX5, a protein highly conserved among eukaryotes, which shuttles its cargo to the peroxisome membrane and, after docking to the pore complex, into the peroxisomal matrix where the cargoes are released. Incidentally, P15, but not P15ΔN6, was found to interact with the *Arabidopsis* PEX5 ortholog (Kragler et al., 1998) in a yeast-two-hybrid screen (data not shown).

This property of peroxisomal piggybacking (or lack thereof) has also allowed us to uncouple the suppression activity of P15 on non-cell autonomous RNAi from that on cell-autonomous RNAi, in the context of PCV infection (**Figure S1B-C and Figure 4**). The stark contrast between the systemic accumulation in Col-0 and *dcl4* mutant background of PCV-ΔN6, a virus otherwise as proficient as PCV-wt to accumulate in isolated BY-2 cells, clearly illustrates the powerful contribution of the systemic aspect of RNAi in dampening viral infection. As such, these viruses may constitute an interesting tool to further investigate mobile, systemic antiviral RNAi.

Finally, although it is well-established that proteins with no peroxisomal targeting signal can `piggyback' into peroxisomes by interacting with PTS-containing proteins (Leon et al., 2006), this study also reports that nucleic acid can be imported into these organelles. In light of these results, it would be interesting to re-assess the role of peroxisomal import of VP4, the spike protein of rotaviruses that cause some 600,000 deaths per year worldwide. The conservation of a PTS1 in all 153 known rotavirus VP4 sequences (Mohan et al., 2002) strongly suggests functional significance of its peroxisomal localization, which could be to deliver into these organelles proteins or nucleic acids acting as negative regulators of the viral life cycle, potentially neutralizing them. The same rationale may also apply to viral proteins interacting with imported peroxisomal proteins such as Nef of HIV or NS1 of Influenza virus (Lazarow, 2011).

EXPERIMENTAL PROCEDURES

Plant material

The *dcl4* (*dcl4-2*), *dcl24* (*dcl2-1/dcl4-2*), SUC:*SUL* line in wild-type (Col-0) and *dcl34* (*dcl3-1/dcl4-2*) mutant background were previously described (Dunoyer et al., 2007; Xie et al., 2005). The 35S-*P15* and 35S-*P15ΔN6* constructs were obtained by amplifying the wild-type or ΔN6-deletion P15 sequences from the corresponding pPC1 constructs (Dunoyer et al., 2002) and cloned into a pCTL-35S binary plasmid. The 35S-*P15FHA* and SUC-*P15FHA* constructs were obtained by cloning the P15 sequence without stop codon in frame with a C-terminal double Flag, double HA tag into a pCTL-35S or pCTL-SUC2 binary plasmid. The various constructs were introduced into the appropriate background by the floral dip method (Bechtold and Pelletier, 1998) and transformants were selected

on MS medium containing appropriate antibiotics. Agrobacterium-mediated transient expression in *Nicotiana benthamiana* was as described (Hamilton et al., 2002).

Virus infections

Agrobacterium containing plasmid expressing TuMV-GFP, TuMV-AS9-GFP (Garcia-Ruiz et al., 2010) or TRV-PDS (Liu et al., 2002) were infiltrated at OD 0.5 in 3-4 leaves/plant of 4-week old *Arabidopsis* and systemically infected tissues were harvested at 15 dpi. PVX-GFP sap was prepared as previously described (Garcia et al., 2014) and inoculated on 4-week old *N. benthamiana*. Systemically infected leaves were harvested at 11 dpi. BY-2 protoplast and primary PCV and PCV-ΔN6 infection of *N. benthamiana* were performed as previously described (Dunoyer et al., 2002). Systemically infected leaves where PCV-ΔN6 was detected, along with those infected with PCVwt, were further used as inoculum to infect *N. benthamiana*. Systemically infected leaves from these infections were harvested at 28 dpi for virion purification (see Supplementary Experimental Procedures). The resulting purified virions of PCV or PCV-ΔN6 were used to perform rub-inoculation of 3-4-week old plants with 4µg/plant (*Arabidopsis*) or 300ng/plant (*N. benthamiana*) of purified virions, diluted in 50mM sodium phosphate buffer pH 7.5. Systemically infected leaves were collected at 12 dpi (*Arabidopsis*) or at 7-11 dpi (*N. benthamiana*).

RNA analysis

RNA from total, peroxisomal or immunoprecipitated fractions was extracted with Tri-Reagent (Sigma, St. Louis, MO) according to the manufacturer's instructions. RNA gel blot analysis of high and low molecular weight RNA was on 10 µg of total RNA and was as described previously (Dunoyer et al., 2007). For high molecular weight northern blot, ethidium bromide staining of total RNA before transfer was used to confirm equal loading. Radiolabeled probe for detection of the SUL, TRV-PDS, TuMV-GFP PVX-GFP or PCV siRNAs was made by random priming reactions in the presence of a-32P-dCTP (Amersham). The template used was either a 400-bp long PCR product amplified from Arabidopsis genomic DNA (SUL), the mGFP5 ORF (TuMV-GFP) or the pPC1 (carrying the PCV RNA1 sequence), or a 600-bp long PCR product amplified from Arabidopsis genomic DNA (PDS) or the PVX coat protein ORF (PVX). DNA oligonucleotides complementary to miRNAs were end-labeled with g-32P-ATP using T4 PNK (New England Biolabs, Beverly, MA). For low molecular weight northern blot, detection of the Arabidopsis U6 small nuclear RNA was used to confirm equal loading.

Protein analysis

Total proteins were extracted from *Arabidopsis* or *N. benthamiana* frozen tissues as previously described (Hurkman and Tanaka, 1986). Peroxisomal and immunoprecipitated proteins were extracted with Tri-Reagent (Sigma, St. Louis, MO) according to the manufacturer's instructions. Proteins were

resolved on SDS–PAGE and after electroblotting on Immobilon-P membrane (Millipore), protein gel blot analysis was carried out using the appropriate antiserum.

Immunoprecipitation

The peptide used to raise rabbit polyclonal antibodies against AGO1 and AGO2 was described previously (Garcia et al., 2012; Qi et al., 2005). Antibodies were affinity-purified before use. For AGO1- and AGO2-immunoprecipitation, 0.4 g of 3-week old seedlings were ground in liquid nitrogen, and homogenized in 3ml/g of extraction buffer (50mM Tris-HCl, pH 7.5, 150mM NaCl, 10% glycerol, 0.1% NP-40) containing 1 tablet/50mL of protease inhibitor cocktail (Roche) for 30 minutes at 4°C. Cell debris was removed by centrifugation at 12,000g for 30 min at 4°C. Extracts were precleared by incubation with Protein A-agarose (Roche) at 4°C for 1h. Precleared extracts were then incubated with affinity purified AGO1 or AGO2-specific antibodies and protein A-agarose for 4 hours at 4°C. Immunoprecipitates were washed three times (20 min each) in extraction buffer. Immune complexes were then subjected to Tri-Reagent extraction (Sigma) for immunoprecipitated RNA and protein analysis. For HA-immunoprecipitation, 0.4g of 3-week old seedlings or 6-week old rosette leaves were ground in liquid nitrogen, homogenized in 1 ml of lysis buffer (50mM Tris–HCl, pH 7.5, 150mM NaCl, 1% Triton X-100) containing 1 tablet/50 ml of protease inhibitor cocktail (Roche) for 15 min at 4°C. Cell debris was removed by two successive centrifugations at 12,000g for 10 min at 4°C. After the second centrifugagtion an aliquot of supernatant was taken for input fraction. The remaining extracts were incubated with magnetic microparticles coated with monoclonal HA antibodies (MACS purification system, Miltenyi Biotech) at 4°C for 20 min. Samples were passed through Mcolumn (MACS purification system, Miltenyi Biotech) and an aliquot of the flow-through fraction was taken. The Mcolumn were then washed 2 times with 500µl of lysis buffer and 1 time with 100µl of washing buffer (20 mM Tris–HCl, pH 7.5). Magnetic beads were eluted with 50°C pre-warmed Tri-Reagent (Sigma, St Louis, MO) and immunoprecipited RNA and proteins were extracted according to manufacturer's instructions.

Peroxisome isolation

Performed according to (Reumann and Singhal, 2014), with slight modifications. Briefly, all extractions were performed at 4°C on fresh non-frozen tissue. Before isolation, plants were kept in the dark 16-20hrs, then 20-30g of 6-week old *A. thaliana* plants or *N. benthamiana* leaves were harvested and left on ice 2hrs. After cutting, grinding (in 120ml of 170mM Tricine pH7.5, 1M sucrose, 2mM EDTA, 1% BSA, 10mM KCl, 1mM $MgCl_2$, 0.5% PVP-40, 5mM DTT, Roche Complete protease inhibitor cocktail) and filtering through Miracloth, crude extract was clarified by centrifugation 1 min at 6700g. Next, the extract was deposited on Percoll/sucrose gradients and centrifuged 12 min at 13200g, then without stop 20 min at 27000g. After discarding the top layers, the bottom 2ml of each tube were collected, diluted in 36% sucrose (20mM Tricine, 1mM EDTA) and centrifuged 30 minutes

at 38700g. The bottom 1 ml of each tube was transferred into to a potter, gently homogenized, deposited on a 41.2% to 60% discontinuous sucrose gradient and ultracentrifuged for 40 minutes at 110800g. Finally, 1.5ml of visible white peroxisome fraction in the 50.5% sucrose phase was harvested and frozen at -80°C.

REFERENCES

Azevedo, J., Garcia, D., Pontier, D., Ohnesorge, S., Yu, A., Garcia, S., Braun, L., Bergdoll, M., Hakimi, M.A., Lagrange, T.*, et al.* (2010). Argonaute quenching and global changes in Dicer homeostasis caused by a pathogen-encoded GW repeat protein. Genes Dev. *24*, 904-915.

Bechtold, N., and Pelletier, G. (1998). In planta Agrobacterium-mediated transformation of adult Arabidopsis thaliana plants by vacuum infiltration. Methods Mol. Biol. *82*, 259-266.

Bender, S., Reuter, A., Eberle, F., Einhorn, E., Binder, M., and Bartenschlager, R. (2015). Activation of Type I and III Interferon Response by Mitochondrial and Peroxisomal MAVS and Inhibition by Hepatitis C Virus. PLoS Pathog. *11*, e1005264.

Carbonell, A., Fahlgren, N., Garcia-Ruiz, H., Gilbert, K.B., Montgomery, T.A., Nguyen, T., Cuperus, J.T., and Carrington, J.C. (2012). Functional Analysis of Three Arabidopsis ARGONAUTES Using Slicer-Defective Mutants. Plant Cell *24*, 3613-3629.

Chitwood, D.H., Nogueira, F.T.S., Howell, M.D., Montgomery, T.A., Carrington, J.C., and Timmermans, M.C.P. (2009). Pattern formation via small RNA mobility. Genes Dev *23*, 549-554.

Cohen, G.B., Rangan, V.S., Chen, B.K., Smith, S., and Baltimore, D. (2000). The human thioesterase II protein binds to a site on HIV-1 Nef critical for CD4 down-regulation. J. Biol. Chem. *275*, 23097-23105.

Deleris, A., Gallego-Bartolome, J., Bao, J., Kasschau, K.D., Carrington, J.C., and Voinnet, O. (2006). Hierarchical action and inhibition of plant Dicer-like proteins in antiviral defense. Science *313*, 68-71.

Dixit, E., Boulant, S., Zhang, Y., Lee, A.S., Odendall, C., Shum, B., Hacohen, N., Chen, Z.J., Whelan, S.P., Fransen, M.*, et al.* (2010). Peroxisomes are signaling platforms for antiviral innate immunity. Cell *141*, 668-681.

Dunoyer, P., Himber, C., Ruiz-Ferrer, V., Alioua, A., and Voinnet, O. (2007). Intra- and intercellular RNA interference in Arabidopsis thaliana requires components of the microRNA and heterochromatic silencing pathways. Nat. Genet. *39*, 848-856.

Dunoyer, P., Pfeffer, S., Fritsch, C., Hemmer, O., Voinnet, O., and Richards, K.E. (2002). Identification, subcellular localization and some properties of a cysteine-rich suppressor of gene silencing encoded by peanut clump virus. Plant J. *29*, 555-567.

Dunoyer, P., Schott, G., Himber, C., Meyer, D., Takeda, A., Carrington, J.C., and Voinnet, O. (2010). Small RNA Duplexes Function as Mobile Silencing Signals Between Plant Cells. Science *328*, 912-916.

Ferreira, A.R., Magalhaes, A.C., Camoes, F., Gouveia, A., Vieira, M., Kagan, J.C., and Ribeiro, D. (2016). Hepatitis C virus NS3-4A inhibits the peroxisomal MAVS-dependent antiviral signalling response. J. Cell. Mol. Med. *20*, 750-757.

Garcia, D., Garcia, S., Pontier, D., Marchais, A., Renou, J.P., Lagrange, T., and Voinnet, O. (2012). Ago hook and RNA helicase motifs underpin dual roles for SDE3 in antiviral defense and silencing of nonconserved intergenic regions. Mol. Cell *48*, 109-120.

Garcia, D., Garcia, S., and Voinnet, O. (2014). Nonsense-mediated decay serves as a general viral restriction mechanism in plants. Cell Host Microbe *16*, 391-402.

Garcia-Ruiz, H., Carbonell, A., Hoyer, J.S., Fahlgren, N., Gilbert, K.B., Takeda, A., Giampetruzzi, A., Garcia Ruiz, M.T., McGinn, M.G., Lowery, N.*, et al.* (2015). Roles and programming of Arabidopsis ARGONAUTE proteins during Turnip mosaic virus infection. PLoS Pathog. *11*, e1004755.

Garcia-Ruiz, H., Takeda, A., Chapman, E.J., Sullivan, C.M., Fahlgren, N., Brempelis, K.J., and Carrington, J.C. (2010). *Arabidopsis* RNA-Dependent RNA Polymerases and Dicer-Like

Proteins in Antiviral Defense and Small Interfering RNA Biogenesis during *Turnip Mosaic Virus* Infection. Plant Cell *22*, 481-496.
Hamilton, A.J., Voinnet, O., Chappell, L., and Baulcombe, D.C. (2002). Two classes of short interfering RNA in RNA silencing. EMBO J. *21*, 4671-4679.
Havelda, Z., Hornyik, C., Crescenzi, A., and Burgyan, J. (2003). In situ characterization of Cymbidium Ringspot Tombusvirus infection-induced posttranscriptional gene silencing in Nicotiana benthamiana. J. Virol. *77*, 6082-6086.
Hurkman, W.J., and Tanaka, C.K. (1986). Solubilization of plant membrane proteins for analysis by two-dimensional gel electrophoresis. Plant Physiol. *81*, 802-806.
Incarbone, M., and Dunoyer, P. (2013). RNA silencing and its suppression: novel insights from in planta analyses. Trends Plant Sci. *18*, 382-392.
Kragler, F., Lametschwandtner, G., Christmann, J., Hartig, A., and Harada, J.J. (1998). Identification and analysis of the plant peroxisomal targeting signal 1 receptor NtPEX5. Proc. Natl. Acad. Sci. USA *95*, 13336-13341.
Kräuter-Canham, R., Bronner, R., Evrard, J.-L., Hahne, G., Friedt, W., and Steinmetz, A. (1997). A transmitting tissue- and pollen-expressed protein from sunflower with sequence similarity to the human RTP protein. Plant Science *129*, 191-202.
Laliberte, J.F., and Zheng, H. (2014). Viral Manipulation of Plant Host Membranes. Annu. Rev. Virol. *1*, 237-259.
Lazarow, P.B. (2011). Viruses exploiting peroxisomes. Curr. Opin. Microbiol. *14*, 458-469.
Leon, S., Goodman, J.M., and Subramani, S. (2006). Uniqueness of the mechanism of protein import into the peroxisome matrix: transport of folded, co-factor-bound and oligomeric proteins by shuttling receptors. Biochim. Biophys. Acta *1763*, 1552-1564.
Liu, Y., Schiff, M., and Dinesh-Kumar, S.P. (2002). Virus-induced gene silencing in tomato. Plant J. *31*, 777-786.
Magalhaes, A.C., Ferreira, A.R., Gomes, S., Vieira, M., Gouveia, A., Valenca, I., Islinger, M., Nascimento, R., Schrader, M., Kagan, J.C*., et al.* (2016). Peroxisomes are platforms for cytomegalovirus' evasion from the cellular immune response. Sci. Rep. *6*, 26028.
Mohan, K.V., Som, I., and Atreya, C.D. (2002). Identification of a type 1 peroxisomal targeting signal in a viral protein and demonstration of its targeting to the organelle. J. Virol. *76*, 2543-2547.
Molnár, A., Melnyk, C., Bassett, A., Hardcastle, T., Dunn, R.M., and Baulcombe, D.C. (2010). Small Silencing RNAs in Plants Are Mobile and Direct Epigenetic Modification in Recipient Cells. Science *328*, 872-875.
Qi, Y., Denli, A.M., and Hannon, G.J. (2005). Biochemical specialization within Arabidopsis RNA silencing pathways. Mol. Cell *19*, 421-428.
Reumann, S., and Singhal, R. (2014). Isolation of leaf peroxisomes from Arabidopsis for organelle proteome analyses. Methods Mol. Biol. *1072*, 541-552.
Schott, G., Mari-Ordonez, A., Himber, C., Alioua, A., Voinnet, O., and Dunoyer, P. (2012). Differential effects of viral silencing suppressors on siRNA and miRNA loading support the existence of two distinct cellular pools of ARGONAUTE1. EMBO J. *31*, 2553-2565.
Vargason, J.M., Szittya, G., Burgyan, J., and Hall, T.M. (2003). Size selective recognition of siRNA by an RNA silencing suppressor. Cell *115*, 799-811.
Voinnet, O., Lederer, C., and Baulcombe, D.C. (2000). A viral movement protein prevents spread of the gene silencing signal in Nicotiana benthamiana. Cell *103*, 157-167.
Voinnet, O., Vain, P., Angell, S., and Baulcombe, D.C. (1998). Systemic spread of sequence-specific transgene RNA degradation in plants is initiated by localized introduction of ectopic promoterless DNA. Cell *95*, 177-187.
Wang, X.-B., Jovel, J., Udomporn, P., Wang, Y., Wu, Q., Li, W.-X., Gasciolli, V., Vaucheret, H., and Ding, S.-W. (2011). The 21-Nucleotide, but Not 22-Nucleotide, Viral Secondary

Small Interfering RNAs Direct Potent Antiviral Defense by Two Cooperative Argonautes in *Arabidopsis thaliana*. Plant Cell *23*, 1625-1638.
Xie, Z., Allen, E., Wilken, A., and Carrington, J.C. (2005). DICER-LIKE 4 functions in trans-acting small interfering RNA biogenesis and vegetative phase change in Arabidopsis thaliana. Proc. Natl. Acad. Sci. USA *102*, 12984-12989.

SUPPLEMENTAL INFORMATION

Supplemental Information includes seven figures, Supplemental Experimental Procedures and Source Data of Figures.

AUTHOR CONTRIBUTIONS

M.I. and P.D. designed the experiments. M.I. performed transgene construction, plant transformation and manipulation, viral purification and infection, immunoprecipitation, peroxisome isolation. M.I. and A.Z. performed RNA and protein extraction, RNA and protein gel blot analysis with the assistance of F.M. P.H. performed unpublished MS-MS protein analyses, while M.I. and M.E. performed immunohistochemistry. P.D. and M.I. wrote the manuscript and prepared the figures.

ACKNOWLEDGMENTS

This work was supported by a research grant from Agence Nationale pour la Recherche (ANR-14-CE19-0014-01). It was also performed under the framework of the LABEX: ANR-10-LABX-0036_NETRNA and benefits from a funding from the state managed by the French National Research Agency as part of the Investments for the future program. We deeply thank S. Reumann for invaluable advice on plant peroxisomes isolation and S. Bouzoubaa for advice on PCV purification.

FIGURE LEGENDS

Figure 1: P15 efficiently sequesters 21-nt siRNAs. (**A**) Phenotypes of SUC:*SUL* plants in wild-type, 35S:*P15FHA* or 35S:*FHAP19* transgenics. (**B**) Northern analysis of *SUL* siRNA, miR159, miR172, miR173 and miR398 accumulation in total RNA and immunoprecipitated (IP) fractions of AGO1-bound small RNA in control, 35S:*P15FHA*- or 35S:*FHAP19*-expressing SUC:*SUL* plants (top). AGO1 immunoprecipitation was confirmed by protein blot analysis (bottom). (**C**) HA epitope-specific immunoprecipitation in SUC:*SUL* reference plants or in 35S:*P15FHA* or 35S:*FHAP19*-expressing SUC:*SUL* transgenics. Total RNA was extracted from IPs and low-molecular-weight RNA subjected to Northern analysis (top). P15FHA and FHAP19 immunoprecipitation was confirmed by protein blot analysis (bottom). Accumulation of snRNA U6 (top) or coomassie staining (bottom) was used to confirm equal loading. Figure source data can be found with the Supplemental information.

Figure 2: Companion-cell specific P15 expression suppresses cell-to-cell SUL-silencing movement in a dose-dependent manner. (**A**) SUL-silencing phenotype in wild-type (WT), *dcl34*, SUC:*P15FHA*

high (line #14) or low-expressing (line #26) transgenic plants in WT background, and SUC:*P15FHA* low-expressing (lines #2 and #7) transgenic plants in *dcl34* mutant background. (**B**) Northern analysis of *SUL* siRNA and miR159 accumulation (top) and western analysis of P15FHA accumulation (bottom) in plants depicted in (A). (**C**) HA epitope-specific immunoprecipitation in SUC:*SUL* reference plants or in high and low SUC:*P15FHA*-expressing SUC:*SUL* transgenics. Total RNA was extracted from IPs and low-molecular-weight RNA subjected to Northern analysis (top panel). P15HA immunoprecipitation was confirmed by protein blot analysis (bottom panel). (**D**) Same as in (C) but for SUC:*SUL*x*dcl34* and SUC:*P15FHA* in SUC:*SUL*x*dcl34* (line #7) transgenic plants. Accumulation of snRNA U6 (top) or coomassie staining (bottom) was used to confirm equal loading. Figure source data can be found with the Supplemental information.

Figure 3: P15 and P15-bound siRNAs are imported into peroxisomes. (**A**) Phenotypes of non-infected (n.i.), or TRV-PDS-infected, 35S:*P15*- or 35S:*P15ΔN6*-expressing SUC:*SUL* plants. (**B**) Western analysis of P15 or P15ΔN6 accumulation in total or purified peroxisomal fractions of plants depicted in (A). Accumulation of the hydroxypyruvate reductase (@HPR), a leaf peroxisomal enzyme is used to confirm equal loading of the peroxisomal fractions. (**C**) Northern analysis of TRV-PDS-derived and SUL siRNAs accumulation in total or purified peroxisomal fractions of plants depicted in (A). (**D**) Phenotypes of wild-type (WT), or VSR-deficient (AS9), TuMV-GFP-infected 35S:*P15*- or 35S:*P15ΔN6*-expressing SUC:*SUL* plants. (**E**) Same as in (B) but for plants depicted in (D). (**F**) Same as in (C) but for plants depicted in (D). Coomassie staining (top) or accumulation of snRNA U6 (bottom) was used to confirm equal loading. Figure source data can be found with the Supplemental information.

Figure 4: P15-mediated piggybacking of vsiRNAs potentiates PCV systemic spread. (**A**) Phenotypes of non-infected or PCV-infected Col-0 *Arabidopsis* (left) and northern analysis of PCV viral RNA accumulation (right). (**B**) Western analysis of P15 accumulation in total or purified peroxisomal fractions of plants depicted in (A). Accumulation of the hydroxypyruvate reductase (@HPR), a leaf peroxisomal enzyme is used to confirm equal loading of the peroxisomal fractions. (**C**) Northern analysis of PCV-derived vsiRNAs accumulation in total or purified peroxisomal fractions of plants depicted in (A). (**D**) Phenotypes of non-infected, PCV- or PVX-infected *Nicotiana benthamiana* and northern analysis of PCV or PVX viral RNA accumulation. (**E**) Same as in (B) but for plants depicted in (D). (**F**) Same as in (C) but for plants depicted in (D). Coomassie staining (top) or accumulation of snRNA U6 (bottom) was used to confirm equal loading. (**G**) Northern analysis of PCV viral RNA accumulation in systemically infected leaves of WT Col-0, *dcl4* or *dcl2/dcl4* mutant background. Out of the 15 plants analyzed per genotype, four individuals spanning the range of viral titers are shown.

(**H**) Same as in (G) but for PCV-ΔN6 viral RNA. Ribosomal RNA (rRNA) is used to confirm equal loading. Figure source data can be found with the Supplemental information.

Figure 1

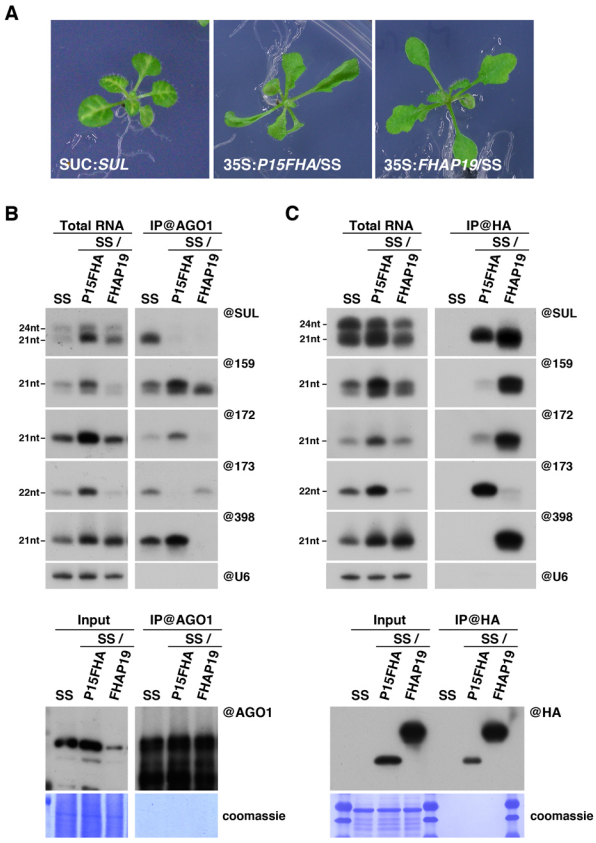
A
SUC:SUL
35S:P15FHA/SS
35S:FHAP19/SS
B
Total RNA
IP@AGO1
SS /
SS
P15FHA
FHAP19
24nt
21nt
@SUL
@159
@172
22nt
@173
@398
@U6
Input
@AGO1
coomassie
C
IP@HA
@HA

Figure 2

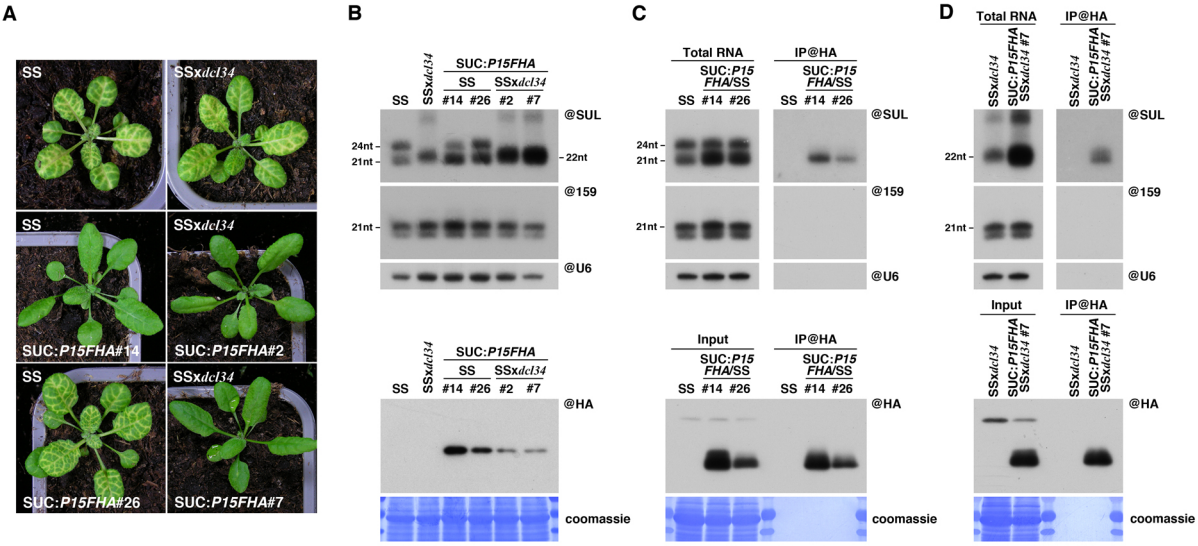
A
SS
SSxdcl34
SUC:P15FHA#14
SUC:P15FHA#2
SUC:P15FHA#26
SUC:P15FHA#7
B
SS
SSxdcl34
SUC:P15FHA
SS
SSxdcl34
#14 #26 #2 #7
@SUL
24nt
21nt
22nt
@159
@U6
@HA
coomassie
C
Total RNA
IP@HA
SUC:P15 FHA/SS
Input
D
Total RNA
IP@HA
SUC:P15FHA SSxdcl34 #7
Input

Figure 3

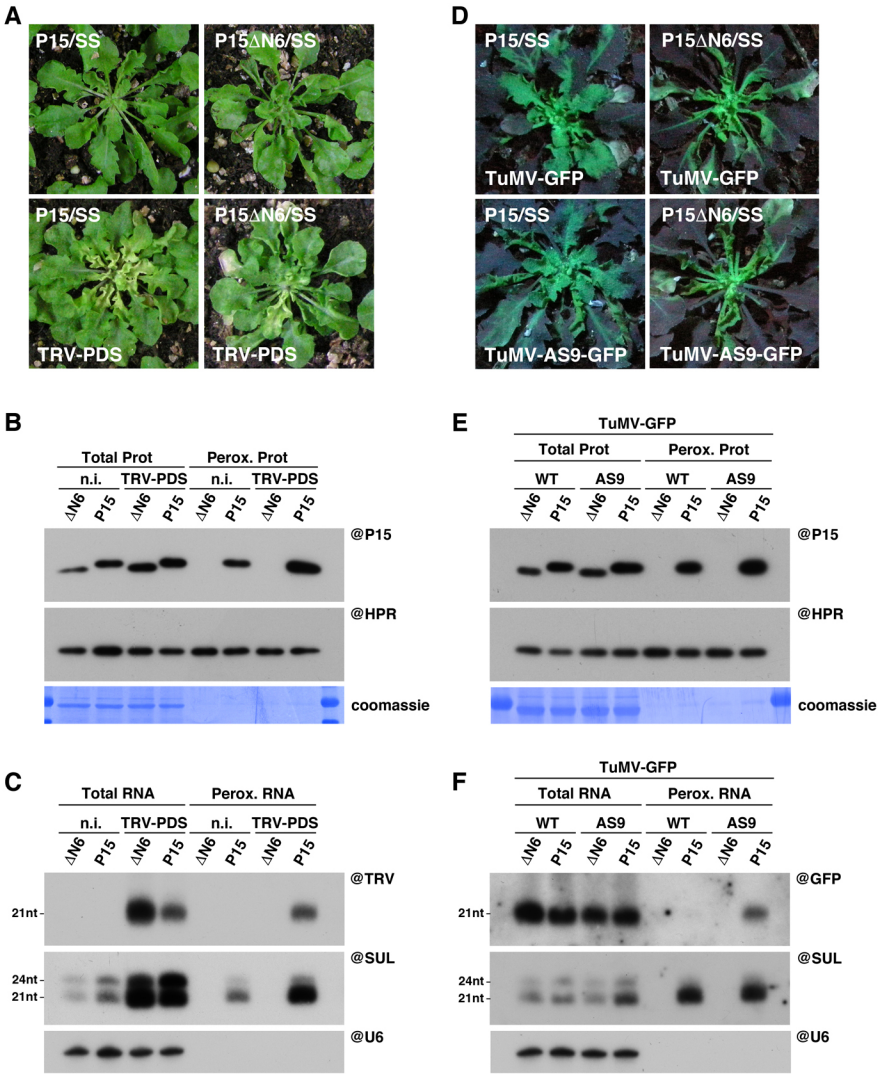
A
P15/SS
P15ΔN6/SS
P15/SS
P15ΔN6/SS
TRV-PDS
TRV-PDS
D
P15/SS
P15ΔN6/SS
P15/SS
P15ΔN6/SS
TuMV-GFP
TuMV-GFP
TuMV-AS9-GFP
TuMV-AS9-GFP
B
Total Prot
Perox. Prot
n.i.
TRV-PDS
n.i.
TRV-PDS
ΔN6
P15
@P15
@HPR
coomassie
E
TuMV-GFP
Total Prot
Perox. Prot
WT
AS9
WT
AS9
@P15
@HPR
coomassie
C
Total RNA
Perox. RNA
@TRV
21nt
@SUL
24nt
21nt
@U6
F
TuMV-GFP
Total RNA
Perox. RNA
@GFP
21nt
@SUL
24nt
21nt
@U6

Figure 4

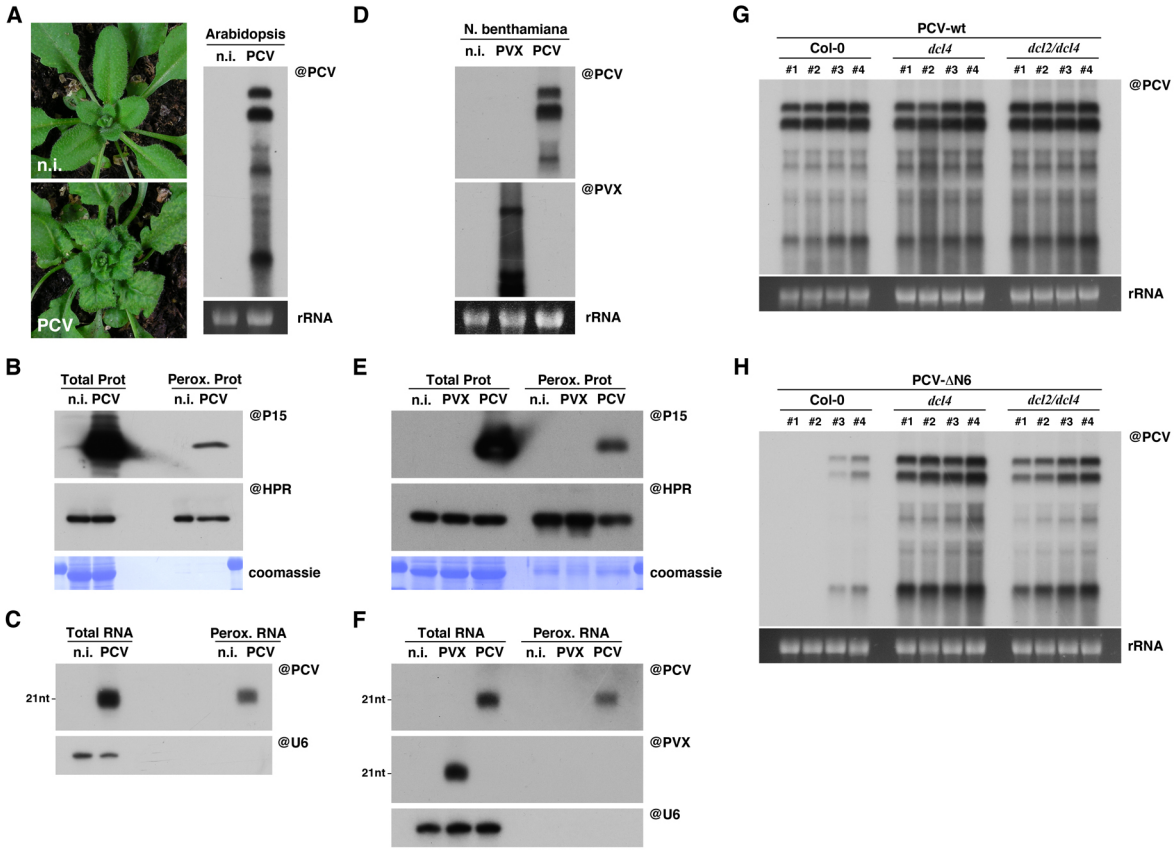
A
n.i.
PCV
Arabidopsis
n.i. PCV
@PCV
rRNA
D
N. benthamiana
n.i. PVX PCV
@PCV
@PVX
rRNA
G
PCV-wt
Col-0
dcl4
dcl2/dcl4
#1 #2 #3 #4
@PCV
rRNA
B
Total Prot
Perox. Prot
n.i. PCV
@P15
@HPR
coomassie
E
n.i. PVX PCV
@P15
@HPR
coomassie
H
PCV-ΔN6
C
Total RNA
Perox. RNA
21nt
@PCV
@U6
F
@PCV
@PVX
@U6

This PDF file includes:

Figures S1 to S3
Supplemental Experimental Procedures

Other Supplemental Information for this manuscript includes the following:

Figure source data for Figures 1 to 4 and Figures S1, S2, S3 as a zip file.

SUPPLEMENTAL FIGURES

Figure S1. Related to Figure 4.

P15 peroxisomal localisation is dispensable for intracellular silencing suppression and PCV viral RNA accumulation but required for PCV viral movement. (**A**) UV illumination of *N. benthamiana* leaves agroinfiltrated with GFP alone or in combination with TBSV P19, PCV P15 or PCV P15ΔN6 (left). Northern analysis of GFP-derived siRNA, miR159 (middle panels) or GFP mRNA (right panel) accumulation in the corresponding agroinfiltrated tissues. (**B**) Viral RNA accumulation of wild-type (WT) or P15ΔN6-mutated PCV in BY-2 protoplasts at 24 or 48 hours post-infection (hpi). (**C**) same as in (B) but in *N. benthamiana* systemic leaves at 7 or 11 days post-infection (dpi). Accumulation of snRNA U6 or ribosomal RNA (rRNA) was used to confirm equal loading. (**D**) Northern analysis of wild-type (WT) or P15ΔN6-mutated PCV in systemic leaves of Col-0 or *dcl24* infected plants at 15 dpi. Out of the 15 plants analyzed per genotype, four individuals spanning the range of viral titers are shown. Ethidium-bromide staining of rRNA was used to verify equal loading. Figure source data can be found with the Supplemental information.

Supplemental Figure S1

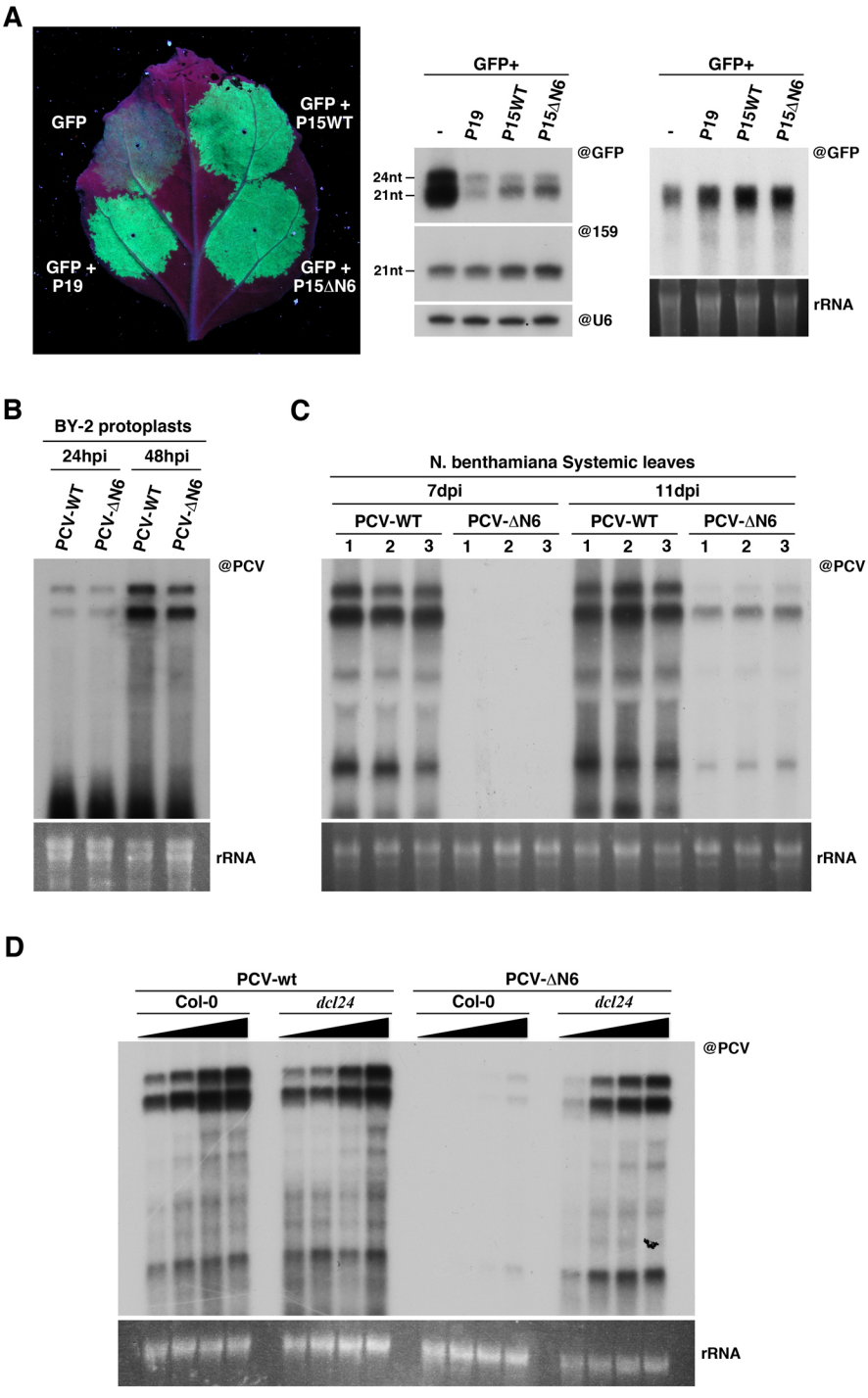

Figure S2. Related to Figure 1.

(**A**) P15 inhibits loading of siRNAs in AGO2. Northern analysis of *SUL* siRNA accumulation in total RNA and immunoprecipitated (IP) fractions of AGO2-bound small RNAs in control, 35S:*P15FHA*- or 35S:*FHAP19*-expressing SUC:*SUL* plants. AGO2 immunoprecipitation was confirmed by protein blot analysis (bottom). Accumulation of snRNA U6 (top) or coomassie staining (bottom) was used to confirm equal loading. Note that the total RNA panels are the same as the ones depicted in Fig. 1B as AGO1 and AGO2 IP experiments were performed on the same set of plants. (**B**) P15FHA is not imported into peroxisomes. Western analysis of P15FHA and P15 accumulation in total or purified peroxisomal fractions of transgenic plants depicted in Figure 1 and 3, respectively. Accumulation of the hydroxypyruvate reductase (@HPR), a leaf peroxisomal enzyme is used to confirm equal loading of the peroxisomal fractions. Coomassie staining was used to confirm equal loading. Figure source data can be found with the Supplemental information.

Supplemental Figure S2

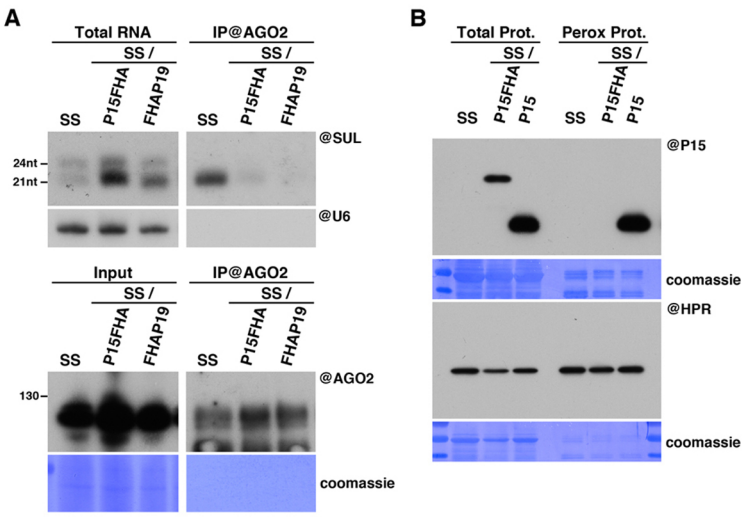

Figure S3. Related to Figure 2.

(**A**) Companion-cell specific expression of P15FHA in SUC:*P15FHA* transgenics. P15FHA immuno-staining in transversal leaf sections of SUC:*P15FHA*-expressing SUC:*SUL* transgenics (lines #14 and #26) and SUC:*SUL* control plants. (**B**) Same as in (A) but in transversal leaf sections of SUC:*P15FHA*-expressing SUC:*SUL*/*dcl34* transgenics (lines #2 and #7). (**C**) PCV but not TuMV viral RNA are efficiently processed by both DCL4 and DCL2 in wild-type plants. High resolution northern blot analysis of TuMV-(top) and PCV-derived siRNA (bottom) accumulation in Col-0 or *dcl4* TuMV-GFP-infected plants. Accumulation of snRNA U6 was used used to confirm equal loading. Figure source data can be found with the Supplemental information. (**D**) Western analysis of DCL4 (top), DRB4 (middle) or P15 (bottom) accumulation in non-infected or PCV-infected Col-0 plants. For DCL4 and DRB4 accumulation, protein extract from T-DNA knock-out plants (*dcl234* and *drb4*, respectively) was loaded in parallel to more easily visualize the specific band. Coomassie staining of the membrane was used to confirm equal loading. Figure source data can be found with the Supplemental information.

Supplemental Figure S3

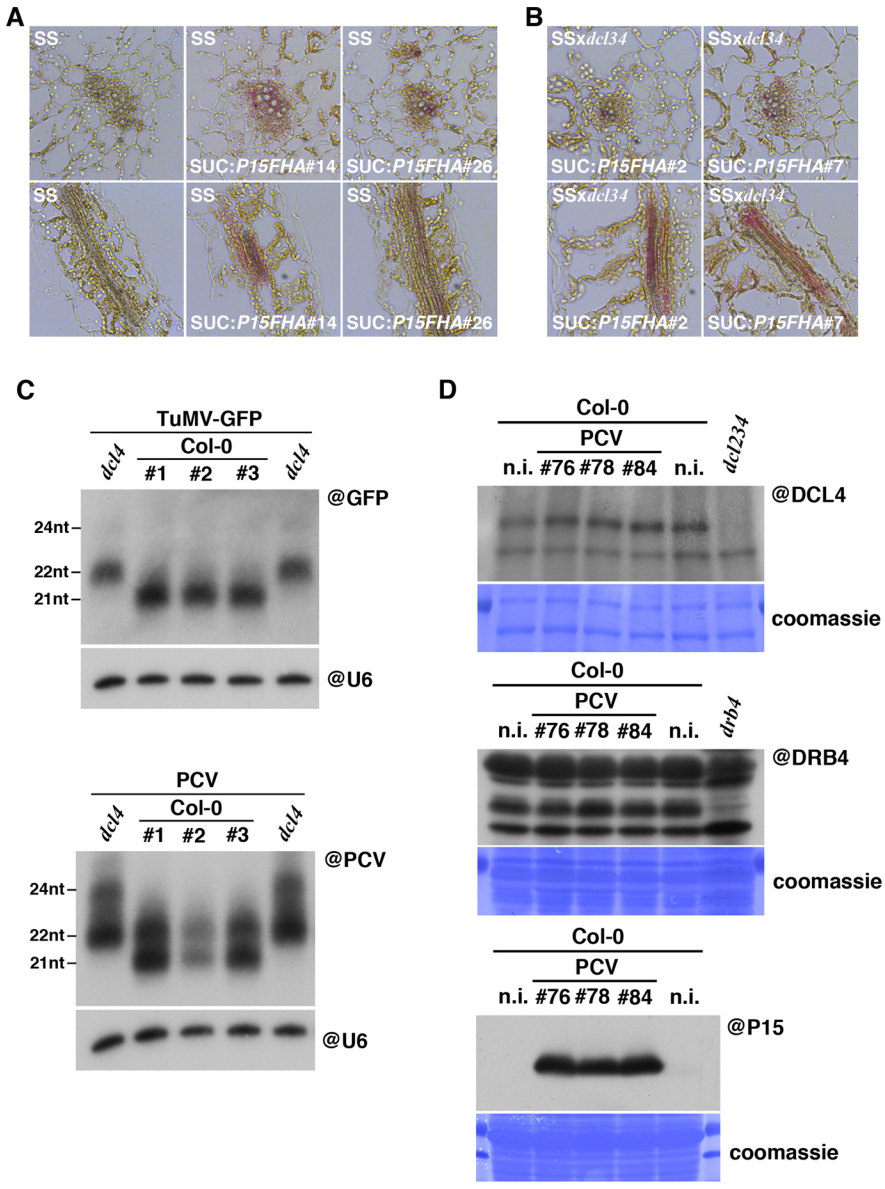

SUPPLEMENTAL EXPERIMENTAL PROCEDURES

PCV virion purification

PCV purification was performed from frozen *N. benthamiana* leaves systemically infected with PCV-wt and PCV-ΔN6 (harvested at 28 dpi). All steps were performed at 4°C. 50 g of frozen tissue were mixed in an electric blender with 120 ml borate buffer 100 mM ($Na_2B_4O_7$, pH 9), 1% Triton X-100, 0.2 % sodium sulphite and 150 ml chloroform. The lysate was centrifuged 15 min at 8670g, and the resulting supernatant was filtered through sterile Miracloth. Precipitation was allowed O/N with 1.2% (w/v) NaCl and 3% (w/v) PEG6000 with gentle stir before centrifugation for 30 min at 14330g. The supernatant was removed and the pellet resuspended in 100 ml borate buffer 40 mM, 0.2 % sodium sulphite for at least 2 hrs. The resulting suspension was further clarified by centrifugation at 8670g for 15 min and the supernatant precipitated for 4 hours with 1.2 % NaCl and 3% PEG6000. After centrifugation for 30 min at 14330g, the supernatant was discarded and the pellet resuspended in 20 ml borate buffer 40 mM, 0.2 % sodium sulphite. After clarification at 4420g for 5 min, the supernatant was deposed onto a 7 ml sucrose cushion (25% sucrose in 40 mM borate buffer, 0.2 % sodium bisulphite) and ultracentrifuged 3 hrs at 100000g. The supernatant was discarded and the pellet resuspended O/N in 1 ml borate buffer 40 mM, 0.2 % sodium bisulphite. After a last clarification to remove the remaining aggregates, the virus concentration was measured by OD and after RNA extraction, quality was evaluated by agarose gel electrophoresis. Virus was stored at 4°C, for up to three months.

Immunohistochemistry

Arabidopsis leaves were fixed in PFA (4% paraformaldehyde, 1x PBS), embedded in paraplast and sectioned as previously described (Kräuter-Canham et al., 1997). Pretreatment of the samples included deparaffination and rehydration. The samples were washed twice in 1x PBS, 1% BSA for 1h. Incubation with a 1:200 dilution of anti-HA antibody coupled to alkaline phosphatase (Sigma-Aldrich) was performed overnight at 4°C in 1x PBS, 1% BSA. This incubation was followed by three washes of 15 min each with 1x PBS, 1% BSA. Sections were then equilibrated in Fast Red buffer. Buffer was then removed and Fast Red was added (SigmaFAST FastRed TR/Naphthol AS-MX) and incubated 3 hours at RT. Reaction was stopped with water and sections were prepared for microscopy in PBS 50% Glycerol 50%. Photos were taken with an E800 Nikon optical microscope and an IDS color camera.

SUPPLEMENTAL REFERENCE

Kräuter-Canham, R., Bronner, R., Evrard, J.L., Hahne, G., Friedt, W. and Steinmetz, A. (1997). A transmitting tissue- and pollen-expressed protein from sunflower with sequence similarity to the human RTP protein. Plant Science *129*, 191-202.